Aus dem Institut für Physiologie und Pathophysiologie

Geschäftsführender Direktor: Prof. Dr. Dominik Oliver

des Fachbereichs Medizin der Philipps-Universität Marburg

Unraveling the complexity of *Drosophila* immune cells: a focus on blood cell heterogeneity, plasticity, and dynamics

Inaugural-Dissertation zur Erlangung

des Doktorgrads der Naturwissenschaften

dem Fachbereich Medizin der Philipps-Universität Marburg

vorgelegt von

Alexander Hirschhäuser

aus Marburg

Marburg, 2023

Angenommen vom Fachbereich Medizin

der Philipps-Universität Marburg am: 15.09.2023

Gedruckt mit Genehmigung des Fachbereichs Medizin

Dekanin: Frau Prof. Dr. Denise Hilfiker-Kleiner

Referent: Herr Prof. Dr. Sven Bogdan

1. Korreferent: Herr Prof. Dr. Alexander Brehm

Summary

Until recently, *Drosophila* immune cells, named hemocytes, were only characterized and clustered into subpopulations based on morphology, function, and a limited number of marker genes. Thus, the cells were subdivided into plasmatocytes, crystal cells, and lamellocytes, and the population of *Drosophila* plasmatocytes has been thought to be a relatively homogenous sub-group. However, new single-cell RNA sequencing approaches revealed a complex heterogeneity and plasticity within this cell population. Particularly, the transcriptional profile of hemocytes changes in response to the significant environmental changes during the transition from the larval to the pupal stage of development. Additionally, the here identified complex heterogeneity of *Drosophila* immune cells includes cells derived from embryonic and lymph gland precursors with a highly migratory and immune responsive Posterior Signaling Center (PSC) niche-like blood cell type that persists into the adult fly. Those niche-like progenitor cells could be potential precursor cells for known hemocyte subpopulations like the lamellocytes. However, so far, lamellocytes have only been reported to differentiate from progenitor hemocytes in response to infestation by parasitoid wasps.

Hemocytes rely on the ability to rapidly adapt to different immune challenges and migrate to locations where they are needed. This is only possible because of the highly regulated actin cytoskeleton. Dynamic remodeling of this dense network – especially inside the lamellipodium - is highly regulated and a crucial step for the necessary cell shape changes to allow locomotion and efficient immune defense. A key regulator, which builds lamellipodial protrusions and thereby drives cell migration, is the Arp2/3 complex, which in turn is activated by the hetero-pentameric WAVE regulatory complex. The role of phosphorylation in regulating WAVE, an indispensable part of the complex, has been addressed in various *in vitro* studies. However, the *in vivo* relevance of WAVE phosphorylation on actin dynamics is still poorly understood and further investigated in this study.

CK1α is a constitutively active and ubiquitously expressed serine/threonine kinase, which is involved in regulating many cellular processes ranging from cell division, and signaling to circadian rhythm and has now emerged as an

essential regulator of WAVE. MARCM induced c*k1α* missense mutant hemocytes phenocopy WAVE depletion resulting in the disruption of the actin network that causes reduced lamellipodia formation and impaired migratory behavior. Rescue experiments using a phosphorylation-deficient mutation in the CK1α target sequence within the VCA domain of WAVE outline the dependency on CK1α phosphorylation for WAVE stability. Remarkably, loss of phosphorylation leads to proteasomal degradation of WAVE. This suggests that WAVE has a basal level of phosphorylation by CK1α, which protects it from degradation and thus promotes its function *in vivo*.

Zusammenfassung

Bis vor einigen Jahren wurden die Immunzellen der Fruchtfliegen *Drosophila*, genannt Hämozyten, nur basierende auf deren Zellstruktur, Funktion und einer beschränkten Anzahl an Signaturgenen beschrieben und unterteilt. Daraus folgte eine Unterteilung in Plasmatozyten, Crystal Cells und Lamellozyten, wobei die Population der Plasmatozyten als relativ homogene Gruppe vermutet wurde. Mit der Weiterentwicklung der Einzelzell RNA Sequenzierungsmethode wurde jedoch festgestellt, dass diese Zellpopulation eine komplexe Heterogenität und Variabilität aufzeigt. Insbesondere verändert sich das transkriptionelle Profil der Hämozyten als Reaktion auf signifikante Veränderungen während des Übergangs von der Larven- zur Puppentwicklungsphase.. Die Ergebnisse bestätigen zudem, dass es sich um eine Vereinigung von Immunzellen, die entweder embryonalen Ursprungs sind oder von Vorläuferzellen aus der Lymphdrüse abstammen, handelt. Zusätzlich umfasst die hier identifizierte komplexe Heterogenität der Immunzellen von *Drosophila* einen hoch migratorischen und immunreaktiven Zelltyp des posterioren Signalzentrums der Lymphdrüse, welcher bis zur adulten Fliege erhalten bleibt. Diese nischenartigen Zellen könnten als potenzielle Vorläuferzellen für bekannte Subpopulationen von Hämozyten wie die Lamellozyten fungieren. Bisher wurde berichtet, dass Lamellozyten als Reaktion auf den Befall durch parasitäre Wespen nur aus Vorläufer-Hämozyten differenzieren..

Wichtig für das Migrationsverhalten der Immunzellen ist die schnelle Anpassungsfähigkeit in der Immunabwehr. Das ist vor allem möglich aufgrund des dynamisch regulierten Aktin-Zytoskelettes. Veränderungen des verzweigten Aktin-Netzwerkes ist ein entscheidender Schritt für diese Anpassung und durch viele Faktoren reguliert. Der Arp2/3 Komplex ist dabei der wichtigste Regulator im Aufbau von lamellipodialen Ausstülpungen, was die treibende Kraft der Zellmigration ist. Dieser Komplex wiederum wird aktiviert durch den hetero pentamerischen WAVE regulatory complex. Die Phosphorylierung von WAVE als Regulationsmechanismus dieses Komplexes wurde in den letzten Jahren intensiv *in vitro* untersucht. Jedoch wurde bisher die Bedeutung der

Phosphorylierung von WAVE und den Einfluss dadurch auf die Aktin Dynamiken *in vivo* nicht gezeigt.

In einem ausführlichen Screen stellte sich heraus, dass die Casein Kinase 1α ein entscheidender Faktor in der Regulation von WAVE ist. Bei dieser Kinase handelt es sich um eine konstitutiv aktive und ubiquitär exprimierten Serin/Threonin Kinase. MARCM induzierten *ck1α* – Verlustmutanten zeigen eine ähnliche Störung des Aktin-Netzwerkes wie bei einer WAVE Herrunterregulierung. Das stellt sich in einer reduizerte Lamellipodienbildung und beeinträchtigten Migration der Hämozyten dar. Rettungsexperimente mit einer Phosphorylierungs-defizienten WAVE-Mutante zeigen deutlich die Bedeutung der CK1α Phosphorylierung für die WAVE-Stabilität. Ohne diese Phosphorylierung wird das WAVE Protein proteasomal abgebaut, ein Prozess, der dem kontrollierten Abbau von Proteinen in der Zelle, z.B. bei fehlerhaften Proteinfaltung, dient. Diese Ergebnisse deuten darauf hin, dass WAVE eine basale Phosphorylierung durch CK1α aufweist und dadurch sowohl der frühzeitige Abbau verhindert als auch die Funktionalität *in vivo* geschützt ist.

Table of Contents

List of Figures

List of Tables

List of used abbreviations

µm	micrometer
A	alanine
Abi	Abelson interactor
Abl	Abelson tyrosine kinase
ADP	adenosine diphosphate
AMP	antimicrobial peptide
Antp	Antennapedia
APF	after pupae formation
Arp	actin-related protein
ATP	adenosine triphosphate
Atxn7	Ataxin-7
B	lipid-binding basic region
BMP	Bone morphogenetic protein
ci	cubitus interruptus
CK1	casein kinase 1
CK2	casein kinase 2
Cobl	Cordon bleu
Col	Collier
CRIB	Cdc42-Rac interactive binding domain
CRL	cullin-RING ligase
crq	croquemort
Cul	cullin
CYRI	CYFIP-related Rac Interactor
CysCs	cyst stem cell
CZ	cortical zone
D	aspartate
Da	Dalton
DBT	doubletime
DIF	Dorsal-related immunity factor
Drs	Drosomycin
Drs-5	Drosomycin-like 5
DUBm	deubiquitylating module
DV	dorsal vessel
E	glutamate
E1	ubiquitin-activating enzyme
E2	ubiquitin-transferring enzyme
E3	ubiquitin ligase
ECM	extracellular matrix
EGFR	epidermal growth factor receptor
en	engrailed
Ena	Enabled
ER	endoplasmatic reticulum
ERGIC	ER-Golgi intermediate compartment
F-actin	filamentous actin
FH	formin homology domain
FOG	friend of GATA
FSC	follicle stem cells
G-actin	globular actin
GBD	GTPase binding domain

gcm	glial cell missing
gcm2	glial cell missing 2
GFP	green fluorescent protein
GSC	germline stem cell
G-TRACE	Gal4 technique for real-time and clonal expression
GUKh	GUK-holder
HECT	homologues to the E6AP carboxyl terminus
Hh	Hedgehog
hml	Hemolectin
Hnt	Hindsight
Hox	homeobox
HPs	hematopoietic pockets
HS1	hematopoietic lineage cell specific protein 1
HSPC300	haematopoietic stem/progenitor cell protein 300
HSPCs	hematopoietic stem and progenitor cells
i.e.	id est, that is
Imd	immune deficiency
IZ	intermediate zone
JAK	Janus kinase
JMY	junction-mediating regulatory protein
JNK	Jun N-terminal kinase
K	lysin
kn	knot
LLS	lamellipodia like structure
Lmod	Leiomodin
Lsp	Larval serum protein
Lz	Lozenge
msn	misshapen
mys	myospheroid
MZ	medullary zone
(N-) WASP	(neural-) Wiskott-Aldrich syndrome protein
NF-κB	nuclear factor κ B
NHSL1	Nance-Horan Syndrome-like 1 protein
NimC4	Nimrod C4
nm	nanometer
NPF	nucleation promoting factor
NuRD	Nucleosome Remodeling and Deacetylation
OXPHOS	oxidative phosphorylation
PIP_3	Phosphatidylinositol-3,4,5-triphosphat
PKA	Protein kinase A
PL	Plasmatocyte
Pnr	pannier
PO	phenoloxidase
PRD	C-terminal Proline-rich domain
proPO/PPO	prophenoloxidase
PSC	posterior signaling center
Pxn	Peroxidasin
RBR	RING-between-RING
Rho GTPase	Rho family of small guanosine triphosphatases
RING	Really Interesting New Gene
ROCK	Rho-associated kinase

ROS	reactive oxygen species
rpr	reaper
S	serine
SCAR	suppressor of cAR
scRNA	single-cell RNA sequencing
smo	smoothened
Sra1	specifically Rac1-associated protein 1
Srp	Serpent
STAT	signal transducer and activator of transcription
T	threonine
Tep	Thioester-containing protein
TGN	trans-Golgi network
Tir	intracellular Toll/Interleukin-1 receptor
TLR	Toll-like Receptor
Ub	ubiquitin
Ubx	Ultrabithorax
Ush	u-shaped
VASP	Vasodilator-stimulated phosphoprotein
VCA	verprolin central acidic
WAHD	WASH-homology domain
WAS	Wiskott-Aldrich syndrome
WASH	WASP and SCAR homolog
WAVE	WASP-family verprolin homolog
WH	WASp-homology
WHAMM	WASP homolog associated with actin, membranes, and microtubules
WRC	WAVE regulatory complex
α-2MS	alpha2-macroglobulin

1. Introduction

1.1. *Drosophila* immune system is closely related to the human innate immune system

The innate immune system is the first line of defense in most multicellular organisms, including humans and the fruit fly *Drosophila melanogaster*. It is a collection of cells and molecules that recognize and respond to various pathogens, including bacteria, viruses, fungi, and parasites. Unlike the adaptive immune system, which takes several days to develop a response to a specific pathogen, the innate immune system provides immediate defense against infection (Janeway & Medzhitov, 2002).

In humans, the innate immune system can be divided into two major components: the humoral immune response and the cellular immune response (Medzhitov & Janeway, 2000). Both components work together in a coordinated manner to provide the innate immune response.

The cellular immune response involves the activation and migration of immune cells, such as phagocytes, natural killer cells, and dendritic cells, to the site of infection. These cells recognize and engulf invading pathogens and secrete cytokines and chemokines to activate other immune cells to the site of infection. The humoral immune response involves producing and releasing of soluble factors such as complement proteins, cytokines, and antimicrobial peptides (AMPs) that circulate in the blood and lymphatic system. These factors act to neutralize pathogens directly or activate other immune system cells to do so (Iwasaki & Medzhitov, 2015; Janeway & Medzhitov, 2002; Medzhitov, 2007).

The *Drosophila* blood system closely resembles the myeloid blood cell system in mammals developmentally and functionally (Gold & Brückner, 2015, 2016; Hartenstein, 2006). It contributes to the innate immune response, tissue integrity, wound healing, and various forms of stress responses (Gold & Brückner, 2014). But unlike mammals, *Drosophila* has an open circulatory system in which the heart pumps blood, the so-called hemolymph, into the body cavity circulating all organs. However, it is worth mentioning that the molecular pathways are highly conserved besides the differences in tissue types (Bergman et al., 2017; Buchon et al., 2014). The development of the innate

immune system in both humans and *Drosophila* is closely linked to hematopoiesis, the process by which blood cells are produced. In both species, hematopoiesis occurs in specialized tissues, such as the bone marrow in humans and the lymph gland in *Drosophila*. The hematopoietic process is regulated by various signaling pathways and transcription factors that control the differentiation of blood cell progenitors into mature cell types (Banerjee et al., 2019; Evans et al., 2014; Gold & Brückner, 2014). Hematopoiesis will be introduced in more detail in a later chapter.

Similar to mammals, the *Drosophila* immune system can be divided into humoral and cellular components. The humoral immune response involves the production and release of effector molecules, such as AMPs, into the hemolymph, and directly kill or inhibit the growth of invading pathogens (Bergman et al., 2017; Vlisidou & Wood, 2015).

1.2. AMPs are essential in the humoral immune response

AMPs are an essential component of the humoral immune response. They play a critical role in the early stages of the immune response by providing the first line of defense against invading pathogens. These peptides are typically small, cationic, and amphipathic, allowing them to target and disrupt the negatively charged cell membrane of bacterial, viral, and fungal pathogens (Joo et al., 2016). AMPs are produced in various tissues like the trachea, midgut, oviduct, spermatheca, ganglia, and a subpopulation of *Drosophila* immune cells (D. Ferrandon, 1998; Tzou et al., 2000). Human AMPs can be classified into several families, such as defensins, cathelicidins, and histatins, each with different modes of action and specifies for different pathogens. In contrast, *Drosophila* AMPs are more limited in their diversity, with seven well-characterized families, such as the drosomycin and attacin families. Corresponding to their target, AMPs are further classified into three categories: response to fungi, gram-positive bacteria, and gram-negative bacteria (Hanson et al., 2019; Hanson & Lemaitre, 2020; Martínez et al., 2020; Tzou et al., 2000). The production and secretion of AMPs are regulated by nuclear factor κ B (NF-κB)-related Toll and immune deficiency (Imd) pathways in *Drosophila*, which is described as the hallmark of humoral immunity. In addition, several transcription

factors, including Relish, Dif, and Dorsal, are involved in regulating AMP gene expression (Hanson et al., 2019; Younes et al., 2020).

1.3. *Drosophila* Toll signaling pathway

Both Toll and Imd signaling pathways play essential roles in the humoral immune response in *Drosophila*, and their relative importance may depend on the specific pathogen being encountered. The Toll pathway is more important for defense against fungi and gram-positive bacteria, while the Imd pathway is more important for defense against gram-negative bacteria (Lemaitre & Hoffmann, 2007). However, the relative importance of these pathways can also vary depending on the tissue and cell type involved in the immune response, as well as the developmental stage of the fly. Both play crucial roles in the immune response, but regarding the results of this work, the introduction will focus on the Toll pathway.

The Toll signaling pathway is an evolutionarily conserved signaling pathway that plays a critical role in humans' and *Drosophila's* innate immune response. The pathway was first identified in *Drosophila* and was subsequently found to have analogous components in humans. Dysregulation of the pathway has been implicated in various diseases, including infections, autoimmune disorders, and cancer (Valanne et al., 2011; Shichao Yu et al., 2022). With the advances in single-cell sequencing, more information on the relationship between immune cell subpopulation and the immune signaling pathways will be provided.

In humans, Toll-like receptors (TLRs) are located on the surface of immune cells and recognize specific ligands associated with pathogens, such as bacterial lipopolysaccharides or viral nucleic acids. TLR binding triggers a signaling cascade that activates NF-κB and other transcription factors, which regulate gene expression in the immune response. In *Drosophila*, the Toll receptors play a similar role in recognizing and responding to pathogens. The Toll signaling pathway is mainly activated by fungi and gram-positive bacteria. Extracellular pathogen recognition leads to a serine protease cascade which ultimately ends in the cleavage of the ligand Spätzle. The Toll signaling pathway is activated by the binding of Spätzle to the Toll receptor on the surface of cells. This binding triggers a cascade of events that leads to the activation and translocation of the transcription factor Dorsal or Dorsal-related immunity factor

(DIF) into the nucleus, where it regulates the expression of genes involved in the immune response, including AMPs (Bergman et al., 2017; Lemaitre & Hoffmann, 2007; Valanne et al., 2011). In the cellular immune response, the Toll signaling pathway has been described to be involved in the development, lamellocyte differentiation, and encapsulation (Shichao Yu et al., 2022).

1.4. Cellular immune response in Drosophila

Cellular response in *Drosophila* is far less understood. The cellular immune response in *Drosophila* involves activating and migrating of the mammalian equivalent of blood cells, collectively called hemocytes, to the site of infection. They engulf and eliminate invading pathogens and activate other immune system cells to respond to the infection (Bergman et al., 2017; Gold & Brückner, 2015; Vlisidou & Wood, 2015).

Drosophila hemocytes can be subdivided into three groups: (1) plasmatocytes, which make up about 95% of all hemocytes, (2) crystal cells; and (3) lamellocytes (Rizki, 1962). The next chapter will detail the difference between those cell types. In short, crystal cells mainly function in the melanization of wounds, which is a form of encapsulation that helps to isolate and kill invading pathogens. Lamellocytes usually are not present in healthy flies but are dramatically induced upon infestation by parasitoid wasps. Plasmatocytes are functionally closely related to vertebrate bone-marrow-derived macrophages (Gold & Brückner, 2016). They are the main phagocytic cells in *Drosophila* and play a similar role to human macrophages. Remarkably, the differentiation process into such mature cell types does not require the involvement of stem cells, but, unlike in mammals, they are derived from precursor prohemocytes. Additionally, vertebrate blood cell types are more varied, whose functions in *Drosophila* are resembled by only few terminally differentiated cell types.

1.5. Functions and characteristics of plasmatocytes, crystal cells, and lamellocytes

Hemocytes have been traditionally classified into three main effector cell types based on their morphology: plasmatocytes, crystal cells, and lamellocytes (Rizki, 1962). But with the advances of single-cell RNA sequencing (scRNA), hemocyte's diverse gene expression patterns at the single-cell level were investigated. This technique enables the identification and classification of

different hemocyte classes and subtypes based on their transcriptional profiles. Thus, recent studies confirmed the existence of different effector cell types as initially described. In addition, many marker genes have been discovered, which are characteristic for each cell type and expand the possibilities for cell lineage research (Cattenoz et al., 2020; Cho et al., 2020; Fu et al., 2020; Tattikota et al., 2020).

90-95% of the total hemocytes are comprised by plasmatocytes, the main phagocytic cells in *Drosophila*, and fulfill a similar role to human macrophages. The primary immune functions are the phagocytosis of pathogens, the production of AMPs in response to bacterial challenge and the first stages of encapsulation of large parasitic invaders (Baer et al., 2010; Basset et al., 2000; Dominique Ferrandon et al., 2004; Gold & Brückner, 2015; Sears et al., 2003; Yasothornsrikul et al., 1997). Without infection, they fulfill an essential role in development, such as embryonic morphogenesis and tissue homeostasis. For instance, plasmatocytes remove large amounts of debris that result from the remodeling activities associated with metamorphosis (Lanot et al., 2001; Regan et al., 2013). Additionally, in the development from embryo to larvae, many genes for different extracellular matrix (ECM) molecules are upregulated (Yasothornsrikul et al., 1997) and secreted by plasmatocytes (Wood & Jacinto, 2007; Yasothornsrikul et al., 1997). Thus, circulating plasmatocytes are the main source for delivering ECM molecules such as papilin, laminin, and collagen IV to develop basement membranes, covering all cell surfaces that are in contact with the hemolymph (Fessler & Fessler, 1989). In later stages, this membrane component deposition is essential for organogenesis and morphogenesis (Matsubayashi et al., 2017; Tepass et al., 1994). Following tissue damage or injury, plasmatocytes are recruited to the site of injury, where they phagocytose debris and initiate tissue repair.

The detailed mechanism of how plasmatocytes detect and eliminate both apoptotic cells and invading particles has been intensely studied. This process is important for maintaining the organism’s overall health by preventing the accumulation of pathogens in the hemolymph. In general, the cell-surface proteins involved are Croquemort (crq), NimC4, Draper, and Eater, which also serve as a marker for mature plasmatocytes (Bretscher et al., 2015; Franc et

al., 1996; Kocks et al., 2005; Kurucz, Márkus, et al., 2007; Kurucz, Váczi, et al., 2007; Nelson et al., 1994). Each protein recognizes and binds to apoptotic cells or pathogens, leading to their internalization and degradation within the plasmatocytes. Moreover, depletion experiments of *crq* revealed that plasmatocytes are indispensable for both removing apoptotic cells during embryogenesis and cellular debris during pupal development (Charroux & Royet, 2009; Defaye et al., 2009; Guillou et al., 2016).

Crystal cells are a specialized type of blood cells that are involved in the innate immune response. They represent 2-5% of the total hemocyte population (mainly in the larval stages) and owe their name to their crystalline inclusions (Kurucz, Váczi, et al., 2007; Rizki, 1962). Their function is more relevant during embryogenesis and in larvae than in the adult fly, where they are present to a minor degree (Ghosh et al., 2015; Hultmark & Andó, 2022). Interestingly, the head mesoderm already contains a cluster of 20-30 crystal cells during stages 10-12 of embryogenesis (Lebestky et al., 2000) (Figure 1, Figure 2, Figure 3)

Crystal cells facilitate wound healing and are active in the immune response. They play a crucial role in the melanization process by releasing prophenoloxidases (proPO/PPO) activating enzymes and related factors into the hemolymph. The *Drosophila* genome contains three genes encoding PPOs. Two of them, PPO1 and PPO2, are found in the crystal cells and the hemolymph at the larval stage. Once a pathogen is recognized and the PPOs are released, a complex serine protease cascade known as the proPO activation system is activated. This ultimately results in the cleavage of the zymogen prophenoloxidase to its active form, phenoloxidase (PO). Once the PO enzyme is activated, it catalyzes the oxidation of phenolic compounds, such as catechols, to quinones, which spontaneously polymerize to form melanin. The melanin is deposited on the surface of the invading microorganisms or foreign particles, forming a dark insoluble coating that encapsulates and immobilizes them, preventing their spread and promoting their clearance by phagocytic cells (Binggeli et al., 2014; Lemaitre & Hoffmann, 2007). Those phenoloxidase and melanization reactions bridge the humoral and cellular arms of the innate immune response. The proteins PPO1 and PPO2 are well-characterized for their activity in crystal cells and, together with Lz and

pebbled/hindsight (Hnt), are used as marker genes (Jung et al., 2005; Lebestky et al., 2000; Tokusumi et al., 2009). Remarkably PPOs are incorporated in crystalline inclusions, which in turn define the specific cell morphology of crystal cells (Kurucz, Váczi, et al., 2007).

Commonly not seen in healthy flies are the larger blood cells called lamellocytes. Besides their large size, they are distinguished from other blood cells by their irregular morphology and the presence of large lamellae or flat, sheet-like extensions of their plasma membrane, which allows them to spread out and adhere to the surface of a foreign capsule (Banerjee et al., 2019; Shresthaa & Gateff, 1982). They can be recognized by the expression of the surface protein Atilla and ßPS-integrin Myospheriod (mys) and are mainly required to neutralize invading pathogens too large to be phagocytosed, for instance for the encapsulation of parasite eggs that are injected into larvae by a parasitic wasp (Anderl et al., 2016; Honti et al., 2009; Irving et al., 2005; Kurucz, Váczi, et al., 2007). Upon infection, lamellocyte differentiation starts within the first 2-10 hours. Even though lamellocytes are present in larvae and pupae, in adult flies, it appears that they do no longer exist (Boulet et al., 2021).

Unlike mammals, where such comparable giant cells arise through the fusion of macrophages (McNally & Anderson, 2011), in *Drosophila,* there are three known and described pathways of lamellocyte hematopoiesis, which have been studied in the context of infestation by wasp eggs into the larvae (Anderl et al., 2016; Banerjee et al., 2019). In general, differentiation is regulated by a variety of signaling pathways, including the Janus kinase (JAK)/signal transducer and activator of transcription (STAT), Jun N-terminal kinase (JNK), and Toll pathway. Activation of these pathways leads to gene expression changes, producing the transcription factors that induce lamellocyte differentiation (Krzemień et al., 2007; Tokusumi et al., 2009; Zettervall et al., 2004). When a parasitic wasp egg is detected in the *Drosophila* larva, it triggers a systemic immune response. Host defense starts as a cascade of events by which the host attempts to neutralize the wasp egg through encapsulation (Labrosse et al., 2005; Letourneau et al., 2016; Nappi & Carton, 2001). In the first 2-10 hours after infestation into the larvae, spreading of the already existing sessile plasmatocytes from the hematopoietic pockets is initiated. They bind the wasp

egg, which leads to the formation of a multicellular structure called the melanotic capsule. This is followed by either recruitment of the already available low number of lamellocytes or transdifferentiation of existing plasmatocytes into lamellocytes (Russo et al., 1996). Noticeably, those cells can be recognized by expression of both, the plasmatocyte-specific gene *eater* and the lamellocyte surface protein Atilla (Anderl et al., 2016; Evans et al., 2014). About 10 hours after the infestation, the progenitor cells within the lymph gland differentiate (Crozatier et al., 2004), the number of circulating hemocytes increases (Russo et al., 2001), and the lymph gland disintegrates already in the 3rd instar larva (around 20 hours post-parasitism) (Eleftherianos et al., 2021; Letourneau et al., 2016). Subsequently, the number of lamellocytes dramatically increases (Lanot et al., 2001; Louradour et al., 2017). Those lamellocytes are distinguishable from these lamellocytes, which transdifferentiate earlier from plasmatocytes, by a missing expression of *eater* (Anderl et al., 2016). Interestingly, the Posterior Signaling Centre (PSC) of the lymph gland fulfills an indispensable role in lamellocyte differentiation (Crozatier et al., 2004; Krzemień et al., 2007; Sinenko et al., 2012). This was first investigated by targeted expression of the pro-apoptotic gen *reaper* (*rpr*) in the PSC. Ablating PSC cells by targeted expression of *rpr* leads to a repression of lamellocyte differentiation. (Benmimoun et al., 2015). In this context, a critical factor is the reactive oxygen species (ROS) level. Upon wasp parasitation, the level of ROS dramatically increases in the PSC, which in turn activates the EGFR and Toll/NFκB pathways. Both act parallel to initiate lamellocyte differentiation of prohemocytes in the lymph gland. Thus, PSC cells contribute to the differentiation either by signaling to progenitors of the Lymph Gland or by providing signals to circulating blood cells (Benmimoun et al., 2015; Krzemień et al., 2007; Oyallon et al., 2016).

Correct timing of differentiation linked to the release of the lamellocytes into hemolymph occurs through a breakdown of the lymph gland´s basement membrane. This in turn is regulated by Toll/NFκB signaling (Louradour et al., 2017). Remarkably this dependency is restricted to the PSC.

Encapsulation of the foreign pathogen requires intracellular signaling for recruitment and cooperation of different immunocompetent hemocytes and for

adhesion and cell shape (L. Yang et al., 2021). As described above, the first step of encapsulation is the disposal of a protein layer on the surface of the parasite egg capsule made by extracellular matrix proteins. Lamellocytes are known to adhere to each other via septate junctions mediated by integrins to build a capsule. Integrins in turn can directly bind to ECM. This suggests an indispensable role for integrins in this process (Howell et al., 2012). Additionally, recent studies have demonstrated that Rac GTPases are critical regulators of the actin cytoskeleton during lamellocyte encapsulation. Specifically, Rac1 and Rac2 have been shown to be required for lamellocyte spreading and adhesion to the surface of the parasitic wasp egg, as well as for stabilizing the actin cytoskeleton. Localization of mys, an integrin that interacts with its ligand to cause hemocyte capsules to surround the wasp egg, to the lamellocyte periphery depends on Rac1. Rac2 is furthermore essential for integrin formation (Williams et al., 2005; Xavier & Williams, 2011).

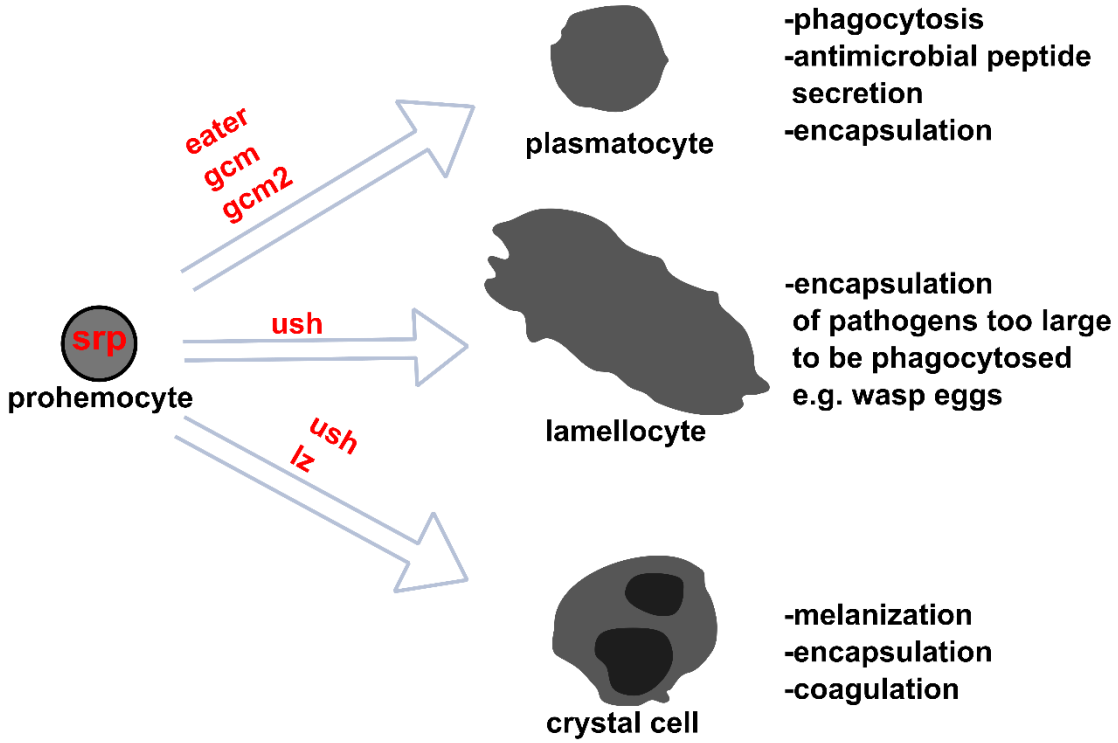

Figure 1 - Prohemocytes can differentiate into three different cell types regulated by distinct transcription factors. *Overview of the three different hemocyte subgroups of hemocytes. The GATA transcription factor Srp is the master regulator in early hemocyte specification and is already present in undifferentiated prohemocytes. In embryonic hematopoiesis, Srp regulates eater, gcm, and gcm2 for differentiation into plasmatocytes. Ush and Lz define crystal cell differentiation and are both regulated by srp. Crystal cells comprise 2 to 5 % of the larval hemocyte population. Normally are not seen in healthy flies are the lamellocytes. Ush regulates transdifferentiation. Note the different cell morphology.*

The GATA family of zinc transcription factors, which are highly conserved from yeast to mammals, play a fundamental role in early cell fate specification, differentiation, and proliferation (Evans et al., 2003). The master regulator is the GATA factor Serpent (Srp), especially in the early hemocyte specification. For example, Srp directly controls the expression of the gene pair *glial cell missing* (*gcm*) and *glial cell missing 2* (*gcm2*). They play a role in the terminal differentiation of functional plasmatocytes determined by their transcriptional targets (Alfonso & Jones, 2002; Vivancos, Roberto Bernardoni & Giangrande, 1997).

Another GATA transcription factor is Pannier (pnr), and there are the friend of GATA (FOG) multi-zinc finger protein U-shaped (Ush), and the RUNX domain

protein Lozenge (Lz) (Banerjee et al., 2019; Fossett et al., 2001; Fossett & Schulz, 2001; Lebestky et al., 2000). Ush and Lz are transcriptional cofactors regulated by Srp and define crystal cell production. From stage 8 of embryogenesis, Ush, represses crystal cell fate, whereas Lz promotes crystal cell development by interacting with Srp (Fossett et al., 2001; Lebestky et al., 2000) (Figure 1). Besides the regulation of hemocyte-specific genes, Ush targets metabolism-related as well as cell cycle regulator genes. Recently, it was shown that Ush interacts with the Nucleosome Remodeling and Deacetylation (NuRD) complex, which represses explicitly hemocyte-specific genes (Lenz et al., 2021). Noticeably, Ush is likewise known to interact with various GATA transcription factors to regulate various steps of hematopoiesis similar to its function in mammals (Fossett et al., 2003; Lebestky et al., 2000; Lenz et al., 2021). Thus, the interaction of Srp with Ush in *Drosophila* is similar to the vertebrate GATA:FOG interactions (Fossett et al., 2003; Tevosian et al., 1999).

Interestingly, Srp is also involved in lamellocytes differentiation together with the FOG homolog Ush (Gajewski et al., 2007) (Figure 1). Knockdown of Ush by RNAi makes it more likely to increase the number of lamellocytes. Additionally, overexpression of the *hop* gene, which encodes for the *Drosophila* JAK, leads to the induction of lamellocyte differentiation within the lymph gland. Thus, downregulation of the JAK-STAT signaling is required for the differentiation of lamellocytes in the lymph gland (Makki et al., 2010).

1.6. Hematopoiesis occurs spatially and temporally divided

Hematopoiesis is the process of blood cell formation that give rise to innate immune cells, which are critical for the defense against pathogens. It occurs in two waves, spatially and temporally divided and closely related to vertebrate primitive and definitive hematopoiesis (overview in Figure 2) (Crozatier & Meister, 2007; Evans et al., 2003). In the first wave, hemocytes derive from the embryonic head mesoderm, whereas the second wave occurs post-embryonically in the lymph gland of larvae (Vlisidou & Wood, 2015).

The lymph gland is a hematopoietic organ structurally divided into multiple lobes and proliferates during the first half of larval development. Those lobes flank the Dorsal Vessel (DV), the cardio-vascular system that originates from the embryo's thoracic mesoderm, posterior to the brain (Mandal et al., 2004). The highest level of hematopoietic activity can be found in the primary lobes, which derivate from the embryonic cardiogenic mesoderm (Mandal et al., 2004). The primary lobes can be further divided into zones based on the differential expression of various marker genes with distinct functions. The Medullary Zone (MZ) is the most inward zone and closest to the DV, then the Cortical Zone (CZ) with an Intermediate Zone (IZ) in between and the Posterior Signaling Center (PSC), which acts as a niche to regulate progenitor maintenance (structural overview Figure 3) (Grigorian et al., 2011; Mandal et al., 2004). The PSC produces signaling molecules, such as cytokines and growth factors, that regulate the differentiation and proliferation of blood progenitors in the adjacent anterior lobes. The differentiation of blood cells in the primary lobes is regulated by a complex network of signaling pathways and transcription factors, including the JAK-STAT pathway, Notch signaling, and GATA factors. The lymph gland undergoes a dramatic remodeling during metamorphosis, leading to the generation of adult blood cells necessary for the fly´s survival. The lymph gland provides a powerful genetic model system for studying the molecular mechanisms underlying blood cell development, differentiation, and homeostasis. Additionally, the ontology of the lymph gland can be described as analogous to the aorta-gonad-mesonephros region of vertebrates (Evans et al., 2003).

As mentioned before, similarly to mammals, hematopoiesis in *Drosophila* starts early in embryonic development and takes place in immune compartments in multiple waves. A loose mass of cells is initially formed in the head of the embryo (Grigorian et al., 2011). There, the first specification of embryonic hemocytes appears in stage 5-embryos and is characterized by the expression of the GATA factor Srp (Holz et al., 2003). Srp is one of the five *Drosophila* GATA factor homologs and represents a conserved transcription factor involved in the blood-lineage specification (Rehorn et al., 1996). *Drosophila* hemocyte precursors expressing *srp* start to differentiate from this state on to form the first subsets of plasmatocytes and crystal cell populations (Banerjee et al., 2019).

In stage 12 of *Drosophila* embryogenesis, a population of about 700 prohemocytes begins to spread throughout the embryo and differentiate. This population resembles the first plasmatocytes characterized by relatively large, actin-rich filopodia and lamellipodia structures (Tepass et al., 1994; Wood et al., 2006). Those cells exhibit phagocytosis to clear the developing tissue of apoptotic debris (Tepass et al., 1994).

In the development of the larval states, hemocytes are found either circulating in the hemolymph or attached to the body walls in sessile pools called hematopoietic pockets (HPs) (Makhijani et al., 2011; Petraki et al., 2015). Those HPs are located between the epidermis and muscle layers of the larval body wall and can disperse through external mechanical disruption but rearrange within 30-60 minutes. Hemocytes in those pockets are named self-renewing “primitive” or “tissue macrophages” (Gold & Brückner, 2014) and have a high rate of self-renewal, expanding the number of 30 cells in the 1st larval instar to around 10000 in the late 3rd instar (Gold & Brückner, 2015). In addition, upon different immune challenges, e.g. through pathogens, tissue macrophages can be released into the circulation on demand and are able to proliferate or differentiate into lamellocytes or crystal cells (Makhijani et al., 2011).

An important fact to keep in mind is that the dispersal and activation of sessile hemocytes upon pupariation are induced by ecdysone signaling. That in turn leads to tissue remodeling during metamorphosis (Regan et al., 2013).

The second lineage of *Drosophila* hemocytes post-embryonically derives from the lymph gland and resembles vertebrates’ definitive hematopoiesis (Evans et al., 2003; Gold & Brückner, 2014). The MZ contains undifferentiated progenitor cells with the potential to differentiate into all three different mature hemocyte types (Figure 2, Figure 3) (Jung et al., 2005).

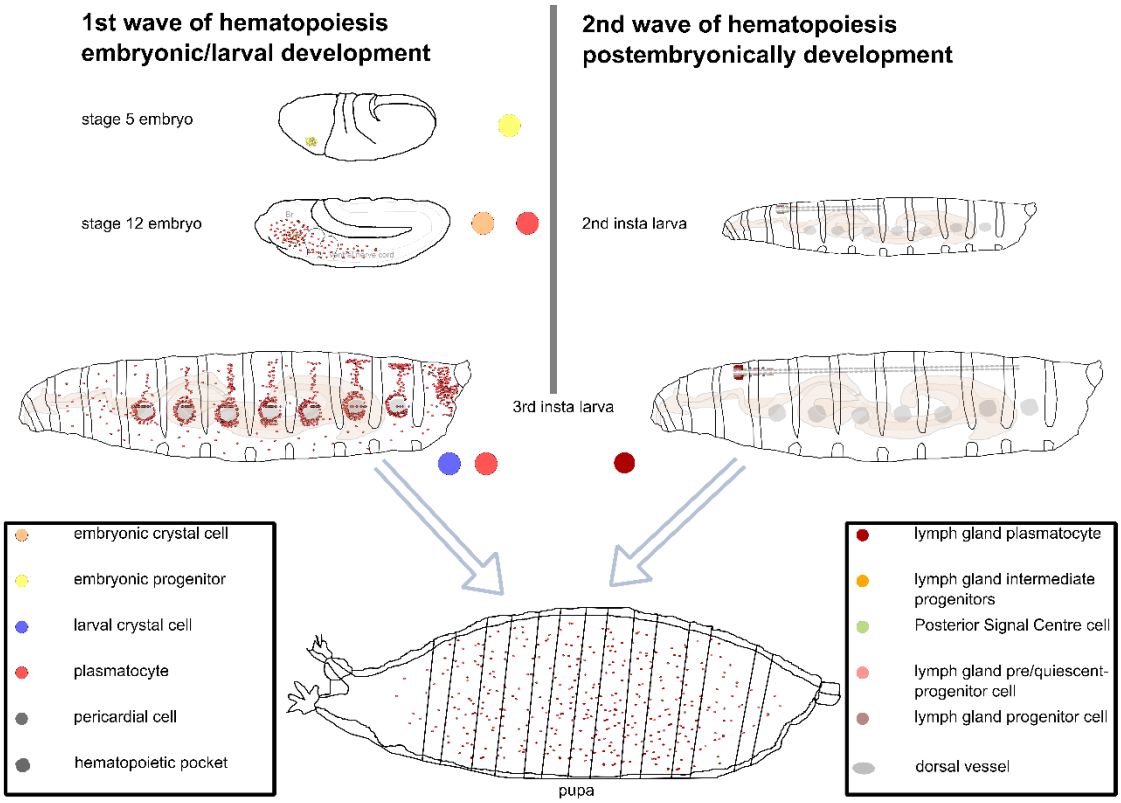

Figure 2 – Drosophila hematopoiesis can be spatiotemporal divided into two waves. *Left panel shows the first wave of hematopoiesis, which begins in the head mesoderm of stage 5 embryo. There embryonic progenitors (yellow) start to differentiate into plasmatocytes and crystal cells (Topaz) and spread out in the embryo. In 3rd instar larva, mature plasmatocytes are located around hematopoietic pockets (dark grey) where they can be released on demand. The right panel shows the second wave of hematopoiesis, which begins with the development of the lymph gland in the 2nd instar larva state. The lymph gland of the 3rd instar larva can be divided into different zones where differentiation of plasmatocytes occurs. For more details, see Figure 3. After lymph gland disintegration, the total hemocyte population is merged in the pupa.*

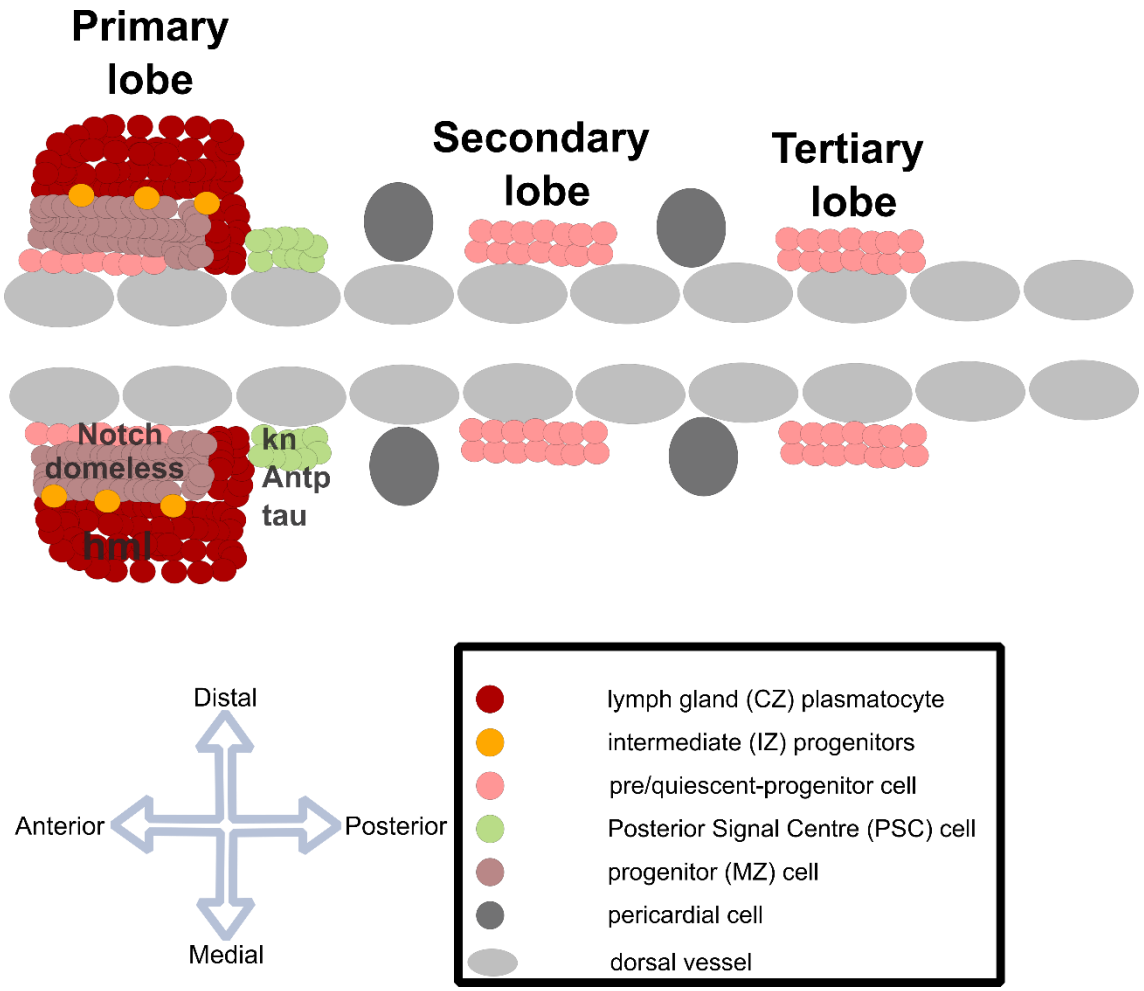

Figure 3 - The lymph gland is the place of the 2nd wave of Drosophila hematopoiesis. *Schematic overview of the lobes of the lymph gland along the dorsal vessel (grey). Most anterior is the primary lobe, which is the largest lobe and is divided into different zones. Those are the Medullar Zone (MZ) with high domeless expression, an Intermediate Zone (IZ), the Cortical Zone (CZ) with high hml expression, and the niche-like Posterior Signal Centre (PSC) with defined by kn, tau, and Antp expression. Plasmatocytes develop from a quiescent-progenitor state to a progenitor state in the MZ. Cells of the IZ represent cells that express both progenitor and mature plasmatocyte markers. Cells of the CZ are mature plasmatocytes that contribute later to the total population of plasmatocytes in the hemolymph. The PSC acts as a niche and maintains the hematopoiesis by signaling to the MZ. The posterior lobes along the dorsal vessel are smaller, consisting of quiescent-progenitor cells, and remain undifferentiated. The posterior lobes are separated by pericardial cells.*

As development proceeds from the late second instar, distinct separation of the CZ appears, and maturation of hemocytes continues until they finally emerge (Jung et al., 2005). A dynamic interplay and regulation exist between the MZ and CZ during development. In the early larval instars, the proliferation state in the MZ is high, but then it slows down dramatically. At the same time, the CZ maintains a high proliferation rate throughout the third instar to expand the

maturating population. This regulation step controls the MZ cells to remain multipotent and undifferentiated. Although it has been shown that the IZ locates between the MZ and CZ, a clear function has not been resolved so far (Jung et al., 2005; Mandal et al., 2004, 2007).

Differentiation of hemocytes within the lymph gland terminates by 12h after puparium formation (APF) with the disintegration of the lymph gland and subsequently releasing of the blood cells into the hemolymph (Grigorian et al., 2011; Holz et al., 2003).

Recently, a lot of effort has been put into the research on the PSC, which comprises a small cluster of about 30-40 cells located at the medio-posterior side of the lymph gland (Figure 3) (Krzemień et al., 2007). Primary markers of the PSC are the homeobox (Hox) protein Antennapedia (Antp), an autonomous determinant of PSC cells, and the *Drosophila* early B cell factor Collier (Col, also known as knot) (Benmimoun et al., 2015; Koranteng et al., 2022; Krzemień et al., 2007). Recent investigations also revealed that *kn* expression in the PSC is required for controlling PSC fate and cell number (Pennetier et al., 2012). Additionally, *kn* is expressed in a low number in the MZ, preventing prohemocytes from premature differentiation (Benmimoun et al., 2015). The expression of *kn* in the posterior lobes was recently investigated and will be introduced in the next chapter. A signature of PSC cells is the extension of numerous filopodia that mediate signaling between the PSC and prohemocytes in the MZ. Various signaling factors, including Hedgehog (Hh) signals, are secreted by PSC cells and transferred to progenitor cells by filopodia structures which enable direct cellular contact between PSC cells and MZ progenitors (Krzemień et al., 2007; Mandal et al., 2007). This signaling by the PSC cells into the MZ maintains hemocyte progenitors in a quiescent state, thereby regulating differentiation (Krzemień et al., 2007). Worth to notice is that the Ush/dNuRD complex represses the Hh enhancer activity in cells of the MZ and CZ and keeps *hh* expression restricted to the PSC (Lenz et al., 2021). Conclusively, the PSC cells significantly influence the fate of the MZ cells (Benmimoun et al., 2015; Crozatier et al., 2004; Krzemień et al., 2007; Mandal et al., 2007; Pennetier et al., 2012; Tokusumi et al., 2009).

Conclusively, the lymph gland is the primary site of hematopoiesis in *Drosophila* larvae. Prohemocytes differentiate into various blood cell lineages and then migrate out of the lymph gland into circulation to carry out their respective functions. Of further notice is that blood cells from the secondary wave of hematopoiesis are most important for immunity, similar to those cells from definitive hematopoiesis in vertebrates (Evans et al., 2003).

One reason most blood cells are produced in the lymph gland is that it provides a highly controlled and regulated environment for hematopoiesis. The lymph gland niche provides various signals and factors that regulate the proliferation and differentiation of prohemocytes, ensuring that the proper balance of blood cell types is maintained. Another reason the lymph gland is the primary site of hematopoiesis is that it provides a mechanism for the rapid production of blood cells, such as during an infection or injury; the lymph gland can rapidly increase its output of blood cells to meet the demand. In addition, the lymph gland provides a mechanism for immune surveillance and defense. The lymph gland contains the three different blood cells that are involved in the innate immune response, as described earlier. These cells quickly recognize and respond to pathogens, helping to prevent infections and protect the organism. Further research will be needed to fully understand the diversity and function of these specialized blood cell subtypes and how they contribute to the overall immune response in *Drosophila*. Single-cell sequencing as described in this work will help to expand the knowledge of different development stages of *Drosophila* immune system. (Cattenoz et al., 2021; Cho et al., 2020; Evans et al., 2003; Lemaitre & Hoffmann, 2007; Tattikota et al., 2020).

1.7. Heterogeneity of the posterior lobes of the *Drosophila* Lymph Gland: An overview of current knowledge

In addition to the anterior lobes of the lymph gland, the posterior lobes are located along the dorsal vessel (Figure 3) (Banerjee et al., 2019; Kanwal et al., 2021; Rodrigues et al., 2021). Cells of these lobes were neither analyzed in detail in recent research about hematopoiesis nor subjected to scRNA-seq experiments (Benmimoun et al., 2015; Kanwal et al., 2021; Rodrigues et al., 2021). A contribution to the hematopoiesis has not been described so far, and the cells of the posterior lobes stay as undifferentiated progenitors with no

expression of known marker genes for mature hemocytes like *hemolectin* (*hml*), P1/NimC1 or *Pxn*, but high expression levels of progenitor marker like *Tep4*, *E-cad* and *dome* until dispersal. This leads to the suggestion that these cells dissociate as incompletely differentiated hemocytes (Grigorian et al., 2011; Rodrigues et al., 2021). To further outline the heterogeneity, common markers of the PSC Antp and Hh are not present in the posterior lobes, but *kn* is expressed at least in one of the lobes (Rodrigues et al., 2021). Furthermore, Ghosh and colleagues proposed that the posterior lobes also contribute to the adult population of hemocytes (Ghosh et al., 2015). Because cells of the posterior lobes persist until 10 to 15 hours APF in a progenitor state and the lobes disintegrate later than the anterior lobes; their contribution might be as a long-term pool of progenitors.

As mentioned earlier, expression of the Hox gene *Antp* in the primary lobes depends on *kn* expression (Mandal et al., 2007). However, Antp is absent in the posterior lobes. Instead, recently, the Hox gene Ultrabithorax (Ubx) was found to be strongly expressed in the posterior lobes (Kanwal et al., 2021). Consequently, it was proposed that the dependency on Antp for maintaining the hematopoietic niche is recapitulated in the posterior lobes by Ubx. Comparable to the PSC, the Ubx-Kn interplay defines the progenitor pool (Kanwal et al., 2021).

1.8. Cytoskeleton dynamics of Hemocytes

The routine immune and phagocytic functions of hemocytes rely on their ability to migrate. Cells utilize the dynamic formation of filamentous actin filaments (F-actin) to rapidly adjust the actin cytoskeleton to move and communicate. (Blanchoin et al., 2014). The dense F-actin-based branched and crosslinked network, which forms a structure called lamellipodia within the actin cytoskeleton, pushes a cell forward during migration. The diversity and flexibility for the cellular functions are furthermore achieved through the additional possibility of forming parallel actin filaments called filopodia, for instance, for phagocytosis and long-range cell-cell communication (Figure 4). Additionally, anti-parallel filaments called stress fibers are made of F-actin and span the cell body.

In addition, microtubules provide structural support for the actin cytoskeleton, whereby both, F-actin and microtubules, influence and stabilize each other, particularly in their structure and function (Akhshi et al., 2014). To maintain an appropriate balance of the essential processes, actin filament assembly must be regulated accurately in time and space (Blanchoin et al., 2014).

Figure 4 - Organization of the actin cytoskeleton (see next page). *(A) Dynamic rearrangement of F-actin structures enables a rapid adaption to environmental immune challenges. The lamellipodia and filopodia are the driving structures of motility and phagocytosis. Reprinted and modified from (Rottner et al., 2021), with permission from Elsevier. (B-D) Parallel actin filaments create filopodia. (B) Platinum-replica electron microscopy of the cytoskeleton at the leading edge. Filopodia extension is made of actin filament bundles (cyan) spanning the dense actin filament network of the lamellipodia (brown). Sometimes they get through to the more stable region behind the lamellipodia named lamella (purple). Scale bar is 1 µm. (C) Enlarged box region from (B) shows long parallel actin filaments (cyan) extending beyond the leading edge. A complex of regulatory proteins (pink) is located at the filopodia tip. (D) Branched actin network. Platinum-replica electron microscopy of the cytoskeleton at the leading edge shows the actin filament organization in the lamellipodium. A region outlined by the yellow box is enlarged in the yellow-framed inset to highlight branched actin filaments. Scale bar is 500 nm. (B-D) Reprinted from* (T. Svitkina, 2018) *by permission of Cold Spring Harbor Laboratory Press.*

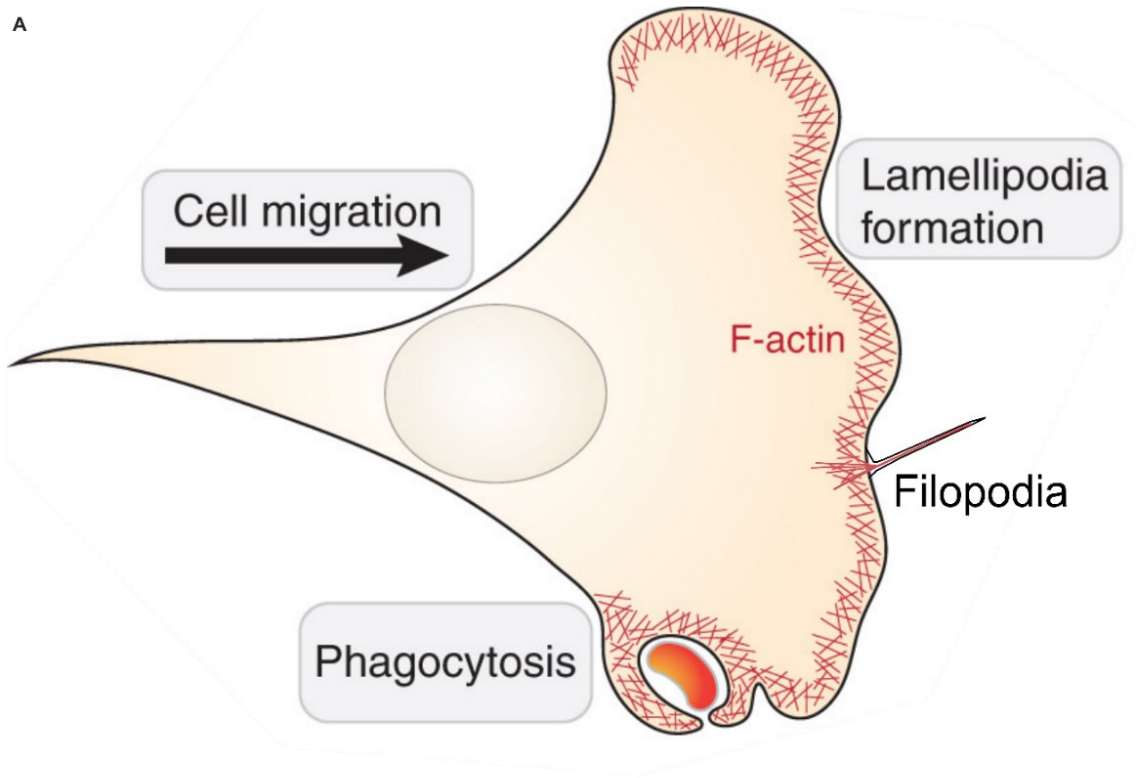
A
Cell migration
Lamellipodia formation
F-actin
Filopodia
Phagocytosis

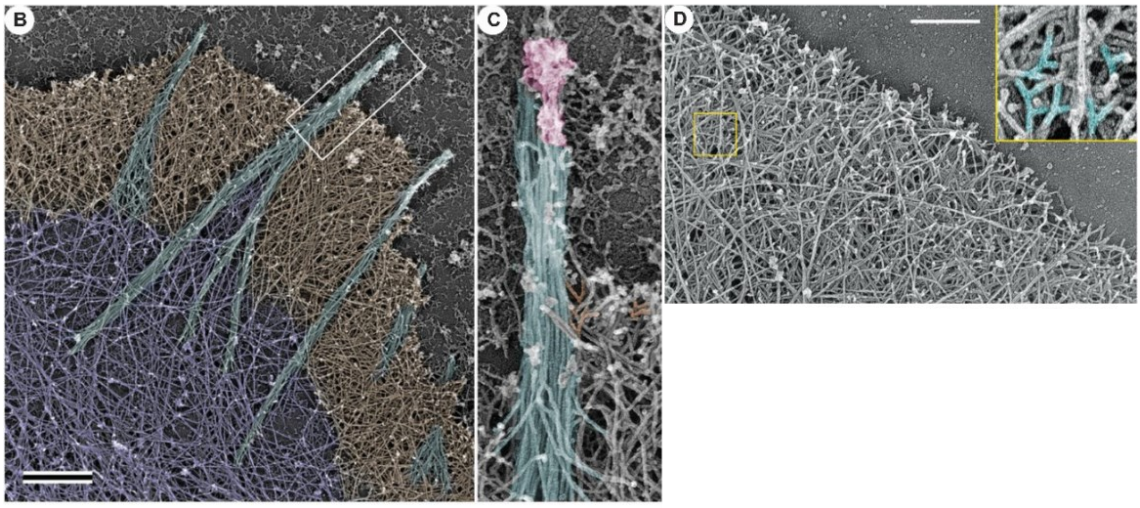
B
C
D

1.9. The dynamic and regulated network of the actin cytoskeleton: A comprehensive overview of actin-binding proteins and polymerization mechanisms

The actin cytoskeleton is composed of monomeric globular actin (G-actin; a 42kDa ATP-binding protein), which assembles into helically twisted filamentous actin (F-actin) microfilaments (Blanchoin et al., 2014; Holmes et al., 1990). Actin filaments continually assemble and disassemble as required by the cell, creating a dense and dynamic network. The underlying mechanism is an ATP-based polymerization at the fast-growing barbed end in contrast to the slower polymerization at the pointed end. Consequently, the combination and co-occurring of both mechanisms create a directionality of the pushing force mediated by actin polymerization. Elongating barbered ends produce the sustained forces that are required to extend the outer part of the lamellipodia forward at the front, leading edge of a migrating cell. Disassembly at the more flexible pointed end guides the release of monomers for recycling (Pollard, 2016). The polymerization mechanism is regulated by numerous actin-binding proteins, which balance each other´s competing activities to build a dense and dynamic network (Overview in Figure 5).

Profilin is an actin monomer-binding protein that promotes nucleotide exchange and restores the G-actin pool, resulting in a faster polymerization rate (Pinto-Costa & Sousa, 2020). Recent research shows an indispensable role in regulating the actin cytoskeleton (Rotty, 2020). Capping proteins prevent further elongation of growing actin filaments and keep up a sufficient amount of free actin monomers. Cofilin enhances the depolymerization rate of actin-ADP and functions in the debranching of the existing dynamic network. The group of actin nucleators stabilizes the nucleus formation to enhance the polymerization rate. In addition, there are formins, which stabilize intermediates, initiate, and elongate unbranched filaments. They are autoinhibited by intramolecular interactions of two domains and only activated by binding Rho-family GTPases. Similar to formins, proteins of the Enabled (Ena)/Vasodilator-stimulated phosphoprotein (VASP) family can associate with growing actin filament barbed ends and promote elongation. Both formins and Ena/VASP locate at the barbed ends of growing actin filaments and produce long and unbranched filaments

within an existing branched network antagonistic to capping proteins. Those linear, unbranched actin filaments are for example important to build finger-like protrusion emerging from the lamellipodium, called filopodia (Campellone & Welch, 2010; Chan et al., 2009; Chesarone et al., 2010; Cooper & Sept, 2008; Edwards et al., 2014; Nadkarni & Brieher, 2014; Pollard, 2016; Pollard & Borisy, 2003; T. M. Svitkina et al., 2003).

The most prominent actin nucleator is the Arp2/3 complex, which, in principle, mimics an actin dimer and subsequently builds a more stable oligomer by adding a fourth subunit (Goley & Welch, 2006) (Figure 5, Figure 6). Monomers are likewise supplied by profilin to the Arp2/3 complex to promote branched actin assembly at the leading edge of a cell. Consequently, there is a dynamic competition between different actin polymerization factors utilizing profilin-bound G-actin. A recent research study uncovered that especially with low concentrations of profilin, bundled filaments generated by Ena/VASP are favored over Arp2/3-mediated branched F-actin (Skruber et al., 2020). Therefore, a cell can rapidly shift the leading-edge actin architecture by modulating the profilin concentration. The mechanism of how the Arp2/3 complex produces actin filament branches will be introduced in more detail in the next chapter.

Lastly, there are the nucleators Spire, Cordon bleu (Cobl), and Leiomodin (Lmod), which all have a tandem actin monomer-binding WASp-homology 2 (WH2) domain. They bind and align multiple G-actin monomers, forming a polymerization seed (Chesarone & Goode, 2009).

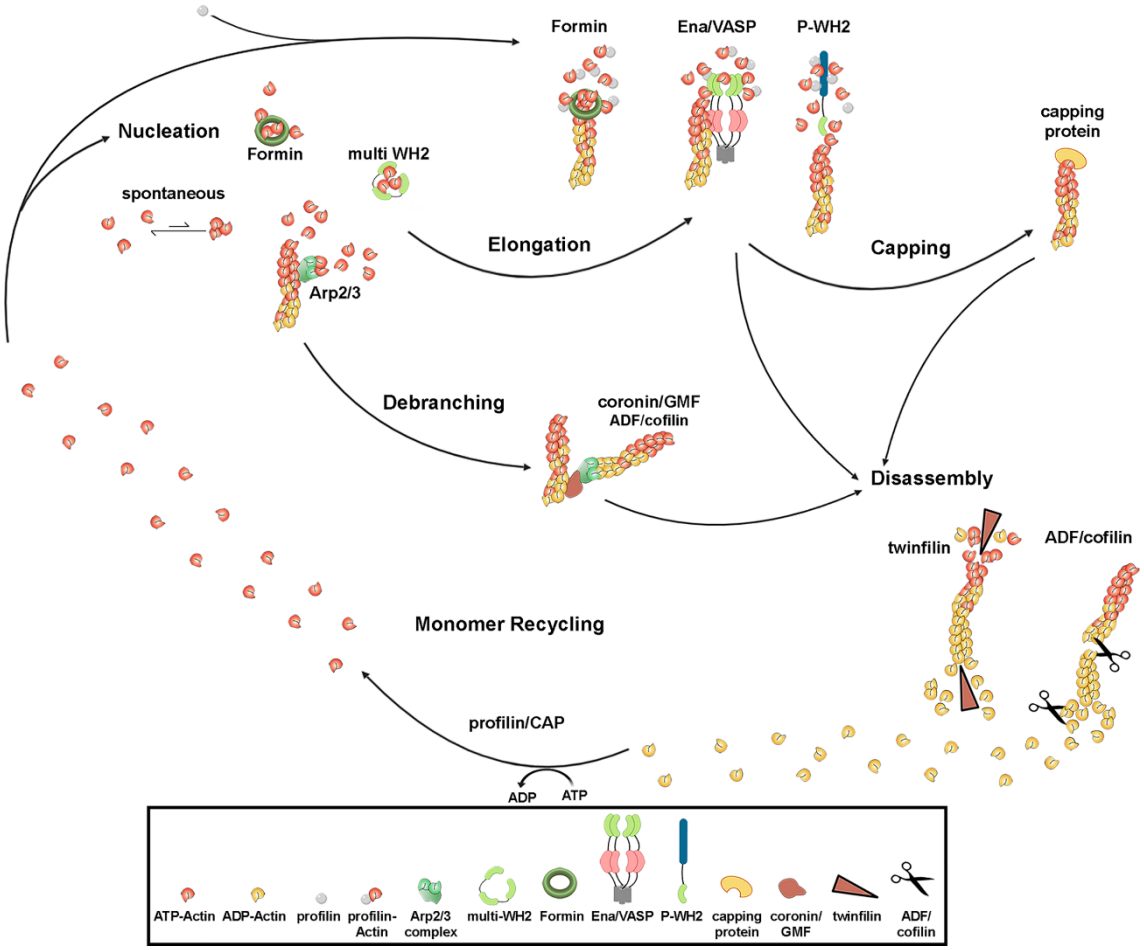

***Figure 5 - Cycle of actin polymerization from* (Schaks et al., 2019).** *Overview of the variety of factors involved in the regulation of actin polymerization. Monomer ADP-Actin is recycled by profilin, which promotes a nucleotide exchange from ADP to ATP. Subsequently, ATP-Actin is ready for nucleation of a new filament or elongation of an existing filament. Either formin, a multi-WH2 protein, or Arp2/3 promote nucleation. Elongation occurs with the help of formin, Ena/VASP, or a P-WH2 protein. Capping proteins protect a filament from further growing. Disassembly is ensured by twinfilin and ADF/cofilin. Used with permission of Portland Press, Ltd., from* (Schaks et al., 2019)*; permission conveyed through Copyright Clearance Center, Inc.*

1.10. The Arp2/3 complex: a key regulator of actin nucleation and cell migration

The Arp2/3 complex consists of seven subunits, including the actin-related proteins Arp2 and Arp3 and the Arp 2/3 complex subunits 1-5 (ARPC1-5). Arp2 and Arp3 show high similarities to monomeric actin and are thereby able to mimic the first units of the growing filament to overcome the instability of actin dimers and trimers. In that way, the complex binds pre-existing mother filaments via Arp2/3. It brings three monomeric actin proteins in close proximity to form a nucleation core at which spontaneous polymerization can occur. As a result, the

newly formed daughter filament has an angle of 70 degrees relative to its mother filament (Figure 6). The resulting dense actin meshwork – which is stabilized by cortactin -builds the lamellipodium that constitutes the driving force in cell migration.

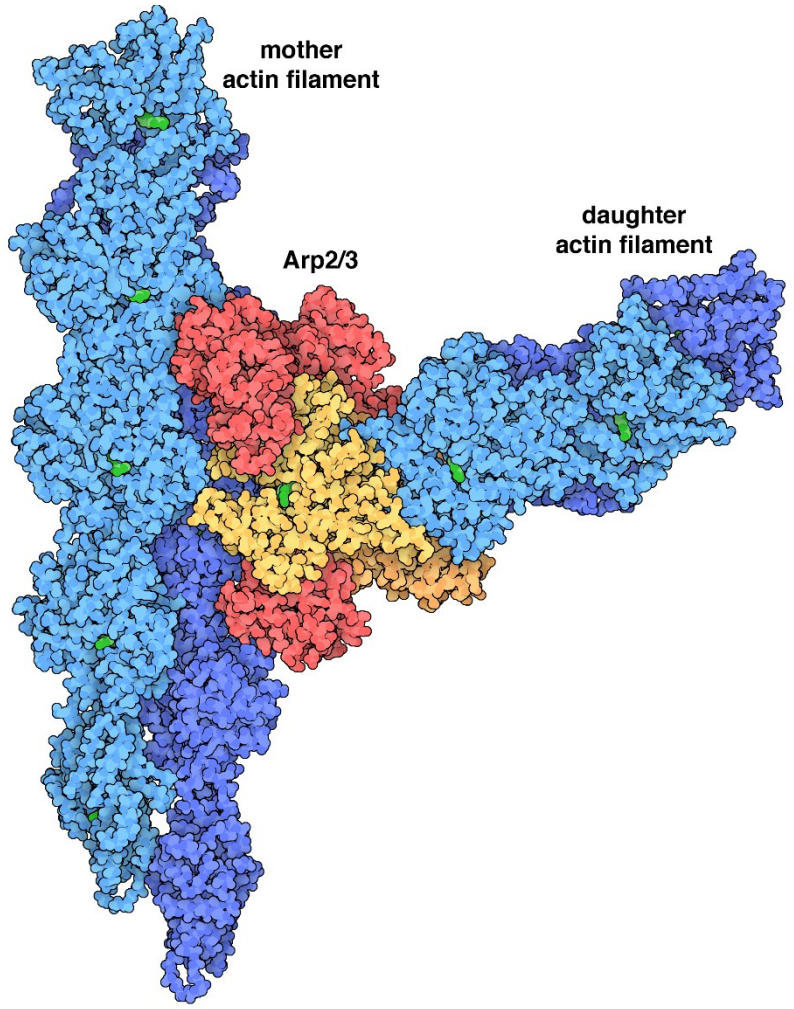

Figure 6 - Actin branching by Arp2/3 complex. *A branch between two actin filaments (blue) created by Arp2/3 complex (red and yellow). The Arp2/3 complex binds to an existing actin filament (the "mother filament"), mimics the first actin monomer to overcome the instability of actin self-assembly, and nucleates the assembling of a new actin filament (the "daughter filament"). Note the resulting angle of 70 degrees between the mother and daughter filament. ATP is shown in green. Image with permission from the RCSB PDB November 2022 Molecule of the Month feature by David Goodsell* (Goodsell, 2022).

The Arp2/3 complex itself is mostly inactive and subject to regulation by multiple nucleation-promoting factors (NPFs) through direct protein-protein interaction (Goley & Welch, 2006; Rotty et al., 2013). These are additional tools to regulate the overall actin assembly by tuning nucleation activity. There are two

subfamilies of Arp2/3 NPFs. The verprolin central acidic (VCA) domain-containing proteins of the Wiskott-Aldrich syndrome protein (WASP) family belong to the NPFs type Ⅰ family. The weaker Arp2/3 activators of the NPFs type Ⅱ family are for instance cortactin, hematopoietic lineage cell-specific protein 1 (HS1), and coronin (Rotty et al., 2013), all of which lack a WH2 domain, which is part of the VCA domain, for binding G-actin (Campellone & Welch, 2010). Instead of using the acidic VCA domain for binding to Arp2/3, these proteins have an acidic domain at their amino terminus to bind and activate the complex along with tandem repeat domains to bind to F-actin (Rotty et al., 2013).

In contrast, the interaction of Arp2/3 and NPFs type Ⅰ relies on the acidic nature of the C-terminal VCA domain (Higgs et al., 1999; Machesky & Insall, 1998). The V domain binds G-actin and delivers it to the Arp2/3 complex, whereas the CA domain is responsible for binding the Arp2/3 complex (Chereau et al., 2005; Marchand et al., 2001). A dimerization of two individual CA sequences induces conformational changes and increases the VCA binding to the Arp2/3 complex (Kramer et al., 2022; Padrick et al., 2008, 2011; Padrick & Rosen, 2010).

The N-terminus is more variable between members of the type Ⅰ NPFs, which enables differences in activity regulation, membrane localization and ligand interactions (Goley & Welch, 2006).

1.11. NPFs are indispensable for the activation of the Arp2/3 complex

The mammalian NPF type Ⅰ family proteins can be further subdivided into five groups: (1) WASP and neural WASP (N-WASP); (2) three WASP-family verprolin homolog (WAVE1 – WAVE3; also known as SCAR) isoforms; (3) WASP and SCAR homolog (WASH); (4) WASP homolog associated with actin, membranes, and microtubules (WHAMM) and (5) junction-mediating regulatory protein (JMY). Additionally, WHAMY - a novel WASP-like protein - was found in the regulation of Arp2/3 in Drosophila blood cells (Alekhina et al., 2017; Brinkmann et al., 2015; Campellone et al., 2008; Derry et al., 1994; Miki et al., 1996, 1998; Suetsugu et al., 1999). All these NPFs, except for WAVE, are

intrinsically inactive because their binding site for actin monomers and Arp2/3 complex is sequestered. Each one is activated by the binding of small Rho GTPase in response to upstream signals, i.e. Rac1 activates WAVE, and Cdc42 activates WASP.

WASP is the first member of the WASP protein family that was discovered as the gene mutated in patients with the Wiskott-Aldrich syndrome (WAS), which is characterized by actin cytoskeletal defects in blood cells, leading to thrombocytopenia, eczema, and immunodeficiency (Derry et al., 1994; Massaad et al., 2013; Orange et al., 2002). Loss-of-function mutations of WASP revealed an essential role in mammals linked to the actin-associated processes that are affected in cells (Facchetti et al., 1998; Gallego et al., 1997; Kenney et al., 1986; Molina et al., 1992). Mammalian WASP is mainly expressed in hematopoietic cells, whereas neural WASP (N-WASP) is present in most cell types (Campellone & Welch, 2010). Both have functional versatility and are autoinhibited by intramolecular interactions of the VCA domain with the CRIB domain. This is stabilized by binding of the WASP-interacting Protein (WIP) to the N-terminal WASP homology 1 domain (WH1), protecting the protein from degradation. They are activated by binding of the small GTPase Cdc42, causing conformational changes in the VCA domain. The binding of Cdc42 together with phosphatidylinositol-4.5-bisphosphate changes the conformation and releases the VCA domain for binding to the Arp2/3 complex, facilitated by binding of profilin-G-actin to the polyproline region (Alekhina et al., 2017; Antón et al., 2007; Campellone & Welch, 2010; Rottner et al., 2010).

The WASP-family verprolin-homologous protein (WAVE) is the second group of the WASP-family proteins and contains three orthologs in vertebrates: WAVE1, WAVE2 and WAVE3. In mammals, WAVE1 and WAVE3 are enriched in the brain, whereas WAVE2 is mainly expressed in all tissues, particularly in peripheral blood leukocytes (Suetsugu et al., 1999; Uhlén et al., 2015).

WAVE was first discovered in 1998 by multiple laboratories. Bear and colleagues identified the protein as a suppressor of cyclic AMP receptor downstream of Rac signaling in regulating the actin cytoskeleton in *Dictyostelium*. This led to its first name SCAR (suppressor of cAR) (Bear et al., 1998). Meanwhile, two other labs were searching for an Arp2/3-interaction

partner and WH2-containing protein and identified the human homolog SCAR1 and introduced the name WAVE (Machesky & Insall, 1998; Miki et al., 1998).

Similar to the other NPFs, WAVE can be structurally divided into four domains. It possesses an N-terminal WHD Domain, a lipid-binding basic region (B), a PRD, and the VCA domain, common for the NPFs. Unlike WASP, WAVE lacks the GBDs that are usually essential for binding of the GTPases, which in turn indicates a further regulatory mechanism (Miki et al., 1998). Additionally, first *in vitro* studies revealed that WAVE itself is fully active and exhibits a basal actin nucleation activity by interacting with Arp2/3 (Machesky et al., 1999).

However, in contrast to WASP, *in vivo* studies showed that WAVE is incorporated into the heteropentameric WAVE regulatory complex (WRC) (Gautreau et al., 2004; Innocenti et al., 2004), which is crucial for most of the interactions and activity regulation and especially for the activation by Rac1 (Miki et al., 1998). The WRC can be described as a central signaling hub through which a large diversity of membrane ligands can transmit signals to Arp2/3 complex-mediated actin polymerization (S. Yang et al., 2022). Deleting one subunit of this complex diminishes the functionality of the whole complex. In this manner, WAVE is a central Arp2/3 regulator for driving actin assembly and consequently mediating cell shape and cell migration. The importance of WAVE in regulating actin dynamics will be introduced in more detail in the following chapters.

WASH is another Arp2/3 NPF different from other NPFs due to its N-terminal WASH-homology domain (WAHD). WASH exists in a stable pentameric complex similar to the WRC. Alone, WASH is inactive, whereas the complex is constitutively active, which differs from the WRC. Moreover, WASH is crucial for early development and is not functionally redundant with WASP or WAVE. Furthermore, WASH promotes F-actin branching at endosomes/endocytic vesicles and regulates endolysosomal system structure and integrin receptor trafficking (Alekhina et al., 2017; Gomez & Billadeau, 2009; B. M. Nagel et al., 2017).

WHAMM and JMY are other NPFs that function in regulating vesicle transport and Golgi morphology and accumulate in the nucleus upon DNA damage, respectively (Campellone et al., 2008; Zuchero et al., 2009, 2012).

1.12. Hemocytes utilize actin-based protrusion for migration and phagocytosis

As mentioned before, cell migration is based on membrane protrusions. The most important migratory mechanism is based on the branched actin network facilitated by the Arp2/3 complex. This dendritic F-actin network constructs the leading edge of a motile cell, which is the outermost 1 µm part of the lamellipodia (Figure 4, Figure 5, Figure 7). To exhibit a dynamic forward movement, the cell must be polarized, and the Arp2/3 complex needs to be located accordingly to the moving direction. A dynamic extension of the lamellipodia is made possible through the addition of monomeric actin between pre-existing growing ends of filaments and the membrane interface (Bisi et al., 2013). This is initiated by the small GTPase protein Rac1 which activates the WRC binding to the Arp2/3 complex at the leading-edge membrane leading to actin polymerization. Arp2/3 mediated actin polymerization constantly creates barbed ends, which are elongated by formins or Ena/VASP, which form long branched filaments that structure the mesh network. Notably, the pointed ends of the newly formed filaments are capped and anchored in the existing network.

Typically, the lamellipodia have a fan-like structure. As mentioned before, the angle between the branched actin filaments is 70°, which leads to the fact that the angle between the elongating barbed ends and the plasma membrane is approximately 45°. This is described as an optimal angle for translating filament elongation into membrane displacement (Mogilner & Oster, 1996; Mullins et al., 1998). Although the WRC was described to target the Arp2/3 complex to the front leading edge, it is noteworthy that actin polymerization also occurs throughout the lamellipodium (Watanabe & Mitchison, 2002).

Additionally, filament elongation by Ena/VASP and formins contribute to the overall structure of the actin network at the plasma membrane and are critical for maintaining network organization (Figure 5, Figure 7) (Chesarone & Goode,

2009). It was discovered that formins also play an important, but not essential role in the constitution of the lamellipodial actin network, as they can adjust the stability and protrusive dynamics of the lamellipodium (Kage et al., 2017). Even when lamellipodia-based migration is dominant, they contribute to an efficient migration by nucleating and elongating of individual filaments. Without this support, the lamellipodia width is reduced, leading to a less effective force generation (Kage et al., 2017; Pfisterer et al., 2020). Coexistence of filopodia and branched lamellipodia structures (T. Svitkina, 2018) is tightly regulated and variable among different cell types. The equilibrium is balanced between the need for fast lamellipodia-based locomotion versus filopodia-based precise navigation. (T. Svitkina, 2018)

A more stable region directly behind the lamellipodia is called lamella. It is formed out of a parallel array of filaments that interacts with myosin-II. In this way, the actin network is coupled to myosin-II mediated contractility and cross-linking functions (Lehne et al., 2022). Opposing to the dynamic elongation at the front leading edge, the small GTPase RhoA activates the Rho-associated protein kinase (ROCK) in the rear end of the cell. This leads to actomyosin contraction and the cell actively retracts at the trailing edge which dynamically regulates the protrusion rate (Lämmermann & Sixt, 2009).

Besides lamellipodial-based motility, a cell can utilize filopodia to fulfill immune functions efficiently. Filopodia-based migration relies on the pushing force created by the F-actin polymerization (Bischoff et al., 2021). Interestingly, filopodia can thereby drive migration independently of lamellipodia. This was first discovered during investigating an explorative role for filopodia (Karp & Solursh, 1985; Malinda et al., 1995). Additionally, various cancer cells utilize filopodia structures for migration (Jacquemet et al., 2015).

Generally, filopodia are small and rod-like protrusions of linear actin filament bundles (Rottner & Schaks, 2019). While Arp2/3 complex-mediated actin polymerization promotes a branched actin network formation, formins like Ena/VASP proteins are important for linear actin elongation and are therefore found in filopodia. F-actin elongation at the barbed ends promoted by Ena/VASP occurs mainly by protecting the tip’s growing end from capping. Since filopodia structures are linear bundles, growing actin filaments are

additionally cross-linked by fascin to keep the F-actin filament densely packed (Vignjevic et al., 2006). Furthermore, Fascin enables elongation of filopodia beyond the leading edge, which underlies their importance in long-rage cell-cell communication (Mattila & Lappalainen, 2008).

Filopodia are also formed to explore the surrounding environment and to capture various particles for subsequent phagocytosis, which in turn is mediated by Arp2/3-dependent actin branches (Vignjevic et al., 2006).

They are further regulated by cofilin, which severs actin filaments at the pointed end to fine-tune the dissociation rate and contractile properties of myosin II (T. Svitkina, 2018). Therefore, a constant retrograde flow is given and can even completely counterbalance the polymerization. This would lead to an apparently stationary state. Conclusively, a regulated dissociation and binding to actin filaments promote the force for filopodia assembly.

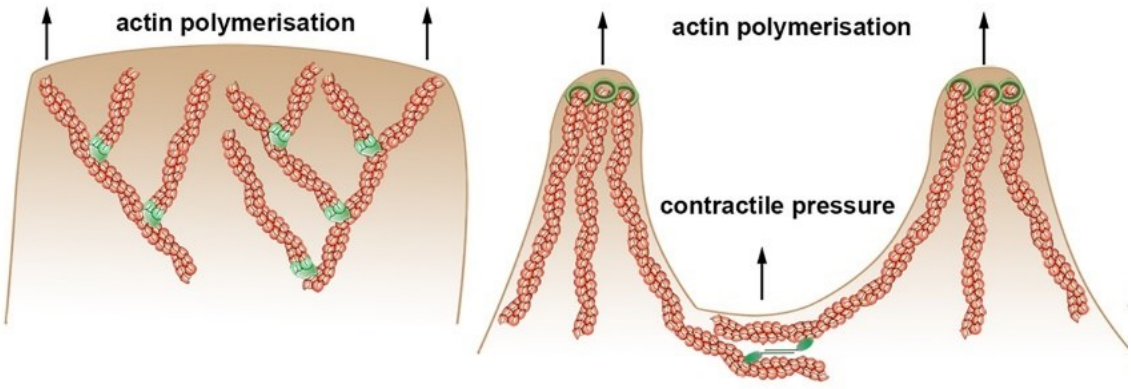

Figure 7 – Actin based membrane protrusions. *From left to right are shown a branched lamellipodia structure and filopodia structures. The Arp2/3 complex (light green, left panel)-dependent lamellipodia actin network creates protrusion of the plasma membrane essential for a dynamic forward moving of a cell. Filopodial actin bundles are decorated with formins at the top barbered (green ring, right panel). Space between two filopodia structures is filled by the contractile activity of myosin II (green, right panel). Note that lamellipodia and filopodia membrane protrusions are based on actin polymerization. Used with permission of Portland Press, Ltd., from* (Schaks et al., 2019)*; permission conveyed through Copyright Clearance Center, Inc.*

1.13. An overview of the WAVE complex: Regulating actin dynamics and cell migration

WAVE is a central Arp2/3 regulator driving actin network remodeling and consequently mediating cell shape and migration.

As mentioned earlier, WAVE is incorporated into the WRC. Other members of this complex are Abi (Abelson interactor), Sra1 (specifically Rac1-associated protein 1, also known as Cyfip), Nap1 (also known as Kette), and HSPC300 (haematopoietic stem/progenitor cell protein 300) (Gautreau et al., 2004; Innocenti et al., 2004). The complex can be described as an assembly of a large, elongated dimer formed by Sra1 and Nap1, and a smaller trimer formed by WAVE, Abi and HSPC300 (Figure 8). The trimer forms a four-helix bundle and is aligned along the axis of the α-helical Sra1-Nap1 dimer. Importantly, only the amino termini of WAVE (i.e., its WHD domain), Abi and HSPC3000 make this intracomplex association (Fokin & Gautreau, 2021). The remaining extending part of WAVE plays essential regulatory roles. The first 90 amino acids are known as the meander region. They are necessary for stabilizing the VCA domain and thereby essential for inhibiting and activating the WRC. The C-terminal VCA domain inhibits WRC function by intracomplex sequestration into a conserved recess of Sra1.

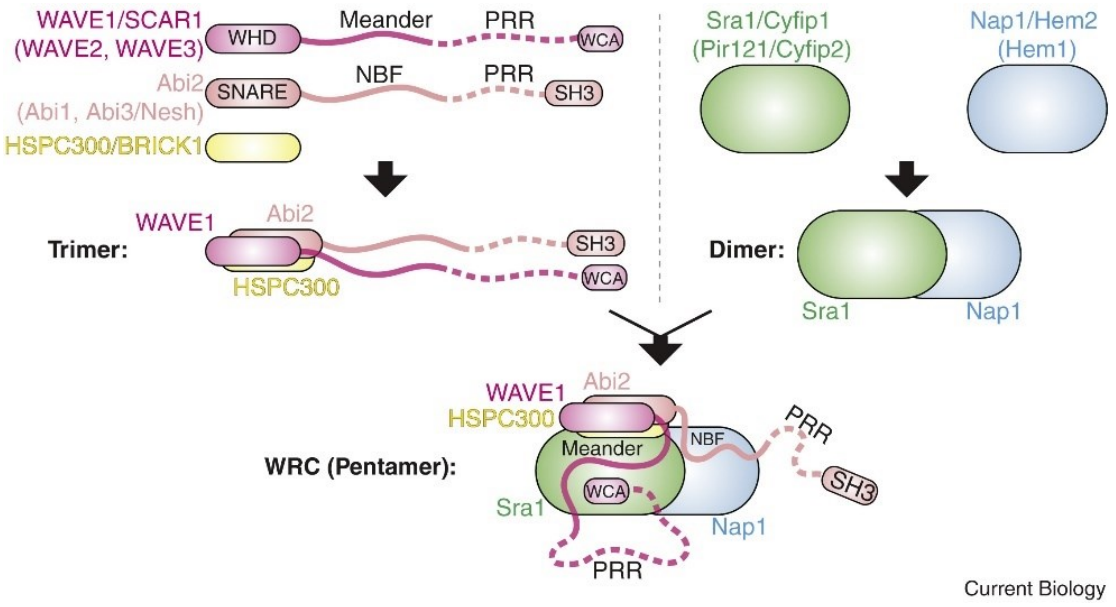

Figure 8 – Assembly of the WRC. *Assembly of the pentameric WRC appears through two parallel assembly routes. The left panel shows the assembly of a trimer of WAVE, Abi and HSPC300. The left panel shows the assembly of a dimer of Sra1 and Nap1. Subsequently, the trimer forms a four-helix bundle aligned along the axis of the α-helical dimer. Reprinted from* (Rottner et al., 2021)*, with permission from Elsevier.*

Various membrane ligands can directly interact with the WRC, which in turn recruit the complex to the plasma membrane and facilitate its interaction with the Arp2/3 complex. The binding of Rac1 as the canonical activator of the WRC to two distinct locations on the opposite ends of the Sra1 subunit leads to the release of the VCA domain. This is followed by recruitment to the plasma membrane, thereby binding and activating the Arp2/3-mediated actin polymerization to generate a dense actin meshwork responsible for cell shape and migration (Figure 9). Noticeably, Rac1 binding affinity is increased to a WRC with the VCA domain deleted, which leads to the conclusion that Rac1 binds at the body of the WRC competitively to the VCA (Buracco et al., 2022). This observed link between Rac1 and WRC components highlights their importance in lamellipodia formation, thereby regulating migratory behavior. Since a high concentration of Rac1 is necessary for the structural change (B. Chen et al., 2017; Steffen et al., 2004; Stradal et al., 2004), there are more mechanisms to further regulate the WRC activity.

Recently Yang and colleagues identified a novel binding site for the small GTPase Arf, which is distinct from the canonical binding site for Rac1. The

authors demonstrated that Arf could activate the WRC and promotes actin polymerization through this binding site. They also showed that this Arf-mediated activation of the WRC is important for normal actin cytoskeleton dynamics in *Drosophila* cells. These findings suggest a previously unrecognized mechanism for WRC regulation and highlight the complex interplay between different small GTPases in controlling actin cytoskeleton dynamics (S. Yang et al., 2022). Interestingly, a recent publication reports the existence of a novel actin network in cells lacking the WRC. The study found that the new network called lamellipodia-like structure (LLS) appears to be formed through a pathway involving the Arp2/3 complex and essentially requires Rac1 and Cdc42 signaling and is similar in appearance to lamellipodia. Additionally, the authors observed neither a WRC-mediated Arp2/3 complex activation nor an Ena/VASP-dependent actin assembly in WRC knockout clones. The findings suggest that there may be multiple pathways for generating lamellipodia-like structures (Kage et al., 2022).

An important step in WRC regulation is recruiting the complex to the plasma membrane. This is further facilitated by PIP3 (Lebensohn & Kirschner, 2009; Oikawa et al., 2004) and multi-module scaffold proteins, including IRSp53, Toca1, and WRP, which also tend to promote clustering of the WRC (X. J. Chen et al., 2014; Z. Chen et al., 2010; Fricke et al., 2009; Padrick et al., 2008; Padrick & Rosen, 2010; Takenawa & Suetsugu, 2007).

So far, research has been focused mainly on the positive control mechanism of WAVE2 in actin dynamics, but the pathway of how WAVE2 is negatively regulated, effectively ending up in degradation, has yet to be investigated in the same way. One example is that Ura and colleagues mentioned that dephosphorylated WAVE is subject to degradation (Ura et al., 2012). They conclude that when WAVE is activated, it is degraded even when incorporated into its regulatory complex. This degradation is the physiological process that removes the activated WAVE and controls actin branching.

Even though it has been proposed that even the loss of only one member of the WRC leads to an improper function of the whole complex, a WAVE:Abi:HSPC300 complex that lacks Sra-1 and Nap-1 is active (Padrick et al., 2008). However, with cell type-specific knockdown experiments of

Drosophila immune cells, it was proven that a loss of Abi leads to a disruption of lamellipodia formation comparable to a knockdown of *wave*. Interestingly the same study also revealed an important interaction of Abi, as part of the complex, with Ena/VASP proteins that sequentially enhances the WRC-mediated actin polymerization (X. J. Chen et al., 2014). Until then, Ena/VASP was thought to stimulate cell migration by antagonizing actin filament capping and acting as processive actin polymerases.

Besides the regulation based on degradation, the Nance-Horan Syndrome-like 1 protein (NHSL1) has been identified in human BF16-F1 cells as a novel negative regulator. NHSL1 belongs to the Nance-Horan Syndrome family, and one ortholog has been identified in *Drosophila*, GUK-holder (GUKh) (S P Brooks, 2004; Caria et al., 2018). Mutations in the NHS gene have been linked to Nance-Horan Syndrome, a rare genetic disorder. The NHSL1 protein contains a functional WHD domain and was first described to maintain the integrity of the circumferential ring, a structure formed by actin filaments in the cell cortex that plays a role in cell shape and division (Simon P. Brooks et al., 2010). Recently it was shown in human BF16-F1 cells that NHSL1 is recruited to the leading edge by binding to membrane-associated active Rac1. Subsequently, NHSL1 binds with its WHD domain to the SH3 domain of Abi and reduces Arp2/3 activity by negatively regulating the WAVE regulatory complex by controlling the complex stability and activity (Law et al., 2021). Loss of NHSL1 leads to a persistent overactivation of the complex, increases Arp2/3 activity, and in the lamellipodium, Arp2/3 and actin densities are higher than the wild-type (Law et al., 2021). However, this has yet to be demonstrated *in vivo* for the *Drosophila* ortholog GUKh.

Additionally, Arpin has been described as a negative regulator of the Arp 2/3 complex, which inhibits the activity of the complex that is essential for actin filament nucleation and branching. Similar to the NPF WAVE, Arpin function is regulated by Rac1. However, this mechanism is so far unknown. Arpin itself is thought to inhibit the Rac-WAVE-Arp2/3 complex interaction to control the directional persistence of migration (Krause & Gautreau, 2014). Recently it was found that Arpin binds to the Arp2/3 complex in a manner that directly competes with the binding of actin-NPF to the Arp3 subunit. This, in turn prevents the

binding of the actin-NPF to the Arp2 subunit required for the Arp2/3 complex to undergo the conformational changes necessary for filament nucleation (Fregoso et al., 2022).

A so far poorly described negative regulator of the WRC is CYRI (CYFIP-related Rac interactor). CYRI interacts with Rac1 at a specific domain called the DUF1394 domain leading to a restricted activity of Rac1 at the cell membrane. In that way, CYRI decreases the activity of the WRC. However, CYRI is needed to maintain the cell's flexibility and allow the actin structures at the front leading edge to respond quickly to environmental changes (Whitelaw et al., 2019).

Moreover, members of the WRC possess different consensus sequences that kinases and phosphatases can recognize. It has been described that phosphorylation might regulate activity and localization (Krause & Gautreau, 2014; Singh et al., 2021). Most recently, for Abi, a phosphorylation-dependent regulation of degradation was reported. It was proposed that phosphorylation of Abi could increase the proteolysis rate of the complex or make the active complex shorter-lived (Singh et al., 2021).

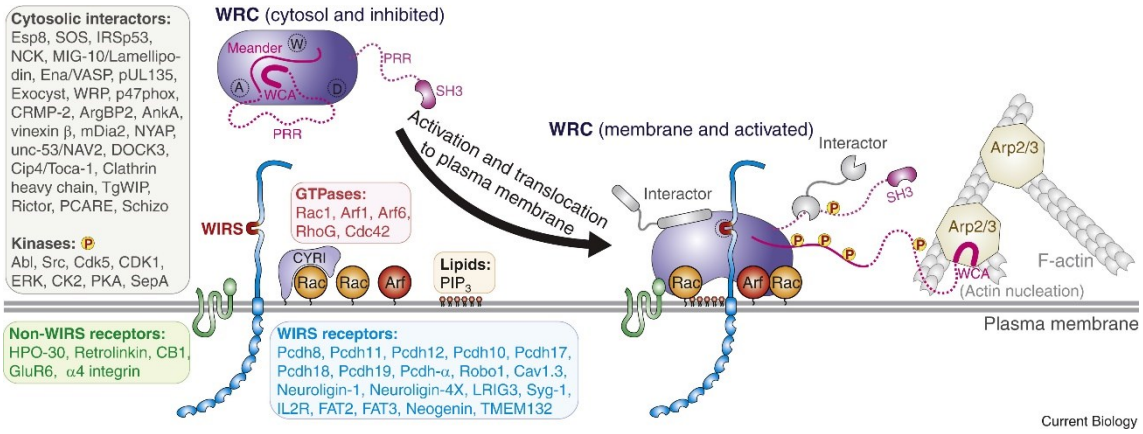

Figure 9 – Activation of the WRC at the plasma membrane. *Schematic overview of simultaneous activation of the WRC and its translocation to the plasma membrane. The WCA (another name for VCA) domain is sequestered and stabilized by the meander region, which leads to an inhibition of the WRC. Activation by GTPases and interaction with various membrane ligands and PIP_3 lipids, in turn, leads to the release of the WCA domain, translocation to the plasma membrane and activation of the complex. Subsequently, the WCA domain gets phosphorylated and binds to the Arp2/3 complex to stimulate actin nucleation. WCA stands for WH2-central-acidic and is equal to the VCA domain. Different groups of ligands that interact with the WRC are listed in the text boxes. In addition, important regulators are explained in the text in more detail. Reprinted from* (Rottner et al., 2021)*, with permission from Elsevier.*

1.14. The role of tyrosine and serine phosphorylation in regulating WAVE-mediated actin dynamics

Previous studies indicated that the phosphorylation of WAVE regulates various aspects of actin dynamics. Several kinases such as Cdk5, Erk, Abl, CK2, and Src have been described to phosphorylate tyrosine and serin residues of both WAVE and Abi (Z. Chen et al., 2010; Danson et al., 2007; Kramer et al., 2022; Mendoza, 2013; Pocha & Cory, 2009; Singh et al., 2021; Ura et al., 2012).

Primary observation proposed that phosphorylation, especially of three tyrosine within the meander domain of WAVE, is important for WRC-mediated actin dynamics (Leng et al., 2005). Particularly a specific role of tyrosine phosphorylation in the interaction between Abi and WAVE has been investigated. It has been shown *in vitro* that the Abelson tyrosine kinase (Abl) localizes Abi upon phosphorylation to WAVE, followed by additional phosphorylation of WAVE (Leng et al., 2005). Conclusively, the interaction of Abi and WAVE, and a subsequent activation of the WRC by Rac1, is favored through tyrosine phosphorylation of one or both proteins. However, this has not been proven *in vivo* yet (Leng et al., 2005). Later, it was demonstrated that

phosphorylation of tyrosine residues within the meander region destabilizes the binding to Sra1. This leads to the release of the VCA domain and favors the WRC activation (Z. Chen et al., 2010).

More recently, the phosphorylation of serine residues within the VCA domain became more interesting and was further investigated. Experiments focused more on a serine-dependent phosphorylation by Casein Kinase 2 (CK2) interacting with the NPFs N-WASP and WAVE. Different studies commonly revealed the importance of phosphorylation. However, the results can be considered controversial regarding the way of regulation (Cory et al., 2003; Mendoza, 2013; Nakanishi et al., 2006; Pocha & Cory, 2009; Singh & Insall, 2021).

It has been shown that the activity of WASP depends upon the phosphorylation of its VCA domain by CK2 (Cory et al., 2003). More precisely, phosphorylation of the VCA domain has distinct effects on its Arp2/3 complex binding and activation properties. Phosphorylation of WASP increases the affinity to the Arp2/3 complex. However, a subsequent enhancement of Arp2/3 activity and thereby actin polymerization has not been detected *in vitro*. It is suggested that other components contribute to this complex interaction (Cory et al., 2003).

Because of the homology of the target residues in the WASP-VCA domain with the WAVE sequence, further research focused on outlining the interaction between CK2 and WAVE (Pocha & Cory, 2009). Pocha and colleagues found that WAVE´s VCA domain is phosphorylated at five serine residues by CK2 *in vitro*. However, further *in vitro* investigations with either a CK2-specific inhibitor or a variety of other kinase inhibitors did not abolish phosphorylation (Pocha & Cory, 2009). Nevertheless, the authors proposed multiple phosphorylation events necessary for high-affinity binding of WAVE to the Arp2/3 complex. Moreover, they pointed out that phosphorylation of the WAVE VCA domain is essential for normal WAVE function (Pocha & Cory, 2009).

Ura and colleagues used *Dictyostelium discoideum,* which expresses a WAVE (in *Dictyostelium,* the name for WAVE is SCAR) with sequence homology to the human WAVE2 and *Drosophila* WAVE. This protein has five conserved putative serine residues that are targeted for phosphorylation in the VCA domain. They

proposed that dephosphorylation of SCAR is the essential step (Ura et al., 2012). They found that the acidic domain is basally phosphorylated and an intramolecular inhibition through binding of the acidic residues to the basic region occurs. Ura and colleagues mutated the potential serine residues within the VCA domain to mimic an unphosphorylated state (serine to alanine) or a constitutively phosphorylated state (serine to aspartate). Interestingly both mutants rescued the growth and cell size *in vivo*, however, not to the same extent as the wildtypic protein. That led to the assumption that phosphorylation regulates the extent rather than the initiation of SCAR activation (Ura et al., 2012).

Another casein kinase family member with a canonical target consensus sequence in the VCA-domain of WAVE, like the CK2 phosphorylation site, is the Casein Kinase 1α (CK1α). This phosphate-directed protein kinase has not been widely described to be involved in WAVE regulation. However, independent RNAi screens both in S2 cells as well as *ex vivo* macrophages revealed a potential interaction of CK1α with the WRC (D'Ambrosio & Vale, 2010; B. Nagel, 2018).

1.15. Identification of a new WAVE regulator driving immune cell shape dynamics: Casein Kinase 1α

Casein Kinase 1α (CK1α) is a widely distributed monomeric Serine/Threonine (S/T) protein kinase with a size of 39.5 kDa (Tuazon & Traugh, 1991). In *Drosophila*, there are 10 known isoforms of casein kinase 1 family members, of which CK1α, CK1ε and CK1γ are well described (L. Zhang et al., 2006). CK1α is present in the nucleus and cytoplasm and mainly consists of the 288 amino acid long kinase domain (Figure 10). Its activity depends only on ATP and no other cofactors (Flotow et al., 1990). In contrast to other CK1 family members, CK1α does not harbor a C-terminal regulatory domain (Cegielska et al., 1998; Gietzen & Virshup, 1999; Graves & Roach, 1995). For example, it has been shown that the human CK1δ, a homolog of the *Drosophila* CK1ε (Knippschild et al., 2005), has an inhibitory domain that functions as a pseudosubstrate thereby inhibiting its own kinase activity (Cegielska et al., 1998; Rivers et al., 1998). Lacking this inhibiting domain, CK1α is constitutively active and is not subject to further regulatory interactions. Thus, the primary regulation mechanisms are the

subcellular localization because the kinase must be in close proximity to its substrate to successfully phosphorylate (P. C. Wang et al., 1992), and additionally, the nature of the target sequence.

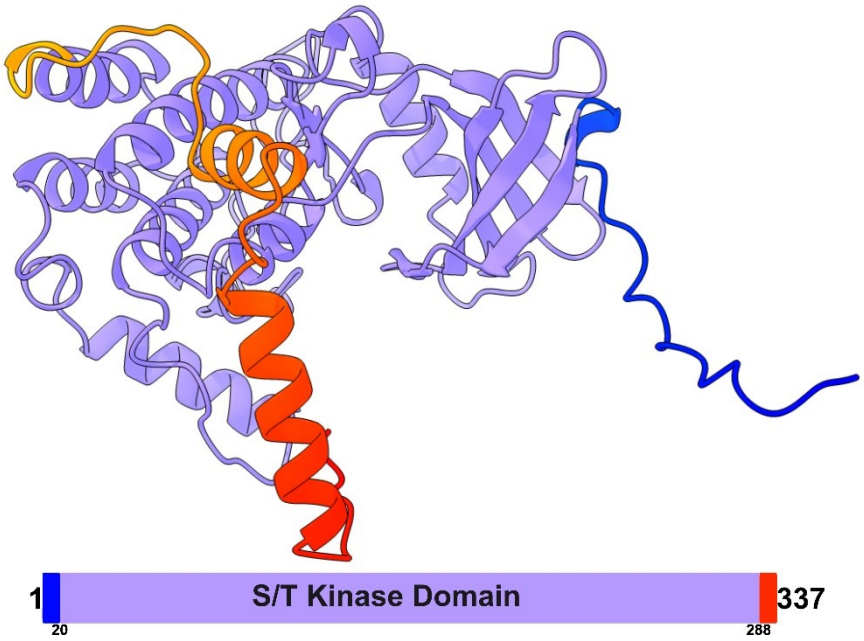

Figure 10 – Predicted three-dimensional (3D) structure of CK1α. *Representation of the predicted 3D structure of CK1α using the UCSF Chimera software* (Pettersen et al., 2021). *The S/T Kinase Domain from amino acids 20 to 288 is highlighted in purple. The C-terminus is highlighted in blue, and the N-terminus in red. The total length of the protein is 337 amino acids.*

CK1α substrate recognition has first been described for acidic protein substrates such as casein and phosvitin (Flotow et al., 1990; Flotow & Roach, 1991). Initial research exclusively focused on the role of aspartate (D) and glutamate (E) residues in phosphorylation sites for kinase activity. However, consecutive studies shed light on the importance of phosphorylation as well as the location of the phosphate groups relative to the phosphate acceptor for kinase activity. Subsequently, the recognition site was determined as S(p)/T(p)-X-X-S/T, where S(p)/T(p) indicates a phosphorylated residue and X represents any amino acid. Nevertheless, a cluster of 3 or 4 acidic residues ending at the -3 position can permit phosphorylation by CK1α but in a weaker nature (Flotow & Roach, 1991; Marin et al., 1994; Pulgar et al., 1999).

Since CK1α is widely distributed and constitutively active, various studies of interaction partners pointed out the diversity of phosphorylation by CK1α. Therefore, the number of proven substrates involved in various pathways is still increasing. Overall, the kinase is involved in many different cellular functions like cell cycle progression, cell morphogenesis, erythrocyte survival, circadian rhythm, Hh and Wnt signaling, *trans*-Golgi network maintenance and cellular differentiation (Chia et al., 2014; J. Jia et al., 2005; Knippschild et al., 2005; Legent et al., 2012; Price, 2006; L. Wang et al., 2013; Zelenak et al., 2012).

Jia and colleagues observed that CK1α targets an inactive form of the transcription factor Cubitus Interruptus (Ci), a regulator of Hh signaling (J. Jia et al., 2005). Phosphorylation of Ci by CK1α initiates two different processing steps depending on the Hh signal and the interplay with other kinases. Ci is either ubiquitinated, which is mediated by the F-Box protein Slimb, to promote subsequent proteasome-mediated degradation or activated through phosphorylation (Han et al., 2019; J. Jia et al., 2005). This observation shed light on the role of CK1α-mediated phosphorylation leading to subsequent ubiquitination followed by proteasome-mediated degradation (Jiang, 2017). Additionally, CK1α regulates the Hh pathway by interacting with the Hh signal transducer Smoothened (Smo), which is hyperphosphorylated among others by CK1α (Yongbin Chen et al., 2011). Consequently, CK1α plays a dual role in regulating the Hh pathway and acts on multiple levels (Han et al., 2019). Noticeably this interplay with other kinases also highlights that the desired target residues for CK1α are determined through sequential phosphorylation events by various kinases.

While investigating the role of CK1α in Wnt signaling, it has been shown that the CK1α substrates NF-AT and beta-catenin are phosphorylated even without the common recognition site. In this case, a non-canonical motif consisting of the sequence SLS combined with a C-terminal cluster of acidic amino acid residues appeared sufficient for CK1α phosphorylation. However, phosphorylation efficiency for this target was 15-25 fold lower. This leads to the assumption that the tertiary structure of the target protein might also play an important role in CK1α phosphorylation activity (Cegielska et al., 1998; Knippschild et al., 2005; Marin et al., 2003; Rivers et al., 1998).

In Drosophila, CK1α function was thoroughly investigated over the last years regarding cellular circadian rhythm. Especially the collaborating activity with the key clock kinase DOUBLETIME (DBT) targeting the clock protein PER1 to maintain the 24 hours length of circadian clocks revealed the indispensable role of CK1α in the circadian rhythm (Hirota et al., 2010; Lam et al., 2018). However, CK1α has not been widely described to be involved in actin regulation. As mentioned earlier, CK2 has been mainly described as potentially phosphorylating WAVE2 (Pocha & Cory, 2009). Even though both belong to the family of casein kinases, they are structurally completely different (Pinna, 1994). CK2 comprises two catalytic CK2α and two regulatory CK2β subunits that form a hetero-tetrameric holoenzyme (Bandyopadhyay et al., 2016). For CK2, the substrate recognition site has been carefully described in terms of D or E residues. Remarkably it has been proposed that phosphorylation processes can be hierarchal (Flotow et al., 1990). In case of the casein kinase family, it could be that serine or threonine residues in a cluster of acidic residues are first phosphorylated by CK2, leading to the phosphorylation of serine +3 by CK1α (Flotow et al., 1990). Thus, CK2 acts cooperatively with CK1α, but it remains unclear if one kinase alone or various kinases are responsible for multiple hierarchical phosphorylation events. Different studies support this hypothesis by showing a CK1α-mediated phosphorylation coupled to the activity of another kinase (H. Jia et al., 2009; J. Jia et al., 2005; Leng et al., 2005).

1.16. Aim of this work

The present work aims to characterize the diversity and functional plasticity of *Drosophila* blood cells, the so-called hemocytes, as well as novel insights into the regulation of the actin cytoskeleton necessary for their immune and phagocytic functions, representing *Drosophila* as a suitable model organism.

Despite the differences in the detail of hematopoiesis between flies and vertebrates, many of the molecular and cellular mechanisms underlying blood cell development and function are conserved, making *Drosophila* a powerful tool for studying hematopoiesis and innate immunity. Recent Bulk RNA-sequencing analysis performed by our lab (Lehne et al., 2022) revealed a remarkable amount of differentially expressed genes between the larval and

pupal states. Single-cell transcriptomics will further investigate the complex heterogeneity of activated pupal hemocytes. Subsequently high-resolution microscopy aims to uncover phenotypically and functionally subpopulations that first appear during pupal development when plasmatocytes become more active. Especially a small group of immune cells that resembles cells of the PSC, a niche that controls blood cell differentiation and maintains hematopoietic progenitors equivalent to the hematopoietic niche of vertebrate bone marrow, highlights the emerging role of niche cells in developmental processes. The role of the PSC cells beyond lymph gland niche function is subject of further investigation with lineage tracing and *in vivo* laser-ablation experiments.

The immune and phagocytic functions of hemocytes rely on their ability to migrate, which is mediated through dynamic changes of the actin cytoskeleton, resulting in cell shape changes. A central regulator of the dense actin network is the Arp2/3 complex, which, in turn, is regulated by WAVE. Phosphorylation is an essential modification in this regulation process. In order to determine the *in vivo* relevance of the phosphorylation of WAVE, a wide screen of putative WAVE interaction partners was performed (B. Nagel, unpublished results) in *Drosophila* hemocytes. Screening 162 kinases by using the RNAi system under control of the *Drosophila* hemocyte-specific driver revealed CK1α as the most prominent candidate regulating the actin machinery. Thereby, it has been shown that knockdown of CK1α alters the morphology of *Drosophila* hemocytes comparable to the already described loss of lamellipodia protrusions evoked by WAVE knockdown (Bogdan & Klämbt, 2003; Rogers et al., 2003).

Although there are two known recognition sites within the WAVE structure, an unfavored SLS motif in the N-terminus, as well as a canonical CK1α consensus sequence in the C-terminal acidic region comprising the VCA domain, a clear phosphorylation relevance has not been proposed so far, albeit the described phenotype. Therefore, experiments with phosphorylation-deficient mutations of the putative phosphorylation sites shall reveal the role of phosphorylation of WAVE. Various loss-of and gain-of function and rescue experiments will be performed to further uncover the substrate specificity to CK1α.

2. Publications

2.1. Publication 1 (under review)

submitted to Development; under review

Single-cell transcriptomics identifies new blood cell populations in *Drosophila* released at the onset of metamorphosis.

Alexander Hirschhäuser, Darius Molitor, Gabriela Salinas, Jörg Großhans, Katja Rust, Sven Bogdan

Single-cell transcriptomics identifies new blood cell populations in *Drosophila* released at the onset of metamorphosis

Alexander Hirschhäuser[1#], Darius Molitor[1#], Gabriela Salinas[2], Jörg Großhans[3], Katja Rust[1*] and Sven Bogdan[1*]

[1] Institute of Physiology and Pathophysiology, Dept. of Molecular Cell Physiology, Philipps University Marburg, Germany

[2] NGS-Integrative Genomics Core Unit, Department of Human Genetics, University Medical Center Göttingen, Germany

[3] Department of Biology, Philipps University Marburg, Germany

[#]) These authors contributed equally to this work.

*) to whom correspondence should be addressed
rustka@staff.uni-marburg.de,
sven.bogdan@staff.uni-marburg.de

Key words

Drosophila, blood, progenitor, scRNA-seq analysis, PSC, migration, hemocytes, plasmatocytes, lamellocytes

Abstract (149 words)

Drosophila blood cells called hemocytes form an efficient barrier against infections and tissue damage. During metamorphosis, hemocytes undergo tremendous changes in their shape and behavior preparing them for tissue clearance. Yet, the diversity and functional plasticity of pupal blood cells have not been explored. Here, we combine single-cell transcriptomics and high-resolution microscopy to dissect the heterogeneity and plasticity of pupal hemocytes. We identified undifferentiated and specified hemocytes with different molecular signatures and cellular functions clearly distinct from other stages of hematopoiesis. Strikingly, we identified that PSC cells, which function as lymph gland niche, are highly migratory and immune responsive cells in the pupa. PSC cells can transdifferentiate to lamellocytes triggered by wasp infection. Altogether, our data highlight a remarkable cell heterogeneity, and identifies a cell population that acts not only as a stem cell niche in larval hematopoiesis, but functions as new cell type in pupal and adult blood.

Introduction (1070 words)

The innate immune system depends on a wide array of conserved cellular and molecular strategies to mediate pathogen defense, tissue remodeling and repair. *Drosophila* is a powerful genetic model organism to study blood cell development and innate immunity (Banerjee et al., 2019; Evans et al., 2003; Lemaitre and Hoffmann, 2007). The fruit fly has an open circulatory system in which the heart pumps blood, the so-called hemolymph into the body cavity circulating all organs. To fight against infections, flies evolved a large variety of defense responses that share highly conserved features with the human innate immunity (Bergman et al., 2017; Buchon et al., 2014). Similar to mammals, the first line of defense against invading pathogens and wounds in *Drosophila* relies on both, a humeral response by which effector molecules such as antimicrobial peptides are secreted into the hemolymph and a cellular response, in which pathogens are phagocytosed by blood cells, the so-called hemocytes (Gold and Bruckner, 2015; Vlisidou and Wood, 2015). Hemocytes have been traditionally classified by their cell morphology into three different effector cells, plasmatocytes, crystal cells, and lamellocytes (Rizki, 1962). Plasmatocytes, the most abundant immune cell type in flies, are professional phagocytes similar to mammalian bone marrow-derived macrophages (Gold and Bruckner, 2015). Circulating and tissue-resident plasmatocytes are immediately recruited to sites of wounding and infections and mediate the major cellular immune response by phagocytosing pathogens and secreting antimicrobial and clotting factors (Evans and Wood, 2014; Sander et al., 2013). Upon injury, platelet-like crystal cells are required for the melanization of wounds, a process that involves the rapid synthesis of the black pigment melanin required for wound healing and encapsulation of invading parasites. Lamellocytes, by contrast, are rarely observed in healthy flies, but are dramatically induced in response to infection by parasitic wasps (Anderl et al., 2016).

Blood-lineage specification in flies requires a similar conserved set of transcriptional regulators and signaling pathways to those that control mammalian hematopoiesis including the GATA factor Serpent (Srp) and the friend of GATA (FOG) transcription factor U-shaped (Crozatier and Vincent, 2011). *Drosophila* hematopoiesis occurs in two spatially and temporally distinct phases with clear parallels to mammals (Crozatier and Meister, 2007). Blood cells initially derive from the head mesoderm of the developing embryo and give rise to both plasmatocytes and crystal cells. These

cells colonize and self-renew in segmentally repeated epidermal-muscular niches in larvae (Crozatier et al., 2004; Makhijani et al., 2011) (Jung et al., 2005; Mandal et al., 2004). The hematopoietic pockets provide both an attractive and trophic microenvironment, promoting proliferation of the initial 600-700 embryonic cells to about 9000-10000 cells per third-instar in the differentiated state (Petraki et al., 2015). The second wave of hematopoiesis in flies occurs post-embryonically in the lymph gland of larvae, a specialized hematopoietic organ of mesoderm origin, which is arranged in multiple paired lobes along the anterior part of the dorsal aorta (Lanot et al., 2001). The lymph gland harbors progenitors, differentiating and mature blood cells within distinct zones, the cortical zone (CZ) with mature hemocytes, the medullary zone (MZ) with progenitors and the posterior signaling center (PSC). PSC is thought to function as a stem cell niche to control the differentiation of all three effector types from progenitors (Jung et al., 2005). The PSC comprises a small cluster of about 30-40 cells and are mitotically inactive in the mature lymph gland. These cells are marked by high levels of the conserved member of the Early B-cell Factor (EBF) family of transcription factors, Collier/Knot (Col/Kn) that controls PSC specification and cell numbers, the expression of the homeobox protein Antennapedia (Antp) and the absence of Ultrabithorax (Ubx) expression (Krzemien et al., 2007; Krzemien et al., 2010; Mandal et al., 2007; Boulet et al. 2021; Rodrigues et al. 2021; Kanwal et al. 2021). Genetic ablation experiments showed that the PSC is dispensable for blood cell progenitor maintenance but vital for induction of lamellocyte formation (Benmimoun et al., 2015; Oyallon et al., 2016). Interestingly, PSC-like cells have been identified by single-cell RNA-sequencing (scRNA-seq) among circulating blood cells of larvae and adults (Cattenoz et al. 2020; Tattikota et al. 2020; Fu et al. 2020; Li et al. 2022). In the adult, these PSC-like cells can proliferate and differentiate to plasmatocytes in response to bacterial infection (Boulet et al. 2021).

Under normal conditions, progenitors in the lymph gland give rise to plasmatocytes and crystal cells. Both effector cell types are released into the circulation as the lymph gland dissociates at the onset of metamorphosis (Csordas et al., 2021). Thus, with the onset of pupation, both embryo and lymph gland-derived blood cells mix together and populate the pupa. Recent advances in scRNA technologies further revealed a much larger diversity of the hemocytes present in the *Drosophila* larva as well as in the lymph gland and adult fly (Cattenoz et al., 2020; Cho et al., 2020; Fu et

al., 2020; Girard et al., 2021; Leitao et al., 2020; Li et al., 2022; Tattikota et al., 2020). Comparative analysis of these datasets showed important differences in the molecular signatures between hemocytes during embryogenesis and larval stages and further suggest an even increased complexity of hemocyte populations in metamorphosis and in adult flies (Cattenoz et al., 2021; Hultmark and Ando, 2022; Li et al., 2022; Liegeois and Ferrandon, 2020). Metamorphosis goes along with dramatic and systemic physiological changes that requires an integration of the innate immune system. In response to ecdysone, hemocytes rapidly upregulate cell motility and phagocytosis of apoptotic debris, and acquire the ability to chemotax to tissue damage. (Regan et al., 2013; Sampson et al., 2013; Sander et al., 2013). Bulk RNA-seq gene expression analysis recently uncovered thousands of genes that are differentially expressed in pupal hemocytes compared to larvae (Lehne et al., 2022). However, whether this striking differential expression pattern of pupal hemocytes might also reflect the differentiation of new hemocyte subtypes or cell types has not yet been addressed. Insights into heterogeneity of these activated hemocytes would, however, also shed light on how tissue clearance is regulated during development.

Here, we employ the scRNA-seq technology to characterize the molecular signatures of pupal hemocyte subpopulations in early stages of metamorphosis. Our data reveals the presence of different undifferentiated and specified hemocytes with distinct transcriptomic signatures and cellular functions including antimicrobial peptide production, proteasomal degradation, fatty acid oxidation, and phagocytosis. Cross-stage dataset analysis provides evidence that most pupal hemocyte populations display distinct transcriptomic profiles suggesting specific functions during metamorphosis. Among the pupal blood cell types, we identified a highly migratory and immune responsive PSC cell cluster that persists into the adult fly. Lineage tracing experiments analysis reveal that these plastic PSC cells are able to differentiate to lamellocytes in response to wasp infection. This displays the remarkable ability of a niche cell to differentiate in response to environmental cues.

Results

Drosophila pupal hemocytes display remarkable cellular heterogeneity

Recent comparative scRNA-seq analyses revealed cellular heterogeneity in the molecular signatures of *Drosophila* hemocytes but also important differences during

embryogenesis and larval stages (Cattenoz et al., 2021; Cattenoz et al., 2020; Fu et al., 2020; Girard et al., 2021; Hultmark and Ando, 2022; Leitao et al., 2020; Tattikota et al., 2020). Both, embryo and lymph gland-released hemocytes mix together at the onset of pupariation and persist into adulthood. Our recent bulk RNA analysis already revealed a highly differential expression profile in pupal hemocytes compared to larvae (Lehne et al., 2022). To analyze this mixed blood cell population in more detail, we used scRNA-seq technology to dissect the cellular heterogeneity of the total blood cells in *Drosophila* early pupa. We applied a high-throughput full coverage of transcripts approach using the SMART-Seq technology on the ICELL8 system (Figure 1A). (Shomroni et al., 2022). The use of the ICELL8 platform allows beside the use of flexible chemistry for library preparations on a one-nanowell chip reaction the analysis of living or fixed cells with a large range of sizes (Shomroni et al., 2022). Hemocytes were isolated from 2-10h APF pupae. Wild type live or fixed single cells were dispensed on the iCell8 platform (Figure 1A). After alignment to the *Drosophila* genome using STAR, downstream analysis and batch effects correction were performed using Seurat (Stuart et al., 2019). We filtered cells based on the number of detected genes as well as the percent of mitochondrial genes (Supplementary figure S1A). A total of 2811 high-quality cells from three replicates were used for subsequent cluster analyses. Using hierarchical clustering, we identified a total of 15 cell clusters. Two of these clusters revealed a large overlap of expressed markers and differential gene expression analysis failed to identify markers to discriminate between these clusters. We decided to merge these two clusters (resulting in the cluster “undifferentiated PL”). For the resulting 14 clusters we identified unique sets of differentially expressed genes (DEG, Figure 1B-C, supplementary data 1-2). All three datasets contributed to each of these 14 clusters (Supplementary figure S1B-D). The name of each cluster corresponds to the name of marker genes or to specific biological features (see subsequent GO term analysis, using DEGs in supplementary data 3-16).

Cellular identity is driven by transcription factor activity. To identify gene regulatory networks that characterize the clusters, we performed a regulon analysis using SCENIC (Aibar et al., 2017). SCENIC analysis highlights several populations of specific transcription factor activities (Figure 1D, supplementary data 17-18). 12 cell clusters showed significant expression of the pan-hemocyte markers *serpent* (*srp*) and *hemese* (*he*), but also to a varying extent of known pan-plasmatocyte markers

such as genes encoding the phagocytosis receptor NimC1 (antigen marker P1) and the scavenger receptor Croquemort (Crq) (Supplementary figure S1E). We did not observe a population expressing lamellocyte markers, as expected for non-infested animals (Supplementary figure S1E). Remarkably, we also did not identify a distinct crystal cell cluster in our dataset differentially expressing known transcription factors such as the Runt related transcription factor *lozenge* (*lz*) or *hindsight* (*hnt*) (Supplementary figure S1E). Compared to wandering third instar larvae we only found very few circulating Hnt-positive hemocytes in pupal hemolymph preparations suggesting that crystal cells represent a rare cell type in *Drosophila* pupae and adults as recently reported (data not shown, (Ghosh et al., 2015). Additionally, crystal cells may have been lost due to the sensitive nature of crystal cells, which tend to burst after bleeding (Bidla et al., 2007; Hultmark and Ando, 2022).

Two of the clusters contain non-hemocytes that express muscle or neuron specific DEGs and transcription factors, respectively (Supplementary figure S2A-D). Muscle- and neuron-specific cell clusters are characterized by increased activities of the transcription factors that specify or maintain muscle or neuronal identity such as *ase*, *onecut*, *Rbp6*, *SoxN*, *E(spl)m3-HLH*, *E(spl)m7-HLH*, *E(spl)mdelta-HLH* and *twi* (Supplementary figure S2E-L).

We previously identified several cytoskeleton and cell motility genes upregulated in pupal hemocytes using a bulk RNA-sequencing approach (Lehne et al., 2022). Among the top 50 of these genes, 37 genes showed cluster specific expression profiles (Supplementary figure S2M). Many of these genes were highly expressed in undifferentiated PL, the most abundant cell cluster we identified. This is plausible since bulk RNA-sequencing experiments tend to reflect the expression profile of the most abundant cell types. Another subset of these genes showed differential expression in OxPhos-PL or Adhesive-PL and Hydrolyzing-PL, suggesting that these populations change transcription profiles with the onset of pupariation to become motile. One gene, *tau*, was specifically detected in a cluster that we later identified as posterior signaling center (PSC) cells. Hemocyte extracts isolated from pupal stages contain the dissolved lymph gland cells, including PSC cells, in contrast to larval hemocyte extracts where the lymph gland is still intact. Thus, the upregulation of *tau* reflects differences of cell population composition at the onset of pupariation.

In order to examine which pupal hemocyte populations may correspond to hemocyte cell types identified in other developmental stages we examined cell type specific marker genes identified in other scRNA-seq studies (Cattenoz et al., 2020; Cho et al., 2020; Fu et al., 2020; Girard et al., 2021; Leitao et al., 2020; Li et al., 2022; Tattikota et al., 2020). Most of the pupal hemocyte populations indeed express marker genes suggesting that they correspond to specific larval, lymph gland and/or adult hemocyte populations (Supplementary Figure S3A, supplementary table 1). These similarities are discussed in more detail below.

Undifferentiated plasmatocyte subtypes with the potential to specify

Several clusters express higher levels of *srp* and SCENIC revealed higher *srp* activity levels in these clusters (undifferentiated PL, transitory PL1-2, Osiris-PL and Secretory-PL; figure 2A-B). Expression analysis of a *srp* Gal4 promoter trap that we expect to reflect *srp* mRNA levels confirmed that *srp* expression is heterogeneous in hemocytes (Figure 2C). In contrast, a *srp* exon trap, which allowed us to monitor Srp protein expression, showed little differences in Srp protein expression across hemocytes (Figure 2D). In the embryo, *srp* mRNA is high in undifferentiated prohemocytes and decreases during hemocyte differentiation (Rehorn et al., 1996). In contrast, Srp protein is expressed in all lymph gland hemocytes (Jung et al., 2005; Lebestky et al., 2000). Adult flies appear to have hemocyte populations with varying Srp protein levels (Ghosh et al., 2015) but the presence of a proliferating hemocyte precursor stage in adults has been refuted (Sanchez Bosch et al., 2019). Undifferentiated PL displayed the highest levels of *srp* expression and transcription factor activity (Figure 2A, B). According to the expression of markers identified in other studies this cluster corresponds to a larval plasmatocyte population (PL-0, Cattenoz et al., 2020; PLASM1; Leitao et al., 2020) and/or a lymph gland plasmatocyte population (PM1-2; Cho et al., 2020; PL2, Girard et al., 2021) as well as an adult plasmatocyte subtype (Plasmatocytes nAChRalpha3/troll (Li et al., 2022; Supplementary Figure S3A, supplementary table 1). Pseudotime trajectory and RNA velocity analysis have placed these clusters midway through the development from a precursor stage to highly specialized plasmatocyte cell types in both circulating larval hemocytes and lymph gland hemocytes (Cattenoz et al., 2020; Cho et al., 2020). We surveyed the expression of cell cycle genes to investigate whether *srp* high undifferentiated PL have proliferative potential and found that they display little

expression of M-phase specific genes, as all other hemocyte populations (Supplementary figure S3B). Taken together, *srp* high hemocyte populations correspond to the most undifferentiated hemocyte cell types in pupae but do not display an actively proliferating precursor stage. Consistently, undifferentiated PL expresses genes which encode proteins involved in hematopoiesis (Figure 2E).

Markers expressed in undifferentiated PL were also detected in other clusters with high *srp* expression (Figure 2F, E). This was particularly true for transitory PL-1. However, this cluster differs from undifferentiated PL by sharing markers with the low *srp* expressing cluster Spermatid-Marker-PL (Figure 2E, G-I), suggesting that transitory PL-1 could be a transition state towards a more specified plasmatocyte fate. To test this hypothesis using an unbiased approach, we applied pseudotime analysis using monocle3 (Trapnell et al., 2014). This method orders cells based on stepwise transcriptomic changes with the most undifferentiated state on one end and more differentiated states on the other end. Indeed, the pseudotime analysis located the undifferentiated PL cluster on one end of the trajectory, suggesting that these are the most undifferentiated plasmatocytes (Figure 2J-K). Transitory PL-1 located between undifferentiated PL and Spermatid-Marker-PL, confirming that it is likely a transition state during plasmatocyte specification. We also found transitory PL-2 to be a transition state towards the more differentiated AMP-PL state. The remaining high *srp* expressing clusters Osiris-PL and Secretory-PL were not identified as a transition states.

Despite overlapping marker genes, transitory PL-2 and Osiris-PL can be distinguished from undifferentiated PL by the expression of cluster specific markers and cluster specific transcription factor activity as well as the enrichment of distinct GO-terms (Figure 2E, L-M; supplementary figure S3C). The same was true for Secretory-PL, which we will revisit later. Osiris-PL expressed many genes important for immunity, providing further support that Osiris-PL are differentiated cells rather than undifferentiated cells (Figure 2E). Additionally, the Osiris-PL cluster is eponymously characterized by the expression of insect-specific gene family Osiris encoding putative transmembrane proteins linked to the development of resistance against a range of different plant and fungi toxins (Figure 2E)(Lanno et al., 2019; Smith et al., 2018; Trienens et al., 2017). The Osiris-PL cluster showed a characteristic increased activity of *invected* (*inv*), encoding a lineage specific homeodomain transcription factor that is specifically required for anti-fungal defense

(Supplementary figure S3D, E) (Jin et al., 2008). In addition, we identified increased activities of transcription factors selectively controlling a subset of JAK/STAT pathway target genes such as *ken and barbie* (Ekengren and Hultmark, 2001) that in turn regulates *slow border cells* (*slbo*) gene expression (Supplementary figure S3F, G). Interestingly, Osiris-PL did not express a gene profile suggesting that these cells correlate to a larval, lymph gland or adult cell population (see Supplementary Figure S3A, supplementary table 1). Thus, the Osiris-PL cluster might be a new cell population of specialized hemocytes specific for metamorphosis.

Identification of specialized plasmatocyte subtypes with distinct molecular signatures

We identified six types of *srp* low-expressing hemocyte populations with distinct markers and molecular signatures that indicate that these are specialized immune cells (Figure 3A-H). Many of these clusters were active for *Relish*, a well-known transcription factor that acts downstream of the immune deficiency (IMD) pathway, regulating antibacterial responses (Figure 3L; Imler and Hoffmann, 2000). Among them, we identified Spermatid-Marker-PL, Lsp-Bomanin-PL, OxPhos-PL, Chitinase-PL, Adhesive-PL, and AMP-PL.

The Spermatid-Marker-PL cluster expresses immunity genes and a high number of genes that have previously been identified in spermatids (Figure 3A, G). A cluster with similar marker gene expression has been identified among adult hemocytes but is absent in earlier stages, suggesting that Spermatid-Marker-PL specify during metamorphosis (compare supplementary figure S3A; supplementary table 1; Li et al., 2022). This cluster is further characterized by highly specific activity of several transcription factors including CG34367, CG11294 and HGTX (Figure 3J-L). Among the immunity genes we found a member of the conserved Niemann-Pick type C protein family (Npc2h) protein, which is involved in immune signaling, particularly in the recognition of pathogen related products such as lipopolysaccharides, lipid A, peptidoglycan and lipoteichoic acid (Shi et al., 2012). In addition, Spermatid-Marker-PL cluster is enriched for *CG42830* encoding a protein related to Akirins, which play a conserved central role in immune gene expression in insects and mammals, linking the SWI/SNF chromatin-remodeling complex with the transcription factor NF-kappaB (Goto et al., 2008). Furthermore, we identified *milkah* (*mil*) as cluster-specific

marker encoding a conserved nucleosome assembly factor of the Nap family involved in spermatogenesis and long-term memory formation (Dubnau et al., 2003; Kimura, 2013). Interestingly, the human homologue, NAP1L has been implicated in stress response and apoptosis through control of the NF-kappaB pathway acting on the anti-apoptotic Mcl-1 gene (Tanaka et al., 2017). Recent studies identified NAP1L as a novel prognostic biomarker associated with macrophages promoting hepatocellular carcinoma (Shen et al., 2022). Spermatid-Marker-PL also display high expression of *TrxT* encoding the cytoprotective thioredoxin against oxidative stress which is also a known conserved marker for inflammatory macrophages. This further suggests that Spermatid-Marker-PL represents an immune-active plasmatocyte population (El Hadri et al., 2012; Itoh and Bryson, 2018).

Lsp-Bomanin-PL expresses several genes encoding larval serum proteins like Lsp1alpha and its receptor Fbp1 (Figure 3B, G). Plasmatocyte populations expressing these genes have previously been identified in larvae (Cattenoz et al., 2020; Fu et al., 2020) and consistently, we can identify a larval plasmatocyte cluster (PL-Lsp; Cattenoz et al., 2020) and Lsp+ (Fu et al., 2020) with a corresponding expression profile (compare supplementary figure S3A; supplementary table 1). Other genes expressed by Lsp-Bomanin-PL include Bomanin genes like *BomS3* and genes encoding secreted anti-fungal and antibacterial peptides such as *Drosomycin* (*Drs*) or *Drosomycin-like 5* (*Drs-5*) (Figure 3G). Overall, a GO-term analysis revealed an enrichment for genes important for the defense response to Gram-positive bacteria (Figure 3H). Further, these cells expressed several genes whose products are secreted from the fat body including stress-induced humeral factors such as Turandot A and B (TotA, TotB) and the coagulation factor encoding *fondue* (*fon*; Figure 3G; Bajzek et al., 2012, Ekengren and Hultmark, 2001).

Thus, the gene expression profile of Lsp-Bomanin-PL partially resembles fat body cells. However, this cell cluster is different from the fat body as it expresses all known hemocyte markers including *srp*, *He*, Pxn and *crq* (Supplementary figure S1E) and its overall gene expression profile correlates well with the other plasmatocyte cell clusters (Supplementary figure S4A). Further, we used ICELL8 imaging data to confirm that the nuclei of these cells were not significantly bigger than other hemocyte populations (27,76 px for Lsp-Bomanin-PL in comparison to 31,97 px for all other plasmatocytes), as one would expect from a fat cell population. Hence, this

cell type represents plasmatocytes of larval origin with the expression of fat body specific genes.

OxPhos-PL contained mostly cells from dataset2 (Supplementary figure S1C-D) and expressed fewer genes than other plasmatocyte clusters (Figure S4B). However, the number of detected UMIs as well as the percentage of mitochondrial genes were similar (Fig. S4C-D), leading us to keep this cluster as high-quality cells. In agreement, a cell type with a similar expression pattern is present among larval circulating hemocytes (PM12, Tattikota et al., 2020; supplementary figure S3, supplementary table 1. OxPhos-PL show a striking increased expression of several genes involved in mitochondrial oxidative phosphorylation system (OXPHOS, figure 3G, H). This cluster also specifically expresses genes encoding several ribosomal proteins (Figure 3G) which might reflect an important cross-regulatory mechanism between mitochondrial energy production and increased ribosomal assembly and translation as recently described for macrophage tissue invasion in the *Drosophila* embryo (Emtenani et al., 2022). For professional phagocytes, sufficient ATP as the critical energy source is even required to drive endocytic and phagocytic processes, especially at the onset of metamorphosis when plasmatocytes encounter and clear apoptotic cells from massive larval tissue histolysis. Interestingly, OxPhos-PL plasmatocytes show an increased expression of genes encoding known actin nucleators and actin-binding proteins required for phagocytosis such as single subunits of the WAVE regulatory complex (WRC; HSPC300) and the Arp2/3 complex (Arpc4) suggesting a role of this cluster in the clearance of the larval body during metamorphosis (Figure 3G). OxPhos-PL also strongly expresses the Ribonuclease Kappa (RNASEK) encoding a V-ATPase-associated factor involved in clathrin-mediated endocytosis of large cargo, such as viruses (Hackett et al., 2015; Perreira et al., 2015).

Chitinase-PL show *abd-A* activity and express high levels of immunity relevant genes such as persephone (psh) and spirit which encode serine proteases , but also diverse genes encoding regulators of the Toll signaling pathway including *windbeutel* (*wbl*), *Gram-negative bacteria binding protein 3* (*GNBP3*), *Gamma-interferon-inducible lysosomal thiol reductase 1* (*GILT1*), *Transferrin 1* (*Tsf1*) and *Thioester-containing protein 2* (*Tep2*) that mediate the cellular immune response to bacteria

(Figure 3G, M). The characteristic high expression of *Cht6* encoding a chitinase, an evolutionarily conserved enzyme involved in ecdysis, organization of the exoskeletal barrier, but also in immune defense in vertebrates, prompted us to name this cluster accordingly (Figure 3G). Recent studies further revealed that the functions of chitinases are not exclusive to catalyze the hydrolysis of chitin producing pathogens, but also include a crucial role in bacterial infections and inflammatory diseases (Di Rosa et al., 2016). Interestingly our GO-term analysis not only identified the enrichment of genes involved in innate immune response but also an increased expression of genes implicated in cell-cell adhesion and septate junction assembly (Figure 3H), a special feature that we could already observe in our previous bulk RNA seq analysis of pupal hemocytes (Supplementary figure S2M, (Lehne et al., 2022). Septate junction (SJ) proteins play an essential role in regulating hematopoiesis in the *Drosophila* lymph gland, but might be also essential for an effective response to parasitic wasp attack (Khadilkar et al., 2017) (Williams, 2009). Lamellocytes are known to encapsulate wasp eggs by forming an encapsulation epithelium sealed by SJs that protects the larval tissue (Russo et al., 1996). Hence, Chitinase-PL might assume similar functions.

Similar but even more prominent, the Adhesive-PL cluster expresses several genes implicated in cell-cell adhesion prompting us to name this cluster accordingly (Figure 3G, supplementary figure S4E). The expressed markers range from cadherin-encoding genes like *shotgun* (*shg*), *echinoid* (*ed*) *cad87A*, *fat* (*ft*) to *Fasciclin 3* (*Fas3*), *prickle* (*pk*) and *piopio* (*pio*) known to be involved in epithelial cell polarity. Interestingly, the Adhesive-PL cluster is characterized by low levels of *Atilla* and *Cherrio* expression (compared to other clusters, supplementary figure S1E) and might be an intermediate state with the potential to transdifferentiate into terminally differentiated lamellocytes as recently described (Anderl et al., 2016; Csordas et al., 2021)

AMP-PL express a high number of immunity genes and our GO-term analysis revealed an enrichment in genes involved in defense to Gram positive bacteria (Figure 3G, H). Among the immunity genes we identified a large repertoire of AMP-encoding genes like *Attacin-A*, *Attacin-B*, *Drosomycin-like 1*, *Drosomycin-like 6*, *Cecropin A*, *Cecropin B* and *Drosocin* (Figure 3H). Several of these genes, those encoding Cecropins in particular, have been identified as markers of larval (PL-AMP,

(Cattenoz et al., 2020) and adult plasmatocytes (plasmatocytes Cec and other immunity genes high, (Li et al., 2022; supplementary figure S3A; supplementary table 1). However, AMP-PL show an increased number of ecdysone inducible genes involved in pupal morphogenesis (*Eig71Ek*, *Eig71Ej*, *Eig71Ec*, *Eig71Ef*, *Eig71Eh*, *Eig71Eb*) (Figure 3G) (Wright et al., 1996). AMP-PL also express several genes encoding extracellular matrix components, including salivary gland secretion proteins (Sgs) which are also induced by ecdysone (Figure 3G) (Lehmann, 1996). This suggests that the gene expression profile of AMP-PL changes upon metamorphosis. These pupal AMP-PL may therefore assume a pupa-specific function.

Secretory-PL are among the *srp*-high expressing clusters but without any descending clusters (Figure 2A-B, J-K). This cluster expresses some markers identified in circulating larval blood cells (PL-Pcd, (Cattenoz et al., 2020; Thanacytes; Fu et al., 2020; supplementary figure S3A; supplementary table 1), suggesting that it may be of embryonic origin. This cluster expresses many genes encoding proteins involved in proteolysis with annotated serine-type endopeptidase activity (*CG30098*, *CG31174*, *CG30083*, *CG18636*, *CG14088*) and the intracellular membrane system as well as protein export, inspiring us to name this cluster Secretory-PL (Figure 4A-E, Supplementary figure S5A). SCENIC further identified high activity of cAMP response element binding (CREB) protein CrebA a transcription factor regulating components of the secretory pathway (Johnson et al., 2020; figure 4F). In addition, target genes of *dorsal*, encoding the executive transcription factor downstream of Toll signaling pathway were highly expressed in Secretory-PL, confirming the importance of this cell type in innate immunity (Figure 4G).

Secretory-PL expresses a highly distinct set of marker genes and shared some marker genes with another cluster that we later identified as PSCs (Figure 4B-E). Shared markers included *Tep4*, *Ance* and *ham* (Figure 4B-D). Using Gal4-enhancer traps and GFP-exon traps for these genes we identified two morphologically distinct cell types: plasmatocyte-shaped cells and small spiky cells (Figure 4H-K). In contrast, *CG31174*, which was not detected in PSCs in our bioinformatic data (Figure 4A) was solely detected in cells with a normal plasmatocyte morphology (Figure. 4K). To confirm that these morphologically different cells are indeed transcriptomic distinct cell types, we co-labeled CG31174 with Tep4 and indeed, while plasmatocyte-shaped cells co-expressed both markers, small spiky cells were never CG31174 positive. Thus, Secretory-PL are plasmatocytes with a classical cellular morphology

(Figure 4L). *CG31174* has been recently shown to be expressed in crystal cells (Fu et al., 2020). We did not detect any classical crystal cell markers in the Secretory-PL cluster (Supplementary figure S1E) and neither larval nor pupal CG31174 cells with plasmatocyte morphology express the crystal cell marker Hnt. As mentioned above, we detect a very low number of crystal cells in pupal bleeds. Among the six replicates of pupal bleeds in which we stained CG31174 cells with Hnt, representing about 3000 blood cells, we identified one CG31174 positive cell that was Hnt positive. This cell displayed crystal cell morphology. In larval bleeds, CG31174 cells with crystal cell morphology and positive for Hnt were more abundant (data not shown). Thus, CG31174 is expressed in crystal cells, as recently reported (Fu et al., 2020). However, the pupal CG31174 positive cell cluster represents a plasmatocyte cell type distinct from crystal cells. To further confirm that Secretory-PL are distinct from crystal cells, we made use of datasets available in public single cell databases from various stages (Cattenoz et al., 2020; Cho et al., 2020; Li et al., 2022), merged and batch corrected the data with our dataset (Supplementary figure S5B). As suggested by the large shift in gene expression detected in our bulk RNA-sequencing analysis, pupal hemocytes were largely located on a distinct region in the resulting UMAP-plot (Supplementary figure S5C). This confirms that pupal hemocytes are, indeed, transcriptomically distinct from other stages. Due to the availability of cell annotation, we were able to map larval as well as adult crystal cells identified by the authors (Cattenoz et al., 2020; Li et al., 2022). While larval and adult crystal cells located on the same region in the UMAP plot, Secretory-PL located differently, confirming that Secretory-PL are different from crystal cells (Supplementary figure S5D-F).

In addition to these major plasmatocyte clusters, our scRNA-seq also identified a small cell cluster that expresses a very unique set of markers, including the early hemocyte marker *srp*, but without detectable levels of more mature hemocyte markers like *He*, *Pxn* and *crq* (Figure 2A, E, S1E, GO-term analysis in S6A). Remarkably, this cell cluster expresses striking markers of the posterior signaling center (PSC) present in the lymph gland, such as the transcription factors encoding gene *knot/collier* (*kn*) (Makki et al., 2010) and the recently identified new PSC marker such as *tau* (Cho et al., 2020) (Figure 5A-D). *kn* is also expressed in a subset of cells in the posterior lymph gland, which have not yet been subjected to scRNA-seq (Benmimoun et al., 2015; Kanwal et al., 2021; Rodrigues et al., 2021). However, in

contrast to posterior lymph gland cells, PSC cells express Antp but do not express Ubx (Benmimoun et al., 2015; Boulet et al., 2021; Kanwal et al., 2021; Rodrigues et al., 2021). In agreement with a lymph gland PSC origin, the PSC cluster expresses *kn*, *tau*, Antp but not Ubx (Figure 5D). Both, Antp as well as Kn were also active in the PSC cluster according to SCENIC analysis (Figure 5E-F). We queried datasets containing larval, lymph gland and adult hemocytes and found a corresponding cluster in each stage (Supplementary figure S6B-D) (Cattenoz et al., 2020; Cho et al., 2020; Fu et al., 2020; Girard et al., 2021; Li et al., 2022). PSCs can be found in the lymph gland and the identification of PSC-like cells in adults suggests that PSCs persist throughout life (Boulet et al., 2021; Li et al., 2022). The identification of PSC-like cells among larval hemocytes from embryonic origin was, however, unexpected. It has previously been suggested that PSC-like cells of embryonic origin are plasmatocytes with PSC-like expression pattern(Cattenoz et al., 2021; Cattenoz et al., 2020). To test whether these cells are indeed distinct from PSCs, we performed cross-stage data integration using datasets for each developmental stage (Cattenoz et al., 2020; Cho et al., 2020; Li et al., 2022). We found that pupal and adult PSCs localize at the same region on the UMAP plot with larval PSC-like PL-Impl2 cells (Supplementary figure S6E-G). While the pupal dataset did not provide cell annotations, we also identified cells from the lymph gland dataset localizing with other PSC-like cells, suggesting that these represent lymph gland PSCs. We then attempted to identify differentially expressed genes across stages of PSC cells, comparing pupal PSCs, adults Hml+ cells with PSC markers, larval PL-Impl2 cells and lymph gland derived cells localizing similarly on the UMAP plot. However, this analysis did not return any significant differences in gene expression among PSC cells from different stages. While this analysis is limited by a low number of cells across all datasets, this result suggests that PSCs remain transcriptionally stable upon lymph gland dissociation. Remarkably, the expression of PSC markers in circulating or sessile larval blood cells has not been confirmed yet (Cattenoz et al., 2020; Fu et al., 2020; Tattikota et al., 2020). Similarly, we could not identify any kn, tau or Antp positive cells in larval bleeds (data not shown). Thus, whether the identification of PSC-like cells in larval stages can be ascribed to issues during dissection or whether some PSC-like cells indeed dissociate from the lymph gland prior to metamorphosis or are specified from an independent source remains to be assessed. We noted that the amount of *kn*, *tau* or *Antp* positive cells with small, spiky

cell morphology exceeded the percentage of PSC cells we identified in our scRNA-seq analysis (0.569 % of cells). We assume that these small cells were lost during centrifugation steps with a higher likelihood than the larger plasmatocytes.

We further validated this distinct gene expression profile of PSC cells and characterized them morphologically in more detail. Using transgenic Gal4-enhancer traps and GFP-exon trap fly lines we found that PSC markers *kn*, *Antp* and *tau* labeled small spiky cells reminiscent of those cells observed by shared markers (*Tep4*, *ham*, *Ance*) labelling Secretory-PL (Figure 4H-L, 5G-J). This cellular morphology is reminiscent of the fusiform PSC-like cells identified recently in adults (Boulet et al. 2021). In contrast to tau, *kn* occasionally labels cells with a more plasmatocyte-like round morphology (Figure 5K). However, this population of *kn* positive plasmatocytes was less frequent than plasmatocytes labelled by the Secretory-PL marker CG31174, suggesting that they are distinct cell populations (Figure 5K). Indeed, co-staining with CG31174 further confirms that PSC cells are morphologically very distinct from Secretory-PL (Figure 5G).

Since *kn* is not only expressed in the PSC but also in the MZ and posterior lobes (Benmimoun et al., 2015; Boulet et al., 2021; Kanwal et al., 2021; Rodrigues et al., 2021), additional *kn* positive cells with plasmatocyte morphology might derive from the MZ or posterior lobes. In contrast, the tau-GAL driver exclusively labeled a subset of cells in the PSC region of the primary lobe of the lymph gland (Figure 5L, L', L''), suggesting that tau is indeed a PSC specific marker gene as recently proposed (Cho et al., 2020).

PSC cell cluster can differentiate into lamellocytes upon wasp infestion

Independent of its role in stem cell maintenance in the lymph gland, the PSC is also required for the induction of lamellocyte formation (Crozatier et al., 2004; Krzemien et al., 2007; Lebestky et al., 2000; Mandal et al., 2007). Next, we addressed whether PSC cells are capable of blood cell differentiation and can respond to parasitoid wasp infection. 48 hours after egg transfer, female wasps were added into vials for infection treatments and allowed to infect larvae. Lamellocytes are identified as large flat cells with a very prominent dense actin cytoskeleton meshwork (Figure 6A). Indeed, induced lamellocytes could be also marked by *kn* expression in pupae (Figure 6A, A'). To test whether these lamellocytes could also derive from PSCs, we

made use of the G-TRACE (GAL4 Technique for Real-time And Clonal Expression) lineage tracing system (Figure 6B)(Evans et al., 2009). This method uses a cell type specific Gal4 driver and a UAS-RFP construct to mark Gal4 positive cells with RFP. Gal4 also induces Flp expression, which removes the stop codons in a ubi-FRT-Stop-FRT-GFP construct, resulting in stable GFP expression. Hence, Gal4 positive cells are RFP and GFP positive, while offspring cells are GFP positive but RFP negative.

Using *kn*-Gal4 to drive G-TRACE we observed small RFP+/GFP+ cells with the PSC specific spiky morphology (Supplementary Figure S7A-A'''). In addition, we detected GFP+/RFP- cells with plasmatocyte-like morphology (Supplementary Figure S7A-A'''). This indicates that *kn* positive posterior lobe cells cease to express *kn* after dissociation from the lymph gland. After wasp infestation we additionally detected GFP+/RFP- cells with prominent lamellocyte morphology (Figure 6C-C'''). As these cells were always RFP-, either the GFP+/RFP+ PSCs or the GFP+/RFP- plasmatocytes with presumably posterior lymph gland lobe origin may be the precursors for these lamellocytes. To determine whether PSCs could indeed transdifferentiate into lamellocytes we also applied the *tau*-Gal4 driver, which we do not detect outside the PSC niche (compare also Figure 5L-L''). Supporting this notion, *tau* driven G-TRACE marks small, spiky PSC cells with both GFP as well as RFP (Supplementary Figure S7B-B'''). Remarkably, upon wasp infestation, we further identify GFP+/RFP- cells with a distinct lamellocyte morphology (Figure 6D-D'''). This confirms that the cells of the PSC cluster are able to differentiate into lamellocytes upon parasitoid infection and suggests that the PSC apart from being a lymph gland hematopoietic niche also functions as a cell reservoir to pupal and adult blood cells.

PSC cells are migratory immune responsive cells persisting into adult

To better characterize PSC cells *in vivo*, we used the *kn*-Gal4 as well as *tau*-Gal4 drivers to perform live-cell imaging in developing pupae (Figure 7). While kn-Gal4 also occasionally marks plasmatocytes (Figure 5K), our in-depth analysis of different PSC markers allowed us to determine that PSCs are smaller with a distinct morphological shape. We therefore focused our analysis on cells with the typical PSC morphology. High-resolution spinning disc live cell imaging microscopy of 4h APF old pupae revealed migrating single *kn*-marked and *tau*-marked PSC cells that form polarized dynamic lamellipodial protrusions and start to redistribute from the

dorsal patches of the body wall as similarly observed for plasmatocytes (Figure 7A, B, C; Supplementary movie M1, M2) (Lehne et al., 2022; Sander et al., 2013). PSC cells are highly motile but much smaller as compared to *hml*-marked plasmatocytes (Supplementary movies M1). This difference in cells size becomes more evident in later pupal development (> 16h APF) when cell dispersal in the pupa is further advanced and cell numbers are increased (Supplementary movie M3). Compared to *hml*-marked plasmatocytes, which are more evenly distributed in the whole developing pupa, *kn*-marked PSC cells become more restricted to the abdomen during pupal development until hatching (compare stages 4h APF and 16h APF in Figure 7 D, D' and E, E'). Remarkably, cells marked either by *kn*-Gal4 or *tau*-Gal4 are not only highly motile, but also immune-responsive as shown by laser-ablation wounding experiments (Figure 7F, G, supplementary movie M3, M4 and M5). Upon wounding cells switch from random to directed migration towards the wounding site as indicated (Figure 7D, E). No significant differences in directionality were found between *kn*-positive cells and *hml*-marked plasmatocytes as quantified by measuring the cell bias angle (Figure 7F). We also visualized migrating *tau*-marked PSC cells in the living prepupae and 16h APF old pupae which look morphologically exactly the same as *kn* positive cells (Figure 7, supplementary movies M3). *tau*-marked PSC cells are also cable to phagocytose cell debris upon wound damage and in rare cases we observed dividing tau-positive cells (Supplementary movie M5). The overall number of cells marked by tau-Gal4 in 16h APF old pupae are significantly lower than those marked by the *kn*-Gal4 driver. This reflects the presence of *tau*-marked PSC cells in contrast to *kn*-marked PSC cells as well as posterior lymph gland cells, a cell population which has been recently designated as the posterior lobe signaling center (PLSC; Kanwal et al. 2021).

Combined, these data strongly suggest a dual function of PSC cells in *Drosophila* hematopoiesis. Apart from its well-known important function as larval hematopoietic progenitor niche, PSC cells can function as tissue resident immune-responsive cell reservoir with limited phagocytic ability but still capable of blood cell differentiation upon immune challenge later in development. Our data also further highlight a second new pupal blood cell type derived from the posterior lobe signaling center persisting to adulthood.

Discussion

In this study we present a comprehensive single-cell transcriptome analysis of *Drosophila* pupal hemocytes at the onset of metamorphosis when larval structures are degraded and replaced by adult tissues and organs. This developmental stage represents a striking example of dramatic and systemic physiological changes that requires an integration of the innate immune system. In response to ecdysone, hemocytes rapidly upregulate cell motility and phagocytosis of apoptotic debris, and acquire the ability to chemotax to tissue damage (Regan et al., 2013; Sampson et al., 2013; Sander et al., 2013). At this early stage of metamorphosis (2-10 h APF), the primary lobes of the lymph glands have disintegrated but the posterior lobes are largely intact (Rodrigues et al., 2021). In agreement, we do not identify a hemocyte cluster with expression patterns described for posterior lobe cells (eg. *kn*+, *Ubx*+, *Antp*-). While we cannot exclude the presence of posterior lymph gland lobe cells in our data, comparative marker analyses suggest that our study is well comparable with previous scRNA-seq studies which have covered hemocytes of embryonic origin or the primary lymph gland lobe but disregarded the posterior lymph gland lobes (Cattenoz et al., 2020; Cho et al., 2020; Fu et al., 2020; Girard et al., 2021; Leitao et al., 2020; Tattikota et al., 2020).

Recent bulk RNA-seq analysis revealed 1542 differentially regulated genes, from which 804 genes are up-regulated in pupal hemocytes compared to quiescent larval hemocytes (Lehne et al., 2022). These striking differences in the global gene expression likely reflect both transcriptional changes of embryo-derived hemocytes and the emergence of new progenitor-derived hemocytes of the lymph gland since both hemocyte lineages mix together and disperse in the pupa (Holz et al., 2003). Consistently, our single cell RNA-seq data analysis revealed both cell clusters common in other stages of hematopoiesis and new subgroups appearing with the onset of metamorphosis and persisting into adulthood. The most abundant *srp*-high expressing undifferentiated PL represents a good example for a cluster present across all stages of hematopoiesis, annotated as PL-0 or PLASM in larvae (Cattenoz et al., 2020; Leitao et al., 2020), as PM1/PM2 or PL2 in lymph glands (Cho et al., 2020; Girard et al., 2021) and as nAChRalpha3/trol-high in adult flies (Li et al., 2022). Undifferentiated PL contain unspecified cells with a broad gene expression profile. However, these cells are committed to the plasmatocyte fate and are likely able to differentiate towards more specialized fates. Undifferentiated PL appear to not

display a proliferative precursor stage comparable to *srp* high embryonic prohemocytes (Rehorn et al., 1996). This is in agreement with the recent finding that adult flies are devoid of a prohemocyte stage and do not display active hematopoiesis and suggests that active hematopoiesis ceases in larval stages (Sanchez Bosch et al., 2019). Lsp-Bomanin-PL correlate with the comparable PL-Lsp and Lsp+ clusters in larvae (Cattenoz et al., 2020; Fu et al., 2020), however, no correlations are found in lymph glands or adult suggesting that this cell population derives from the embryonic/larval lineage with distinct functions in metamorphosis. By contrast, Spermatid-Marker-PL only has a common expression profile with the Hml+ with sperm markers cluster found in adults (Li et al., 2022) suggesting that it represents an immune-active plasmatocyte population with important functions beyond metamorphosis.

Remarkably, some plasmatocyte clusters do not correlate to larval plasmatocytes from either embryonic or LG origin, which highlights the diverse hemocyte functions during pupal development. The Chitinase-PL and Adhesive-PL clusters might represent such effector cells both sharing an increased expression of several genes implicated in cell-cell adhesion and septate-junction formation required for encapsulation of parasitic wasp egg. Most known parasitoid wasp species attack the larval or pupal stages of *Drosophila*. While *Trichopria* drosophilae infect the pupal stages of the host, females of the genus *Leptopilina* and *Ganaspis* attack the larval stages (Chen et al., 2018; Small et al., 2012). Core components of Toll pathway are highly upregulated in Adhesive-PL that control the immuno-genetic circuit of host immune response against parasitoid wasp attack by activating the NF-kappaB transcription factor, *Dorsal*. Future high-resolution live-imaging combined with genetics will be further required to dissect in more detail how these newly identified plasmatocyte effectors contribute to this fascinating process of encapsulation. Another example is the Osiris-PL cluster, for which we could not identify correlating cell types in any other developmental stage.

Besides the identification of new specialized plasmatocyte subpopulations that first appear during pupal development, we identified a small group of immune cells that resembles the PSC, a well-known stem cell niche that controls the differentiation of effector types from progenitors in the lymph gland, but also participate in the larval response to wasp parasitization (Banerjee et al., 2019). PSC cells are clearly

distinguished by their co-expression of Antp and Collier/knot from other regions within the lymph gland (Crozatier et al., 2004; Lebestky et al., 2000; Mandal et al., 2007) and we confirmed tau as an additional specific marker. Previous work has shown that PSC cells reside in the lymph gland and provide signals to regulate progenitor maintenance or differentiation (Crozatier et al., 2004; Krzemien et al., 2007; Lebestky et al., 2000; Mandal et al., 2007). Recently, circulating PSC-like cells have been identified in the adult fly and the presence of larval circulating PSC-like cells has been suggested, although the presence of such a cell type remains to be proven *in vivo* (Boulet et al., 2021; Cattenoz et al., 2020; Fu et al., 2020; Tattikota et al., 2020). In this work, we identified PSC cells from the hemolymph of early pupa that are characterized by the expression of Antp and Collier (Kn), but also by the recently identified new PSC markers such as Tau (Fu et al., 2020). High-resolution live-imaging microscopy analysis using kn-Gal4 and tau-Gal4 enhancer traps further confirmed the existence of single motile and immune-responsive PSC cells persisting throughout pupal development, thus, far longer than described for progenitor cells from histolyzing lymph glands (Rodrigues et al., 2021).

Our lineage tracing results demonstrate that pupal PSC cells are able to differentiate into lamellocytes in response to wasp infection. While *kn* positive cells contain PSCs as well as other immune cell populations (Benmimoun et al., 2015; Boulet et al., 2021; Ghosh et al., 2015), the identification of *tau* as a specific marker for PSCs allowed us to determine the PSCs as the cell pool transdifferentiating into lamellocytes. Further, adult PSC-like cells have been shown to transdifferentiate into plasmatocytes upon bacterial infection (Boulet et al., 2021). While the importance of PSC cells as stem cell niche in larval hematopoiesis has been extensively proven, the existence as well as relevance of circulating PSC cells was unclear (Hultmark and Ando, 2022). Our results corroborate recent findings that PSC cells also serve as a reservoir for blood cells upon immune challenges and show that this function is not limited to the adult stage (Boulet et al., 2021).

In summary, this study identified new pupal undifferentiated and differentiated effector hemocytes with distinct molecular signatures and cellular functions clearly distinct from other stages of hematopoiesis. Our data further uncovers an additional route for lamellocyte differentiation. Besides the transdifferentiation from existing

plasmatocytes or from differentiating lymph gland prohemocytes, we provide first evidence that PSC cells can differentiate into lamellocytes. This work will allow future genetic studies to better understand immune cell plasticity and function during metamorphosis and innate immunity.

Experimental procedures

Drosophila Genetics

Fly husbandry and crossing were carried out according to the standard methods. Crosses were maintained at 25°C. The following fly lines were used: *hml*-DsRed (D. Siekhaus), srpHemo-3xmCherry (Gyoergy et al., 2018); srp-GFP (VDRC 318053); *hml* -Gal4, UAS-eGFP (Sinenko and Mathey-Prevot, 2004); UAS-eGFP (BL 6874). tep4-Gal4 (BL 76750), Ance^{MiMiC}-GFP (BL 59828), kn-Gal4 (BL 67516), pcol85-Gal4 (Crozatier et al., 2004), Antp-Gal4 (BL 26817), ham(GMR80G10)-Gal4 (BL 40090), tau-Gal4 (BL 77641), CG31174^{MiMic}-GFP (BL 24040); UAS-mCherry-NLS (BL 38425). G-TRACE (UAS-RedStinger, UAS-FLP, Ubi-p63E(FRT.STOP)Stinger) (BL 28281). For wasp infection, flies were transferred into a fresh food vial and placed at 25°C for 48h. Flies were then removed and larvae submitted to egg laying by wasps of the species *Leptopilina boulardi,* strain G486. Wasps were removed before dissecting pupae as described below.

Isolation of Drosophila hemocytes for single-cell RNA-sequencing

50-60 2-10h APF pupae were collected and washed in 1 x PBS. The pupae were then transferred to 1 x Schneider´s *Drosophila* medium (Gibco) supplemented with 10% FBS, 50 units/mL penicillin, and 50 µg/mL streptomycin and opened using forks to rinse out the hemolymph. Cells were filtered through a 50-µm cell strainer and collected in a total volume of 500 µL. Subsequently, centrifugation at 500 x g and 4°C for 20 minutes was performed. The supernatant was discarded, and the pellet was resuspended with 500 µL PBS + 0.01 % BSA for single-cell sequencing of live cells. For fixed samples, the previous pellet was resuspended with 100 µL 1 x PBS and subsequently fixed by adding 4 volumes of ice-cold 100% methanol (final concentration of 80% methanol in PBS) and thoroughly mixed with a pipette. Cells were stored at -20°C until use (1-3 days). For single-cell sequencing, cells were moved to 4°C and kept on ice throughout the procedure. Fixed cells were pelleted at

500 x g for 15 minutes and rehydrated in 500 µL PBS + 0.01 % BSA. For datasets 1 and 2 we used fixed samples, while we used live cells for dataset 3.

Single-cell RNA-sequencing of Drosophila pupal hemocytes

The Takara ICELL8 5,184 nano-well chip was used with the full-length SMART-Seq ICELL8 Reagent Kit. Cell suspensions were fluorescent-labelled with live/dead stain, Hoechst and propidium iodide (NucBlue Cell Stain Reagent, Thermo Fisher Scientific) for 15 min prior to their dispensing into the Takara ICELL8 5,184 nano-well chip. CellSelect Software (Takara Bio) was used to visualize and select wells containing single and live cells. Next, cDNA was synthesized via oligo-dT priming in a one-step RT-PCR reaction. P5 indexing primers for subsequent library preparation were dispensed into all wells receiving a different index, in addition to Terra polymerase and reaction buffer. Transposase enzyme and reaction buffer (Tn5 mixture) were dispensed to selected wells. P7 indexing primers were dispensed to wells. Final Illumina libraries were amplified and pooled as they were extracted from the chip. Pooled libraries were purified and size selected using Agencourt AMPure XP magnetic beads (Beckman Coulter) to obtain an average library size of 500 bp. A typical yield for a library comprised of ~ 1,300 cells was ~ 15 nM. Libraries were sequenced on the HiSeq 4000 (Illumina) to obtain on average ~ 0.3 Mio reads per cell (SE; 50 bp). A list of Gal4-enhancer trap and GFP-exon trap fly lines used for ex vivo validation can be found in Supplementary data 19.

Bioinformatic analysis

Raw sequencing files (bcl) were converted into a single fastq file using Illumina bcl2fastq software (v2.20.0.422) for each method. Each fastq file was de-multiplexed and analyzed using Cogent NGS analysis pipeline (CogentAP) from Takara Bio (v1.0). In brief, “cogent demux” wrapper function was used to allocate the reads to the cells based on the cell barcodes provided in the well-list files. Subsequently, “cogent analyze” wrapper function performed a preliminary analysis, including: read trimming with cutadapt (version 3.2); genome alignment to Drosophila M. Version 103 using STAR (version 2.7.2a); read counting for exonic, genomic and mitochondrial regions in Drosophila M. genes from ENSEMBL gene annotation version 103 using featureCounts (version 2.0.1); and summarizing the gene counts into gene matrices with number of reads expressed for each cell in each gene. Raw

gene matrices underwent quality-control filtering for cells and genes using the following parameters: for cells, only those with at least 10,000 reads associated to at least 300 different genes were kept, and for genes, only those containing at least 100 reads mapped to them from at least 3 different cells were kept. Subsequent analyses were performed using Seurat v4.1.1 in Rstudio 2022.02.2. Low-quality cells were filtered out based on the number of detected genes and percentage of mitochondrial genes (Supplementary figure S1A). Batch correction between the three replicates was performed, UMAP coordinates were calculated and unsupervised clustering was perfomed with 16 dimensions and the default resolution factor. Clustering was controlled by testing for sufficient distinct marker genes using the FindAllMarkers() command and two clusters were merged due to insufficient distinct markers (resulting in Precursor-PL-1) (Script 1). Pseudotime analysis was performed using monocle3 v1.0.0 using UMAP coordinates calculated with Seurat v4.1.1 and with learn_graph_control = list(ncenter=480) in the learn_graph() command (Script 2). SCENIC analysis was performed with SCENIC v1.3.1 using the cisTarget v8 motif collection mc8nr (Script 3). For a GO-term analysis we used differentially expressed genes identified using FindMarkers(). Gene names were converted to FlybaseIDs and analysed with DAVID 2021. Cross-dataset analysis was performed using Seurat v4.1.1 including batch correction and UMAP calculation (Script 4). Scales in Seurat expression plots and maps display the expression in $\log((\text{UMI} + 1/\text{total UMI})\times 10^4)$. To determine M-phase gene expression, we monitored the expression of the M-phase specific genes *polo*, *aurB*, *Det* as applied in (Cho et al., 2020) .

Data and Code availability

Raw data is available at GEO with the accession number GSE216339. Output files as well as data associated with figures are published as Supplementary data files. In addition, the final processed data will be made available for download from Mendeley as a .rds file. To allow easy use of this file, we provide Script 5, which aims to guide users without prior knowledge in R. Code used in this study is submitted in Scripts 1-4 and any further details can be obtained upon request.

Immunohistochemistry

Pupal macrophages were isolated as described previously (Lehne et al., 2022). In short, white to light brownish prepupae (2-4h APF) were collected and washed in 1 x

PBS. The prepupae were then transferred to 1 x Schneider´s *Drosophila* medium (Gibco) supplemented with 10% FBS, 50 units/mL penicillin, and 50 µg/mL streptomycin and opened using forks to rinse out the hemolymph. Cells were spread on glass coverslips, previously coated for 30 minutes with ConcanavalinA (0.5 mg/mL, Sigma), for 1 h at 25°C. The supernatant was removed and adherent cells were subsequently fixed for 15 min with 4% paraformaldehyde in 1 x PBS at RT. Cells were treated shortly with 1 x PBS + 0.1 % Triton X-100 followed by three washing steps with 1 x PBS. If no antibody staining was performed, the treatment with PBS-T was omitted. Cells were stained with antibody for 2 h at RT and secondary antibody with Phalloidin and DAPI for 1 h at RT in a humidified dark chamber. Stained cells were mounted in Mowiol 4-88 (Carl Roth).
The following antibodies were used: anti-Atilla (1:10), anti-Hnt (1:5, 1G9 from DSHB). The following secondary antibody were used: polyclonal Alexa Flour-647-conjugated goat-anti-mouse (1:1000 dilution; #A21236, Invitrogen). F-actin staining was visualized using Phalloidin-iFlour 405 (1:100 dilution, Abcam #176752) or Alexa Flour-Phalloidin 568 (1:100 dilution, #A12380, Invitrogen) and nucleus by DAPI staining (1 µg/mL, #62248, Thermo Scientific).

Preparation of larval lymph glands

Wandering L3 larvae were anesthetized on ice and placed ventral side up on a silicone dissection pad in a drop of PBS. The larvae were pinned in place with one insect pin at the mouth hooks and one between the posterior spiracles, then sliced open lengthwise with a fine cataract scissor. The ventral cuticle was pinned to the side and the gut and fat body were carefully removed. The larva was fixed by removing the PBS and adding 10 µl of 4% PFA for 20 minutes at RT. The lymph gland was then carefully pulled from the fillet along with the attached brain and transfered to a drop of Fluoromount with DAPI (Invitrogen) on a microscope slide. The brain was severed and removed from the lymph gland before placement of the coverslip. Lymph glands were imaged using a Leica TCS SP8 confocal microscope (20x objective).

Image acquisition and microscopy

Pupae were imaged as a whole with Leica Fluorescence Stereo Microscope and Leica Application Suite X (LasX, Version 3.5.2.18963).

Confocal fluorescent images were taken with a Leica TCS SP8 with an HC PL APO CS2 63x/1.4 oil objective and Leica Application Suite X (LasX, Version 3.5.2.18963). Live imaging of macrophage cultures was performed using a Zeiss CellObserver Z.1 with a Yokogawa CSU-X1 spinning disc scanning unit and an Axiocam MRm CCD camera (6.45 µm x 6.45 µm) and ZenBlue 2.5 software. Ablation experiments were done using the UV ablation system DL-355/14 from Rapp OptoElectronics, as reported previously [9,89].

Live-cell imaging of pupal macrophages

Live imaging of pupal macrophages 4 h APF for random migration as well as 16 h APF for directed migration experiments were performed as described previously [89]. 4 h APF prepupae were collected and glued to a glass coverslip on their dorsal-lateral side. Spinning disk time-lapse movies were taken with images every 20 s for 30 min. 16-18 h APF pupae were dissected out of their cuticles and laid on a glass coverslip on their dorsal abdomen. Single cells were ablated as described in the previous chapter. Spinning disk-time-lapse movies were taken every 30 s for 60 min.

Quantification of directed migration of macrophages

Tracking of migrating macrophages was performed using the spots module in the Imaris 9.3 (Bitplane) software. The reference frame module was set at the ablation site. After automatic tracking, all time laps movies were checked for correct results and were manually corrected. The bias angle between the vector toward the ablated cell and the direction vector of the cell was calculated in R (R Studios Version 1.4). The angle between the vector directly towards the ablation cell and the direction vector of the cell at each time point was calculated with ——,

i.e., the scalar product of vectors *a* and *b* divided by the multiplication of the length of each vector .

For directed migration only cells within a 10-80 µm radius of the wounding site were analyzed. Results were statistically analyzed using GraphPad Prism 7 by GraphPad Software.

References

Aibar, S., Gonzalez-Blas, C.B., Moerman, T., Huynh-Thu, V.A., Imrichova, H., Hulselmans, G., Rambow, F., Marine, J.C., Geurts, P., Aerts, J., *et al.* (2017). SCENIC: single-cell regulatory network inference and clustering. Nat Methods *14*, 1083-1086.

Anderl, I., Vesala, L., Ihalainen, T.O., Vanha-Aho, L.M., Ando, I., Ramet, M., and Hultmark, D. (2016). Transdifferentiation and Proliferation in Two Distinct Hemocyte Lineages in Drosophila melanogaster Larvae after Wasp Infection. PLoS Pathog *12*, e1005746.

Bajzek, C., Rice, A.M., Andreazza, S., and Dushay, M.S. (2012). Coagulation and survival in Drosophila melanogaster fondue mutants. J Insect Physiol *58*, 1376-1381.

Banerjee, U., Girard, J.R., Goins, L.M., and Spratford, C.M. (2019). Drosophila as a Genetic Model for Hematopoiesis. Genetics *211*, 367-417.

Benmimoun, B., Polesello, C., Haenlin, M., and Waltzer, L. (2015). The EBF transcription factor Collier directly promotes Drosophila blood cell progenitor maintenance independently of the niche. Proc Natl Acad Sci U S A *112*, 9052-9057.

Bergman, P., Esfahani, S.S., and Engstrom, Y. (2017). Drosophila as a Model for Human Diseases-Focus on Innate Immunity in Barrier Epithelia. Curr Top Dev Biol *121*, 29-81.

Bidla, G., Dushay, M.S., and Theopold, U. (2007). Crystal cell rupture after injury in Drosophila requires the JNK pathway, small GTPases and the TNF homolog Eiger. J Cell Sci *120*, 1209-1215.

Boulet, M., Renaud, Y., Lapraz, F., Benmimoun, B., Vandel, L., and Waltzer, L. (2021). Characterization of the Drosophila Adult Hematopoietic System Reveals a Rare Cell Population With Differentiation and Proliferation Potential. Front Cell Dev Biol *9*, 739357.

Buchon, N., Silverman, N., and Cherry, S. (2014). Immunity in Drosophila melanogaster--from microbial recognition to whole-organism physiology. Nat Rev Immunol *14*, 796-810.

Cattenoz, P.B., Monticelli, S., Pavlidaki, A., and Giangrande, A. (2021). Toward a Consensus in the Repertoire of Hemocytes Identified in Drosophila. Front Cell Dev Biol *9*, 643712.

Cattenoz, P.B., Sakr, R., Pavlidaki, A., Delaporte, C., Riba, A., Molina, N., Hariharan, N., Mukherjee, T., and Giangrande, A. (2020). Temporal specificity and heterogeneity of Drosophila immune cells. EMBO J *39*, e104486.

Cho, B., Yoon, S.H., Lee, D., Koranteng, F., Tattikota, S.G., Cha, N., Shin, M., Do, H., Hu, Y., Oh, S.Y., *et al.* (2020). Single-cell transcriptome maps of myeloid blood cell lineages in Drosophila. Nat Commun *11*, 4483.

Crozatier, M., and Meister, M. (2007). Drosophila haematopoiesis. Cell Microbiol *9*, 1117-1126.

Crozatier, M., Ubeda, J.M., Vincent, A., and Meister, M. (2004). Cellular immune response to parasitization in Drosophila requires the EBF orthologue collier. PLoS Biol *2*, E196.

Crozatier, M., and Vincent, A. (1999). Requirement for the Drosophila COE transcription factor Collier in formation of an embryonic muscle: transcriptional response to notch signalling. Development *126*, 1495-1504.

Crozatier, M., and Vincent, A. (2011). Drosophila: a model for studying genetic and molecular aspects of haematopoiesis and associated leukaemias. Dis Model Mech *4*, 439-445.

Csordas, G., Gabor, E., and Honti, V. (2021). There and back again: The mechanisms of differentiation and transdifferentiation in Drosophila blood cells. Dev Biol *469*, 135-143.
Di Rosa, M., Distefano, G., Zorena, K., and Malaguarnera, L. (2016). Chitinases and immunity: Ancestral molecules with new functions. Immunobiology *221*, 399-411.
Dubnau, J., Chiang, A.S., Grady, L., Barditch, J., Gossweiler, S., McNeil, J., Smith, P., Buldoc, F., Scott, R., Certa, U.*, et al.* (2003). The staufen/pumilio pathway is involved in Drosophila long-term memory. Curr Biol *13*, 286-296.
Ekengren, S., and Hultmark, D. (2001). A family of Turandot-related genes in the humoral stress response of Drosophila. Biochem Biophys Res Commun *284*, 998-1003.
El Hadri, K., Mahmood, D.F., Couchie, D., Jguirim-Souissi, I., Genze, F., Diderot, V., Syrovets, T., Lunov, O., Simmet, T., and Rouis, M. (2012). Thioredoxin-1 promotes anti-inflammatory macrophages of the M2 phenotype and antagonizes atherosclerosis. Arterioscler Thromb Vasc Biol *32*, 1445-1452.
Emtenani, S., Martin, E.T., Gyoergy, A., Bicher, J., Genger, J.W., Kocher, T., Akhmanova, M., Guarda, M., Roblek, M., Bergthaler, A.*, et al.* (2022). Macrophage mitochondrial bioenergetics and tissue invasion are boosted by an Atossa-Porthos axis in Drosophila. EMBO J *41*, e109049.
Evans, C.J., Hartenstein, V., and Banerjee, U. (2003). Thicker than blood: Conserved mechanisms in Drosophila and vertebrate hematopoiesis. Dev Cell *5*, 673-690.
Evans, C.J., Olson, J.M., Ngo, K.T., Kim, E., Lee, N.E., Kuoy, E., Patananan, A.N., Sitz, D., Tran, P., Do, M.T.*, et al.* (2009). G-TRACE: rapid Gal4-based cell lineage analysis in Drosophila. Nat Methods *6*, 603-605.
Evans, I.R., and Wood, W. (2014). Drosophila blood cell chemotaxis. Curr Opin Cell Biol *30*, 1-8.
Fu, Y., Huang, X., Zhang, P., van de Leemput, J., and Han, Z. (2020). Single-cell RNA sequencing identifies novel cell types in Drosophila blood. J Genet Genomics *47*, 175-186.
Ghosh, S., Singh, A., Mandal, S., and Mandal, L. (2015). Active hematopoietic hubs in Drosophila adults generate hemocytes and contribute to immune response. Dev Cell *33*, 478-488.
Girard, J.R., Goins, L.M., Vuu, D.M., Sharpley, M.S., Spratford, C.M., Mantri, S.R., and Banerjee, U. (2021). Paths and pathways that generate cell-type heterogeneity and developmental progression in hematopoiesis. Elife *10*.
Gold, K.S., and Bruckner, K. (2015). Macrophages and cellular immunity in Drosophila melanogaster. Semin Immunol *27*, 357-368.
Goto, A., Matsushita, K., Gesellchen, V., El Chamy, L., Kuttenkeuler, D., Takeuchi, O., Hoffmann, J.A., Akira, S., Boutros, M., and Reichhart, J.M. (2008). Akirins are highly conserved nuclear proteins required for NF-kappaB-dependent gene expression in drosophila and mice. Nat Immunol *9*, 97-104.
Gyoergy, A., Roblek, M., Ratheesh, A., Valoskova, K., Belyaeva, V., Wachner, S., Matsubayashi, Y., Sanchez-Sanchez, B.J., Stramer, B., and Siekhaus, D.E. (2018). Tools Allowing Independent Visualization and Genetic Manipulation of Drosophila melanogaster Macrophages and Surrounding Tissues. G3 (Bethesda) *8*, 845-857.
Hackett, B.A., Yasunaga, A., Panda, D., Tartell, M.A., Hopkins, K.C., Hensley, S.E., and Cherry, S. (2015). RNASEK is required for internalization of diverse acid-dependent viruses. P Natl Acad Sci USA *112*, 7797-7802.
Holz, A., Bossinger, B., Strasser, T., Janning, W., and Klapper, R. (2003). The two origins of hemocytes in Drosophila. Development *130*, 4955-4962.

Hultmark, D., and Ando, I. (2022). Hematopoietic plasticity mapped in Drosophila and other insects. Elife *11*.
Imler, J.L., and Hoffmann, J.A. (2000). Signaling mechanisms in the antimicrobial host defense of Drosophila. Curr Opin Microbiol *3*, 16-22.
Jin, L.H., Shim, J., Yoon, J.S., Kim, B., Kim, J., Kim-Ha, J., and Kim, Y.J. (2008). Identification and functional analysis of antifungal immune response genes in Drosophila. PLoS Pathog *4*, e1000168.
Johnson, D.M., Wells, M.B., Fox, R., Lee, J.S., Loganathan, R., Levings, D., Bastien, A., Slattery, M., and Andrew, D.J. (2020). CrebA increases secretory capacity through direct transcriptional regulation of the secretory machinery, a subset of secretory cargo, and other key regulators. Traffic *21*, 560-577.
Jung, S.H., Evans, C.J., Uemura, C., and Banerjee, U. (2005). The Drosophila lymph gland as a developmental model of hematopoiesis. Development *132*, 2521-2533.
Kanwal, A., Joshi, P.V., Mandal, S., and Mandal, L. (2021). Ubx-Collier signaling cascade maintains blood progenitors in the posterior lobes of the Drosophila larval lymph gland. PLoS Genet *17*, e1009709.
Khadilkar, R.J., Vogl, W., Goodwin, K., and Tanentzapf, G. (2017). Modulation of occluding junctions alters the hematopoietic niche to trigger immune activation. Elife *6*.
Kimura, S. (2013). The Nap family proteins, CG5017/Hanabi and Nap1, are essential for Drosophila spermiogenesis. FEBS Lett *587*, 922-929.
Krzemien, J., Dubois, L., Makki, R., Meister, M., Vincent, A., and Crozatier, M. (2007). Control of blood cell homeostasis in Drosophila larvae by the posterior signalling centre. Nature *446*, 325-328.
Krzemien, J., Oyallon, J., Crozatier, M., and Vincent, A. (2010). Hematopoietic progenitors and hemocyte lineages in the Drosophila lymph gland. Dev Biol *346*, 310-319.
Lanno, S.M., Shimshak, S.J., Peyser, R.D., Linde, S.C., and Coolon, J.D. (2019). Investigating the role of Osiris genes in Drosophila sechellia larval resistance to a host plant toxin. Ecol Evol *9*, 1922-1933.
Lanot, R., Zachary, D., Holder, F., and Meister, M. (2001). Postembryonic hematopoiesis in Drosophila. Dev Biol *230*, 243-257.
Lebestky, T., Chang, T., Hartenstein, V., and Banerjee, U. (2000). Specification of Drosophila hematopoietic lineage by conserved transcription factors. Science *288*, 146-149.
Lehmann, M. (1996). Drosophila Sgs genes: stage and tissue specificity of hormone responsiveness. Bioessays *18*, 47-54.
Lehne, F., Pokrant, T., Parbin, S., Salinas, G., Grosshans, J., Rust, K., Faix, J., and Bogdan, S. (2022). Calcium bursts allow rapid reorganization of EFhD2/Swip-1 cross-linked actin networks in epithelial wound closure. Nat Commun *13*, 2492.
Leitao, A.B., Arunkumar, R., Day, J.P., Geldman, E.M., Morin-Poulard, I., Crozatier, M., and Jiggins, F.M. (2020). Constitutive activation of cellular immunity underlies the evolution of resistance to infection in Drosophila. Elife *9*.
Lemaitre, B., and Hoffmann, J. (2007). The host defense of Drosophila melanogaster. Annu Rev Immunol *25*, 697-743.
Li, H., Janssens, J., De Waegeneer, M., Kolluru, S.S., Davie, K., Gardeux, V., Saelens, W., David, F.P.A., Brbic, M., Spanier, K.*, et al.* (2022). Fly Cell Atlas: A single-nucleus transcriptomic atlas of the adult fruit fly. Science *375*, eabk2432.
Liegeois, S., and Ferrandon, D. (2020). An atlas for hemocytes in an insect. Elife *9*.

Makhijani, K., Alexander, B., Tanaka, T., Rulifson, E., and Bruckner, K. (2011). The peripheral nervous system supports blood cell homing and survival in the Drosophila larva. Development *138*, 5379-5391.
Makki, R., Meister, M., Pennetier, D., Ubeda, J.M., Braun, A., Daburon, V., Krzemien, J., Bourbon, H.M., Zhou, R., Vincent, A.*, et al.* (2010). A short receptor downregulates JAK/STAT signalling to control the Drosophila cellular immune response. PLoS Biol *8*, e1000441.
Mandal, L., Banerjee, U., and Hartenstein, V. (2004). Evidence for a fruit fly hemangioblast and similarities between lymph-gland hematopoiesis in fruit fly and mammal aorta-gonadal-mesonephros mesoderm. Nat Genet *36*, 1019-1023.
Mandal, L., Martinez-Agosto, J.A., Evans, C.J., Hartenstein, V., and Banerjee, U. (2007). A Hedgehog- and Antennapedia-dependent niche maintains Drosophila haematopoietic precursors. Nature *446*, 320-324.
Oyallon, J., Vanzo, N., Krzemien, J., Morin-Poulard, I., Vincent, A., and Crozatier, M. (2016). Two Independent Functions of Collier/Early B Cell Factor in the Control of Drosophila Blood Cell Homeostasis. PLoS One *11*, e0148978.
Perreira, J.M., Aker, A.M., Savidis, G., Chin, C.R., McDougall, W.M., Portmann, J.M., Meraner, P., Smith, M.C., Rahman, M., Baker, R.E.*, et al.* (2015). RNASEK Is a V-ATPase-Associated Factor Required for Endocytosis and the Replication of Rhinovirus, Influenza A Virus, and Dengue Virus. Cell Rep *12*, 850-863.
Petraki, S., Alexander, B., and Bruckner, K. (2015). Assaying Blood Cell Populations of the Drosophila melanogaster Larva. J Vis Exp.
Regan, J.C., Brandao, A.S., Leitao, A.B., Mantas Dias, A.R., Sucena, E., Jacinto, A., and Zaidman-Remy, A. (2013). Steroid hormone signaling is essential to regulate innate immune cells and fight bacterial infection in Drosophila. PLoS Pathog *9*, e1003720.
Rehorn, K.P., Thelen, H., Michelson, A.M., and Reuter, R. (1996). A molecular aspect of hematopoiesis and endoderm development common to vertebrates and Drosophila. Development *122*, 4023-4031.
Rizki, T.M. (1962). Experimental Analysis of Hemocyte Morphology in Insects. Am Zool *2*, 247-256.
Rodrigues, D., Renaud, Y., VijayRaghavan, K., Waltzer, L., and Inamdar, M.S. (2021). Differential activation of JAK-STAT signaling reveals functional compartmentalization in Drosophila blood progenitors. Elife *10*.
Russo, J., Dupas, S., Frey, F., Carton, Y., and Brehelin, M. (1996). Insect immunity: early events in the encapsulation process of parasitoid (Leptopilina boulardi) eggs in resistant and susceptible strains of Drosophila. Parasitology *112 (Pt 1)*, 135-142.
Sampson, C.J., Amin, U., and Couso, J.P. (2013). Activation of Drosophila hemocyte motility by the ecdysone hormone. Biol Open *2*, 1412-1420.
Sanchez Bosch, P., Makhijani, K., Herboso, L., Gold, K.S., Baginsky, R., Woodcock, K.J., Alexander, B., Kukar, K., Corcoran, S., Jacobs, T.*, et al.* (2019). Adult Drosophila Lack Hematopoiesis but Rely on a Blood Cell Reservoir at the Respiratory Epithelia to Relay Infection Signals to Surrounding Tissues. Dev Cell *51*, 787-803 e785.
Sander, M., Squarr, A.J., Risse, B., Jiang, X.Y., and Bogdan, S. (2013). Drosophila pupal macrophages - A versatile tool for combined ex vivo and in vivo imaging of actin dynamics at high resolution. Eur J Cell Biol *92*, 349-354.
Shen, B., Zhu, W., Liu, X., and Jiang, J. (2022). NAP1L1 Functions as a Novel Prognostic Biomarker Associated With Macrophages and Promotes Tumor

Progression by Influencing the Wnt/beta-Catenin Pathway in Hepatocellular Carcinoma. Front Genet *13*, 876253.
Shi, X.Z., Zhong, X., and Yu, X.Q. (2012). Drosophila melanogaster NPC2 proteins bind bacterial cell wall components and may function in immune signal pathways. Insect Biochem Molec *42*, 545-556.
Shomroni, O., Sitte, M., Schmidt, J., Parbin, S., Ludewig, F., Yigit, G., Zelarayan, L.C., Streckfuss-Bomeke, K., Wollnik, B., and Salinas, G. (2022). A novel single-cell RNA-sequencing approach and its applicability connecting genotype to phenotype in ageing disease. Sci Rep *12*, 4091.
Sinenko, S.A., and Mathey-Prevot, B. (2004). Increased expression of Drosophila tetraspanin, Tsp68C, suppresses the abnormal proliferation of ytr-deficient and Ras/Raf-activated hemocytes. Oncogene *23*, 9120-9128.
Smith, C.R., Morandin, C., Noureddine, M., and Pant, S. (2018). Conserved roles of Osiris genes in insect development, polymorphism and protection. J Evol Biol *31*, 516-529.
Stuart, T., Butler, A., Hoffman, P., Hafemeister, C., Papalexi, E., Mauck, W.M., 3rd, Hao, Y., Stoeckius, M., Smibert, P., and Satija, R. (2019). Comprehensive Integration of Single-Cell Data. Cell *177*, 1888-1902 e1821.
Tanaka, T., Hozumi, Y., Iino, M., and Goto, K. (2017). NAP1L1 regulates NF-kappaB signaling pathway acting on anti-apoptotic Mcl-1 gene expression. Biochim Biophys Acta Mol Cell Res *1864*, 1759-1768.
Tattikota, S.G., Cho, B., Liu, Y., Hu, Y., Barrera, V., Steinbaugh, M.J., Yoon, S.H., Comjean, A., Li, F., Dervis, F.*, et al.* (2020). A single-cell survey of Drosophila blood. Elife *9*.
Trapnell, C., Cacchiarelli, D., Grimsby, J., Pokharel, P., Li, S., Morse, M., Lennon, N.J., Livak, K.J., Mikkelsen, T.S., and Rinn, J.L. (2014). The dynamics and regulators of cell fate decisions are revealed by pseudotemporal ordering of single cells. Nat Biotechnol *32*, 381-386.
Trienens, M., Kraaijeveld, K., and Wertheim, B. (2017). Defensive repertoire of Drosophila larvae in response to toxic fungi. Mol Ecol *26*, 5043-5057.
Vervoort, M., Crozatier, M., Valle, D., and Vincent, A. (1999). The COE transcription factor Collier is a mediator of short-range Hedgehog-induced patterning of the Drosophila wing. Current Biology *9*, 632-639.
Vlisidou, I., and Wood, W. (2015). Drosophila blood cells and their role in immune responses. Febs J *282*, 1368-1382.
Williams, M.J. (2009). The Drosophila cell adhesion molecule Neuroglian regulates Lissencephaly-1 localisation in circulating immunosurveillance cells. BMC Immunol *10*, 17.
Wright, L.G., Chen, T., Thummel, C.S., and Guild, G.M. (1996). Molecular characterization of the 71E late puff in Drosophila melanogaster reveals a family of novel genes. J Mol Biol *255*, 387-400.

Acknowledgements

We thank the Bloomington Stock Center and VDRC for fly stocks. We thank Daria Siekhaus for sharing fly stocks. The work was supported by grants to S.B. (BO1890/5-1) from the Deutsche Forschungsgemeinschaft (DFG), and by J.G. from the VW Stiftung. "Big Data in den Lebenswissenschaften der Zukunft", Nr. A129197.

Author contributions

S.B. designed the project. S.B. and K.R. made the figures and wrote the manuscript. A.H. and D.M. performed the experiments. K.R. performed the bioinformatic analysis. G.S. and J.G. managed and coordinated RNA seq analysis. All authors commented on the manuscript.

Competing interests

The authors declare no competing interests.

Figure legends

Figure 1. scRNA-seq analysis of pupal *Drosophila* hemocytes reveals a remarkable cellular heterogeneity

A) Workflow for the full-length SMART scRNA-Seq approach using the ICELL8 platform. Hemocytes were isolated from 2-10 h APF *Drosophila* pupae. Cells were stained with Hoechst (additionally, propidium iodide for live cell dataset) prior to their dispensing into the Takara ICELL8 5,184 nanowell chip. Only wells containing single cells were selected using the CellSelect Software prior to the on-chip RT-reaction, library preparation and sequencing. Exemplary images of Lsp-Bomanin-PL, PSC and Secretory-PL cells are shown. **B**) UMAP plot of 2811 high quality cells in fourteen transcriptomically distinct clusters. **C**) Heatmap of the top 50 differentially regulated genes per cluster showing transcriptomic differences between cell groups. **D**) Transcription factor activity of selected transcription factors identified by SCENIC identifies distinct activities between clusters.

Figure 2. Identification of several precursor plasmatocyte populations

A-B) UMAP plots. *srp* is highly expressed (**A**) and active (**B**) in several clusters. **C-D**) Maximum intensity projection of confocal images of differential expression of the transcription factor *srp* in pupal hemocytes using (**C, C'**) srpHemo-3xmCherry; white arrowheads highlight low-expressing cells. Scale bar represents 10 µm. (**D, D', D''**) *srp* GFP trap; scale bar represents 10 µm. **E**) Dotplot showing the average expression and percent expression per cluster for marker genes of clusters with high *srp* expression: undifferentiated PL, transitory PL1-2 – 3 and Osiris-PL. **F**) Expression of *CG8046*, a undifferentiated PL marker, on the UMAP plot. **G-I**) Expression of transitory PL-1 markers on the UMAP plot. **G**) *CG4822* expression is also detected in undifferentiated PL. **H**) *CG31141* expression is also detected in Spermatid-Marker-PL. **I**) Combined expression of *CG4822* and *CG31141* is only detected in transitory PL-1. **J-K**) Monocle3 pseudotime analysis. **J**) Pseudotime trajectory on the UMAP plot. **K**) UMAP plot with pseudotime trajectory and cells colored based on pseudotime. **L-M**) Expression of marker genes on the UMAP plot. **L**) *CG13012*, identified as a marker for transitory PL-2. **M**) *ich*, identified as a marker for Osiris-PL.

Figure 3. Identification of effector cells with distinct molecular signatures

A-F) Expression of selected markers on the UMAP plot. **A**) *mil* is a marker for Spermatid-Marker-PL. **B**) *Lsp1alpha* is expressed in Lsp-Bomanin-PL. **C**) *28SrRNA-Psi:CR40596* is highly expressed in OxPhos-PL. **D**) *CG6426* is a marker for Adhesive-PL. **E**) *CG15905* marks Adhesive-PL. **F**) *CG5402* marks AMP-PL. **G**) Dotplot of selected marker genes with average expression and percent expression per cluster for the following clusters: Spermatid-Marker-PL, Lsp-Bomanin-PL, OxPhos-PL, Chitinase-PL, Adhesive-PL and AMP-PL. **H**) Representative terms of the top seven annotation clusters identified with DAVID 2021 GO-term analysis of differentially expressed genes of the clusters Spermatid-Marker-PL, Lsp-Bomanin-PL, OxPhos-PL, Chitinase-PL, Adhesive-PL and AMP-PL. The barplot height reflects the enrichment score of the annotation cluster and is colored based on the p-value of the GO-term. **I-M**) Activity of transcription factors on the UMAP plot identified with

SCENIC. **I**) *Rel* is highly active in Precursor-PL-3, AMP-PL and Hydrolyzing-PL. **J-L**) *CG34367* (J) and *CG11294* (K) and *HGTX* (L) are active in Spermatid-Marker-PL. **M**) *abd-A* is active in Chitinase-PL.

Figure 4. Secretory-PL, a new plasmatocyte type in pupae, is transcriptomically distinct from other developmental stages.

A-D) UMAP plots showing the expression of Secretory-PL markers. **A**) *CG31174* is specific for Secretory-PL. **B-D**) *Tep4* (B), *ham* (C) and *Ance* (D) expression can also be detected in PSC. **E**) Average expression and percent expression of Secretory-PL markers on a Dotplot. Note the importance of many genes in immunity or their function in proteolysis. **F-G**) Activity of transcription factors highly active in Secretory-PL on the UMAP plot as identified by SCENIC. **F**) *CrebA*. **G**) *dl*. **H-L**) Maximum intensity projection of confocal images of pupal hemocytes expressing GFP; cells with plasmatocyte-like cell shape are marked by the white arrowhead; small spiky cells with filopodial protrusions are marked by yellow arrowheads; Alexa568-labeled phalloidin was used to stain the actin cytoskeleton. (**H**) Tep4-Gal4. (**I**) Ham-Gal4. (**J**) Ance ^{mimic}-GFP. (**K**) CG31174 ^{mimic}-GFP. (**L, L', L''**) Small spiky cells are not CG31174 positive. CG31174 ^{mimic}-GFP co-expressing Tep4-Gal4-nls-mCherry. Small spiky cells are marked by a yellow asterisk and plasmatocyte-like shaped cells co-expressing both markers are marked by a white asterisk. Scale Bar represents 10 µm

Figure 5. Identification of individual tissue-resident PSC cells in pupae

A-C) Expression of PSC markers on the UMAP plot. **A**) *kn*. **B**) *Antp*. C) *tau*. **D**) Dotplot with average expression and percent of expression of PSC markers. **E-F**) Activity of transcription factors *kn* (E) and *Antp* (F) on the UMAP plot. **G-J**) Maximum intensity projection of confocal images of the actin cytoskeleton in pupal macrophages; phalloidin (white) was used to stain the actin cytoskeleton and DAPI for the nuclei (blue). (G) PSC cells and Secretory-PL cells represent different cell types. CG31174 mimic-GFP co-expressing kn-Gal4-mCherry. PSC cells are marked by a yellow asterisk and CG31174-positive cells are marked by a white asterisk. **H**) kn-Gal4 driving UAS-GFP. **I**) A*ntp*-Gal4 driving UAS-GFP. **J**) *tau*-Gal4 driving UAS-GFP. **K**) Quantification of GFP-positive spiky PSC cells, GFP-positive and GFP-negative cells with plasmatocyte morphology frequency represented by *kn* (n=462; GFP-positive =3%; PSC = 16%; GFP-negative = 81%), *tau* (n=464; GFP-positive =

0%; PSC = 8 %; GFP-negative = 92%) and CG31174 (n =3 59; GFP-positive = 24.5%; GFP-negative = 75%). Cells were obtained from six individual experiments. Scale bar represents 10 µm. **L**) A representative wandering third instar larval lymph gland expressing GFP (green) under the control of tau-Gal4 driver co-stained with DAPI (white). Scale bar represents 100 µm. **L', L''**) Expression of GFP is exclusively found in the PSC region of primary lobes. No expression is found in the smaller posterior lobes. Scale bar represents 50 µm.

Figure 6. PSC cells can differentiate into lamellocytes upon wasp infestion

A-D) Maximum intensity projection of confocal images of isolated pupal macrophages; Alexa568-labeled phalloidin was used to stain the actin cytoskeleton. Nuclei were stained by DAPI. **A**) kn-Gal4 > UAS-GFP individuals were infested with wasps. Upon infestion GFP positive cells are either small and spiky (yellow arrowhead) or large with lamellocyte typical morphology (white arrowhead). **B**) Schematic overview of the G-TRACE system. Gal4 protein is specifically expressed in PSCs under the control of the *tau* promoter. PSCs are RFP positive due to the UAS-RFP transgene. Gal4-positive PSCs induce flipase (FLP) expression via UAS-FLP. FLP can remove an FRT-flanked stop codon downstream the ubiquitous ubi promoter. Stop codon removal leads to stable and inheritable expression of GFP, which allows tracing of offspring cells produced by PSCs. Differentiating PSC offspring turn off *tau*-Gal4 resulting into GFP positive but RFP negative cells. **C**, **D**) Cell lineage analysis of pupal hemocytes using **C**) *kn* > G-TRACE. PSCs are small and spiky cells double positive for RFP and GFP (yellow arrowhead). *kn* > GFP cells correspond to the small and spiky PSC morphology, a small number of GFP positive cells displayed plasmatocyte typical morphology (green arrowheads), GFP positive lamellocytes are marked by white arrowheads. **D**) *tau* > G-TRACE. Some lamellocytes are GFP positive (green arrowhead) showing that they derived from PSC cells. Other lamellocytes are GFP negative and may thus differentiated from other cellular sources. Scale bar represents 10 µm.

Figure 7. PSC cells are motile tissue-resident immune responsive cells persisting into adult

A-C) Frames of a spinning disc time-lapse movies of randomly migrating 4h and 16h APF and pupal hemocytes marked by GFP expression under the control of **A**) *kn*-

Gal4 and **B, C**) *tau*-Ga4 in 4h and 16h APF pupae, respectively. Images were taken every 20 s for 30-60 min. A white arrowhead mark the migrating PSC hemocytes. The time point of each image is annotated, scale bar is 20 µm. **D, E**) Still images of spinning disc time-lapse movies of directed macrophage migration upon wounding of a single cell in the **D**) *kn*-Gal4, UAS-GFP and **E**) *hml*-Gal4, UAS-GFP background. Cells were imaged for 60 min after laser ablation in 30 s intervals and tracked by Imaris software. Trajectories indicate that GFP expressing PSC hemocytes are highly motile. Note: *Hml*-marked plasmatocytes are much bigger and contain more phagocytic vacuoles than PSC cells marked by *kn*-Gal4. **F**) Quantification of the directionality of cells marked with *hml* or *kn* towards the wound. Directionality is described with the bias angle of the migrating cells. *kn* positive PSC cells show a similar wound response as *hml*-GFP cells, which serve as a pan-hemocyte control. *kn* (n=129) *hml* (n=103) values from 10 individual experiments. Graphs are depicted in a scatter dot blot with bars indicating mean and standard deviation. ns = p = > 0.03 (Welch´s t test). **G**) Magnification of PSC macrophages close to the ablated cell (marked by a red asterisk) at the indicated time points. Green asterisk marks a migrating wound-responsive PSC hemocyte towards the ablation site.

Supplementary Figure 1

A) Violin plots representing the number of Features, UMI counts and percent of mitochondrial genes per cell and per dataset. B) UMAP plot with cells labeled by dataset origin. c, d) Contribution of cells per dataset in a table (C) or represented as a barplot (D). Note that all datasets (two fixed and one live cell dataset) contribute to every cluster. E) Average expression and percent expression per cluster of known pan-hemocyte, crystal cell and lamellocyte markers.

Supplementary Figure 2

A) Dotplot showing the average expression and percent expression of muscle and neuron markers. B-C) Expression of the muscle marker *sing* (B) and the neuron marker *Appl* (C) on the UMAP plot. D) DAVID 2021 GO-term analysis of Neuron and Muscle markers. For each of the top seven annotation cluster a representative term is presented. Barplot shows enrichment score of the annotation cluster and p-value of the GO-term. E-L) SCENIC determined activity of transcription factors active in Neuron (E-H) or Muscle (I-L) on the UMAP plot. E) *ase*, F) *onecut*, G) *Rbp6*, H)

SoxN, I) *E(spl)m3-HLH*, J) *E(spl)m7-HLH*, K) *E(spl)mdelta-HLH*, L) *twi*. M) Average expression and percent expression per cluster of cytoskeleton and cell motility genes identified in a bulk RNA-sequencing experiment comparing larval and pupal hemocytes.

Supplementary Figure 3

A) Dotplot of the average and percent expression of hemocyte subtype specific markers identified other studies as indicated. B) Expression level of the M-phase specific genes *polo*, *aurB*, *Det* per cluster. C) Marker genes of undifferentiated PL, transitory PL-1-2 or Osiris-PL were analyzed with DAVID 2021. For the top seven annotation cluster one representative GO-term is shown. Barplot shows enrichment score of the annotation cluster and is colored by GO-term p-value.D-G) Activity of transcription factors on the UMAP plot as identified by SCENIC. D) *Hsf*, E) *inv*, F) *ken*, G) *slbo*.

Supplementary Figure 4

A) Cross cluster correlation analysis of hemocyte cell types. *srp*^{high} clusters correlate well with each other and with several differentiated plasmatocyte types. Transcriptomes of plasmatocytes Chitinase-PL and AMP-PL differ dramatically, suggesting a high level of specification. b-d) Violin plot showing the number of (B) features, (C) UMIs or (D) percent of mitochondrial genes per cluster. E) Average and percent expression of genes implicated in cell adhesion identified as markers for Adhesive-PL. Note that most genes are also expressed in Chitinase-PL.

Supplementary Figure 5

A) GO-term analysis of Secretory-PL markers performed with DAVID 2021. Representative GO-terms for the top seven annotation clusters are shown. Enrichment score of annotation clusters and p-value of GO-terms are presented in A barplot. B-F) UMAP plots of integrated hemocyte datasets across different developmental stages. B) Labelled by dataset. C) Pupal cells are highlighted in magenta. D) Adult crystal cells are highlighted in magenta. E) Larval crystal cells are shown in magenta. F) Pupal Secretory-PL are represented in magenta.

Supplementary Figure 6

A) PSC markers were analysed with DAVID 2021 and representative GO-terms of the top seven GO-terms are presented. Barplot shows the enrichment score of the annotation cluster and is colored by p-value of the GO-term. B-D) Dotplots of markers of pupal PSCs showing average expression and percent expression per cluster in B) the normal lymph gland [20] at 120h afer egg laying, C) free larval hemocytes of embryonic origin and D) in adult Hml positive cells. D-F) UMAP plot of integrated datasets across developmental stages showing the location of D) pupal PSC, E) adult Hml positive cells with PSC markers and F) larval PL-Impl2 cells.

Supplementary Figure 7

(A, B) Cell lineage analysis of non-infested pupal hemocytes using (A) *kn* > G-TRACE. (H) *tau* > G-TRACE. Scale bar represents 10 µm.

Supplementary table 1

Pupal blood cell types and likely corresponding cell types identified in studies characterizing other stages of hematopoiesis. Corresponding clusters were identified by examining the respective cluster specific markers in pupal blood cell clusters (compare to Supplementary figure S3A). In addition, we considered previously identified overlap between clusters (Hultmark and Andó, 2022).

Supplementary movies

Supplementary movie M1 *kn*-positive cells randomly migrate in prepupae.

Representative spinning disc microscopy video of randomly migrating pupal *hml*+ (left) versus *kn*+ (right) cells expressing an EGFP transgene imaged from a living prepupa (4h APF). Note the difference of *hml*+ hemocytes marked by a yellow arrow. Scale bar represents 20 µm. Cells were imaged for 30 minutes.

Supplementary movie M2 *tau*-positive cells randomly migrate in prepupae.

Representative spinning disc microscopy video of randomly migrating pupal *tau*+ cells expressing an EGFP transgene imaged from a living prepupa at 4h APF (left) and at 16h APF (right).

Supplementary movie M3 PSC cells are wound responsive and differ in size compared to *hml*-marked plasmatocytes

Representative spinning disc microscopy videos of *hml*+ (left) and *kn*+ (right) cells in the Drosophila abdomen 16h APF upon single cell laser ablation. Cells are imaged for 60 minutes after ablation in a 30 seconds interval and tracked afterwards using Imaris. Representative migratory tracks are shown (colored, jagged lines). Characteristic plasmatocytes are marked by yellow arrows compared to a small, spiky PSC cell marked by a white arrow. Yellow asterisk marks the ablated wounding site. Scale bar represents 20 µm.

Supplementary movie M4 PSC cells switch from random to directed migration upon single cell laser ablation.

Representative spinning disc microscopy video with a magnification (indicated by yellow rectangle) of single *kn*+ cells that migrate towards a laser-ablated cell marked by a yellow asterisk. Note the size difference between plasmatocytes marked by yellow arrows and PSC cells. Scale bar represent 20 µm.

Supplementary movie M5 PSC cells are able to phagocytose cell debris

Representative spinning disc microscopy videos of randomly migrating pupal *tau* positive cells expressing an EGFP transgene imaged from living prepupae (16h APF). **A**) Single *tau*-positive PSC cell (yellow arrowhead) migrate towards a laser-ablated cell marked by a green asterisk. Note the formation of dynamic filopodial protrusion toward the wound. **B**) Single *tau*-positive PSC cell (yellow arrowhead) starts to phagocytose particles derived from the laser-ablated cell (green asterisk). Note the formation of dynamic filopodial protrusion toward the wound. **C**) Single *tau*-positive PSC cell (yellow arrowhead) rounds up and divides.

Supplementary Data 1

List of differentially expressed genes across all 14 clusters identified with Seurat v4.1.1 FindAllMarkers() command.

Supplementary Data 2

Data associated with Figure 1C. This list contains the top50 genes identified with Seurat v4.1.1 FindAllMarkers() and is an abbreviated version of Supplementary Data 1.

Supplementary Data 3

Differentially expressed genes of undifferentiated PL identified with Seurat v.1.1 FindMarkers() used for DAVID 2021 GO-term analysis.

Supplementary Data 4

Differentially expressed genes of transitory PL-1 identified with Seurat v.1.1 FindMarkers() used for DAVID 2021 GO-term analysis.

Supplementary Data 5

Differentially expressed genes of transitory PL-2 identified with Seurat v.1.1 FindMarkers() used for DAVID 2021 GO-term analysis.

Supplementary Data 6

Differentially expressed genes of Osiris-PL identified with Seurat v.1.1 FindMarkers() used for DAVID 2021 GO-term analysis.

Supplementary Data 7

Differentially expressed genes of Spermatid-Marker-PL identified with Seurat v.1.1 FindMarkers() used for DAVID 2021 GO-term analysis.

Supplementary Data 8

Differentially expressed genes of Lsp-Bomanin-PL identified with Seurat v.1.1 FindMarkers() used for DAVID 2021 GO-term analysis.

Supplementary Data 9

Differentially expressed genes of OxPhos-PL identified with Seurat v.1.1 FindMarkers() used for DAVID 2021 GO-term analysis.

Supplementary Data 10

Differentially expressed genes of Chitinase-PL identified with Seurat v.1.1 FindMarkers() used for DAVID 2021 GO-term analysis.

Supplementary Data 11

Differentially expressed genes of Adhesive-PL identified with Seurat v.1.1 FindMarkers() used for DAVID 2021 GO-term analysis.

Supplementary Data 12

Differentially expressed genes of AMP-PL identified with Seurat v.1.1 FindMarkers() used for DAVID 2021 GO-term analysis.

Supplementary Data 13

Differentially expressed genes of Secretory-PL identified with Seurat v.1.1 FindMarkers() used for DAVID 2021 GO-term analysis.

Supplementary Data 14

Differentially expressed genes of PSC identified with Seurat v.1.1 FindMarkers() used for DAVID 2021 GO-term analysis.

Supplementary Data 15

Differentially expressed genes of Neuron identified with Seurat v.1.1 FindMarkers() used for DAVID 2021 GO-term analysis.

Supplementary Data 16

Differentially expressed genes of Muscle identified with Seurat v.1.1 FindMarkers() used for DAVID 2021 GO-term analysis.

Supplementary Data 17

Scaled regulon activity identified by SCENIC v1.3.1. A subset of this data is visually presented in Figure 1D.

Supplementary Data 18

Top active transcription factors per cell type identified by SCENIC v1.3.1.

Supplementary Data 19

Validation of marker genes for each cluster of *Drosophila* hemocytes. A list of Gal4-enhancer trap and GFP-exon trap fly lines used for ex vivo validation is included.

Script 1

R script for data processing steps including quality filtering, normalization, data integration, clustering and cluster annotation using the Seurat package.

Script 2

R script for the pseudotime analysis using Monocle3

Script 3

R script for the identification of transcription factor activity with SCENIC.

Script 4

R script for the integration of datasets from different developmental stages using the Seurat batch correction algorithm.

Script 5

R script containing an overview of how the processed data can be read into R and analyzed for gene expression.

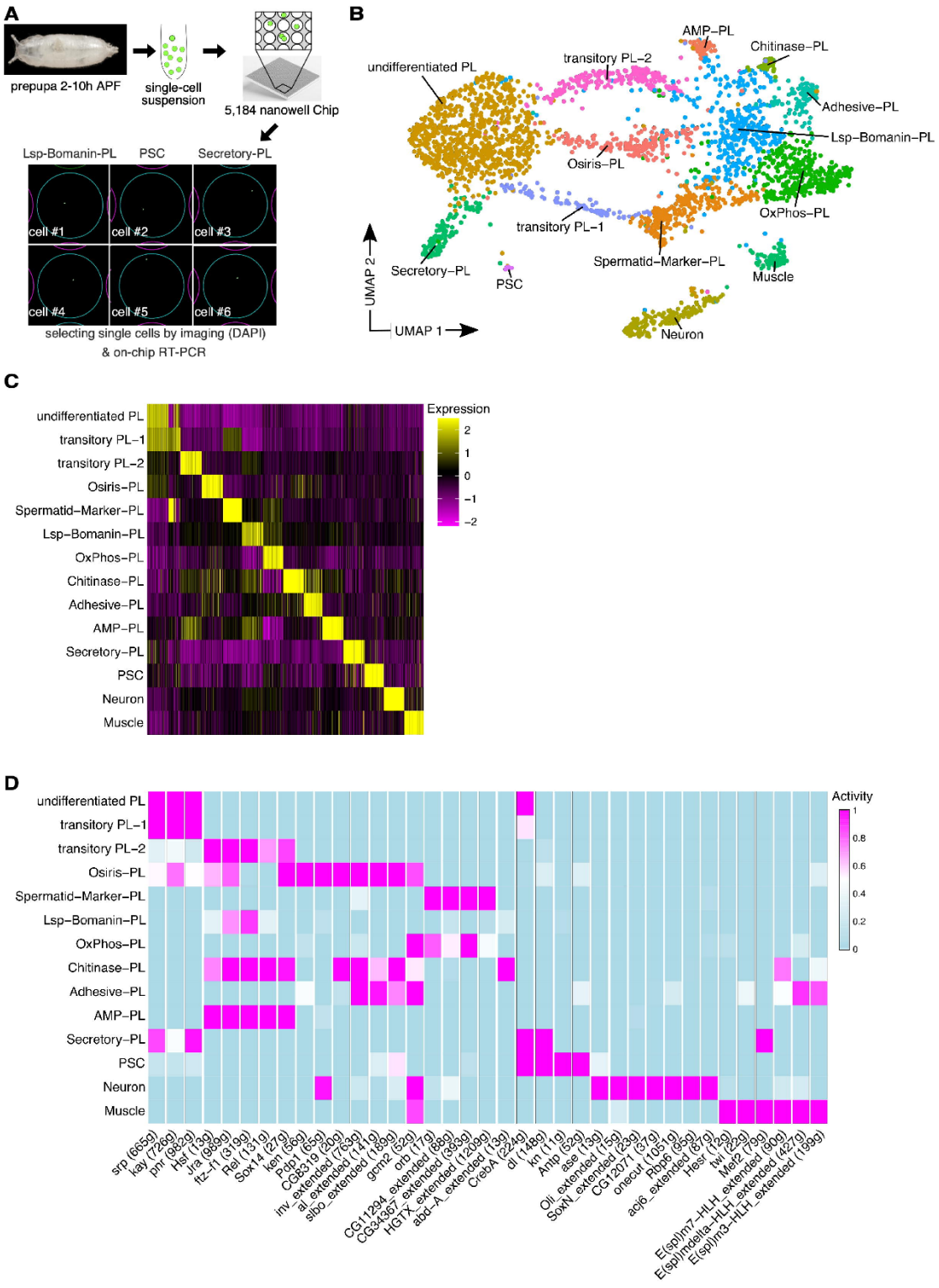

Figure 1, Hirschhäuser et al.

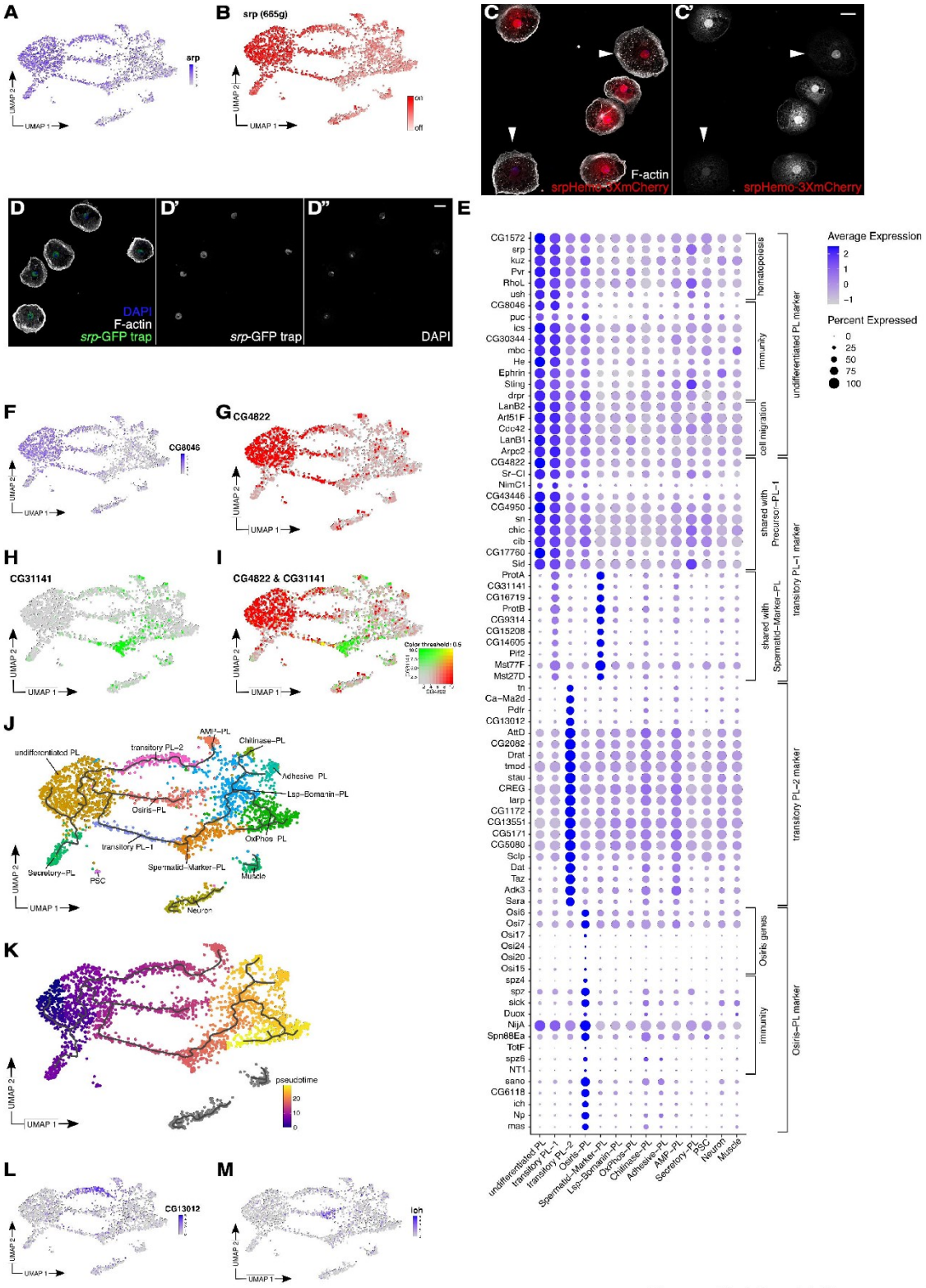

Figure 2, Hirschhäuser et al.

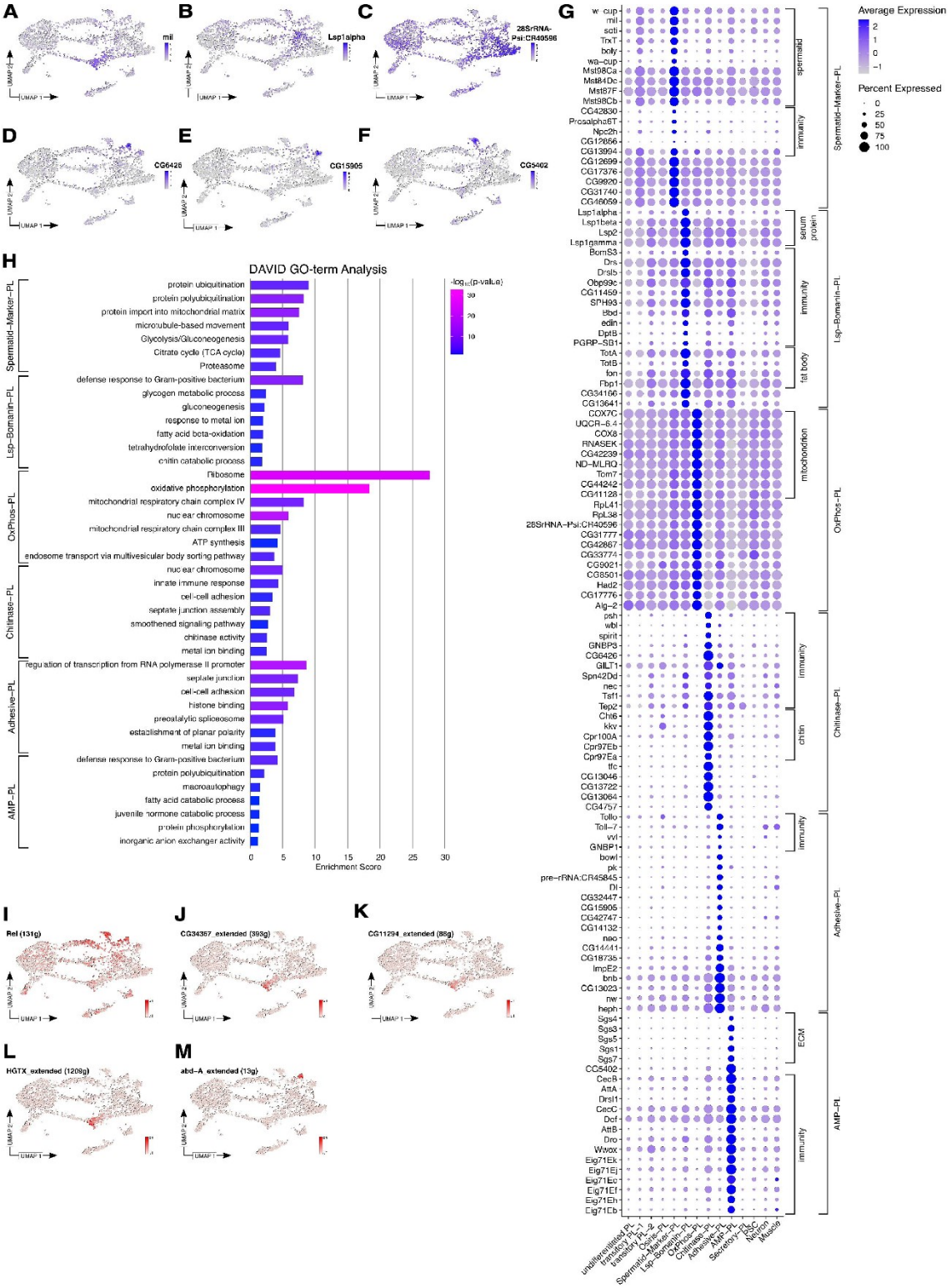

Figure 3, Hirschhäuser et al.

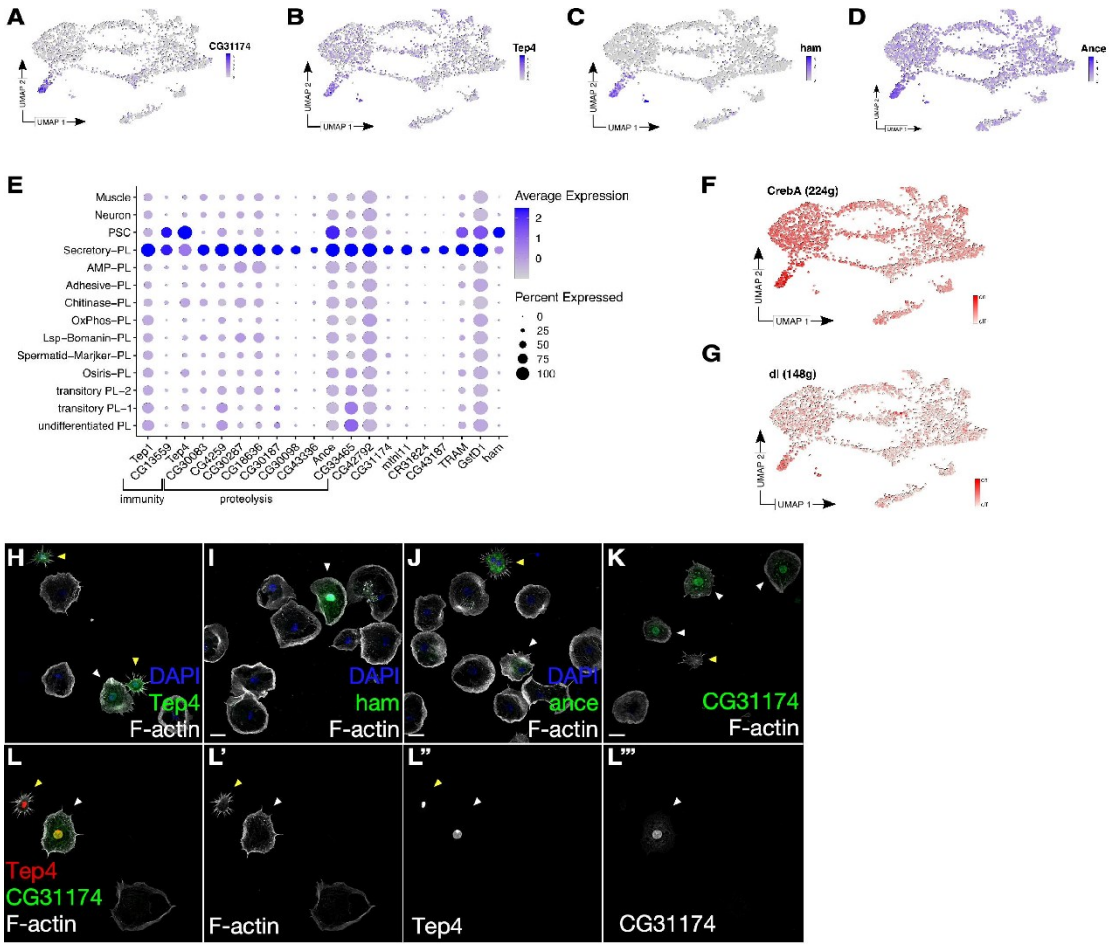

Figure 4, Hirschhäuser et al.

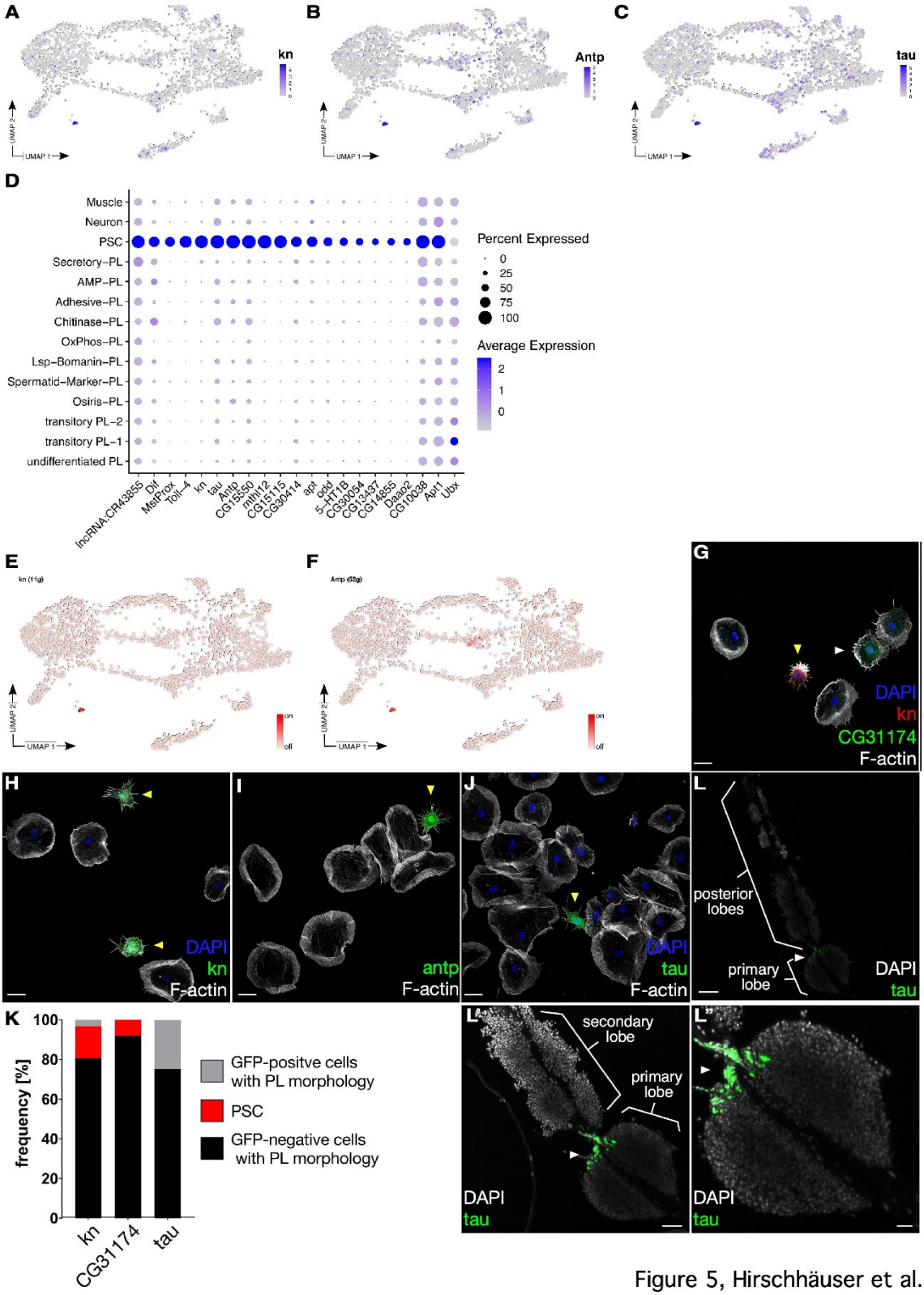

Figure 5, Hirschhäuser et al.

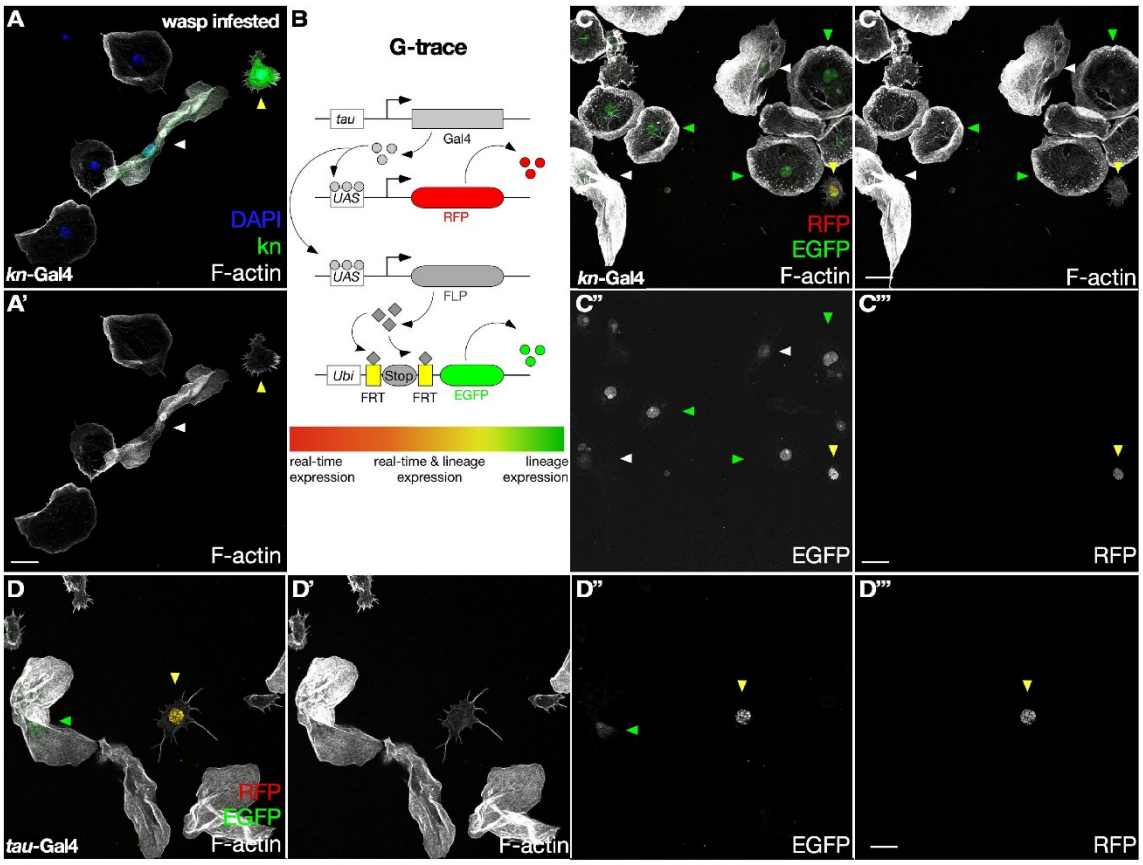

Figure 6, Hirschhäuser et al.

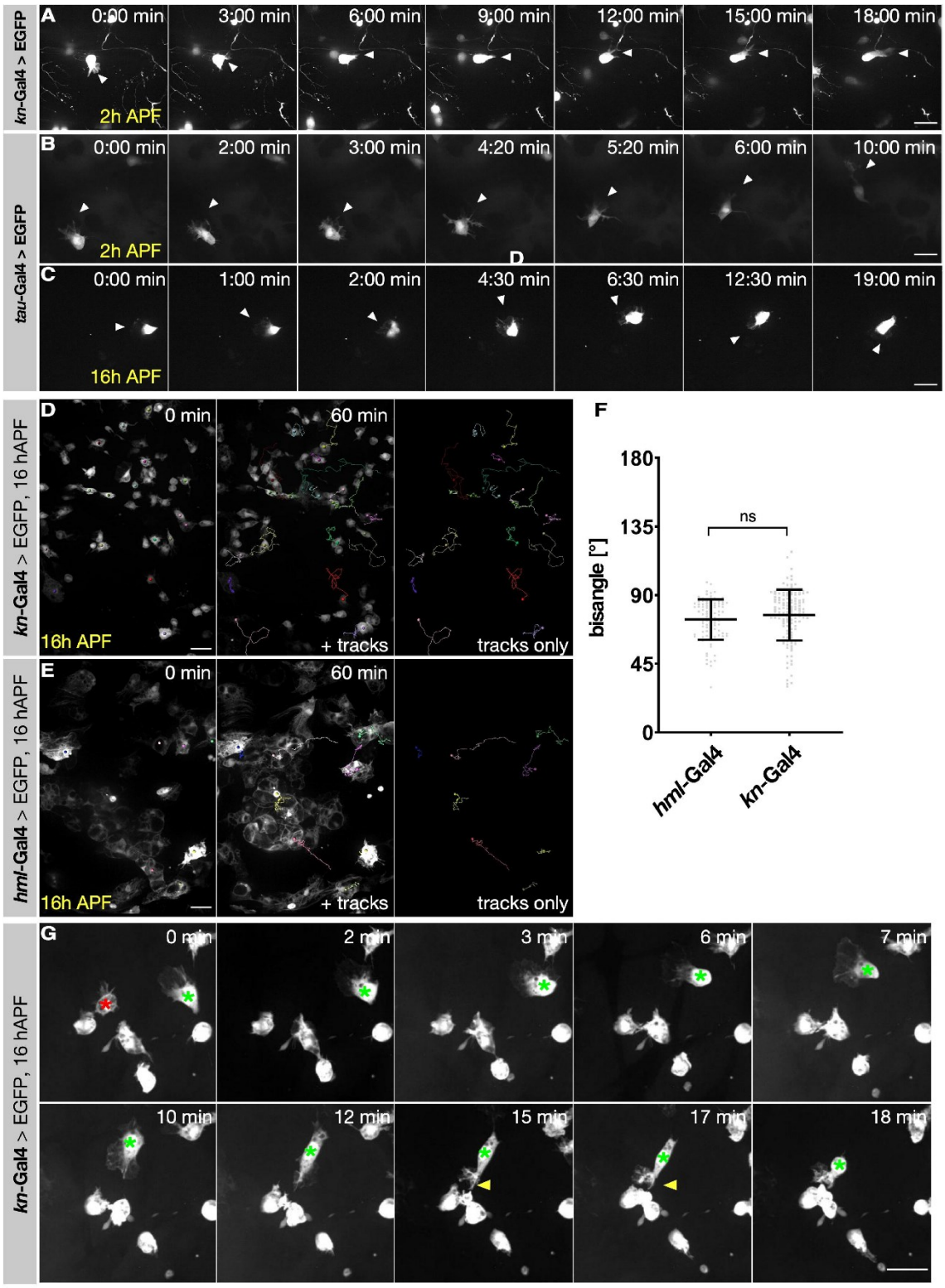

Figure 7, Hirschhäuser et al.

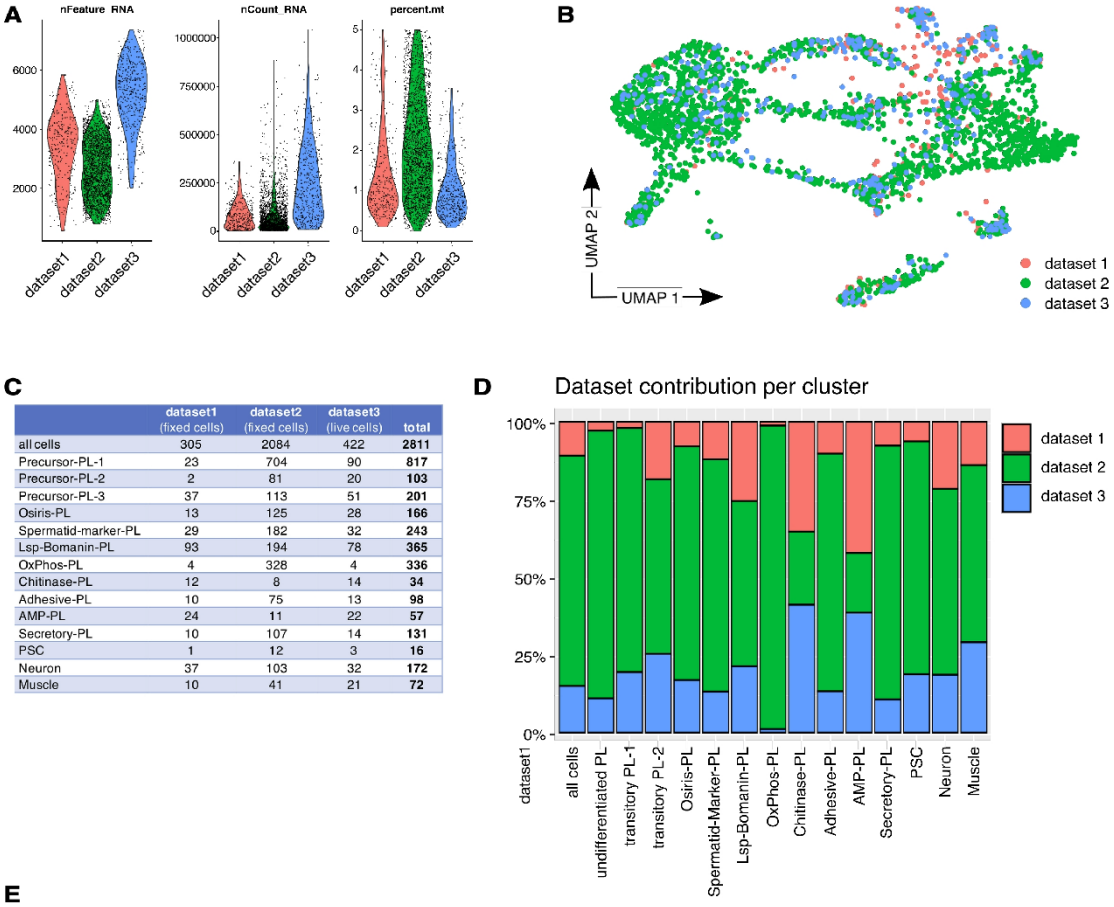

	dataset1 (fixed cells)	dataset2 (fixed cells)	dataset3 (live cells)	total
all cells	305	2084	422	**2811**
Precursor-PL-1	23	704	90	**817**
Precursor-PL-2	2	81	20	**103**
Precursor-PL-3	37	113	51	**201**
Osiris-PL	13	125	28	**166**
Spermatid-marker-PL	29	182	32	**243**
Lsp-Bomanin-PL	93	194	78	**365**
OxPhos-PL	4	328	4	**336**
Chitinase-PL	12	8	14	**34**
Adhesive-PL	10	75	13	**98**
AMP-PL	24	11	22	**57**
Secretory-PL	10	107	14	**131**
PSC	1	12	3	**16**
Neuron	37	103	32	**172**
Muscle	10	41	21	**72**

Supplementary Figure S1, Hirschhäuser et al.

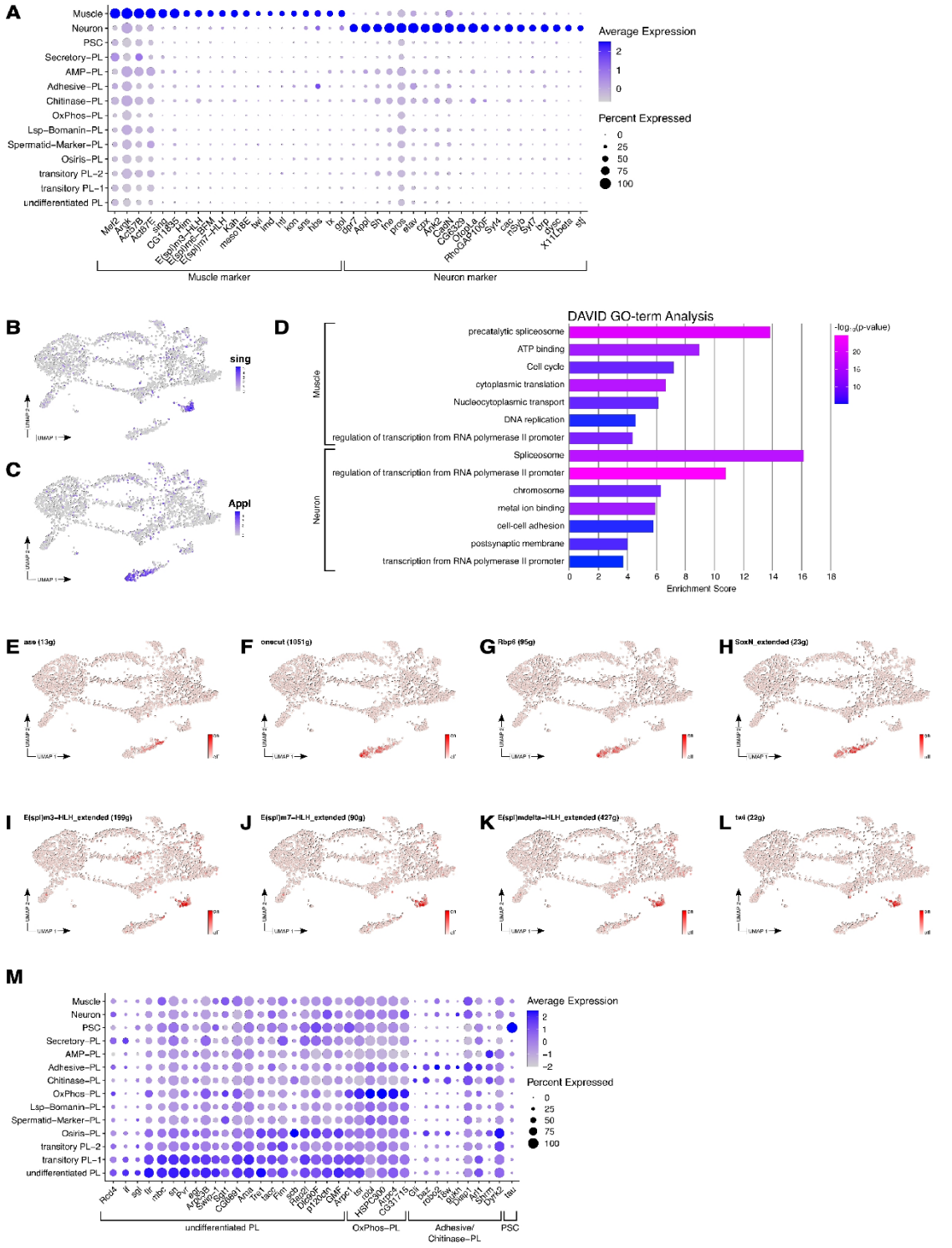

Supplementary Figure S2, Hirschhäuser et al.

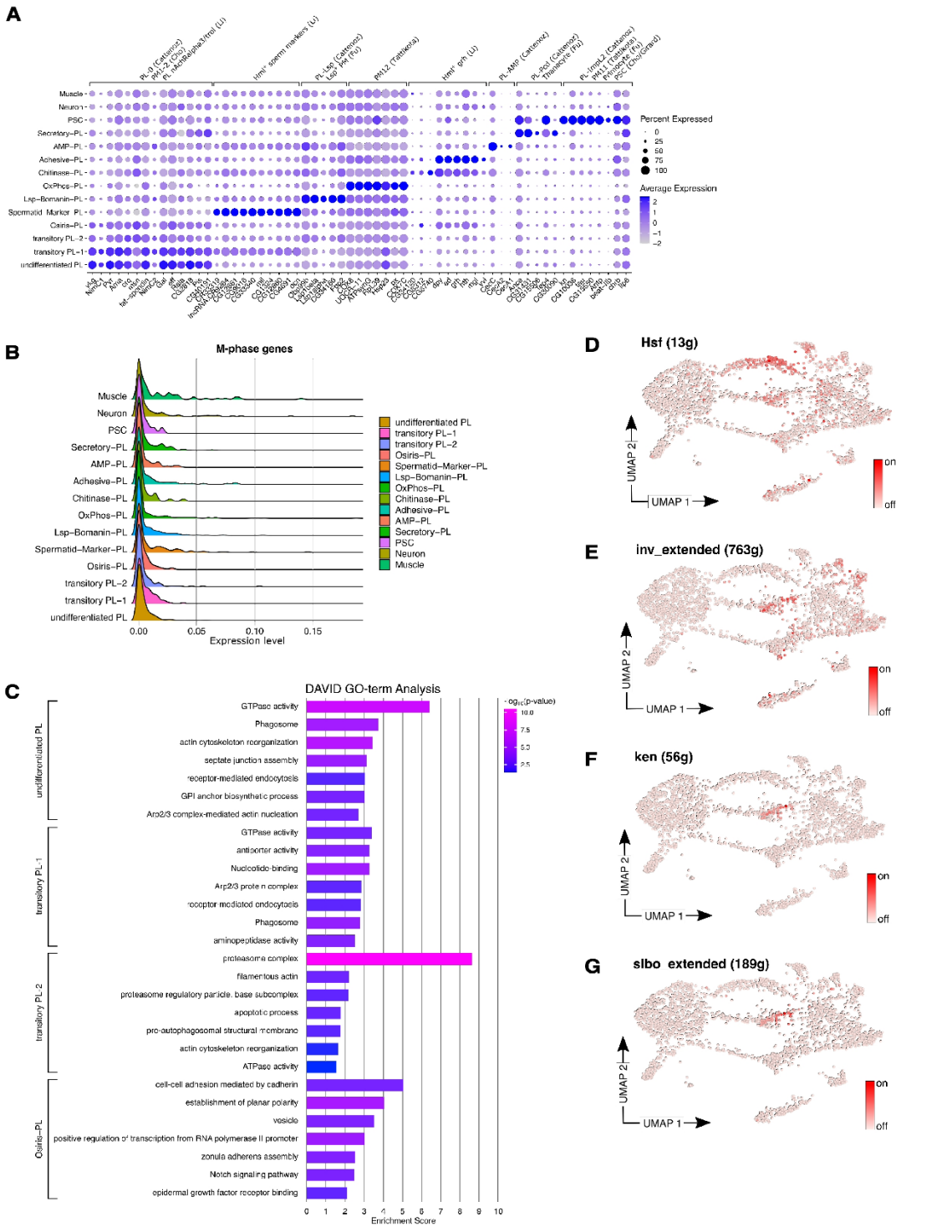

Supplementary Figure S3, Hirschhäuser et al.

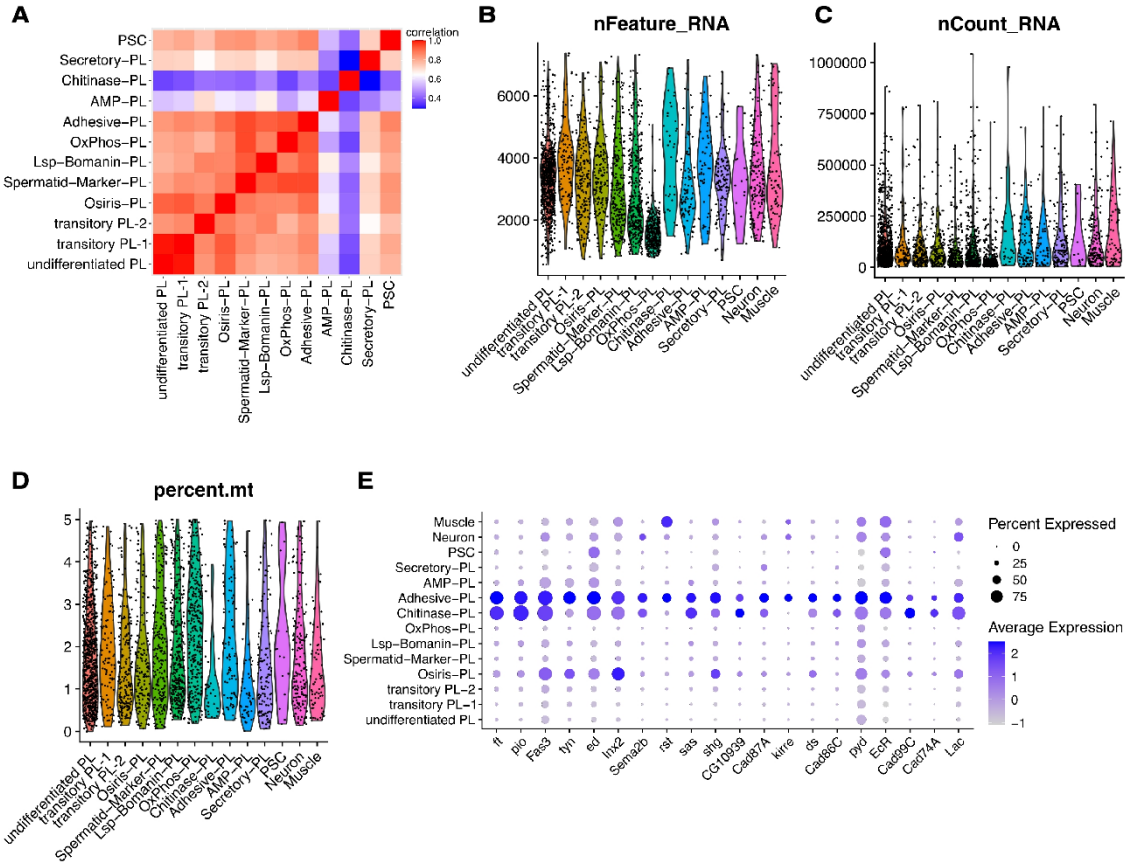

Supplementary Figure S4, Hirschhäuser et al.

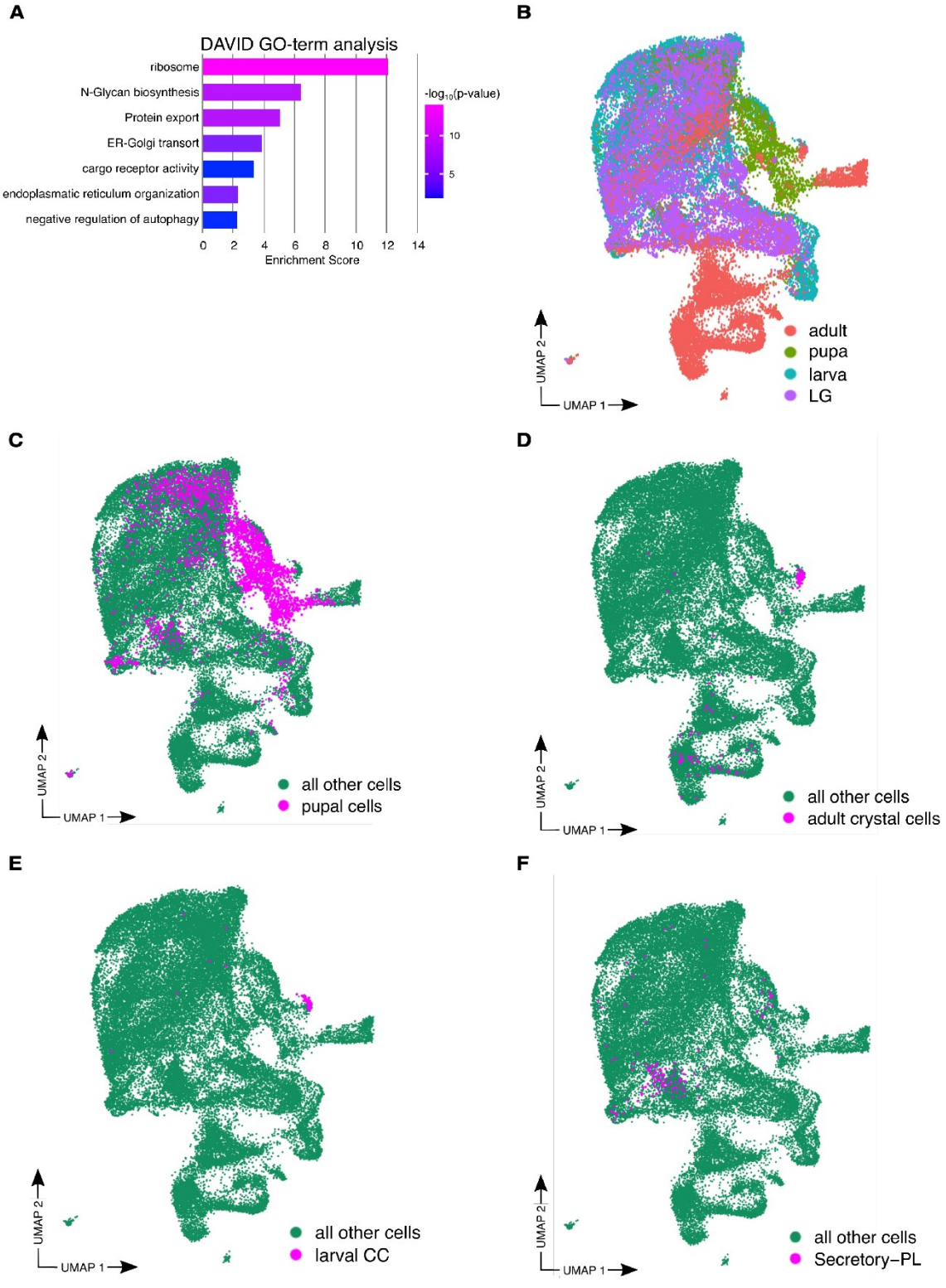

Supplementary Figure S5, Hirschhäuser et al.

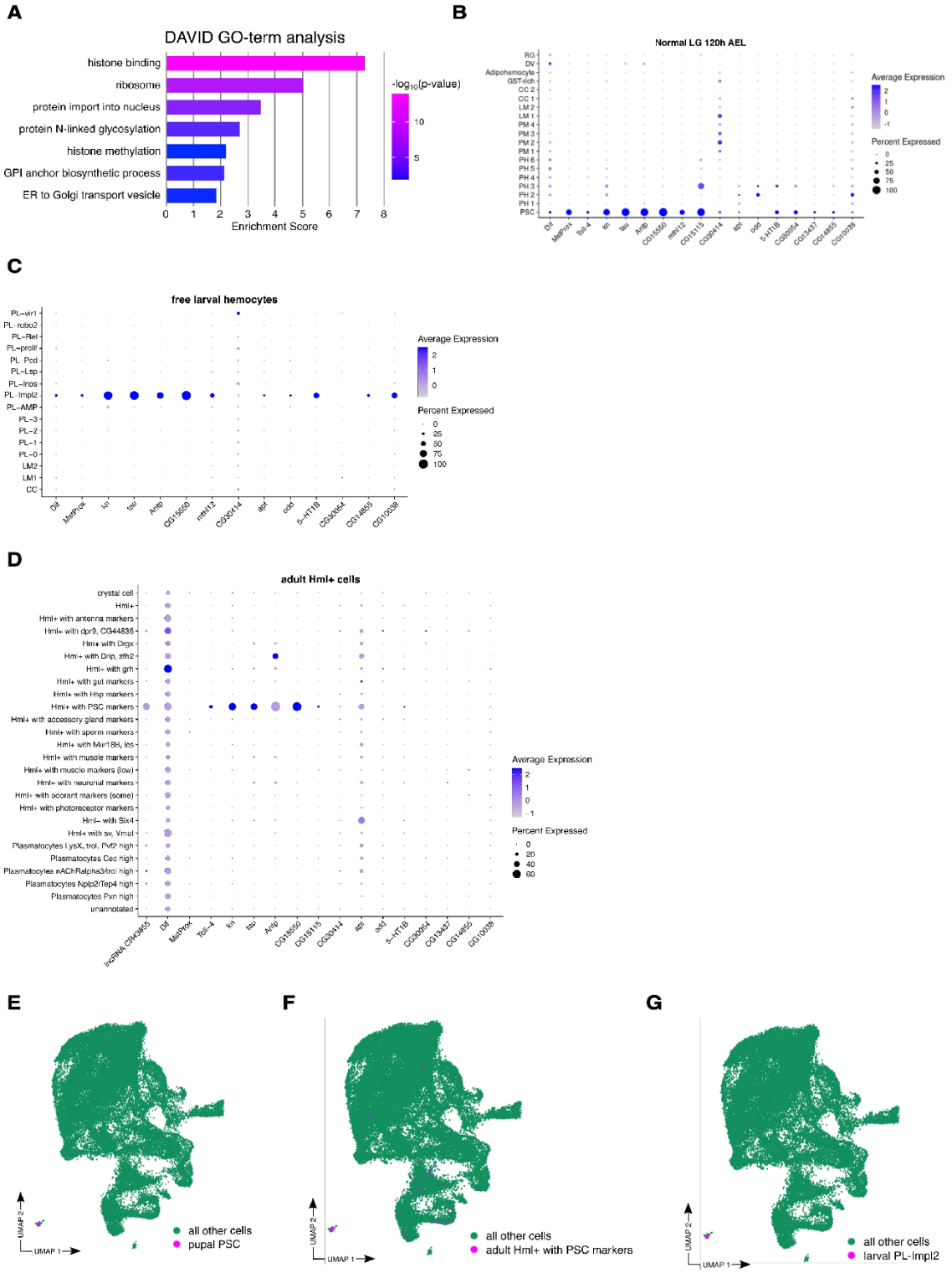

Supplementary Figure S6, Hirschhäuser et al.

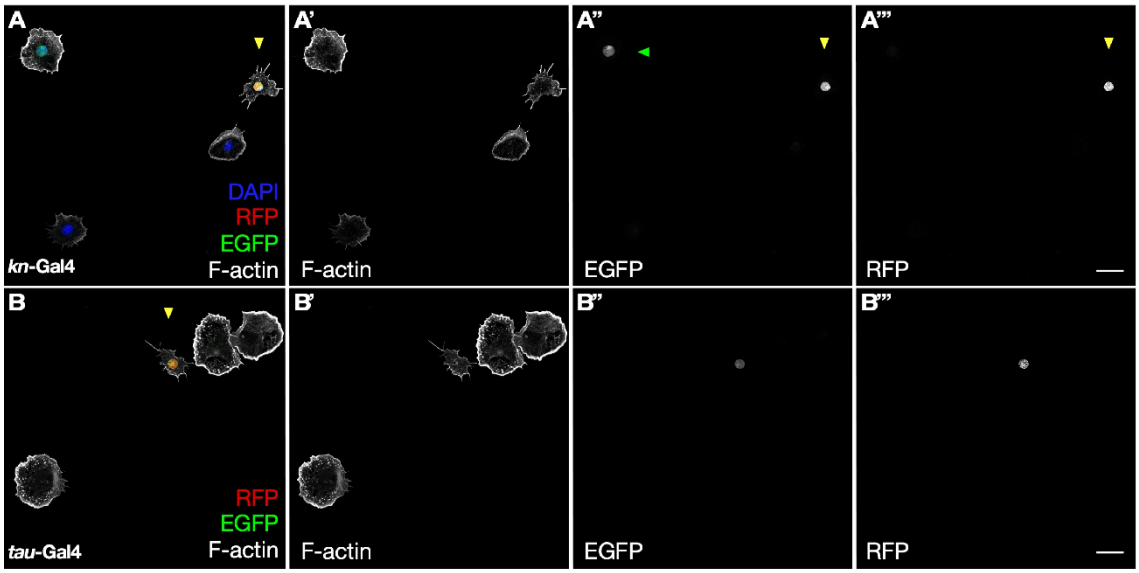

Supplementary Figure S7, Hirschhäuser et al.

2.2. Publication 2

J Cell Sci (2021) 134 (23): jcs258891

CK1α protects WAVE from degradation to regulate cell shape and motility in the immune response

Alexander Hirschhäuser, Marianne van Cann, Sven Bogdan

©2021. Published by The Company of Biologists Ltd | Journal of Cell Science (2021) 134, jcs258891. doi:10.1242/jcs.258891

RESEARCH ARTICLE

CK1α protects WAVE from degradation to regulate cell shape and motility in the immune response

Alexander Hirschhäuser[1], Marianne van Cann[2] and Sven Bogdan[1,2,*]

ABSTRACT

The WAVE regulatory complex (WRC) is the main activator of the Arp2/3 complex, promoting lamellipodial protrusions in migrating cells. The WRC is basally inactive but can be activated by Rac1 and phospholipids, and through phosphorylation. However, the in vivo relevance of the phosphorylation of WAVE proteins remains largely unknown. Here, we identified casein kinase I alpha (CK1α) as a regulator of WAVE, thereby controlling cell shape and cell motility in Drosophila macrophages. CK1α binds and phosphorylates WAVE in vitro. Phosphorylation of WAVE by CK1α appears not to be required for activation but, rather, regulates its stability. Pharmacologic inhibition of CK1α promotes ubiquitin-dependent degradation of WAVE. Consistently, loss of Ck1α but not ck2 function phenocopies the depletion of WAVE. Phosphorylation-deficient mutations in the CK1α consensus sequences within the VCA domain of WAVE can neither rescue mutant lethality nor lamellipodium defects. By contrast, phosphomimetic mutations rescue all cellular and developmental defects. Finally, RNAi-mediated suppression of 26S proteasome or E3 ligase complexes substantially rescues lamellipodia defects in CK1α-depleted macrophages. Therefore, we conclude that basal phosphorylation of WAVE by CK1α protects it from premature ubiquitin-dependent degradation, thus promoting WAVE function in vivo.

This article has an associated First Person interview with the first author of the paper.

KEY WORDS: Drosophila, Macrophages, Cell migration, Cell shape, Lamellipodia, Cell motility, Actin, Arp2/3, WAVE, CK1α, CK2, Phosphorylation, Ubiquitin-dependent protein degradation

INTRODUCTION

Cell shape changes require dynamic remodeling of the actin cytoskeleton. The WASP family verprolin homologous protein (WAVE) is a central Arp2/3 regulator driving lamellipodial protrusions and cell migration in most eukaryotic cells. Together with Abi, NCKAP1/Nap1, CYFIP/Sra-1 and BRK1/HSPC300, WAVE forms a conserved hetero-pentameric complex, the WAVE regulatory complex (WRC). Within the WRC, activity of WAVE towards the Arp2/3 complex is inhibited by intracomplex sequestration of its Arp2/3 activating domain, i.e. the verprolin homology, cofilin homology, acidic region (VCA) domain. One of the central WRC activators is the small RhoGTPase Rac1, which directly binds to the WRC subunit Sra-1 and activates the WRC by allosterically releasing the bound Arp2/3-activating VCA domain of WAVE. Several studies have shown that phosphorylation plays an important role in regulating WRC-Arp2/3-mediated actin filament branching and lamellipodia formation (Mendoza, 2013). WAVE proteins are phosphorylated at numerous sites, and several kinases have been identified as potential regulators (Mendoza, 2013). A previous in vitro study has identified multiple functional phosphorylation events within the acidic VCA domain of mammalian WAVE2 (officially known as WASF2) by casein kinase 2 (CK2), which are required for its activity (Pocha and Cory, 2009). However, the results are based on the overexpression of phosphorylation-deficient mutants in cultured NIH-3T3 cells in the presence of the endogenous wild type protein (Pocha and Cory, 2009). A more recent in vivo study confirmed that the C-terminal acidic region within the VCA domain of the Dictyostelium WAVE is basally phosphorylated at four phosphorylation sites by CK2 and suggested that a regulated dephosphorylation of a fraction of the cellular WAVE pool is a key step in its activation during pseudopod dynamics (Ura et al., 2012).

In this work, we analyze the role of phosphorylation of WAVE (also known as SCAR) in Drosophila in vivo. By using RNA interference (RNAi), we identified casein kinase 1α (CK1α) but not CK2 as an important regulator of lamellipodia formation and immune cell migration. Ck1α-mutant macrophages exhibit a stellate morphology and an altered migratory behavior that phenocopies wave-deficient cells. We also found that CK1α can interact physically with WAVE. Drosophila WAVE contains two conserved CK1α consensus sequences that are located in the N-terminal WHD and the C-terminal acidic domain, overlapping with two conserved CK2 phosphorylation sites within mammalian WAVE2. Phosphorylation-deficient mutations in the N-terminal but not C-terminal domain of WAVE can fully rescue the lethality of the wave mutant and the lamellipodium defects of macrophages deficient for wave. Loss-of and gain-of-function analysis, and pharmacological inhibition of CK1α further suggest that basal phosphorylation of VCA domain by CK1α is crucial for WAVE stability rather than its activity in vivo.

RESULTS

Loss of Ck1α function results in a prominent stellate cell morphology

As previously shown, suppression of Arp2/3-mediated actin polymerization in arp2- or wave-depleted macrophages results in complete loss of lamellipodial protrusions (Rogers et al., 2003; Zobel and Bogdan, 2013). To screen systematically for candidate protein kinases that are required for lamellipodia formation, we used

[1]Institute of Physiology and Pathophysiology, Dept. of Molecular Cell Physiology, Philipps-University Marburg, 35037 Marburg, Germany. [2]Institute for Neurobiology, University of Münster, 48149 Münster, Germany.

*Author for correspondence (sven.bogdan@staff.uni-marburg.de)

M.v., 0000-0002-6388-4937; S.B., 0000-0002-8753-9855

Handling Editor: Michael Way
Received 10 May 2021; Accepted 25 October 2021

Journal of Cell Science (2021) 134, jcs258891. doi:10.1242/jcs.258891

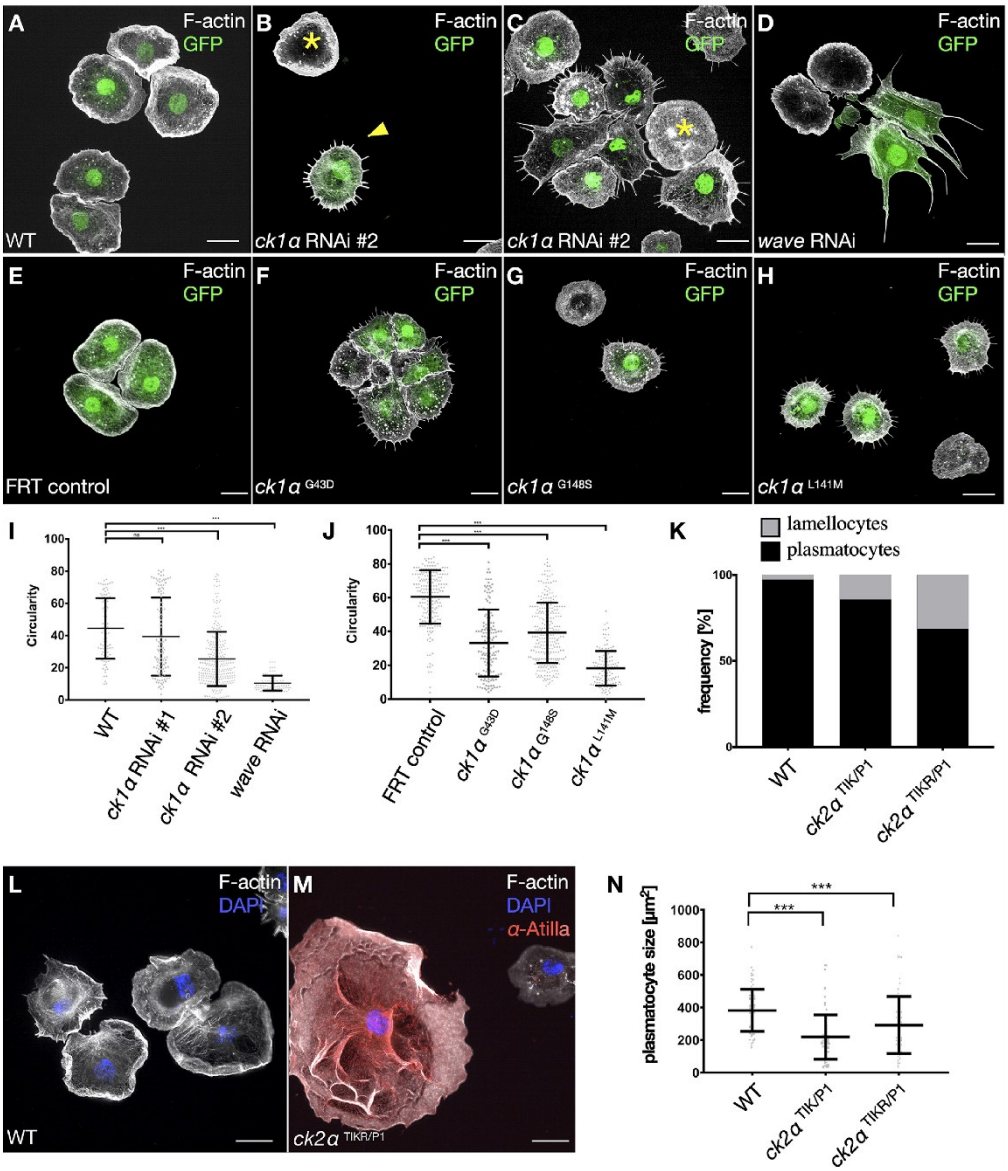

Fig. 1. Loss of CK1α functions disrupt lamellipodia formation. (A-H) Maximum intensity projection of confocal images that show larval macrophages expressing GFP (green); Alexa Fluor 568-labeled phalloidin was used to stain the actin cytoskeleton (white). Scale bars: 10 µm. (A) Wild type macrophages show a highly polarized actin cytoskeleton with a broad lamellipodial cell front. (B,C) Macrophage-specific knockdown of CK1α in larval macrophages using the hemolectin-Gal4 driver disrupts lamellipodia formation. Embryo-derived macrophages that do not co-express Ck1α dsRNA and GFP show wild type cell morphology (asterisk). (D) Macrophage-specific knockdown of wave results in a complete loss of lamellipodial protrusions. (E) MARCM control clones show a wild type cell morphology. (F-H) Ck1α-mutant cells show a stellate cell morphology. (I) Quantification of cell circularity. Macrophage-specific knockdown of Ck1α Wild type (WT; n=99), Ck1α RNAi #1 (n=116), Ck1α RNAi #2 (n=127) and wave RNAi (n=89), depicted in a scatter dot plot with bars indicating mean±s.d. ***P ≤0.001 ANOVA. (J) Quantification of cell circularity. FRT 19 control (n=205), $Ck1\alpha^{G43D}$ (n=152), $Ck1\alpha^{G148S}$ (n=282) and $Ck1\alpha^{L141M}$ (n=135) cells, depicted in a scatter dot blot with bars indicating mean±s.d. ***P ≤0.001 (one-ANOVA with Dunnett's multiple comparison test). I and J show a unitless measure. (L,M) Structured illumination microscopy (SIM) images of lamellocytes isolated from Drosophila larvae stained for Atilla (red) and F-actin (white); nuclei were stained with DAPI (blue). Scale bars: 10 µm. Wild type cells (L), transheterozygous $ck2\alpha^{TIKR/P1}$ mutant cells (M). (K,N) Quantification of lamellocyte frequency (K) and macrophage size (N). Note that loss of ck2α induces not only lamellocytes at the expense of plasmatocytes but also results in macrophages with reduced cells size, likely to represent intermediates.

Journal of Cell Science (2021) 134, jcs258891. doi:10.1242/jcs.258891

Drosophila macrophages as a model system, therefore combining many advantages of cultured cells with a genetic in vivo model system (Rüder et al., 2018; Sander et al., 2013). We tested 308 conditional transgenic RNAi fly lines targeting 162 kinases encoded in the fly genome (see Table S1). Transgene RNAis were specifically coexpressed with GFP in the macrophage lineage using the hmlΔ-Gal4 driver (Sinenko and Mathey-Prevot, 2004). Macrophages were isolated from third-instar larvae, and tested for their phenotypic effects on lamellipodia formation and cell spreading ex vivo.

Wild type macrophages acquire a round, pancake-like shape with a broad lamellipodial actin filament network (Fig. 1A). Expression of most double-stranded RNAs (dsRNAs) induced no defects in the cell morphology and lamellipodia formation (see Table S1). We identified the casein kinase 1α (Ck1α) gene as a candidate that most strongly affected lamellipodia formation and phenocopied wave-depleted cells, characterized by a prominently reduced circularity index (Fig. 1B–D,I). We only found a few more dsRNAs that affected cell shape (see Table S1).

Next, we analyzed Ck1α mutants, bearing distinct missense mutations ($Ck1\alpha^{8B12}$, $Ck1\alpha^{A}$ and $Ck1\alpha^{B}$). Of those, $Ck1\alpha^{8B12}$ ($Ck1\alpha^{G43D}$) is the only functionally characterized Ck1α allele carrying a mutation that transforms the conserved glycine residue at position 43 into an aspartic acid (G43D). It has been first described as a strong hypomorph or amorphic allele (Legent et al., 2012). $Ck1\alpha^{A}$ ($Ck1\alpha^{L141M}$) and $Ck1\alpha^{B}$ ($Ck1\alpha^{G148S}$) have been previously isolated in a large EMS screen, but neither allele has so far been functionally characterized (Haelterman et al., 2014). $Ck1\alpha^{A}$ carries a mutation that leads to replacement of a conserved lysine residue with methionine at position 141 (L141M), constituting the only mutation that yields removal of an H-bond – which might affect the active site of the CK1 (see 3D structure in Movie 1, dashed lines in magenta). By contrast, $Ck1\alpha^{B}$ replaces glycine with a serine at position 148 (G148S) without any obvious structural changes.

To analyze these embryonic lethal Ck1α mutations in macrophages we performed mosaic analysis with a repressible cell marker (MARCM; Wu and Luo, 2006) to generate Ck1α-mutant macrophages in a wild type animal background. Compared

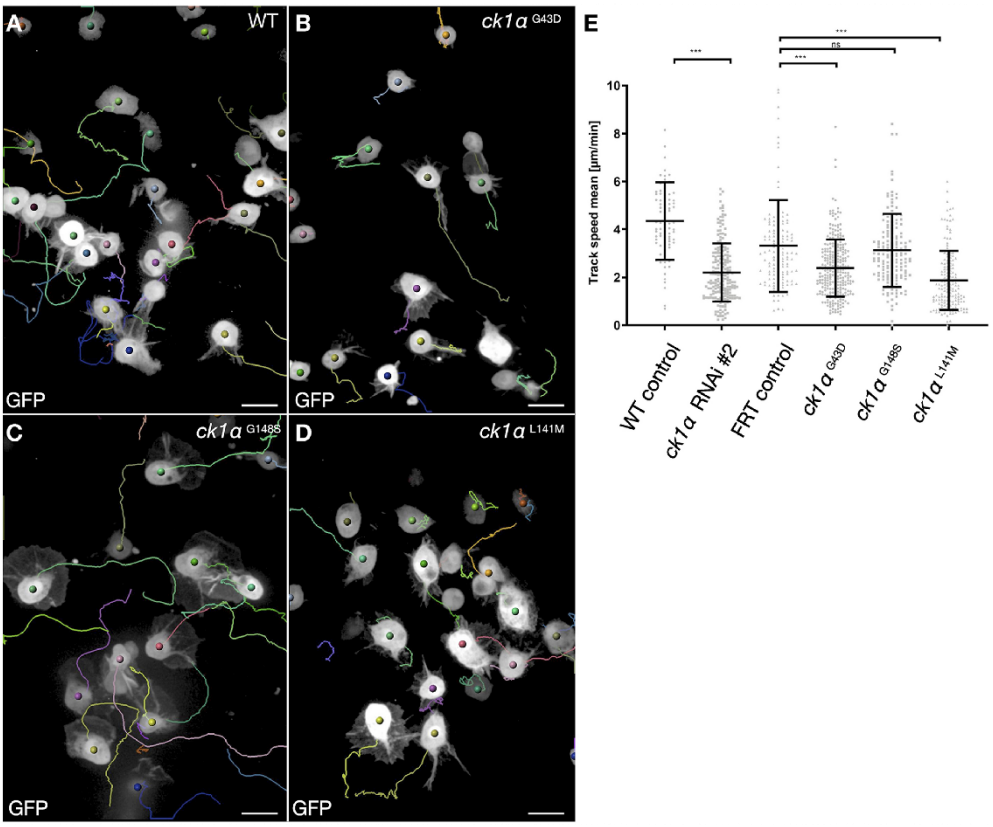

Fig. 2. Loss of CK1α impairs macrophage migration. (A–D) Still images of randomly migrating pupal macrophages (after 20 min recording). Cells were tracked using Imaris software; single trajectories are depicted in different colors. Wild type macrophages (A) expressing GFP show broad lamellipodia that migrate constantly. Mutation of Ck1α (B–D) results in reduced cell speed. Scale bars: 10 µm. (E) Quantification of cell speed. Shown is a scatter dot plot with bars indicating mean±s.d. ***P ≤0.001 (Welch's t-test); ns, not significant. The mean track speed of $Ck1\alpha^{L141M}$>$Ck1\alpha^{G43D}$ mutant cells is significantly reduced comparison to control macrophages. Based on lamellipodium defects and impaired migratory behavior, we ranked the mutations into the following allelic series: $Ck1\alpha^{L141M}$>$Ck1\alpha^{G43D}$>$Ck1\alpha^{G148S}$.

Journal of Cell Science (2021) 134, jcs258891. doi:10.1242/jcs.258891

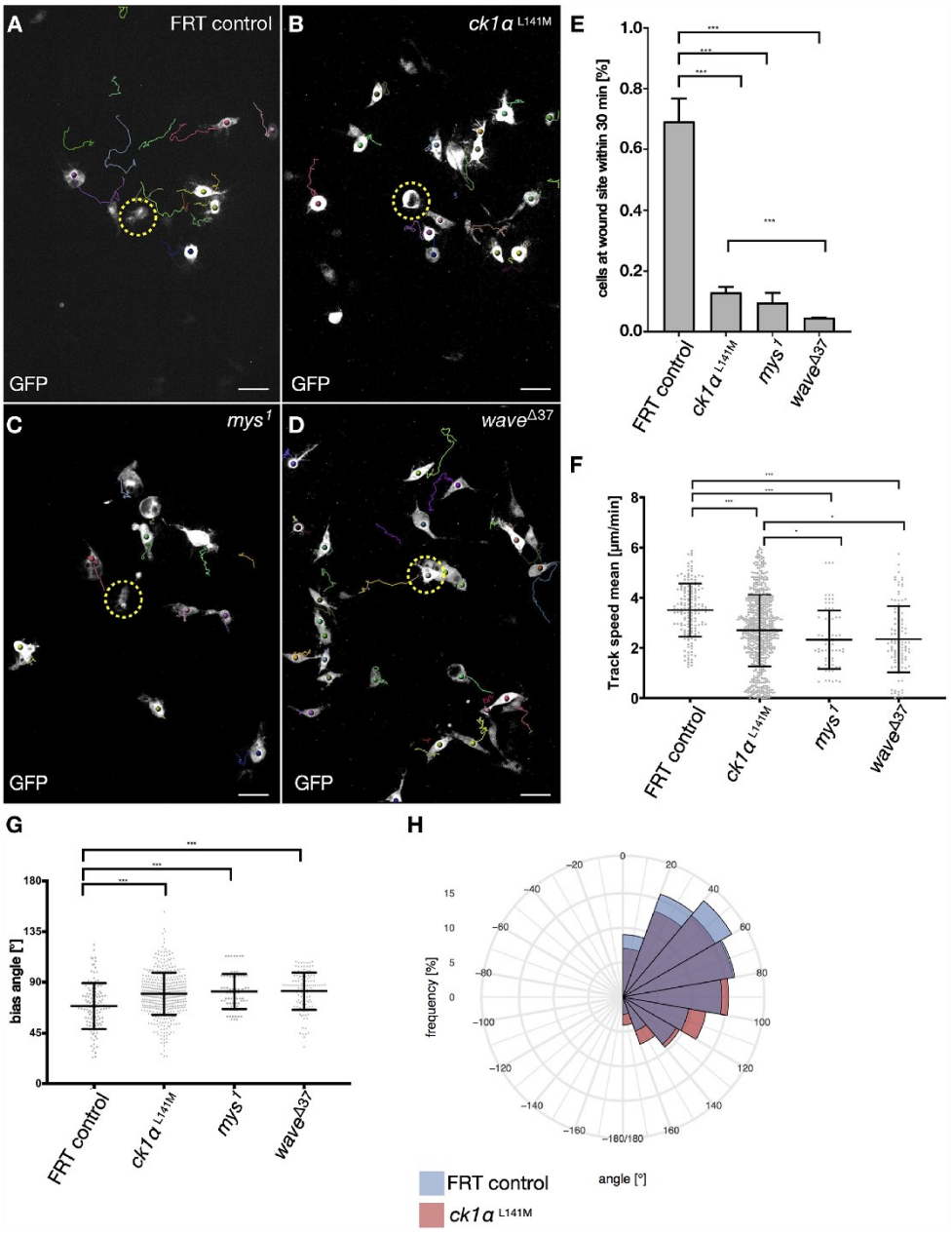

Fig. 3. See next page for legend.

with control cells (Fig. 1E), isolated GFP-positive Ck1α^{L141M} mutant cells displayed the strongest defects in lamellipodia formation, showing a prominent stellate cell morphology compared with Ck1α^{G43D} and Ck1α^{G148S} (Fig. 1E–H, quantification of reduced circularity is shown in Fig. 1J). Thus, we confirmed CK1α as an important novel regulator of cell shape.

A possible role on cell shape has also been suggested for casein kinase 2 (CK2; Kramerov et al., 2011; Pocha and Cory, 2009), a structurally completely different enzyme that was also included in

Fig. 3. Loss of CK1α impairs macrophage directionality upon wounding of a single cell. (A–D) Still images of spinning disc time-lapse movies of directed macrophage migration upon wounding of a single cell (encircled by yellow dashed line, t=0). Scale bars: 20 µm. Cells were imaged for 30 min after laser ablation in 30 s intervals and tracked by using Imaris software. (A) Upon wounding, wild type cells switch from random to directed migration. Within 30 min, most cells within a distinct radius reach the wound site. (B) Trajectories indicate that Ck1α-mutant macrophages are attracted to the wound site, but they migrate with a reduced directionality. A similar, but even stronger impaired migratory behavior was found for mys^{1} (C) and $wave^{\Delta 37}$ (D) mutant macrophages. (E) Quantification of cells at the wounding site 30 min after laser ablation of wild type FRT19 control, $Ck1\alpha^{L141M}$, mys^{1} and $wave^{\Delta 37}$ cells. ***P ≤0.001 (Welch's t-test). (F) Quantification of cell speed. Shown is a scatter dot plot, with bars indicating mean±s.d. ***P ≤0.001, *P ≤0.033 (Welch's t-test). The mean track speed of mys and $wave^{\Delta 37}$>$Ck1\alpha^{L141M}$ mutant cells is significantly reduced compared to that of control macrophages. Wild type FRT19 control (n=130), $Ck1\alpha^{L141M}$ (n=445), mys^{1} (n=72) and $wave^{\Delta 37}$ (n=120). (G) Quantification of the bias angle. Wild type FRT19 control (n=130), $Ck1\alpha^{L141M}$ (n=445), β^{PS}-integrin (mys, n=72) and $wave^{\Delta 37}$ (n=120). Shown is a scatter dot blot with bars indicating mean±s.d. ***P ≤0.001 (Welch's t-test). (H) Polar histogram chart of the bias angle distribution, showing impaired directionality of $Ck1\alpha^{L141M}$ mutant macrophages when compared to wild type FRT control cells.

our initial RNAi screen (see also Table S1). Whereas CK1α is a monomeric serine kinase, CK2 is composed of two catalytic CK2α and two regulatory CK2β subunits that form a hetero-tetrameric (α2β2) holoenzyme (Bandyopadhyay et al., 2017). RNAi-mediated depletion of either CK2α or CK2β subunit did not significantly affect lamellipodia formation but resulted in altered blood cell homeostasis, which could be also confirmed in ck2α (also known as CkIIα)-mutant larvae (Table S1; Fig. 1K–M). Loss of ck2α function induced the formation of Atilla-positive lamellocytes at the expense of macrophages (Fig. 1L,M; quantification in Fig. 1K). Lamellocytes are giant cells that are rarely observed in healthy flies, but transdifferentiation from macrophages is dramatically induced in response to infection by parasitic wasps (Anderl et al., 2016). Transheterozygous $ck2\alpha^{TIK/P1}$ and $ck2\alpha^{TIKR/P1}$ mutant larvae, which lack CK2α kinase activity (Bulat et al., 2014), showed an enlarged lamellocyte compartment (≤30%) and macrophages (70%) whose average size differs compared with control macrophages (Fig. 1N). as recently suggested, these cells might be at an intermediate state of transdifferentiation (Anderl et al., 2016). Our data suggest that CK2 regulates blood cell differentiation, rather than blood cell shape.

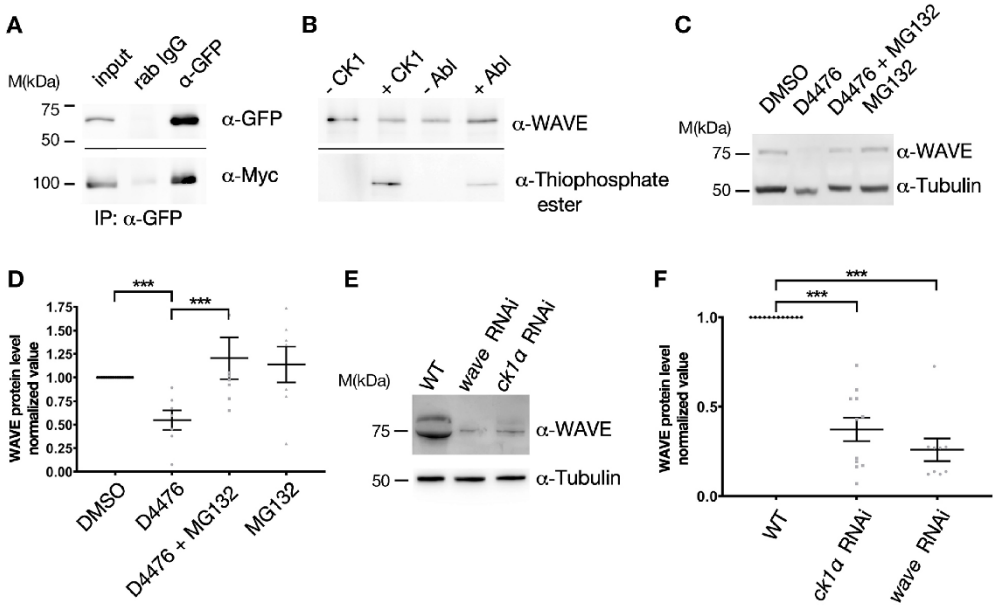

Fig. 4. RNAi-induced depletion of CK1α results in reduction of WAVE protein levels in macrophages. (A) CK1α physically interacts with WAVE. S2 cells were co-transfected with EGFP-tagged CK1α and Myc-tagged WAVE. Total cell lysates (input) were used for immunoprecipitation with a pre-immune control serum [rabbit (rab) IgG] or α-GFP serum (α-GFP). Samples were separated using SDS-PAGE and analyzed by western blotting using antibodies against GFP (α-GFP, top) or Myc (α-Myc, bottom). (B) Detection of in vitro phosphorylated WAVE protein, phosphorylated through recombinant human CK1 or Abl. Reactions were performed using recombinant GST-WAVE purified from E. coli. –/+ indicates absence (–) and presence (+) of the CK1 or Abl (NEB). Reaction conditions depend on the added kinase. Samples were separated by SDS-PAGE and analyzed by western blotting using anti-WAVE and anti-thiophosphate ester antibodies (α-WAVE and α-thiophosphate ester, respectively). (C) Inhibition of CK1α increases WAVE protein levels. S2 cells were treated with vehicle control (DMSO), the CK1α-specific inhibitor D4476, the proteasome inhibitor MG132 or D4476 and MG132 together for 4 h. The cells were collected, lysed and analyzed by immunoblotting with antibodies against WAVE or tubulin. Inhibition of CK1α decreases levels of endogenous WAVE protein, whereas MG132-treated cells show markedly increased levels. Tubulin served as loading control. (D) Quantification of WAVE protein levels in response to pharmacological inhibition of CK1α. Results are the average of five independent experiments normalized to wild type protein level (set at 1). P-values from ratio paired t-test are shown when significantly different from control (***P <0.001). (E) RNAi induced CK1α depletion results in substantial reduction of WAVE protein levels in macrophages. Larval macrophages were isolated, centrifuged and resuspend in SDS-sample buffer, and immunoblotted with antibodies against WAVE or tubulin. RNAi of wave serves as control to clarify specificity and reduction of WAVE protein levels. Tubulin serves as the loading control. (F) Quantification of WAVE protein levels upon RNAi-mediated knockdown. RNAi of wave serves as control. Results are the average of nine independent experiments. P-values from ratio paired t-test are shown when significantly different from control (***P <0.001).

Journal of Cell Science (2021) 134, jcs258891. doi:10.1242/jcs.258891

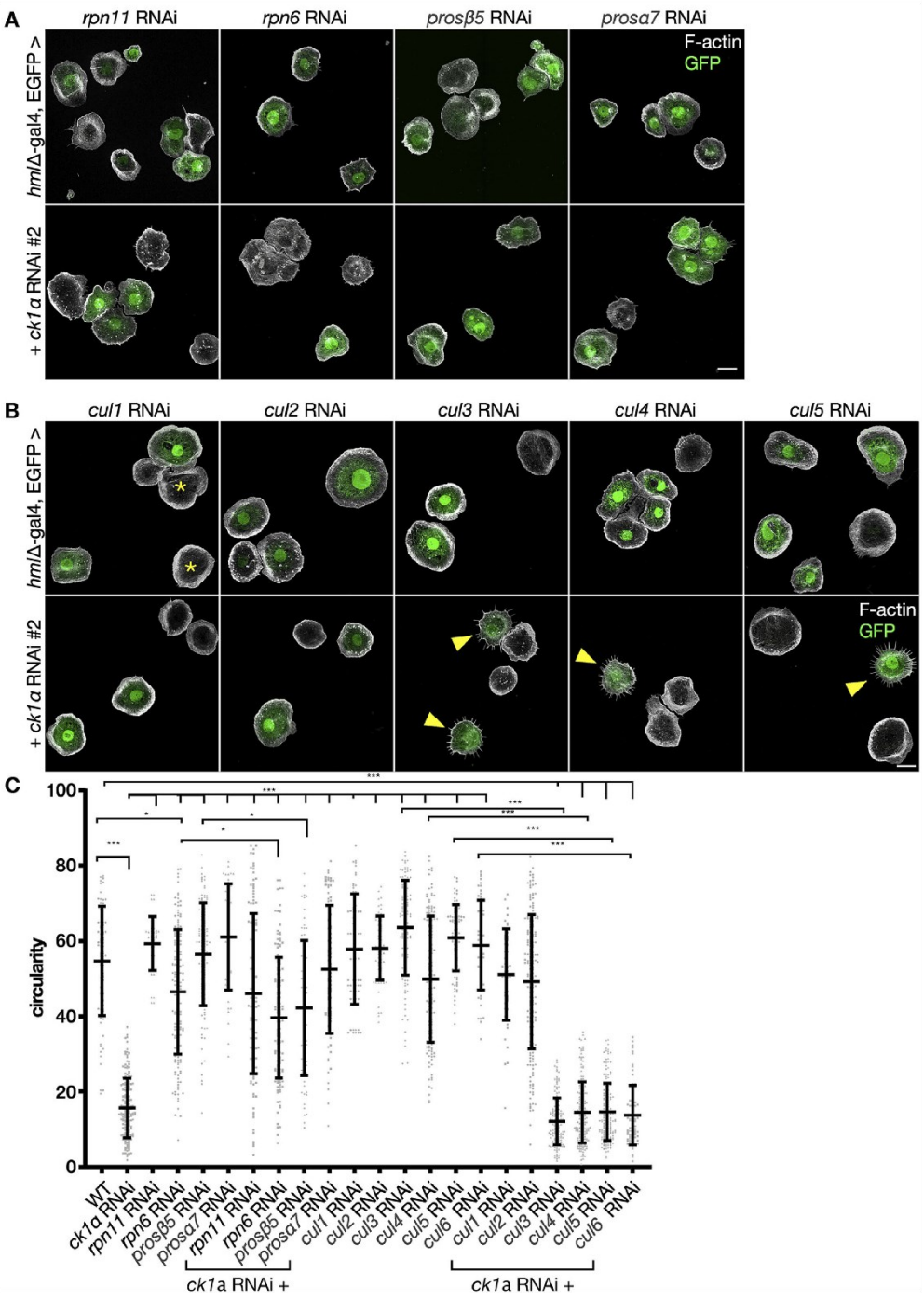

Fig. 5. See next page for legend.

Fig. 5. Lamellipodia defects in CK1α-depleted macrophages are rescued upon inhibition of proteasomal degradation. (A,B) Maximum intensity projection of confocal images that show larval macrophages expressing GFP (green). Alexa Fluor 568-labeled phalloidin was used to stain the actin cytoskeleton (white). Scale bar: 10 µm. (A) Macrophage-specific knockdown of proteasome components rpn11, rpn6, prosβ5 or prosα7 in larval macrophages using the hemolectin-Gal4 driver does not affect cell morphology. Rescue of cell morphology defects of Ck1α RNAi-depleted cells by co-expression of indicated transgenic RNAis against indicated proteasomal components. (B) Macrophage-specific knockdown of any of the six known cullin proteins does not significant impact on cell shape. Embryo-derived macrophages that do not co-express dsRNA and GFP are indicated (asterisks). RNAi-mediated knockdown of Cul1 and Cul2 but not Cul3 to Cul6 rescued cell shape defects of macrophages evoked by Ck1α RNAi. Scale bars: 10 µm. (C) Quantification of cell circularity. Shown is a scatter dot plot, bars indicate mean±s.d. *P ≤0.033, ***P ≤0.001 (one-way ANOVA with Bonferroni's multiple comparison test). Wild type WT (n=78) Ck1α RNAi (n=172), rpn11 RNAi (n=40), Rpn6 RNAi (n=163), prosβ5 RNAi (n=117), prosα7 RNAi (n=47), Ck1α RNAi+rpn11 RNAi (n=124), Ck1α RNAi+rpn6 RNAi (n=145), Ck1α RNAi+prosβ5 RNAi (n=74) and Ck1α RNAi+prosα7 RNAi (n=83), Cullin 1 RNAi (n=61), Cullin 2 RNAi (n=66), Cullin 3 RNAi (n=120), Cullin 4 RNAi (n=130), Cullin 5 RNAi (n=90), Cullin 6 RNAi (n=54), Ck1α RNAi+Cullin 1 RNAi (n=48), Ck1α RNAi+Cullin 2 RNAi (n=174), Ck1α RNAi+Cullin 3 RNAi (n=144), Ck1α RNAi+Cullin 4 RNAi (n=177), Ck1α RNAi+Cullin 5 RNAi (n=170), Ck1α RNAi+Cullin 6 RNAi (n=76).

Loss of Ck1α function impairs macrophage migration and immune response

To further examine a possible role of CK1α in cell migration, we first analyzed the migratory behavior of $Ck1\alpha^{L141M}$ mutant macrophages expressing GFP in pre-pupae. Wild type control macrophages form broad lamellipods to migrate along the epidermis (Fig. 2A). Cell trajectories show wild type macrophages migrate long distances within 20 min of acquisition (Fig. 2A; Movie 2; quantification of migration speed is shown in Fig. 2E). By contrast, $Ck1\alpha^{G43D}$ and $Ck1\alpha^{L141M}$ mutant macrophages migrate considerably slower (Fig. 2B,C,E). No significant differences were observed between (FRT, where FRT indicates the target site for the FLP recombinase) control and $Ck1\alpha^{G148S}$ mutant macrophages, suggesting that $Ck1\alpha^{G148S}$ is a hypomorph (Fig. 2D,E).

To determine the role of CK1α in directed wound response of macrophages, laser ablation experiments were performed in a single cell within the pupal wing (Fig. 3A–D, area encircled by dashed yellow line). Upon wounding, control macrophages (FRT control) switch from random to directed migration towards the wounding site. Cells were automatically tracked within the first 30 min post wounding and trajectories were constructed (Fig. 3A–D; quantification in Fig. 3E–H; Movie 3). Ck1α-deficient macrophages still respond to the cell damage, however, due to reduced lamellipodia formation, $Ck1\alpha^{L141M}$ mutant cells were impaired in their ability to migrate towards the ablated cell. To better characterize defects in the migratory behavior we first counted the number of cells that reached the wound within the first 30 min after wounding (Fig. 3E). Number of cells at the wound were normalized to the total number of cells within 10–80 µm of the ablation site. We also measured the mean track speed of mutant cells compared to that of FRT control cells (Fig. 3F). Both, cell numbers at the wound and cell speed were significantly reduced in $Ck1\alpha^{L141M}$ as well as in myospheroid (mys^{1}) and $wave^{\Delta37}$ mutant cells (Fig. 3E,F; Movie 3). To further describe the impaired migratory behavior of $Ck1\alpha^{L141M}$ mutant cells we also measured the bias angle, i.e. the angle between the motion vector (a step of the cell) and the direction vector pointing towards the wound (Liepe et al., 2016; Weavers et al., 2016). A bias angle of ∼0° indicates the highest directionality to the wound, whereas cells with a value of ∼180° move in the opposite direction. For migrating wild type macrophages, the bias angle had values of <80° (shown in Fig. 3G,H as frequency distribution of the bias angle for each trajectory). By contrast, $Ck1\alpha^{L141M}$ mutant cells move with a bias angle between 80° and 180° (Fig. 3G,H). Ck1α-mutant macrophages showed reduced distance from the origin, with a reduced directionality (indicated by the cell bias angle; Fig. 3F). A similar, but more severely impaired migratory behavior was shown for $wave^{\Delta37}$ and β-integrin (mys^{1}) mutant macrophages (Fig. 3F,G; Moreira et al., 2013). These results indicate that CK1α is required for proper lamellipodia formation and immune cell migration in vivo.

CK1α physically interacts with WAVE and human recombinant CK1δ can phosphorylate Drosophila WAVE in vitro

Given the similar cellular phenotypes, we next tested for a possible physical interaction between CK1α and WAVE. To this end, we transiently co-transfected Drosophila S2R+ cells with EGFP-tagged CK1α and Myc-tagged WAVE, followed by coimmunoprecipitation experiments. Pull-down assays using lysates from cells expressing tagged CK1α and WAVE revealed a physical interaction between the two proteins (Fig. 4A). To further examine whether CK1 can phosphorylate WAVE, we performed an in vitro kinase assay using recombinant human CK1δ kinase (1–317aa) – which has 65% identity to Drosophila CK1α – in the presence of purified glutathione S-transferase (GST)-tagged Drosophila WAVE protein (GST-WAVE). In this assay, ATPγS served as the phosphate donor from which mono-thiophosphate instead of phosphate is transferred to the substrate (Fig. 4B). Alkylated thiophosphate creates an epitope for thiophosphate ester-specific antibodies, which allows detection of phosphorylation (Allen et al., 2007). Our thiophosphorylation assay showed that WAVE can be phosphorylated by CK1 and its positive control Abelson kinase (Abl) (Leng et al., 2005) (Fig. 4B).

CK1α protects WAVE from ubiquitin-mediated degradation

We next analyzed the potential effect of CK1α on endogenous WAVE protein. First, we used the cell-permeable, CK1α-specific ATP-competitive inhibitor D4476 (Rena et al., 2004). Remarkably, inhibition of CK1α activity by D4476 resulted in a significant reduction of WAVE protein levels in S2 cells (Fig. 4C, quantification is shown in Fig. 4D). This was prevented by addition of the proteasome inhibitor MG132, suggesting that phosphorylation of WAVE by CK1α protects WAVE from ubiquitin-mediated degradation (Fig. 4C,D). In addition, we found that CK1α depletion through RNAi results in substantial reduction of WAVE protein levels in larval macrophages (Fig. 4E). Quantification of nine independent experiments is shown in Fig. 4F. To further analyze whether inhibition of ubiquitin-mediated degradation can also revert the lamellipodium defects evoked by depletion of CK1α, we screened for proteasome components and tested various RNAi lines. Ubiquitin-dependent degradation is a multi-step process that involves members of the cullin protein family as part of E3 ligase complexes (Morreale and Walden, 2016) as well as the 26S proteasome, consisting of a 20S catalytic core and a 19S regulatory complex (Saeki, 2017). Upon inhibition of proteasomal degradation by targeting either the 20S catalytic core (Prosβ5, Prosβ7) or the 19S regulatory complex (Rpn11, Rpn6), we found that the lamellipodium defects induced in response to RNAi of Ck1α were significantly rescued, whereas knockdown of rpn11, rpn6, prosβ5 and prosβ7 alone did not show significant differences regarding cell shape (Fig. 5A,C). We also

Journal of Cell Science (2021) 134, jcs258891. doi:10.1242/jcs.258891

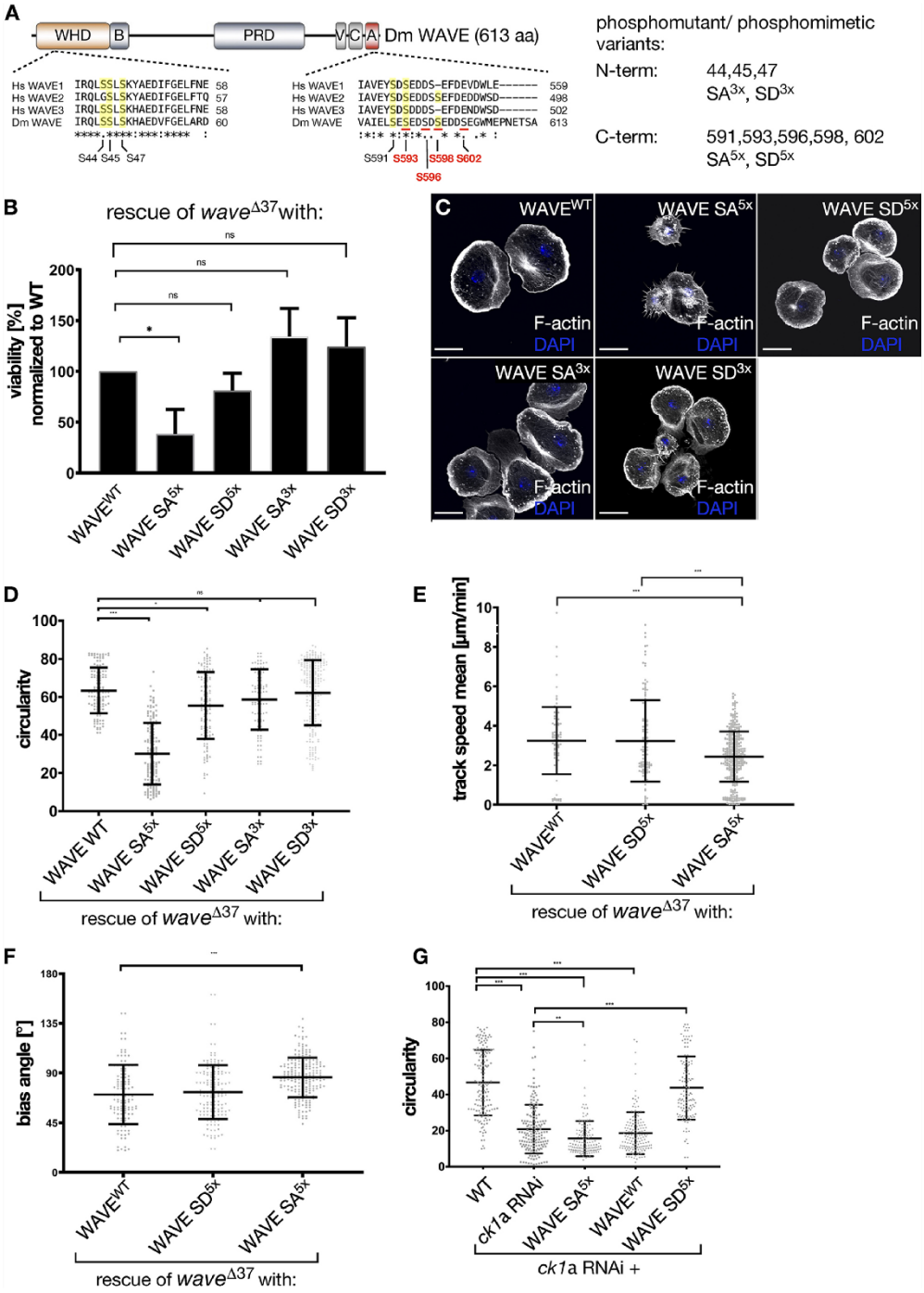

Fig. 6. See next page for legend.

Fig. 6. Phosphorylation of the acidic region within the VCA domain of WAVE is essential for its function. (A) Schematic of domain structure within the Drosophila WAVE protein. Shown are the WAVE homology domain (WHD), basic region – B, proline-rich region – PRG, verprolin domain – V, central region – C and acidic region – A, as well as sequence alignment of N-terminal and C-terminal parts of human of WAVE1, 2 and 3, and Drosophila WAVE. Shown are two CK1α consensus sequences within the WHD and the acidic region of WAVE; conserved serine residues are underlined in yellow. Serine residues that match the CK1α consensus motif are underlined and/or shown in red. Phosphorylatable serine residues that were replaced with alanine in the unphosphorylatable mutant (SA) and with aspartic acid in the phosphomimetic mutant (SD) are indicated on the right. (B) Rescue of wave$^{\Delta 37}$ homozygote lethality into adulthood by ubiquitous re-expression of transgenic WAVE variants as indicated. Results show the averages of three independent crossings. Notice that only the C-terminal phosphomutant SA^{5x} variant is unable to rescue lethality. *P ≤0.03, ns, not significant (one-way ANOVA with Dunnett's multiple comparison test). (C) Maximum intensity projection of confocal images that show larval wave$^{\Delta 37}$ mutant macrophages re-expressing transgenic WAVE variants as indicated. Cells were stained for F-actin (white); nuclei were stained with DAPI (blue). Scale bars: 10 µm. N-terminal (SD^{3x}) and C-terminal phosphomimetic (SD^{5x}) as well as the N-terminal unphosphorylatable mutant (SA^{3x}) can substantially rescue the wave-mutant phenotype. In contrast, lamellipodia formation is still severely defective in macrophages re-expressing the C-terminal unphosphorylatable mutant of the VCA domain (SA^{5x}). (D) Quantification of cell circularity of rescued macrophages. WAVE-WT (n=122), WAVE-SA^{5x} (n=143), WAVE-SD^{5x} (n=131), WAVE-SA^{3x} (n=92), WAVE-SD^{3x} (n=246). Shown is a scatter dot blot with bars indicating mean±s.d. *P=0.010, ***P ≤0.001 ANOVA; ns, not significant. (E) Quantification of mean track speed of directed migration of rescued macrophages upon wounding of a single cell. WAVE-WT (n=94), WAVE-SA^{5x} (n=384), WAVE-SD^{5x} (n=128). Shown is a scatter dot plot with bars indicating mean±s.d. ***P ≤0.001 (Welch's t-test). (F) Quantification of bias angles of directed migration of rescued macrophages upon wounding of a single cell. WAVE-WT (n=296), WAVE-SA^{5x} (n=206), WAVE-SD^{5x} (n=233). Shown is a scatter dot blot with bars indicating mean±s.d. ***P ≤0.001 (Welch's t-test). (G) Quantification of cell circularity. Rescue of cell morphology defects of Ck1α RNAi-depleted cells by co-expression of indicated transgenic WAVE variants. D and G show a unitless measure. WT (n=160), Ck1α RNAi (n=160), Ck1α RNAi+WAVE-SA^{5x} (n=131), Ck1α RNAi+WAVE-WT (n=154) and Ck1α RNAi+WAVE-SD^{5x} (n=120). Graph is depicted in a scatter dot plot with bars indicating mean±s.d. **P ≤0.01, ***P ≤0.001 ANOVA.

tested the six known Drosophila members of the cullin protein family (Cul1, 2, 3, 4, 5 and 6), which function as scaffolds to assemble distinct E3 ligase complexes (Ketosugbo et al., 2017). Interestingly, RNAi-mediated knockdown of Cul1 and Cul2, but not Cul3 to Cul6 (RNAi had already been validated), rescued cell shape defects of macrophages evoked by RNAi of Ck1α (Fig. 5B,C). Knockdown of any cullin protein alone did not show significant differences in cell shape (Fig. 5B,C). Taken together, these data further provide evidence that CK1α protects WAVE from ubiquitin-mediated proteasomal degradation to ensure the proper formation of lamellipodia.

We also tested whether forced overexpression of CK1α might increase WAVE protein levels. For this, we generated a stably transfected S2 cell line expressing CK1α under the control of a Cu^{2+}-inducible metallothionein promoter (pMT). However, induced expression of full-length CK1α did neither induce a phosphorylation-dependent mobility shift of endogenous WAVE nor did it yield increased levels of WAVE protein (Fig. S1A,B), suggesting that prominent basal phosphorylation by CK1α already stabilizes endogenous WAVE levels.

Phosphorylation of the acidic region within the VCA domain of WAVE is essential for its function regarding lamellipodia formation, cell migration and development

CK1α is a monomeric, serine/threonine-specific protein kinase that recognizes the canonical consensus sequence [S(p)/T(p)-X-X-S/T] [where S(p)/T(p) indicates a phosphorylated residue (Flotow et al., 1990) and X represents any amino acid]. In addition, non-canonical consensus sequences recognized by CK1 family members have been described previously, i.e. the SLS motif as found in β-catenin (Marin et al., 2003). WAVE proteins contain a conserved SLS motif in the N-terminal WAVE homology domain (WHD) and a canonical CK1α consensus sequence in the C-terminal acidic region comprising VCA (Fig. 6A, marked in red). To further explore the physiological relevance of phosphorylation, we performed rescue experiments in fly. We generated different mutant WAVE variants, in which the serine residues within the N-terminal WHD (i.e. S44, S45 and S47) or the C-terminal VCA domain (i.e. S591, S593, S596, S598 and S602) were replaced with unphosphorylatable alanine residues yielding SA mutants (N-terminal SA^{3x} and C-terminal SA^{5x} mutant variants) (Fig. 6A) or with phosphomimetic aspartic acid residues yielding SD mutants (i.e. N-terminal SD^{3x}- and C-terminal SD^{5x} mutant variants) (Fig. 6A). To ensure equal expression rates we integrated these transgenes into the same landing site (68E) using the ΦC31-mediated transgenesis strategy (Bischof et al., 2007).

Ubiquitous re-expression of N-terminal phosphomutant or phosphomimetic variants (SA^{3x} or SD^{3x}) fully rescued embryonic lethality of wave mutants, indicating that the SLS motif is dispensable for WAVE function (Fig. 6B). By contrast, phosphorylation of the C-terminal acidic domain of WAVE is crucial for WAVE function. With only a small number of progenies, the phosphomutant variant (SA^{5x}) failed to rescue the lethality of the wave mutant, whereas the C-terminal phosphomimetic variant (SD^{5x}) completely restored viability (Fig. 6B). A similar phenotypic analysis in macrophages further confirmed that basal phosphorylation of the C-terminal acidic domain is required for WAVE function (Fig. 6C). Defects regarding lamellipodia formation in wave-mutant macrophages can be substantially rescued by re-expressing wild type, N-terminal phosphomimetic SD^{3x} or phosphomutant SA^{3x} WAVE protein (Fig. 6C). However, C-terminal phosphomutant SA^{5x} WAVE failed to rescue the lamellipodium defects (Fig. 6C). Cells expressing the SA^{5x} variant still showed strongly reduced circularity and mean track speed compared to cells rescued either by wild type, SA^{3x} or SD^{5x} protein (quantification in Fig. 6D and E). Similarly, we still found significant defects in the migratory directionality of mutant macrophages expressing phosphomutant SA^{5x} WAVE compared to wild type or the phosphomimetic SD^{5x} variant (quantification in Fig. 6F). Finally, we tested whether defects in lamellipodia formation evoked by RNAi of Ck1α can be rescued by overexpression of the phosphomimetic SD^{5x} variant. Indeed, overexpression of the phosphomimetic SD^{5x} but not the phosphomutant SA^{5x} WAVE variant substantially rescued cell shape defects of macrophages deficient for Ck1α (Fig. 6G). Likewise, re-expression of wild type WAVE did not rescue defects evoked by RNAi of Ck1α, suggesting that basal phosphorylation of the acidic domain of WAVE is essential for its stability in vivo.

Phosphorylation of the acidic region within the VCA domain of WAVE promotes its stability rather than its actin nucleation in vivo

We finally tested whether a phosphomimetic WAVE SD mutant of the VCA domain exhibits a higher protein stability or actin polymerization activity in vivo. Here, we used the Drosophila wing imaginal disc as an in vivo model to measure the effect of the WAVE overexpression. We used the en-Gal4 driver, which only

Journal of Cell Science (2021) 134, jcs258891. doi:10.1242/jcs.258891

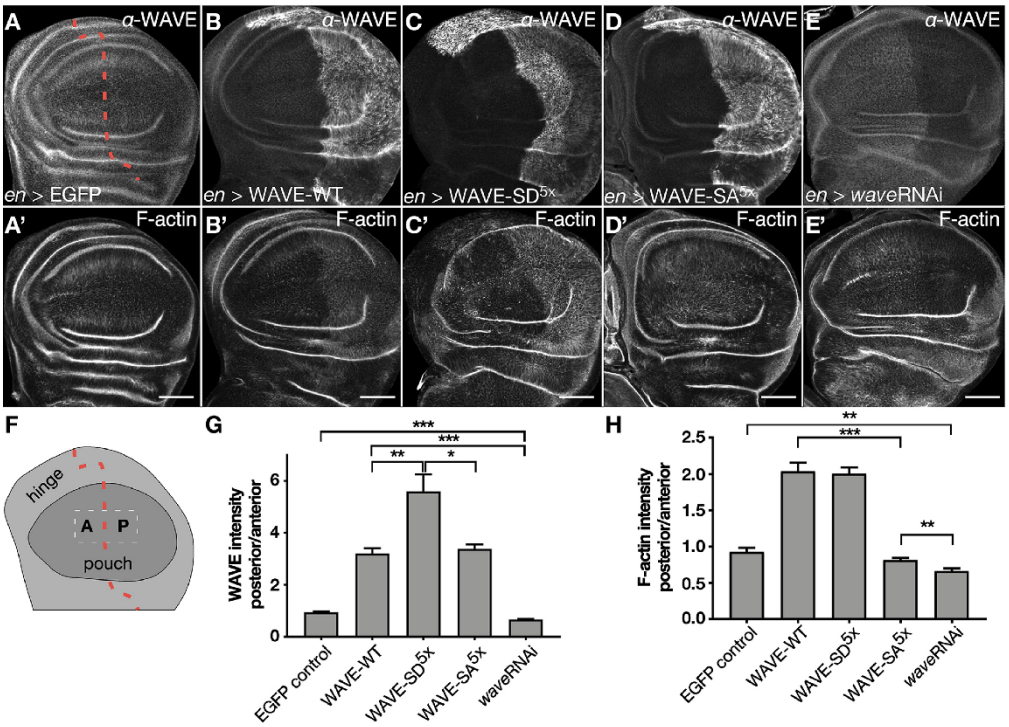

Fig. 7. Phosphorylation of the acidic region within the VCA domain of WAVE promotes its stability rather than its actin nucleation in vivo. (A–E′) Confocal images of wing imaginal discs expressing unphosphorylatable mutant WAVE-SA^{5x} or phosphomimetic WAVE-SD^{5x} constructs in the en-Gal4 pattern. Expression of transgenes is verified by antibody staining as indicated. Anterior is to the left. The anterior–posterior compartment border is indicated by a red dashed line. Scale bars: 50 µm. (F) Schematic representation of third-instar larvae wing imaginal disc. A, anterior; P, posterior. The anterior–posterior compartment border is indicated by a red dashed line. (G) Quantification of WAVE levels upon overexpression of WAVE. Quotient of posterior over anterior signal strength. EGFP serves as a negative control and wave RNAi transgene as a positive control. WAVE-WT (n=15), WAVE-SA^{5x} (n=143), WAVE-SD^{5x} (n=9), WAVE-SA^{3x} (n=14), EGFP (n=5), wave RNAi (n=9). (H) Quantification of F-actin upon overexpression of WAVE as the quotient of posterior/anterior signal intensity. EGFP serves as a negative control and wave RNAi transgene as a positive control. *P ≤0.033, **P ≤0.002, ***P <0.001 (Welch's t-test). WAVE-WT (n=14), WAVE-SA^{5x} (n=143), WAVE-SD^{5x} (n=16), WAVE-SA^{3x} (n=16), EGFP (n=8), wave RNAi (n=7).

induces expression in the posterior compartment of wing imaginal discs, whereas the anterior compartment serves as a negative control (Fig. 7A–E, schematic in F). Expression of an EGFP transgene served as an additional negative control (Fig. 7A,A′) and that of wave RNAi transgene as a positive control (Fig. 7E,E′) for changes in F-actin levels. We found that phosphomimetic WAVE-SD^{5x} (Fig. 7C,C′) is more stable compared to WAVE-wild type (WAVE-WT (Fig. 7B,B′) and phosphomutant WAVE-SA^{5x} (Fig. 7D,D′,G). Protein levels of WAVE-WT and WAVE-SA^{5x} were not significantly different (Fig. 7G). Moreover, despite the fact that phosphomimetic WAVE-SD^{5x} is more stable than the wild type protein, we found no increased activity (F-actin induction) in WAVE-WT and WAVE SD^{5x} cells (Fig. 7H). Thus, these data suggest that phosphorylation of the VCA domain promotes WAVE stability rather than its actin nucleation activity in vivo.

DISCUSSION

WAVE proteins contain a conserved C-terminal VCA domain that directly binds to and activates the Arp2/3 complex, driving branched actin polymerization. A previous study suggested that CK2 phosphorylates serine of mammalian WAVE2 at positions 482, 484, 488, 489 and 497 within the acidic domain of the VCA domain that promotes Arp2/3 complex activity in vitro (Pocha and Cory, 2009). Consistently, overexpression of a GFP-WAVE2 5A construct inhibits lamellipodial protrusion in transfected NIH3T3 cells (Pocha and Cory, 2009). Whether a phosphomimetic WAVE SD mutant of the VCA domain exhibits increased actin polymerization activity in vitro has not been addressed so far. In this work, we found that overexpression of phosphomimetic WAVE-SD^{5x} and wild type WAVE equally induces F-actin in epithelial tissue. This suggests that increased stabilization did not necessarily result into increased actin nucleation activity. However, inhibiting the phosphorylation of the VCA domain (see WAVE-SA^{5x} variant) clearly leads to significantly reduced F-actin induction as compared to overexpression of wild type WAVE (WAVE-WT). Therefore, basal phosphorylation of the VCA domain not only seems to be required for protein stability but also seems to promote WAVE activity. However, the phosphomimetic SD^{5x} variant behaves like the wild type WAVE as it fully rescues wave-mutant lethality and any defects in lamellipodia formation. Thus, our data more closely

Journal of Cell Science (2021) 134, jcs258891. doi:10.1242/jcs.258891

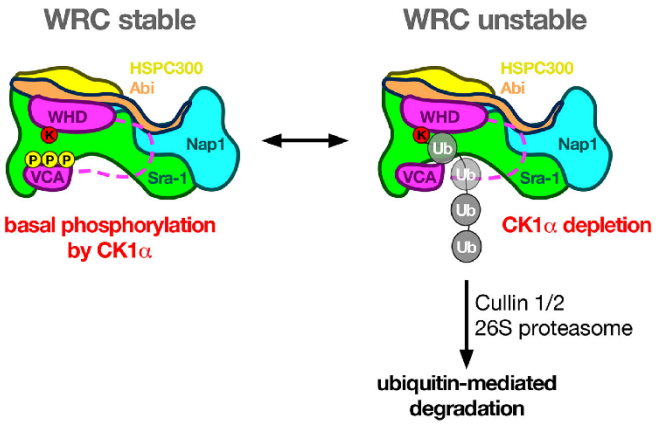

Fig. 8. CK1α protects WAVE from proteasomal degradation. Schematic showing the proposed role of CK1α in regulating WAVE protein stability. The WRC forms a stable pentameric complex that, in Drosophila consists of WAVE (magenta), Abi (orange), Nap1 (blue), Sra-1 (officially known as Cyfip; green), and HSPC300 (yellow). Basal phosphorylation of the VCA domain contributes to protein stability. The VCA domain is normally inhibited through interaction with the meander region of the WAVE WHD domain (Chen et al., 2010) and Sra-1. Release of the autoinhibitory conformation facilitates exposure of WAVE to ubiquitylation, leading to its degradation. Ubiquitylation of WAVE might be mediated by a conserved lysine residue within the WHD domain.

resemble previous observations of WAVE2 in NIH3T3 cells (Pocha and Cory, 2009). Our findings also imply that dephosphorylation is a crucial regulatory step in the regulation of WAVE. Our data further suggest that basal phosphorylation by CK1α protects WAVE against increased ubiquitin-dependent degradation. However, the question remains how phosphorylation of the VCA domain by CK1α impacts on WAVE stability? A recent study has demonstrated that WAVE2 undergoes ubiquitylation in a T-cell activation-dependent manner that is followed by proteasomal degradation dependent on the VCA domain (Joseph et al., 2017). The main WAVE2 ubiquitylation site has been mapped to Lys45, a highly conserved residue within the WHD, and is required for WRC integrity and stability (Joseph et al., 2017). A model has been proposed in which activation of WAVE triggers a conformational change that releases the sequestered VCA domain, exposes the WHD (Lys45), to ubiquitylation and, thereby, promotes WAVE degradation (Joseph et al., 2017). Overall, our data provide first in vivo evidence for CK1α-dependent phosphorylation of WAVE as a so far unknown and crucial mechanism to control WAVE functions (Fig. 8).

Our data also show that CK1α – but not CK2 – is an important regulator of WAVE function in vivo. In contrast to Ck1α-mutant cells, macrophages deficient for the catalytic CK2α subunit formed normal lamellipodia but showed increased differentiation of lamellocytes at the expense of macrophages. Our data suggest that CK2 regulates differentiation, rather than shape and locomotion, of blood cells. Accordingly, previous data revealed that phosphorylation of dMi-2, the catalytic subunit of the nucleosome remodeling and deacetylase (NuRD)/Ush complex, by CK2 modulates nucleosome remodeling activity, which might contribute to the repression of blood lineage-specific genes (Bouazoune and Brehm, 2005; Lenz et al., 2021).

MATERIALS AND METHODS

Drosophila genetics

Fly husbandry and crossing were carried out according to the standard methods. Crosses were maintained at 25°C, UAS-Gal4-based experiments including RNAi were performed at 29°C. The following fly lines were used: CK1α RNAi BL 25786 and VDRC 16645, hmlΔ-Gal4, UAS-eGFP (Sinenko and Mathey-Prevot, 2004); en-Gal4 (Bloomington Stock Center). Transgenic pUASp-wave WT, pUASp-wave SD^{3x}, pUASp-wave SA^{5x}, pUASp-wave SD^{5x} and pUASp-wave SA^{5x} flies were generated using ΦC31-mediated transgenesis (M{3xP3-RFP.attP}ZH-86F (Bischof et al., 2007).

To generate MARCM-ready stocks the following fly lines from Bloomington Stock Center were used: hsFLP, tubP-GAL80, w*, FRT19A; Pin/CyO; (BL#5133); FRT19A;; (BL#1709); mys^{1}FRT19A/FM7c;; (BL#23862), y^{1} w* $Ck1\alpha^{[A]}$ FRT19A/FM7c, Kr-GAL4, UAS-GFP (BL#57084), y^{1} w* $Ck1\alpha^{8B12}$ FRT19A/FM7i, twi-GAL4, UASt-GFP; $snaI^{[Sco]}$/CyO (BL#63802); y^{1} w* Ck1α[A] FRT19A/FM7c, Kr-GAL4, UAS-GFP (BL#64459); hsFLP, w*, y; tubP-GAL80, FRT40A; hmlΔ-GAL4, UAS-eGFP/TM6B; hsFLP; $wave^{\Delta 37}$, FRT40A/Cyo; y* w*;; $ck2\alpha^{[TIkR]}$/TM3 (BL#24511); y* w*;; $ck2\alpha^{TIK}$/TM3 (BL#24512); y* w*;; $ck2\alpha^{P1}$/TM6B, Tb1 (Kyoto 141869). MARCM (Mosaic Analysis with a Repressible Cell Marker; Wu and Luo, 2006) experiments were performed as follows.

Deleted in hemocytes only (DEMON) (Moreira et al., 2013) males were crossed with mutant or FRT19a control virgin flies and placed at 25°C for 48 h. The progeny was submitted to three 1-h heat shocks every 24 h at 37°C. Between heat shocks, crosses were maintained at 29°C. Each heat shock was carried out in a 37°C water bath, followed by 1 h at 18°C to extend the G2 phase and improve MARCM efficiency. Female third-instar larvae containing GFP-expressing hemocytes were then selected for further analysis.

Cell culture, cell transfection

Drosophila $S2R^{+}$ cells were propagated in 1× Schneider's Drosophila Medium, as described previously (Stephan et al., 2008). $S2R^{+}$ cells were transfected as described previously (Nagel et al., 2017).

Cell transfection and maintenance of stable cell line

Drosophila $S2R^{+}$ cells were transfected with 11.37 µg pMT-Ck1α-6×c-myc plasmid expressing Myc-tagged CK1α (Lam et al., 2018). For selection of co-transfected cells, we used the pCoHygro (Invitrogen) selection vector (1.26 µg) expressing the hygromycin resistance gene. Three days after transfection, medium was replaced and cells were cultured in the presence of 300 µg/ml hygromycin-B (ThermoFisher). Stably transfected cells were screened for hygromycin resistance over 5 weeks. During this time, the medium was changed every 4–5 days. Expression of CK1α was induced by addition of $CuSO_4$ (final concentration of 500 µM). Cells were harvested at indicated time points.

Chemical inhibitors

The CK1α inhibitor D4476 (Sigma) was resuspended in DMSO to 5000 µM stock dilution. D4476 was then diluted in cell culture medium and added to cells at final concentrations of 100 µM in 24-well tissue culture plates. Cells were treated for 4 h. The proteasome inhibitor MG132 (Sigma) was resuspended in DMSO to 1 mM stock dilution. Cells were treated with 10 µM MG132 for 4 h. Control-treated cells were treated with equal volumes of DMSO under conditions identical to those of drug treatment.

Phosphorylation assays

Phosphorylation assays were conducted using recombinant glutathione S-transferase (GST)-tagged Drosophila WAVE protein (GST-WAVE) as substrate (0.2 µg/µl in 50 mM Tris buffer pH 8.0). First, GST-WAVE was incubated with ATPγS. Which serves as the phosphate donor from which mono-thiophosphate instead of phosphate is transferred to the substrate. Second, alkylation of thiophosphorylated serine, threonine or tyrosine residues is allowed by addition of para-nitrobenzylmesylate (PNBM). Alkylated thiophosphate creates an epitope for thiophosphate ester-specific antibodies, which allows to detection phosphorylation (Allen et al., 2007). Kinases used were CK1 (truncated human δ isoform) (Graves and Roach, 1995) and Abl [truncated form of murine leukemia virus v-Abl (Foulkes et al., 1985)], both purchased from NEB. Reactions were mixed and incubated for 30 min at 30°C before PNBM was added for alkylation. Alkylation with PNBM occurred for 120 min at 30°C.

Co-immunoprecipitation experiments

Co-immunoprecipitation experiments were performed as described previously (Bogdan et al., 2004). Samples were used for SDS PAGE and western blot analysis as described below.

SDS-PAGE and western blot analysis

Protein extracts were separated by SDS-PAGE and analyzed by western blotting. The following antibodies were used: anti-WAVE (1:1000; Bogdan et al., 2004), anti-Tubulin (1:3000, DSHB AA4.3) and anti-thiophosphate ester (rabbit, ab133473, Abcam). The following secondary antibodies were used diluted 1:5000 in 10% milk TBS-T: goat anti-mouse IgG (H+L), HRP (ThermoFisher) and goat anti-guinea Pig IgG (H+L), HRP. Western blots were quantified using Image studio lite 5.2 software from Li-Cor and statistically analyzed using GraphPad Prism 8 software.

Immunohistochemistry of Drosophila macrophages and wing imaginal discs

Pupal macrophages were isolated as described previously (Ruder et al., 2018). Wing imaginal discs were dissected from third-instar larvae and collected in ice-cold PBS. The discs were fixed with 4% PFA for 45 min at RT on a rotary mixer. 3% (w/v) BSA in PBS, 0.3% Triton X-100 was used as blocking solution. Samples were incubated in primary antibody over night at 4°C. 0.3% PBT was used for every washing step. Primary antibodies used were anti-WAVE (1:1000; Bogdan et al., 2004) and anti-Atilla (1:10; Kurucz et al., 2007). Secondary antibody was goat anti-guinea pig 488 (1:1000, Thermo Fisher Scientific). Actin staining was carried out using Alexa Fluor 568 conjugated to phalloidin (1:100) during the secondary antibody incubation for 2 h. Discs were mounted in Fluoromount G (Thermo Fisher Scientific) and stored at 4°C.

Image acquisition and microscopy

Structure illumination microscopy images were taken with an ELYRA S.1 microscope (Cell Observer SD, 63×/1.4 oil-immersion objective). Confocal fluorescence images were taken using a Leica TCS SP8 with an HC PL APO CS2 63×/1.4 oil objective. Live imaging of macrophage cultures was performed using a Zeiss CellObserver Z.1 with a Yokogawa CSU-X1 spinning disc scanning unit and an Axiocam MRm CCD camera (6.45 µm×6.45 µm). Ablation experiments were done using a 355 nm pulsed UV laser (Rapp, Optoelectronics), as reported previously (Sander et al., 2013; Rüder et al., 2018).

Structural protein visualization and analysis

Molecular visualization, editing and analysis, and image production were carried out using the UCSF Chimera package (Pettersen et al., 2021).

Quantification of Drosophila macrophages and analysis of cell morphology

Cell morphology was analyzed by using FIJI shape descriptor parameter. Circularity ranges were between 0 (infinitely elongated polygon) and 100 (perfect circle), $4\pi \times \text{area} \div \text{perimeter}^2$ (Zdilla et al., 2016).

Quantification of directed migration of macrophages

Tracking of migrating macrophages was performed using the spots module of Imaris 9.3 (Bitplane; https://imaris.oxinst.com/versions/9-3) software. The reference frame module was set at the ablation site. After automatic tracking, all time-lapse movies were checked and were manually corrected if necessary. The mean track speed was measured by using the Imaris software and values were analyzed with Graph Pad Prism. The bias angle between the vector towards the ablated cell and the direction vector of the cell was calculated in R software (R Studios Version 1.4). The angle between the vector directly towards the ablation cell and the direction vector of the cell at each time point was calculated using $\cos w = \frac{e\vec{W}\vec{b}}{|\vec{a}||\vec{b}|}$, i.e. the scalar product $e\vec{W}\vec{b}$ of vectors a and b divided by the multiplication product of the length of each vector $|\vec{a}||\vec{b}|$.

Polar histograms were generated using the package ggplot2. For directed migration only cells within a 10–80 µm radius of the wounding site were analyzed. Results were statistically analyzed with GraphPad Prism 8.

Quantification of actin and WAVE levels in wing imaginal discs

Confocal microscopy images were processed and quantified with FIJI software. F-actin and WAVE intensities were quantified within the same plane. The intensities of three different regions (10×10 µm size) within the posterior and anterior compartment were quantified for each experiment. The integrated density of each square was measured using FIJI software. The mean value of each side was taken to calculate the quotient of posterior over anterior intensity.

Statistics

Results were statistically analyzed with GraphPad Prism 8.

Acknowledgements

We thank the Bloomington Stock Center and VDRC for fly stocks. We thank Moritz Sander (Institute for Neurobiology, University of Münster, Germany) and Benedikt Nagel (Institute of Physiology and Pathophysiology, Philipps-University Marburg, Germany) for performing initial RNAi experiments. We thank Doris Wagner and Kirsten Ramlow (both Institute of Physiology and Pathophysiology, Philipps-University Marburg, Germany) for establishing and testing stable S2 cells and antibodies, Katja Rust and Mailk C. Bischoff (Institute of Physiology and Pathophysiology, Philipps-University Marburg, Germany) for critical reading of the manuscript.

Competing interests

The authors declare no competing or financial interests.

Author contributions

Conceptualization: S.B.; Methodology: A.H., M.v.C.; Data curation: A.H.; Writing - original draft: S.B.; Writing - review & editing: S.B., A.H.; Visualization: S.B., A.H.; Supervision: S.B.; Project administration: S.B.; Funding acquisition: S.B.

Funding

The work was initially supported by the cluster of excellence 'Cells in Motion' (CIM; University of Münster) and by grants to S.B. from the Deutsche Forschungsgemeinschaft (DFG). Open access funding provided by University of Philipps-University Marburg. Deposited in PMC for immediate release.

Peer review history

The peer review history is available online at https://journals.biologists.com/jcs/article-lookup/doi/10.1242/jcs.258891.

References

Allen, J. J., Li, M., Brinkworth, C. S., Paulson, J. L., Wang, D., Hübner, A., Chou, W.-H., Davis, R. J., Burlingame, A. L., Messing, R. O. et al. (2007). A semisynthetic epitope for kinase substrates. Nat. Methods 4, 511-516. doi:10.1038/nmeth1048

Anderl, I., Vesala, L., Ihalainen, T. O., Vanha-Aho, L.-M., Andó, I., Rämet, M. and Hultmark, D. (2016). Transdifferentiation and proliferation in two distinct hemocyte lineages in Drosophila melanogaster larvae after Wasp infection. PLoS Pathog. 12, e1005746. doi:10.1371/journal.ppat.1005746

Bandyopadhyay, M., Arbet, S., Bishop, C. P. and Bidwai, A. P. (2017). Drosophila protein kinase CK2: genetics, regulatory complexity and emerging roles during development. Pharmaceuticals 10, 4. doi:10.3390/ph10010004

Bischof, J., Maeda, R. K., Hediger, M., Karch, F. and Basler, K. (2007). An optimized transgenesis system for Drosophila using germ-line-specific wC31 integrases. Proc. Natl. Acad. Sci. USA 104, 3312-3317. doi:10.1073/pnas.0611511104

Bogdan, S., Grewe, O., Strunk, M., Mertens, A. and Klämbt, C. (2004). Sra-1 interacts with Kette and Wasp and is required for neuronal and bristle development in Drosophila. Development 131, 3981-3989. doi:10.1242/dev.01274

Bouazoune, K. and Brehm, A. (2005). dMi-2 chromatin binding and remodeling activities are regulated by dCK2 phosphorylation. J. Biol. Chem. 280, 41912-41920. doi:10.1074/jbc.M507084200

Bulat, V., Rast, M. and Pielage, J. (2014). Presynaptic CK2 promotes synapse organization and stability by targeting Ankyrin2. J. Cell Biol. 204, 77-94. doi:10.1083/jcb.201305134

Chen, Z., Borek, D., Padrick, S. B., Gomez, T. S., Metlagel, Z., Ismail, A. M., Umetani, J., Billadeau, D. D., Otwinowski, Z. and Rosen, M. K. (2010). Structure and control of the actin regulatory WAVE complex. Nature 468, 533-538. doi:10.1038/nature09623

Flotow, H., Graves, P. R., Wang, A. Q., Fiol, C. J., Roeske, R. W. and Roach, P. J. (1990). Phosphate groups as substrate determinants for casein kinase I action. J. Biol. Chem. 265, 14264-14269. doi:10.1016/S0021-9258(18)77295-5

Foulkes, J. G., Chow, M., Gorka, C., Frackelton, A. R. Jr and Baltimore, D. (1985). Purification and characterization of a protein-tyrosine kinase encoded by the Abelson murine leukemia virus. J. Biol. Chem. 260, 8070-8077.

Graves, P. R. and Roach, P. J. (1995). Role of COOH-terminal phosphorylation in the regulation of casein kinase I delta. J. Biol. Chem. 270, 21689-21694. doi:10.1074/jbc.270.37.21689

Haelterman, N. A., Jiang, L., Li, Y., Bayat, V., Sandoval, H., Ugur, B., Tan, K. L., Zhang, K., Bei, D., Xiong, B. et al. (2014). Large-scale identification of chemically induced mutations in Drosophila melanogaster. Genome Res. 24, 1707-1718. doi:10.1101/gr.174615.114

Joseph, N., Biber, G., Fried, S., Reicher, B., Levy, O., Sabag, B., Noy, E. and Barda-Saad, M. (2017). A conformational change within the WAVE2 complex regulates its degradation following cellular activation. Sci. Rep. 7, 44863. doi:10.1038/srep44863

Ketosugbo, K. F., Bushnell, H. L. and Johnson, R. I. (2017). A screen for E3 ubiquitination ligases that genetically interact with the adaptor protein Cindr during Drosophila eye patterning. PLoS ONE 12, e0187571. doi:10.1371/journal.pone.0187571

Kramerov, A. A., Golub, A. G., Bdzhola, V. G., Yarmoluk, S. M., Ahmed, K., Bretner, M. and Ljubimov, A. V. (2011). Treatment of cultured human astrocytes and vascular endothelial cells with protein kinase CK2 inhibitors induces early changes in cell shape and cytoskeleton. Mol. Cell. Biochem. 349, 125-137. doi:10.1007/s11010-010-0667-3

Kurucz, É., Váczi, B., Márkus, R., Laurinyecz, B., Vilmos, P., Zsámboki, J., Csorba, K., Gateff, E., Hultmark, D. and Andó, I. (2007). Definition of Drosophila hemocyte subsets by cell-type specific antigens. Acta Biol. Hung. 58 Suppl. 1, 95-111. doi:10.1556/ABiol.58.2007.Suppl.8

Lam, V. H., Li, Y. H., Liu, X., Murphy, K. A., Diehl, J. S., Kwok, R. S. and Chiu, J. C. (2018). CK1α collaborates with DOUBLETIME to regulate PERIOD function in the Drosophila circadian clock. J. Neurosci. 38, 10631-10643. doi:10.1523/JNEUROSCI.0871-18.2018

Legent, K., Steinhauer, J., Richard, M. and Treisman, J. E. (2012). A screen for X-linked mutations affecting Drosophila photoreceptor differentiation identifies Casein kinase 1α as an essential negative regulator of wingless signaling. Genetics 190, 601-616. doi:10.1534/genetics.111.133827

Leng, Y., Zhang, J., Badour, K., Arpaia, E., Freeman, S., Cheung, P., Siu, M. and Siminovitch, K. (2005). Abelson-interactor-1 promotes WAVE2 membrane translocation and Abelson-mediated tyrosine phosphorylation required for WAVE2 activation. Proc. Natl. Acad. Sci. USA 102, 1098-1103. doi:10.1073/pnas.0409120102

Lenz, J., Liefke, R., Funk, J., Shoup, S., Nist, A., Stiewe, T., Schulz, R., Tokusumi, Y., Albert, L., Raifer, H. et al. (2021). Ush regulates hemocyte-specific gene expression, fatty acid metabolism and cell cycle progression and cooperates with dNuRD to orchestrate hematopoiesis. PLoS Genet. 17, e1009318. doi:10.1371/journal.pgen.1009318

Liepe, J., Sim, A., Weavers, H., Ward, L., Martin, P. and Stumpf, M. P. H. (2016). Accurate reconstruction of cell and particle tracks from 3D live imaging data. Cell Syst. 3, 102-107. doi:10.1016/j.cels.2016.06.002

Marin, O., Bustos, V. H., Cesaro, L., Meggio, F., Pagano, M. A., Antonelli, M., Allende, C. C., Pinna, L. A. and Allende, J. E. (2003). A noncanonical sequence phosphorylated by casein kinase 1 in β-catenin may play a role in casein kinase 1 targeting of important signaling proteins. Proc. Natl. Acad. Sci. USA 100, 10193-10200. doi:10.1073/pnas.1733909100

Mendoza, M. C. (2013). Phosphoregulation of the WAVE regulatory complex and signal integration. Semin. Cell Dev. Biol. 24, 272-279. doi:10.1016/j.semcdb.2013.01.007

Moreira, C. G. A., Jacinto, A. and Prag, S. (2013). Drosophila integrin adhesion complexes are essential for hemocyte migration in vivo. Biol. Open 2, 795-801. doi:10.1242/bio.20134564

Morreale, F. E. and Walden, H. (2016). Types of ubiquitin ligases. Cell 165, 248-248.e1. doi:10.1016/j.cell.2016.03.003

Nagel, B. M., Bechtold, M., Rodriguez, L. G. and Bogdan, S. (2017). Drosophila WASH is required for integrin-mediated cell adhesion, cell motility and lysosomal neutralization. J. Cell Sci. 130, 344-359. doi:10.1242/jcs.193086

Pettersen, E. F., Goddard, T. D., Huang, C. C., Meng, E. C., Couch, G. S., Croll, T. I., Morris, J. H. and Ferrin, T. E. (2021). UCSF ChimeraX: structure visualization for researchers, educators, and developers. Protein Sci. 30, 70-82. doi:10.1002/pro.3943

Pocha, S. M. and Cory, G. O. (2009). WAVE2 is regulated by multiple phosphorylation events within its VCA domain. Cell Motil. Cytoskel. 66, 36-47. doi:10.1002/cm.20323

Rena, G., Bain, J., Elliott, M. and Cohen, P. (2004). D4476, a cell-permeant inhibitor of CK1, suppresses the site-specific phosphorylation and nuclear exclusion of FOXO1a. EMBO Rep. 5, 60-65. doi:10.1038/sj.embor.7400048

Rogers, S. L., Wiedemann, U., Stuurman, N. and Vale, R. D. (2003). Molecular requirements for actin-based lamella formation in Drosophila S2 cells. J. Cell Biol. 162, 1079-1088. doi:10.1083/jcb.200303023

Rüder, M., Nagel, B. M. and Bogdan, S. (2018). Analysis of cell shape and cell migration of Drosophila macrophages in vivo. Methods Mol. Biol. 1749, 227-238. doi:10.1007/978-1-4939-7701-7_17

Saeki, Y. (2017). Ubiquitin recognition by the proteasome. J. Biochem. 161, 113-124. doi:10.1093/jb/mvw091

Sander, M., Squarr, A. J., Risse, B., Jiang, X. and Bogdan, S. (2013). Drosophila pupal macrophages – a versatile tool for combined ex vivo and in vivo imaging of actin dynamics at high resolution. Eur. J. Cell Biol. 92, 349-354. doi:10.1016/j.ejcb.2013.09.003

Sinenko, S. A. and Mathey-Prevot, B. (2004). Increased expression of Drosophila tetraspanin, Tsp68C, suppresses the abnormal proliferation of ytr-deficient and Ras/Raf-activated hemocytes. Oncogene 23, 9120-9128. doi:10.1038/sj.onc.1208156

Ura, S., Pollitt, A. Y., Veltman, D. M., Morrice, N. A., Machesky, L. M. and Insall, R. H. (2012). Pseudopod growth and evolution during cell movement is controlled through SCAR/WAVE dephosphorylation. Curr. Biol. 22, 553-561. doi:10.1016/j.cub.2012.02.020

Weavers, H., Liepe, J., Sim, A., Wood, W., Martin, P. and Stumpf, M. P. H. (2016). Systems analysis of the dynamic inflammatory response to tissue damage reveals spatiotemporal properties of the wound attractant gradient. Curr. Biol. 26, 1975-1989. doi:10.1016/j.cub.2016.06.012

Wu, J. S. and Luo, L. (2006). A protocol for mosaic analysis with a repressible cell marker (MARCM) in Drosophila. Nat. Protoc. 1, 2583-2589. doi:10.1038/nprot.2006.320

Zobel, T. and Bogdan, S. (2013). A high resolution view of the fly actin cytoskeleton lacking a functional WAVE complex. J. Microsc. 251, 224-231. doi:10.1111/jmi.12020

Zdilla, M. J., Hatfield, S. A., McLean, K. A., Cyrus, L. M., Laslo, J. M. and Lambert, H. W. (2016). Circularity, solidity, axes of a best fit ellipse, aspect ratio, and roundness of the foramen ovale: a morphometric analysis with neurosurgical considerations. J. Craniofac. Surg. 27, 222-228. doi:10.1097/SCS.0000000000002285

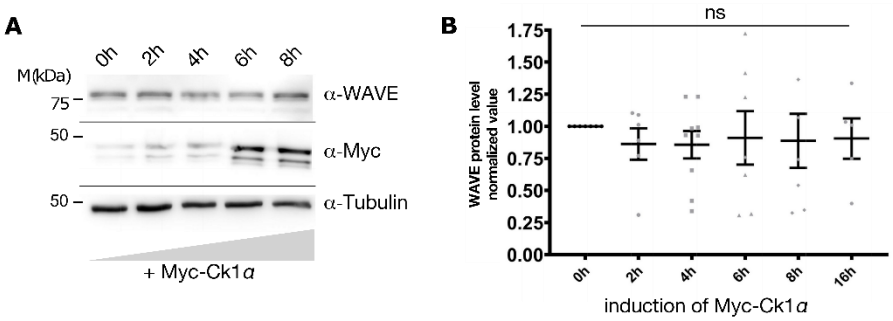

Fig. S1. (A) Induced expression of a myc-tagged CK1α protein in S2 cells. **(B)** Quantification of WAVE protein level upon induced expression. The results are the averages of seven independent experiments. There is no significant increase in WAVE level.

Table S1. A list of transgenic RNAi fly lines screened for cell shape changes.

CG number	Gene name	Phenotype	Fly line ID
CG10023	Fak56D - Focal Adhesion Kinase	no	VDRC 17957 VDRC 108608
CG10244	Cadherin96Ca	no	VDRC 1089
CG10260	Phosphatidylinositol 4-kinase III alpha	a few spiky cells	BL-35256 BL-38242 BL-35643 VDRC 15993 VDRC 105614 NIG 10260Rb-1 NIG 10260Rb-2
CG10295	PAK-kinase	no	VDRC 12553
CG10564	Adenylyl cyclase 78C	no	VDRC 51978
CG10637	Numb-associated kinase	no	VDRC 35482
CG10673	Threonyl-carbamoyl synthesis 5	no	VDRC 35482
CG10776	wishful thinking	no	VDRC 865
CG10895	loki	no	VDRC 44980
CG10951	nimA-like kinase	no	VDRC 16120
CG10967	Autophagy-specific gene 1	no	VDRC 16133
CG1107	auxillin	no	VDRC 103426 VDRC 16182
CG11228	hippo	no	VDRC 7823
CG11420	pan gu	no	VDRC 31500
CG11489	serine-arginine protein kinase at 79D	no	VDRC 47544
CG11533	Asator	no	VDRC 47544
CG11660	CG11660	no	VDRC 18526
CG12066	cAMP-dependent protein kinase 2	no	VDRC 30685
CG12069	CG12069	no	VDRC 23719
CG1210	Phosphoinositide-dependent kinase 1	no	VDRC 18736
CG12147	CG12147	no	VDRC 31658 VDRC 31659
CG1227	CG1227	no	VDRC 38647
CG12306	polo	no	VDRC 20177
CG13388	A kinase anchor protein 200	no	VDRC 5647 VDRC 102374
CG14026	thickvein	no	VDRC 105834

CG14030	bub1 homologue	spiky cells	BL-35260 VDRC 101096 VDRC 24833 NIG 14030R-1 NIG 14030R-2
CG14080	Mitogen-activated protein kinase phosphatase 3	no	VDRC 45415
CG14217	Tao	no	VDRC 17432
CG14226	domeless	no	VDRC 19717
CG14305	CG14305	no	VDRC 17477
CG14895	Pak3	no	VDRC 107260
CG14992	Ack	no	VDRC 39857
CG1506	Ac3	no	VDRC 33217
CG15224	Casein kinase 2 β subunit	a few spiky cells, more lamellocytes	BL-31254 VDRC 32377 VDRC 106845 VDRC 32378
CG15793	Downstream of raf1	no	VDRC 40025
CG15862	cAMP-dependent protein kinase R2	no	VDRC 101763 VDRC 39436 VDRC 39437
CG1594	hopscotch	no	VDRC 40037
CG17090	homeodomain interacting protein kinase	no	VDRC 32854
CG17161	grapes	no	VDRC 11076
CG17174	ACXB	no	VDRC 9748
CG17216	KP78b	no	VDRC 51996
CG17256	Nek2	no	VDRC 40052
CG17348	derailed	no	VDRC 3047
CG17520	Casein kinase 2 α subunit	more lamellocytes	BL-31645 BL-35136
CG17596	Ribosomal protein S6 kinase II	no	VDRC 5702 VDRC 101451
CG17998	G protein-coupled receptor kinase 2	no	VDRC 1835
CG18069	Calcium/calmodulin-dependent protein kinase II	no	VDRC 47280
CG18247	SH2 ankyrin repeat kinase	no	VDRC 105706
CG1830	Phosphorylase kinase γ	no	VDRC 33054
CG18402	Insulin-like receptor	no	VDRC 991
CG1848	LIM-kinase1	no	VDRC 25344

			VDRC 25343
CG18582	mushroom bodies tiny	no	VDRC 46043
CG1951	CG1951	no	VDRC 33431
CG1954	Protein C kinase 98E	no	VDRC 33434
CG1973	yata	no	VDRC 19275
CG2028	Casein kinase 1α	many spiky cells, stellate	BL-35152 BL-35153 BL-41711 BL-25786 VDRC 110768 VDRC 13664
CG2048	discs overgrown	no	VDRC 9241
CG2049	Protein kinase related to protein kinase N	no	NIG 2055R-1
CG2079	Downstream of kinase	no	VDRC 20796 VDRC 108544 VDRC 20796
CG2252	female sterile (1) homeotic	no	VDRC 51227
CG2272	slipper	no	VDRC 33516
CG2577	CG2577	no	VDRC 41693
CG2615	IκB kinase-like 2	no	VDRC 12485
CG2845	pole hole	no	VDRC 20909 VDRC 107766
CG2899	kinase suppressor of ras	no	VDRC 45040
CG3008	CG3008	no	VDRC 52634
CG3051	SNF1A/AMP-activated protein kinase	no	VDRC 1827 VDRC 106200
CG3086	MAP kinase activated protein-kinase-2	no	VDRC 3170
CG3105	PAS kinase	no	VDRC 25661
CG31421	Tak1-like1	no	VDRC 25760
CG32019	bent	no	VDRC 46253
CG32031	Arginine kinase	no	VDRC 34037
CG32134	breathless	no	VDRC 27106
CG3216	CG3216	no	VDRC 29915

CG32417	Myt1	no	VDRC 34547
CG3249	spoonbill	no	VDRC 48005 VDRC 48006
CG3277	CG3277	no	VDRC 7271
CG3319	Cyclin-dependent kinase 7	no	VDRC 10442
CG34361	Diacyl glycerol kinase	no	VDRC 38239
CG34412	Tousled-like kinase	a few spiky cells, some stellate	BL-33983 BL-35298 BL-36102
CG3682	PIP5K59B	no	VDRC 47027
CG3915	Derailed 2	no	VDRC 40484
CG4007	Neurospecific receptor kinase	no	VDRC 36282
CG4012	genghis khan	no	VDRC 107207 VDRC 28367
CG4032	ABL- tyrosine kinase	no	VDRC 2897
CG4041	CG4041	no	VDRC 34780
CG4141	Pi3k92E	no	BL-27690 VDRC 38986 VDRC 107390 VDRC 38986 VDRC 107390 VDRC 38985
CG4154	Guanylyl cyclase at 88E	no	VDRC 21797
CG4201	immune response deficient 5	no	VDRC 26427
CG42341	cAMP-dependent protein kinase R1	no	VDRC 103303 VDRC 26329 VDRC 26328 VDRC 103720 VDRC 103303 VDRC 26329 VDRC 26328 VDRC 103720
CG42349	Protein kinase C δ	spiky cells cells smaller	VDRC 101029 VDRC 31468 VDRC 33837 VDRC 101421 VDRC 31468 VDRC 22755 VDRC 33838
CG4252	meiotic 41	no	VDRC 11251

CG4268	PitsIre	no	BL-35157 BL-56855 VDRC 107303
CG43143	Nuak family kinase	no	VDRC 16334
CG43217	C-terminal Src kinase	no	VDRC 32877 VDRC 102313 VDRC 48282 VDRC 48281
CG4379	cAMP-dependent protein kinase 1	no	VDRC 101524
CG44012	Btk family kinase at 29A	no	VDRC 106962
CG4488	wee	no	VDRC 26543
CG4551	Dyrk2 - Dual-specificity tyrosine phosphorylation-regulated kinase 2	no	VDRC 40534
CG4583	Ire1 - Inositol-requiring enzyme-1	no	VDRC 39561
CG4803	Takl2 - Tak1-like 2	no	VDRC 34898
CG4839		no	VDRC 26641
CG4926	Ror - Ror	no	VDRC 935
CG5072	Cdk4 - Cyclin-dependent kinase 4	no	VDRC 40577
CG5179	Cdk9 - Cyclin-dependent kinase 9	no	VDRC 30448
CG5182	Pk34A - Pk34A	no	VDRC 27368
CG5206	bon - bonus	no	VDRC 44284
CG5363	cdc2 - cdc2	a few spiky cells	VDRC 106130 VDRC 41838
CG5408	trBL- - tribBL-es	no	VDRC 22114
CG5483	Lrrk - Leucine-rich repeat kinase	no	VDRC 22139
CG5680	bsk - basket	no	VDRC 104569 VDRC 34139
CG5790		no	VDRC 45045
CG5974	pll - pelle	no	VDRC 2889
CG5983	ACXB - ACXB	no	VDRC 2870
CG6027	cdi - center divider	no	VDRC 43634
CG6033	drk - downstream of receptor kinase	no	VDRC 105498

CG6114	sff - sugar-free frosting	no	VDRC 22225
CG6355	fab1	no	VDRC 27591
CG6498		no	VDRC 109282 VDRC 35101
CG6518	inaC - inactivation no afterpotential C	no	VDRC 2895 VDRC 2894
CG6535	tefu - telomere fusion	no	VDRC 22502
CG6551	fu - fused	no	VDRC 27663
CG6620	ial - IpIl-aurora-like kinase	no	VDRC 35107
CG6622	Pkc53E - Protein C kinase 53E	no	VDRC 27696 VDRC 27699
CG6703	CASK - CASK ortholog	no	VDRC 34184
CG6715	KP78a - KP78a	no	VDRC 51616 VDRC 26722 VDRC 47658 VDRC 47657
CG6963	gish - gilgamesh	spiky cells cells smaller	VDRC 26003 VDRC 106826 VDRC 26003 VDRC 106826
CG7004	four wheel drive	no	VDRC 27786 VDRC 27785
CG7097	happyhour	no	VDRC 35166
CG7111	Receptor of activated protein kinase C 1	no	VDRC 27859 VDRC 27858
CG7156	CG7156	no	VDRC 26035
CG7177	Wnk	no	VDRC 35193
CG7180	CG7180	no	VDRC 34369
CG7186	Sak kinase	no	VDRC 27904
CG7223	heartless	no	VDRC 27180 VDRC 6692 VDRC 27180
CG7524	Src oncogene at 64B	no	VDRC 35252
CG7597	cdk 12 – Cyclin-dependent kinase 12	spiky cells, cells smaller	BL-35163 BL-34838 BL-42775 VDRC 25508

			VDRC 25510
CG7693	frayed	no	VDRC 41718
CG7717	Mekk1	no	VDRC 25529
CG7838	Bub1-related kinase	no	VDRC 26109
CG7873	Src oncogene act 42A	no	VDRC 26019
CG7892	nemo	no	VDRC 3002
CG8174	SRPK	no	VDRC 26933
CG8201	par-1	no	VDRC 52553 VDRC 52556
CG8203	Cyclin-dependent kinase 5	no	VDRC 35856 VDRC 35855 VDRC 104491
CG8222	PDGF- and VEGF-receptor related	no	VDRC 976 VDRC 43461 VDRC 13502 VDRC 43459 VDRC 105353 VDRC 977
CG8250	Alk	no	VDRC 11446
CG8485	CG8485	no	VDRC 35940
CG8726	CG8726	no	VDRC 40719
CG8767	mos	no	VDRC 36531
CG8789	wallenda	no	VDRC 26910
CG8808	Pyruvate dehydrogenase kinase	no	VDRC 37966
CG8874	Fps oncogene analog 85D	no	VDRC 107266 VDRC 36053 VDRC 36054
CG8878	CG8878	no	VDRC 28970
CG8967	off-track	no	VDRC 30833
CG9210	Adenylyl cyclase 35C	no	VDRC 11547
CG9222	CG9222	no	VDRC 27010
CG9533	rutabaga	no	VDRC 101759 VDRC 5569
CG9738	MAP kinase kinase 4	no	VDRC 26929

CG9774	Rho-kinase	cytokinesis defects	BL-35305 BL-34324 BL-28797 VDRC 3793 VDRC 104675 NIG 9774R-2 NIG 9774R-3
CG9962	CG9962	no	VDRC 36473 VDRC 36178 VDRC 108721
CG9985	skittles	no	BL-35198 BL-27715 BL-101624 VDRC 6229

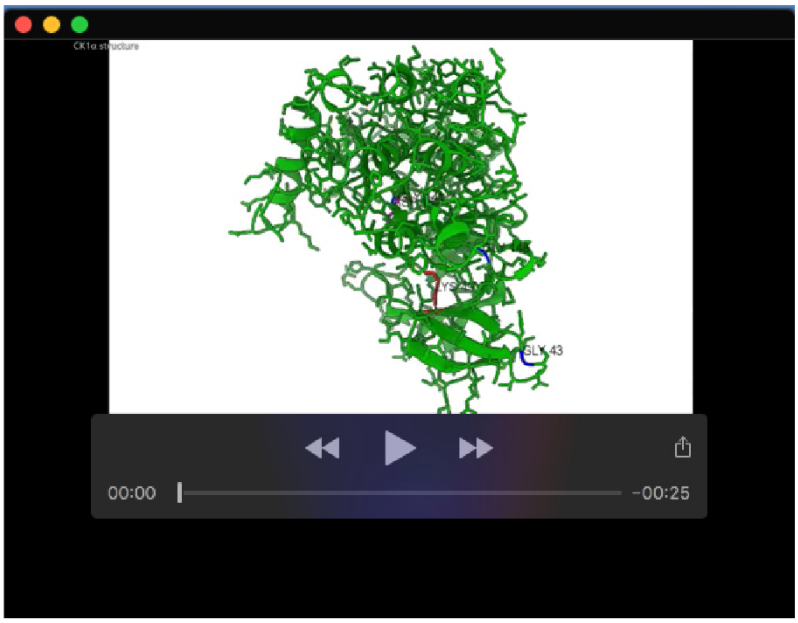

Movie 1. Representation of the three-dimensional (3D) structure of CK1α using the UCSF Chimera software (Pettersen et al., 2021). The ATP-binding Site (Lysin49) is highlighted in red; the active site/ proton acceptor (Asp139) is highlighted in magenta. Residue glycine 43 (*ck1α*^{G43D}), glycine 148 (*ck1α*^{G148S}) and lysine 141 (*ck1α*^{L141M}) that are replaced in the three different available mutant *ck1α* alleles are highlighted in blue. Subsequently, the mutated structure is depicted. The substitution lysine to methionine at position 141 removes an H-bond and favors unfavorable interactions with the active site where atoms are too close together (dashed lines in magenta), highlighted in the last sequence of the video. Labels are located on the upper left side.

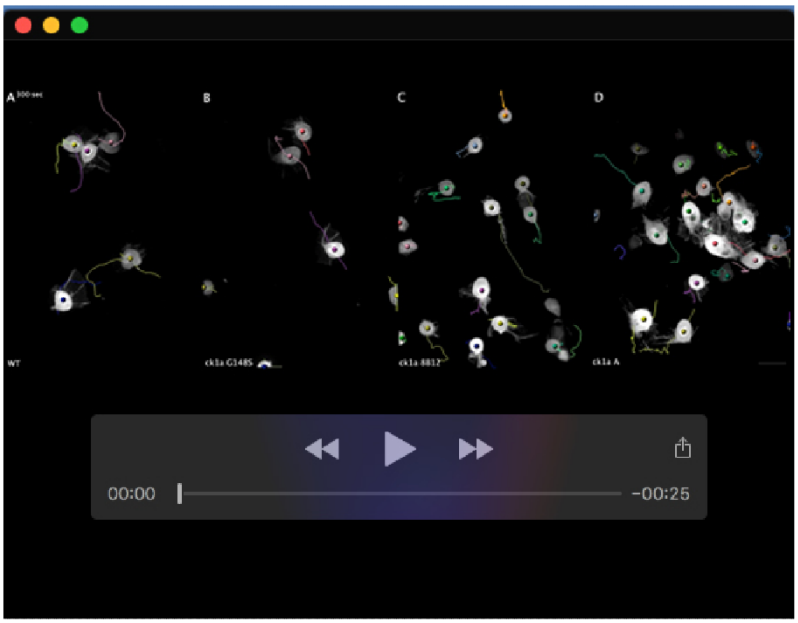

Movie 2. Spinning disc microscopy videos of randomly migrating pupal **(A)** WT wild type, **(B)** *ck1α* ^{G148S} mutant, **(C)** *ck1α* ^{G43D} mutant and **(D)** *ck1α* ^{L141M} mutant macrophages expressing an EGFP transgene imaged from a living prepupa (2 h APF). Migratory tracks of individual cells are indicated (colored, jagged lines). Scale bars represent 10 µm.

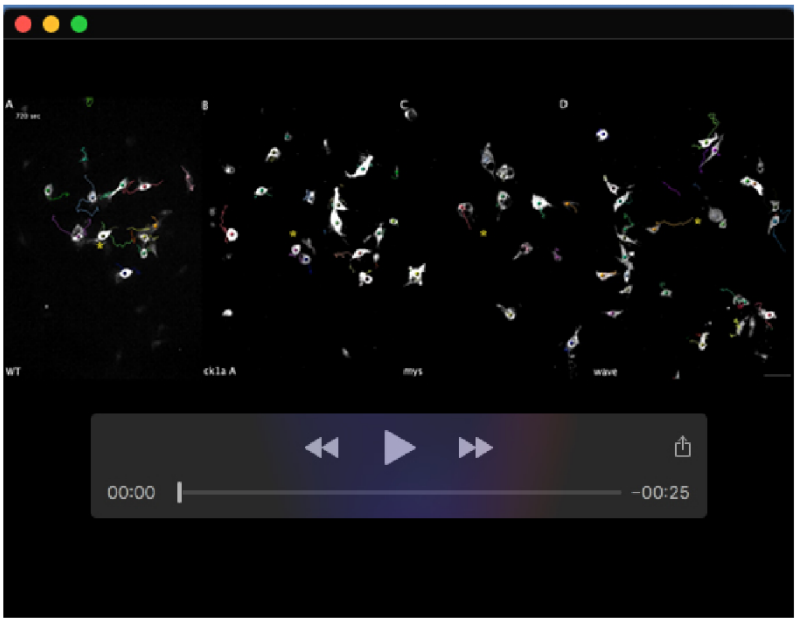

Movie 3. (A-D) Spinning disc microscopy videos of macrophages that migrate towards a laser-ablated cell (indicated by the yellow circle). Cells are imaged for 30 minutes after ablation in a 30 seconds interval and tracked afterwards using Imaris. (**A**) WT wild type (**B**) *ck1α* ^{L141M} mutant, (**C**) *wave*$^{\Delta 37}$ and (D) βPS-integrin (*mys*^{1}) mutant macrophages. Homozygous mutant cells are labeled by GFP expression using the MARCM system. Scale bars represent 10 µm.

3. Additional Results:

3.1. WAVE Lysin 48 is not involved in the degradation

Since we found that the knockdown of CK1α leads to a ubiquitin-mediated proteasomal degradation of WAVE in *Drosophila*, the question arises which lysine residue of WAVE is subject to ubiquitylation. Human WAVE2 was shown to be ubiquitylated at lysine 45 (Joseph et al., 2017). To test whether *Drosophila* WAVE is also ubiquitylated at this residue, I mutated the corresponding lysine 48 to arginine ($WAVE^{K48R}$, Figure 11 A). Arginine residues cannot become ubiquitinated therefore, this mutation is commonly used to investigate the lysine residues that function for ubiquitin association. For further *in vivo* analysis, this transgene was integrated into the 68E landing site using the Φ31-mediated transgenesis strategy (Bischof et al., 2007). First, I confirmed the expression of the WAVE mutant by using the *engrailed (en)*-Gal4 driver, which only induces expression in the posterior part of the wing imaginal disc. In contrast, the anterior compartment serves as a control. Enrichment of WAVE is clearly seen in the posterior part (Figure 11 F-G; Publication 2). As shown previously, depletion of CK1α leads to lamellipodia defects in *Drosophila* hemocytes, which is rescued by simultaneous inhibition of ubiquitin-mediated degradation (Publication 2). Thus, it was suggested that co-expression of $WAVE^{K48R}$ can also rescue this phenotype because ubiquitin binding is supposed to be inhibited on the predicted site. Interestingly, expression of $WAVE^{K48R}$ failed to rescue the lamellipodia defects (Figure 11 B-D). Cells still show a reduced circularity comparable to the depletion of CK1α (Figure 11 E). Furthermore, expression of $WAVE^{K48R}$ alone does not evoke any changes in cell shape (Figure 11 D-E).

Figure 11 – Expression of WAVE^{K48R} is insufficient to rescue lamellipodia defects in CK1α-depleted hemocytes (see next page). *(A) Section of a sequence alignment of Drosophila WAVE (top) and human WAVE2 (bottom), identifying the conserved lysine. (B-D) Maximum intensity projection of confocal images that show larval hemocytes expressing GFP (green). Alexa Flour 568-labeled phalloidin was used to stain the actin cytoskeleton (white). Scale bar: 10 µm. (B) Hemocyte-specific knockdown of CK1α in larval hemocytes using the hemolectin-Gal4 driver disrupts lamellipodia formation. (C) Overexpression of a WAVE^{K48R} mutant in larval hemocytes does not rescue cell shape defects of hemocytes evoked by simultaneous knockdown of CK1α. (D) Overexpression of WAVE^{K48R} mutant in larval hemocytes does not affect cell morphology. (E) Quantification of cell circularity. Rescue of cell morphology defects of Ck1α RNAi-depleted cells by co-expression of indicated transgenic WAVE variants. WT (n=160), Ck1α RNAi (n=160), Ck1α RNAi+ WAVE^{K48R}(n=100), Ck1α RNAi+ WAVE-SD^{5x}(n=120) (see also Publication 2) and WAVE^{K48R} (n=150). Graph is depicted in a scatter dot plot with bars indicating means±s.d. ***P≤0.001 ANOVA. (F-G) Confocal images of wing imaginal discs expressing WAVE^{K48R} in the en-Gal4 pattern. Expression of transgenes is verified by antibody staining. Anterior is to the right. Scale bar is 50 µm. (F) Staining for F-actin with Alexa Flour-labeled phalloidin (G) Antibody staining for WAVE.*

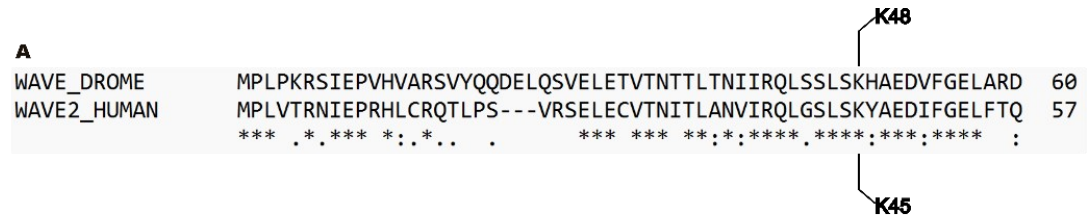
A
K48
WAVE_DROME MPLPKRSIEPVHVARSVYQQDELQSVELETVTNTTLTNIIRQLSSLSKHAEDVFGELARD 60
WAVE2_HUMAN MPLVTRNIEPRHLCRQTLPS---VRSELECVTNITLANVIRQLGSLSKYAEDIFGELFTQ 57
K45

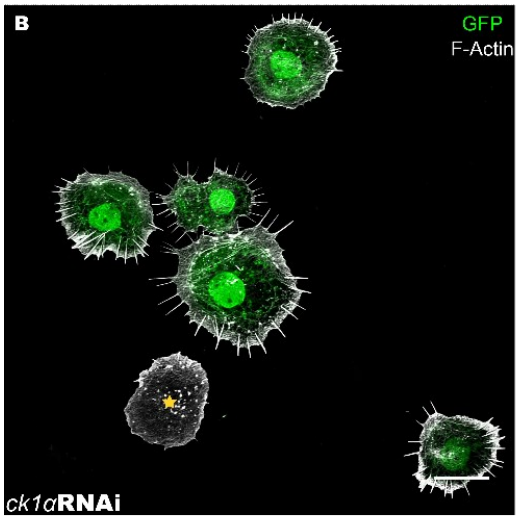
B
GFP
F-Actin
ck1αRNAi

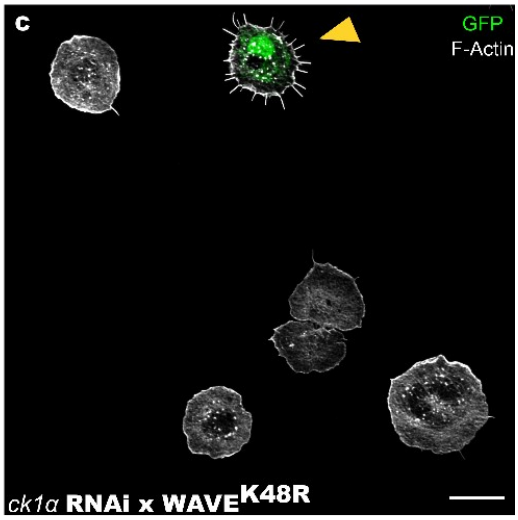
C
GFP
F-Actin
ck1α RNAi x WAVEK48R

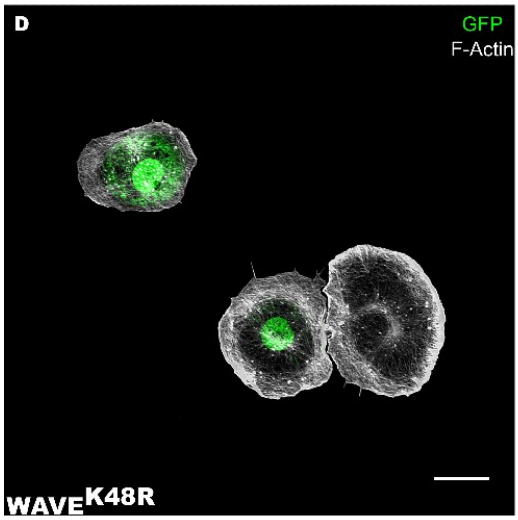
D
GFP
F-Actin
WAVEK48R

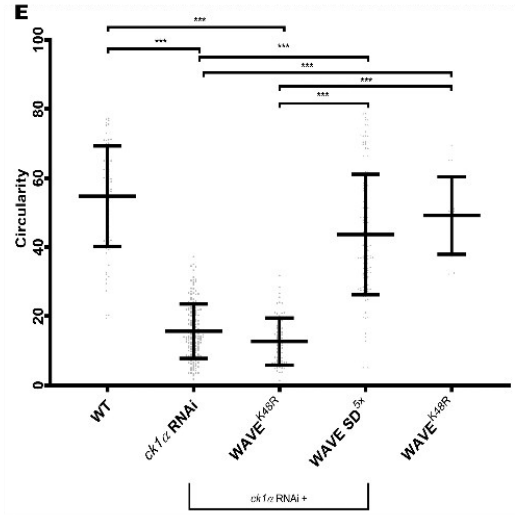
E
Circularity
0
20
40
60
80
100
WT
ck1α RNAi
WAVEK48R
WAVE SD5x
WAVEK48R
ck1α RNAi +

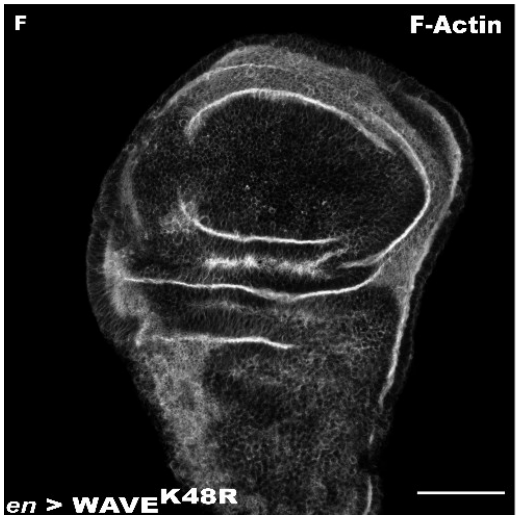
F
F-Actin
en > WAVEK48R

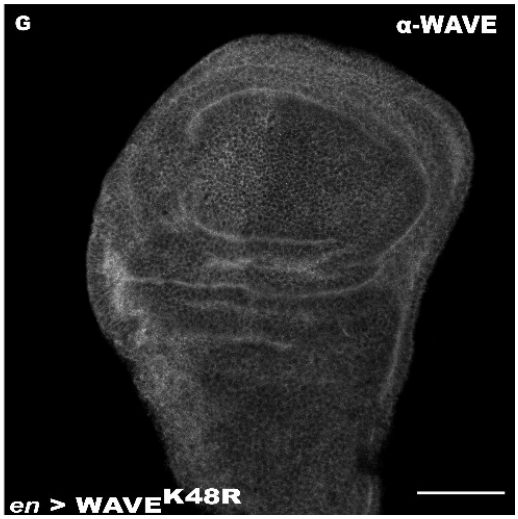
G
α-WAVE
en > WAVEK48R

3.2. CK1 overexpression affects WAVE protein level and activity

Overexpression of a phosphomimetic WAVE-SD mutant in the wing imaginal disc reveals that phosphorylation of the acidic domain of WAVE promotes its stability rather than its nucleation activity (Publication 2). However, inducible expression of full-length CK1α in S2 cells did not significantly increase WAVE protein abundance (Publication 2). To further investigate the influence of increased CK1α abundance *in vivo*, I measured the WAVE protein level as well as the F-actin level upon overexpression in the posterior compartment of the wing imaginal disc (Figure 12). Compared to the control expression of an EGFP transgene, both the WAVE protein and F-actin levels are significantly increased (Figure 12 A-C; quantification in Figure 12 D-E). However, overexpression of the kinase did not lead to the same stability as it appears for the three different WAVE constructs (Figure 12 D-E; Publication 2). Though the WAVE protein level is lower than for the WAVE-SA^{5x} mutant, the F-actin level and accordingly the polymerization activity is increased. Thus, enhanced CK1α abundance leads to a slight increase in WAVE protein level, which favors enhanced F-actin polymerization to a minor degree.

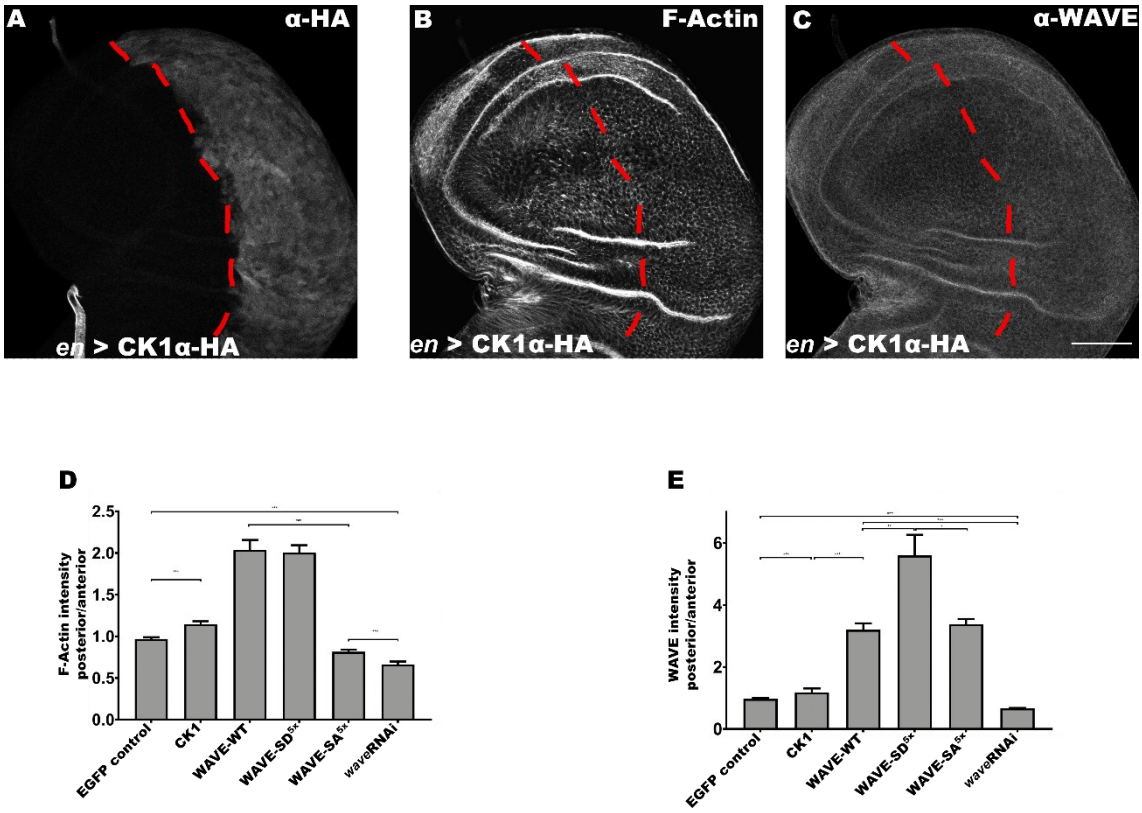

Figure 12 – Overexpression of CK1α increases level of WAVE protein in vivo. *(A-C) Confocal images of wing imaginal discs expressing CK1α in the en-Gal4 pattern. Expression of transgenes is verified by antibody staining. Anterior is to the left. A red dashed line indicates the anterior-posterior compartment border. Scale bar is 50 µm. (A) Overexpression of CK1α. (B) Staining for F-actin with Alexa Flour-labeled phalloidin to measure F-actin intensity between posterior and anterior. Note the difference between anterior and posterior compartments. (C) Antibody staining for WAVE to measure WAVE protein level between anterior and posterior. Note the slightly increased intensity in the anterior compartment. (D) Quantification of F-actin upon overexpression of CK1α as the posterior/anterior signal intensity quotient. EGFP serves as a negative control. Overexpression of different WAVE constructs and wave RNAi transgene are obtained from publication 2. **P≤0.002, ***P≤0.001 (Welch´s t-test). CK1α (n=15) (E) Quantification of WAVE levels upon overexpression of CK1α. The quotient of posterior over anterior signal strength. EGFP serves as a negative control. Overexpression of different WAVE constructs as well as wave RNAi transgene are obtained from publication 2. **P≤0.002, ***P≤0.001 (Welch´s t-test). CK1α (n=15)*

3.3. Lamellocyte transdifferentiation is induced either by knockdown of Ush or loss-of CK2 function

Loss of CK2 kinase activity leads to an enlarged lamellocyte compartment in mutant larvae (Publication 2: Figure 1 K, M) (Figure 13 A). To further investigate the CK2 regulation of blood cell differentiation, I took a closer look at transcriptional factors involved in hemocyte differentiation. Most prominent is the friend of GATA Ush. This factor normally maintains the pluripotency of

progenitor cells and suppresses their differentiation. Indeed, RNAi-mediated knockdown of *Ush* in *Drosophila* hemocytes induces transdifferentiation and increases the number of lamellocytes (Figure 13 B). Thus, this result confirmed the previously described dependency of Ush on cell fate decisions. Previous studies additionally showed that Ush acts cooperatively with the dNuRD complex in cell lineage commitment (Lenz et al., 2021). dMi-2, a member of this complex, is regulated by CK2 phosphorylation (Bouazoune & Brehm, 2005). Consequently, I sought to determine if knockdown of *dMi-2* can resemble the phenotype of reduced Ush activity. Interestingly there is neither an obvious change in cell shape nor a detectable number of lamellocyte (Figure 13 C).

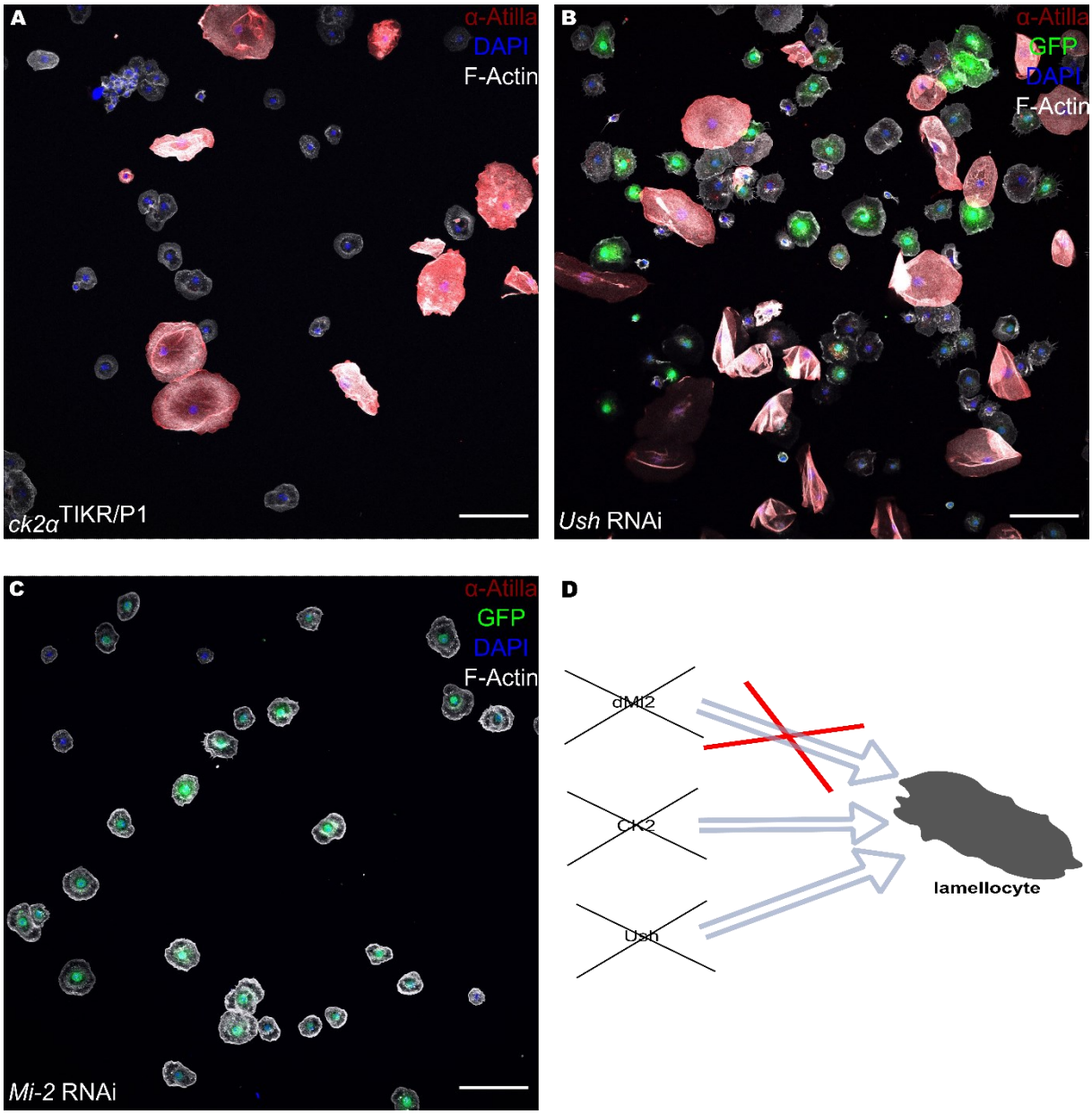

Figure 13 – Downregulation of Mi-2 does not induce lamellocyte transdifferentiation. *(A-C) Maximum intensity projection of confocal images that show lamellocyte frequency marked with Atilla (red) from Drosophila larvae. F-actin was stained with Alexa Flour-labeled phalloidin (white); nuclei were stained with DAPI (blue). Scale bar is 50 µm. (A) Transheterozygous ck2α$^{TIKR/P1}$ mutant larval hemocytes show an enlarged number of lamellocytes. (B) Hemocyte-specific knockdown of the transcription factor Ush in larval hemocytes using the hemolectin-Gal4 driver increases the lamellocyte frequency. (C) Hemocyte specific knockdown of the transcription factor Mi-2 does not induce lamellocyte transdifferentiation. (D) Schematic overview of downregulation of dMi-2, CK2 or Ush. Downregulation of dMi-2 does not increase the transdifferentiation of lammellocytes, whereas downregulation of either CK2 or Ush does.*

3.4. Lamellocytes transdifferentiate from hemocytes through an intermediate state

Since this work demonstrated that there are different ways to induce lamellocyte differentiation (Figure 14), I investigated if there are any apparent differences within the lamellocyte population. For this purpose, I took advantage of transgenic flies expressing the lamellocyte marker misshapen (msn) together with the pan-hemocyte marker eater (Anderl et al., 2016). The *eaterGFP*, *msnmCherry* reporter has been introduced as a specific marker for plasmatocytes and lamellocytes and is widely used to visualize and study the lamellocyte population (Anderl et al., 2016). Thus, it can be used to monitor lamellocyte differentiation. In order to define the blood cell lineages this combination of reporter constructs can be used to study the dynamic nature of the immune response. Particularly, the expression of *eaterGFP* resembles a plasmatocyte origin that suggests a transdifferentiation from plasmatocytes to lamellocytes.

Upon wasp infestation, the number of msn-positive cells without the typical lamellocyte structure increased (Figure 14 B, quantification Figure 15). In addition, a fraction of lamellocytes that do not express the pan-hemocyte marker eater was also observed. This confirms the previous observation that there are intermediate states in transdifferentiation where hemocytes already express the lamellocyte-specific marker msn but are not fully differentiated. Moreover, it demonstrates, again, a possible different origin of lamellocytes. Namely, if lamellocytes differentiate in the lymph gland, they do not exhibit eater expression as previously suggested (Anderl et al., 2016; Banerjee et al., 2019).

Additionally, *ev vivo* analysis of isolated pupal hemocytes revealed that Tep4 marks rare giant cells with lamellocyte morphology (Supplementary Figure S 1). Indeed, quantification demonstrated that in both genetic backgrounds the abundance of differentiated lamellocytes is similar (Figure 15).

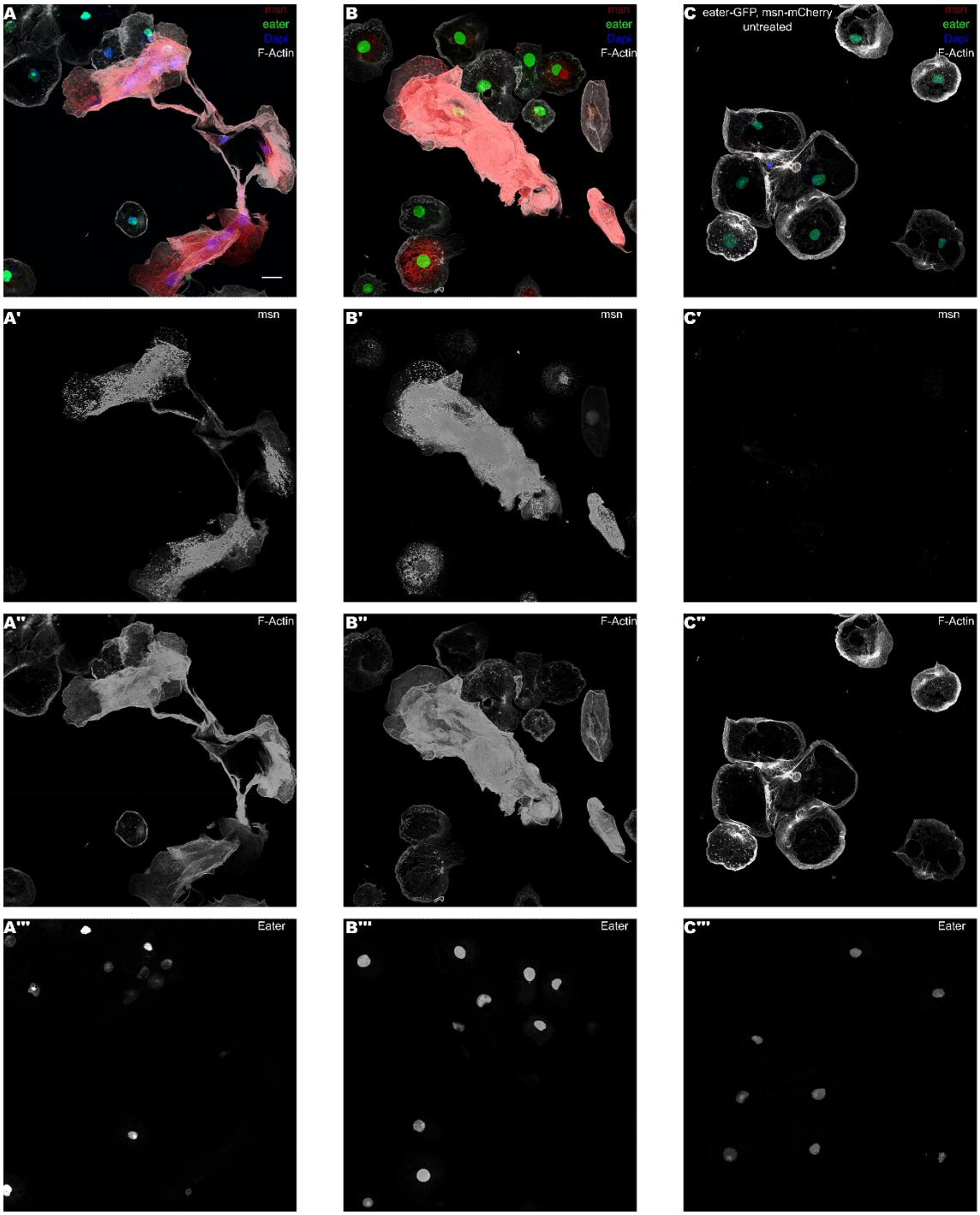

Figure 14 – Plasmatocyte transdifferentiation to lamellocytes occurs through an intermediate state. *(A-C) Maximum intensity projections of confocal microscopy images of pupal hemocytes expressing eater-GFP-NLS (green) as a pan-hemocyte marker and msn-mCherry (red) as a marker for lamellocytes either upon wasp infestation (A, B) or in unchallenged condition (C). Scale bar is 10 µm. (A-B) Cells show various states of differentiation from plasmatocytes to lamellocytes upon wasp infestation. (A) Lamellocytes partially express eater-GFP-NLS. (B) Cells with a plasmatocye-like cell shape already express the lamellocyte marker msn.*

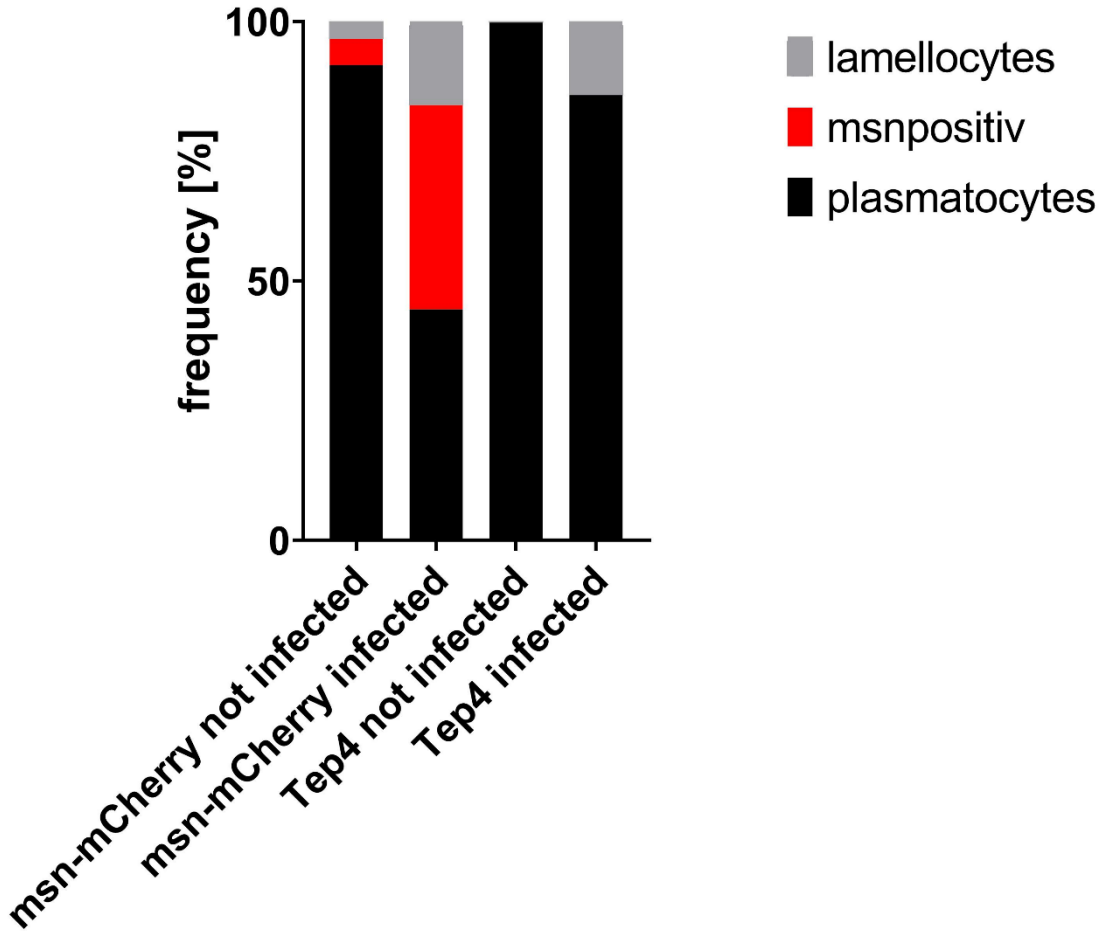

Figure 15 - Quantification of lamellocyte frequency. *Note that wasp infested msn-mCherry cells show many msn-positive cells without the typically lamellocyte morphology.*

4. Discussion

4.1. Single Cell RNA Sequencing identifies subgroups of *Drosophila* plasmatocytes which come along with the onset of metamorphosis

With the onset of metamorphosis and the transition from larval to pupal stage, most larval structures are degraded and replaced by adult tissues and organs (Banerjee et al., 2019; Regan et al., 2013). Recent single-cell analysis has mainly focused on circulating larval hemocytes or cells from the lymph gland of 3rd instar larvae (Cattenoz et al., 2020; Cho et al., 2020; Tattikota et al., 2020). Recent bulk RNA-seq analysis performed by our lab (Lehne et al., 2022) revealed 1542 differentially regulated genes, from which 804 genes are upregulated in pupal hemocytes compared to larvae. The pupal stage of *Drosophila* exhibits a remarkable amount of differentially expressed genes in hemocytes. However, whether this reflects the differentiation of new hemocyte subtypes or cell types is unknown. Thus, it was of further interest to investigate the transcriptional shift from larval to the pupal stage associated with different requirements, for instance, regulation of tissue clearance during development or the metabolic adaption of hemocytes.

After the disintegration of the lymph gland, the hemocyte population derived from both waves of hematopoiesis contributes to the pupal and adult hemocyte populations (Grigorian et al., 2011; Holz et al., 2003). Our single-cell dataset uncovered new pupal precursor and effector hemocytes with distinct molecular signatures and cellular functions clearly distinct from other stages of hematopoiesis (Publication 1). Remarkably the most abundant *srp*-high expression cluster is the undifferentiated PL cluster. Noticeably, *srp* is described to be expressed in low levels in all hemocytes but upregulated in undifferentiated precursor cells (Ghosh et al., 2015; Rehorn et al., 1996). Thus, this cluster reflects the presence of hemocytes which remain in an undifferentiated state and are still able to differentiate into effector cells. Further trajectory-based differential gene expression (monocle3) analysis (Trapnell et al., 2014) located the undifferentiated PL cluster on one end of the trajectory, verifying that those cells resemble the most undifferentiated plasmatocyte subgroup (Publication 1). The transitory PL-2 cluster is located between

undifferentiated PL and the more differentiated AMP-PL state, confirming that this cluster resembles a transition state during plasmatocyte specification. Accordingly, available data of free larval hemocytes showed that although they are identified as specific subgroups, they still have unspecified plasmatocyte markers (Cattenoz et al., 2020; Tattikota et al., 2020). These cells are able to adapt to environmental and probably to the metamorphic changes, which occur with the onset of metamorphosis and in immune challenges.

4.2. The Lsp-Bomanin-PL cluster: A multifunctional effector cell cluster with nutritional and immune functions in *Drosophila*

Overall, some previously described effector cell clusters share high similarities with our results (Cattenoz et al., 2020; Cho et al., 2020; Fu et al., 2020; Tattikota et al., 2020). For instance, the Lsp-Bomanin-PL cluster shares high similarities with the previous described PL-Lsp cluster discovered in circulating hemocytes (Cattenoz et al., 2020; Fu et al., 2020).

The Lsp-Bomanin-PL cluster cells express several genes secreted from the fat body, such as Larval serum protein 1 alpha (Lsp1α) and Bomanin genes like *BomS3*. Lsp1α belongs to the larval serum proteins (Lsp), which serve as nutritional storage proteins. Those might function in anticipation of upcoming starvation as it appears in developmental stages where Lsps are regulated by ecdysone (Handke et al., 2013). At the pupal stages, Lsps are degraded to amino acids and are thought to be used for building new structures (T., 2002). Their role in the development of *Drosophila* and importance in maintaining tissue homeostasis have been demonstrated by depletion of *Lsp* genes, which leads to abnormal development (Liu et al., 2009). The Bomanin peptides are involved in the innate immune response. Studies have shown that *Bomanin* genes are important for Toll-mediated defense against bacterial and fungal infections in *Drosophila*. Thus, Bomanins are critical for survival during infection (Clemmons et al., 2015). It can also be suggested that cells of this cluster are plasmatocytes that have engulfed fat body fragments in preparation for metamorphosis. This hypothesis correlates with the fact that a similar plasmatocyte cluster has been observed in circulating immune cells but not in the lymph gland (Cattenoz et al., 2020; Cho et al., 2020).

Another example is Edin, a small secreted protein, responsible for effective defense against wasp infestation by controlling the number of circulating plasmatocytes (Vanha-Aho et al., 2015). The mobilization of sessile plasmatocytes upon wasp infestation into circulation, where they usually differentiate into encapsulation-specific lamellocytes, initiate the immune response and occurs before the release of immune cells from the lymph gland. It was shown that upon knockdown of *edin*, those sessile plasmatocytes do not leave the sessile bands. This results in an impaired encapsulation, a process in which the wasp egg is surrounded by a first layer of plasmatocytes and encapsulation-specific lamellocytes to sequester it from the hemocoel of the larvae (Vanha-Aho et al., 2015). Additionally, enrichment of genes that are involved in the defense response against Gram-positive bacteria like *Drosomycin* (Drs) or *Drosomycin-like 5* (Drs-5) was identified in the Lsp-Bomanin-PL cell cluster (Publication 1). Thus, this cluster might represent a combination of a nutrition reservoir, for instance, the storage of amino acids, and humoral immune response, and is closely connected to the AMP-PL cluster cells (Cattenoz et al., 2020).

4.3. The multifaceted role of AMP-PL cluster cells in immunity and development during metamorphosis in *Drosophila*

The AMP-PL cluster cells are indispensable for a direct immune response against microbial pathogens. This plasmatocyte subgroup already exists in the larval state and can neutralize pathogens or activate other immune system cells to do so, which is the most common function of plasmatocytes. Furthermore, AMP-PL and Lsp-Bomanin-PL together might function in metabolic processes connected with the immune response (Cattenoz et al., 2020). This outlines a complex relationship between metabolism and immunity. Noteworthy, the AMP-PL cells also express ECM production genes and many ecdysone-inducible genes (Publication 1). As mentioned in the introduction, ECM molecules are necessary for developing basement membranes and ecdysone-inducible genes are important in pupal morphogenesis. A signal triggered by ecdysone, which initiates metamorphosis, may induce both rapid differentiation events occurring in the hours between pupation and lymph gland dissociation, as well as

increased hemocyte motility during normal development (Grigorian et al., 2011). Thus, it can be suggested that these cells provide a pool for forming a defensive barrier against pathogens and are essential in the development from larval to pupal stage. Furthermore, the expression profile of AMP-PL changes upon metamorphosis. This suggests that the pupal AMP-PL assumes pupa-specific functions (Johnson et al., 2020; Lehmann, 1996).

4.4. Identification of a new plasmatocyte subgroup, OxPhos-PL, and its potential role in metabolism and immunity in *Drosophila*

A yet unknown subgroup of plasmatocytes was identified and named OxPhos-PL. Cells of this cluster likely provide energy resources since they show enrichment of mitochondrial gene transcripts and are linked to the ribosome as well as oxidative phosphorylation and ATP synthesis (Publication 1). Thus, they are able to cover the metabolic requirements for removing debris, which is an indispensable function of plasmatocytes at the onset of metamorphosis. It has been described that plasmatocytes, which are associated with tissue repair and clearance of apoptotic cells commit to oxidative phosphorylation (OXPHOS) (Krejčová et al., 2019; O'Neill & Pearce, 2016). Upon an immune challenge, plasmatocytes can increase their glucose consumption to produce sufficient ATP and glycolytic intermediates that facilitate their elevated phagocytic activity. The cellular response to bacterial infections imposes significant metabolic demands, and metabolic adaption is regulated by plasmatocytes throughout the infection (Krejčová et al., 2019). Noteworthy, during embryogenesis, energy is mainly produced by glycolysis (Emtenani et al., 2022). During larval stage, embryo-derived hemocytes shift to lipid beta-oxidation. This in turn is required for blood cell progenitor differentiation in the larval lymph gland (Boulet et al., 2021; Tiwari et al., 2020). Importantly, a functional metabolism is indispensable for an effective immune response, implying that metabolism and immunity share a complex relationship. This was also demonstrated in mammalian blood cells, which shift their metabolism in response to development, aging, infection, or cancer (Faas & de Vos, 2020; Nakamura-Ishizu et al., 2020; Rashkovan & Ferrando, 2019). Conclusively, because recent investigations reveal high similarities between fly and mammalian, *Drosophila* is established as a powerful

model for exploring the molecular mechanisms that control immune cell metabolism.

4.5. Chitinase-PL and Adhesive-PL: A potential axis of adhesion and chitin recognition in the immune response

Interestingly the Chitinase-PL and Adhesive-PL might be of further interest. Both clusters, again, highlight the changes of molecular signatures from larval to pupal stage and do not have any corresponding cluster in larval stages but show similarities with a hemocyte subcluster described in the adult fly (H. Li et al., 2022). Additionally, they are transcriptomically the most distinct plasmatocyte cluster. They also share an increased expression level of several genes implicated in cell-cell adhesion, septate-junction, and immune response. As the introduction mentions, lamellocytes adhere to one another via septate junctions to encapsulate the parasitic egg. However, less is known about the exact mechanism underlying the encapsulation and which genes are involved in this process. It might be of further interest to visualize septate junction proteins by immunostaining to uncover junction proteins involved in the encapsulation process. Subsequent lamellocyte-specific knockdown experiments of Chitinase-PI or Adhesive-PL marker genes and *in vivo* investigation of the wasp egg encapsulation process could reveal the importance of those cluster cells in mediating adhesions. This experiment could further outline that they contribute to an interesting axis of immune response performed by adhesion and chitin recognition. Noteworthy, lamellocytes have a distinctive cytoskeleton that includes numerous actin filaments and other proteins involved in cell adhesion and migration.

Altogether, this study's results broaden the diversity and complexity of *Drosophila* plasmatocyte characterization. It can be suggested that this heterogeneity and plasticity derive from the complex interaction between plasmatocytes and their microenvironment. Functional distinctions of different subpopulations can now be more precisely characterized by developmental stages and immune challenges identifying their involvement in phagocytosis, metabolic homeostasis, and AMP response. With the hallmark of novel distinct marker genes, it will be possible to generate more specific targeted genetic tools for *Drosophila* hemocytes to investigate the role of immune cells in

physiological and pathological conditions. We can now distinguish between different precursor and effector cells.

4.6. Secretory-PL cluster cells represent a precursor state with various functions in innate immune response

Although we identified a still high expression of *srp*, usually representative for an undifferentiated state, the Secretory-PL cluster was not identified as a transition state from undifferentiated to effector cells. However, cells of this cluster might still have the potential to differentiate. Instead, many genes encoding for serine-type endopeptidases involved in proteolysis are found in the Secretory-PL cluster (Publication 1).

A here newly identified marker gene of the Secretory-PL cluster is CG31174. So far, this gene has been barely described but was found in recent single-cell analyses in a crystal cell cluster and described as a potential marker of this cell type (Cho et al., 2020). *Ex vivo* analysis of hemocytes with the known crystal cell antibody Hnt validated a few CG31174 positive crystal cells in the pupae with a distinct cell shape. Among the six replicates of pupal bleeds in which CG31174 cells were stained with Hnt, representing about 3000 blood cells, one CG31174 positive cell that was Hnt positive was identified. They were more abundant in larval than in pupal hemocytes. This observation was further verified by transcriptome analysis (Publication 1).

Additionally, it has been described that crystal cells are lost after the onset of metamorphosis (Lanot et al., 2001). It could be suggested that this appears due to the sensitive nature of crystal cells as they tend to burst (Bidla et al., 2007; Hultmark & Andó, 2022). Using crystal cell specific reporter fly lines, for instance, Lz-GFP, for live-cell imaging could reveal if GPF-positive crystal cells are visible through the pupal case. This experiment would clarify their occurrence in the pupal state. Conclusively, CG31174 can be described to be expressed in crystal cells, as recently reported.

Additionally, it has been shown that crystal cells serve as storage for the rapid delivery of PPOs. After crystal cell rupture, the PPOs are secreted into the hemolymph, where they are activated upon proteolytic cleavage by serine proteases and involved in PO activity (Binggeli et al., 2014; Vlisidou & Wood,

2015). Furthermore, serine proteases are involved in proteolytic cascades regulating both, melanization and Toll signaling pathway (Dudzic et al., 2019; Shichao Yu et al., 2022). Dudzic and colleagues demonstrated two different pathways of activating PO activity that result in melanization. Additionally, two serine proteases, Hayan and Psh, which are downstream of pattern recognition receptors, are responsible for the regulation of both Toll activity and the melanization response (Dudzic et al., 2019; Ligoxygakis, Pelte, Hoffmann, et al., 2002; Ligoxygakis, Pelte, Ji, et al., 2002). Therefore, it might be possible that the Secretory-PL cluster, with various serine proteases upregulated, represents a precursor or activator of crystal cells.

Recently a role for a sub-population of plasmatocytes expressing genes with annotated serine protease activity similar to our Secretory-PL cluster has been described as detrimental to fly survival. It has been proposed that the decrease in infected phagocytic cells may be due to caspase-dependent apoptosis, which could result from the serine-protease activity conferred on this sub-population (Galindo et al., 2023). However, a clear understanding of their function in various processes remains uncharacterized mainly because of the large complexity of serine proteases. Consequently, this has to be addressed in further detail.

Additionally, genes associated with the innate immune response, like *MyD88* or Thioester-containing proteins 1 and 4 (Tep1 and Tep4) are upregulated in the Secretory-PL cell cluster (Publication 1) They have been described to be involved in the immune response against different types of bacteria.

Upregulation of the *MyD88* gene, which encodes an adaptor protein involved in the Toll pathway, further highlights the importance of the Secretory-PL cluster cell type in the innate immune system. MyD88 is an adaptor protein that interacts with the Toll receptor intracellular Toll/Interleukin-1 receptor (TIR) upon activation of the Toll pathway. The following pathway reactions are ultimate in immune-related gene expression (Shichao Yu et al., 2022). Interestingly, this also points out another functional parallel to the vertebrate system. Toll-like receptors can stimulate mammalian bone marrow hematopoietic stem and progenitor cells (HSPCs) in response to pathogens or inflammatory signals, which subsequently activates myeloid differentiation in a MyD88-dependent

manner (J. L. Zhao & Baltimore, 2015). In addition, MyD88 is required to reduce fat stores when exposed to Gram-positive bacteria (Ayyaz et al., 2013). This observation further links Toll pathway signaling and metabolic homeostasis and underlies the immune-metabolic interaction. Of further interest is the upregulation of *dorsal*. This gene encodes another transcription factor regulated by the Toll pathway mainly used during development (Ayyaz et al., 2013).

Tep1 and Tep4 belong to the family of *Tep* genes, which show a similar expression pattern with a defense function against pathogens in barrier epithelia and promote the activation of the Toll pathway (Dostálová et al., 2017). In addition, they have been described to be expressed in hemocytes and function in the innate immune response against pathogens (Bou Aoun et al., 2011). *Ex vivo* analysis performed in this work uncovered an additional function of Tep4, which will be discussed in the next chapter (Supplementary Figure S 1).

4.7. Tep4-positive lamellocytes: A possible dynamic adaption in the immune response of *Drosophila* against pathogens and parasitoid wasps

In general, members of the Thioester-containing protein (TEP) family function in the antimicrobial immune response by opsonization and elimination of pathogens in both vertebrate and invertebrate animals (Shokal & Eleftherianos, 2017a). Tep4, upregulated among others in the Secretory-PL cluster, belongs to the *Tep* family of genes. This protein family is, in total, composed of six genes (*Tep1-Tep6*), of which *Tep5* is a pseudogene as no transcripts are detected. Drosophila TEPs are similar to the complement factors C3/C4/C5 in mammals and the alpha2-macroglobulin (α-2Ms) family of protease inhibitors, both of which have important roles in the immune response against pathogens. Accordingly, their characteristic central hypervariable region corresponds to the bait domain of alpha2-macroglobulin and the anaphylatoxin domain in C3.

Moreover, they share the common 4-amino-acid sequence CGEQ which defines the thioester site responsible for covalent binding to microbial surfaces. However, Tep6, also known as macroglobulin-complement related and C5 in higher vertebrates, is a transmembrane protein that lacks a functional thioester-

binding site (Dostálová et al., 2017). So far, the family of TEPs has been described to be involved in the innate immune response of *Drosophila* against pathogenic bacteria (Bou Aoun et al., 2011).

We found that *Tep4*, besides the upregulation in the Secretory-PL and PSC cluster, marks rare giant cells with lamellocyte morphology (Supplementary Figure S 1, Figure 15). This observation contradicts to a recent single-cell analysis of the lymph gland (Cho et al., 2020), where *Tep4* is not upregulated in the identified lamellocyte clusters. Additionally, a recent study suggested a role for TEPs against parasitoid wasps, but it lacks a precise mechanism for how the TEPs are involved in this immune response (Dostálová et al., 2017). One hypothesis is that Tep4-positive cells represent a population of plastic or responsive subgroup of plasmatocytes capable of a dynamic adaption to the environment.

Remarkably, all detected lamellocytes, verified by anti-Atilla staining, are Tep4 positive (Supplementary Figure S 1). Accordingly, the number of Tep4-positive lamellocytes is enriched in the same amount compared to a control experiment using the lamellocyte-specific marker *msn-mCherry* (Figure 15). However, we observed two different subgroups of lamellocytes in line with the fact that there are different ways of differentiation (Anderl et al., 2016).

One fraction of lamellocytes simultaneously expressing the lamellocyte-specific *msn-mCherry* and the plasmatocyte-specific *eater-GFP* markers suggests a plasmatocyte-lamellocyte conversion. Those are literally called “type II” lamellocytes and are known to transdifferentiate from plasmatocytes (Anderl et al., 2016; Banerjee et al., 2019). Additionally, *eater-GFP*-negative lamellocytes were observed. This fraction is supposed to derivate from dedicated lymph gland progenitors and is called “type I”. Also, there were msn-positive cells detectable that still did not have a lamellocyte-like morphology. Upregulation of *msn* expression happens when circulating plasmatocytes adhere to wasp eggs and start to transdifferentiate into “type II” lamellocytes. Hence, cells with a detectable level of msn, described as cytoplasmatic mCherry-positive foci (Anderl et al., 2016), but not with a lamellocyte-like shape, might represent an intermediate state. A recent postulation underlines this suggestion that the final step of lamellocyte differentiation is a cell morphology change (Leitão et al.,

2020). This was observed while investigating the immune response in flies continuously exposed to parasitic wasps (Leitão et al., 2020). Even though the transcriptional state of the cell is constitutively active with high expression of lamellocyte marker, they noted that changes in cell morphology remain an inducible response (Leitão et al., 2020). Remarkably taking the msn-positive population observed in our study together, it accounts for approximately 60 percent of the hemocyte population (Figure 15).

Another hypothesis to explain the positive Tep4 staining of lamellocytes could be the internalization of secreted Tep4 protein. Previously it has been proposed that secreted TEP molecules in the hemolymph can interact with other tissues to activate signaling pathways that regulate immune functions against invading microbes (Shokal & Eleftherianos, 2017b). Lamellocytes show high endocytic and exocytic pathway activity; however, little is known about the mechanisms. It has been suggested that Atilla take part in internalizing of extracellular vesicles, but this was not further investigated in more detail (Wan et al., 2020). Lamellocyte-specific knockdown of various surface proteins, known to be expressed in lamellocytes, could gain more insights into this process, and clarify a hypothesized Tep4 intake by lamellocytes. Of further notice is that is has been shown that *Tep4* gene transcription can affect PO activity in response to infections. In the absence of *Tep4*, both PO activity in the hemolymph and melanization intensity at the injection site increase substantially when responding to pathogen infection (Shokal & Eleftherianos, 2017a). Conclusively, Tep4 is an interesting candidate to study further the bridge between the humoral and cellular arms of the innate immune response. However, the exact mechanism underlying the emerging role of Tep4 has to be elucidated.

4.8. Discovering a novel pathway of lamellocyte differentiation from Posterior Signaling Center cells of Lymph Glands in *Drosophila*

Generally, the stem cell niche of the lymph gland called Posterior Signal Center (PSC) regulates hemocyte differentiation in the lymph gland during larval development and participates in the larval response to wasp parasitization (Banerjee et al., 2019).

In this study, I showed that motile and immune-responsive PSC cells contribute to the hemolymph of early pupae, persist throughout pupal development and are capable of transdifferentiating into lamellocytes upon an immune challenge (Publication 1, Supplementary Figure S 2).

PSC cells can be clearly distinguished from other regions within the lymph gland by their unique expression profile, including the co-expression of *Antp, kn* and *tau* (Crozatier et al., 2004; Mandal et al., 2007). It has been previously shown that PSC cells reside in the lymph gland and provide signals to regulate progenitor maintenance or differentiation (Crozatier et al., 2004; Krzemień et al., 2007; Mandal et al., 2004). Furthermore, recent studies revealed the presence of circulating PSC-like cells in the adult fly, and single-cell sequencing results suggest the presence of such cell type in the larval hemolymph and lymph gland (Boulet et al., 2021; Cattenoz et al., 2020; Cho et al., 2020; Fu et al., 2020; Tattikota et al., 2020). It has been described that PSC cells persist within the niche until 10 h APF immediately before dissociation of the lymph gland. At this point, the PSC cells are no longer associated with the dorsal vessel, suggesting that they and other hemocytes disperse into the hemolymph (Grigorian et al., 2011).

Ex vivo identification of PSC cells from the hemolymph of early pupae was possible by the expression of *Antp* and *kn* (Crozatier & Vincent, 2011), which also mark a subset of plasmatocytes (Publication 1), and additionally by the recently identified PSC marker *tau* (Cho et al., 2020). In line with previous reports, a small fraction of PSC cells expresses *srp*, and not the crystal cell marker Hnt (Publication 1).

Recent publications showed that adult hemocytes further derivate from posterior lobe progenitors (Boulet et al., 2021; Ghosh et al., 2015; Sanchez Bosch et al., 2019). Furthermore, *kn* and the transcription factor *srp* are expressed in those posterior lymph gland lobes (Sanchez Bosch et al., 2019); thus, this might provide an active hematopoietic hub in *Drosophila* adults and consequently contribute to the total pupal and adult hemocyte population.

Additionally, *kn* expression has been observed in a low but physiologically relevant number of prohemocytes in the MZ, where they suppress further

differentiation to keep cells in a quiescent state (Oyallon et al., 2016). Although a contribution to hemocyte differentiation has not been clarified so far, our G-TRACE (Gal4 technique for real-time and clonal expression) (Evans et al., 2009) lineage tracing data confirmed a *kn* lineage-traced expression cell population with plasmatocyte typical morphology (Publication 1). It could be that lineage-traced *kn*-positive plasmatocytes originate from progenitors of the MZ. They might contribute to the population after lymph gland disintegration. This argument is underlined by the fact that in both *ex vivo* and *in vivo* imaging of pupae, a *kn*-positive population with plasmatocyte typical morphology was observed. However, they can be separated from PSC cells by their small and spiky morphology (Publication 1).

In addition to maintaining hematopoiesis, PSC cells regulate lamellocyte differentiation. It has been previously shown that overexpression of *kn* in the MZ together with wasp infestation leads to reduced lamellocyte production. In contrast, the reduction of *kn* in the MZ is essential for lamellocyte differentiation and dispersal (Oyallon et al., 2016). However, transdifferentiation from PSC cells into lamellocytes has not been described so far. It was generally described that lamellocytes derivate from existing plasmatocytes or differentiating lymph gland prohemocytes. Lineage tracing experiments performed in this work now suggest that *kn*-traced progenitors are able to differentiate into lamellocytes in response to wasp infestation. As mentioned before, *kn*-positive cells comprise both PSC cells and progenitors of the MZ though (Publication 1).

However, we identified Tau as a novel marker for PSCs with expression limited to the PSC niche. This was further validated by showing that expression of GFP under the control of the Tau-Gal4 driver is exclusively found in the PSC region of primary lobes (Publication 1). Thus, we used *tau* for lineage tracing analysis (Cho et al., 2020; Sanchez Bosch et al., 2019). Thereby, the lineage tracing results demonstrate the existence of a progenitor lamellocyte population derived from the PSC cells independent of both the posterior lobes and the MZ of the anterior lobes (Publication 1). Our data shed light on an additional PSC-dependent route for lamellocyte differentiation.

However, the mechanism underlying the transdifferentiation of PSC cells into lamellocytes must be elucidated. In addition, the contribution of PSC-derived

lamellocytes to the innate immune response should be investigated. This is so far not described, and it is assumed that pupal or adult lamellocytes do not contribute to the immune response. A suitable method could be an encapsulation assay with GFP expression under the control of the Tau-Gal4 driver.

So far, it has been described that without the PSC, lamellocyte differentiation fails to occur (Crozatier et al., 2004). ROS level increases in the PSC upon infestation and this in turn activates the Toll signaling pathway to trigger lamellocyte differentiation in the MZ and the disintegration of the lymph gland (Sinenko et al., 2012). Interestingly, similar emergency hematopoiesis in mammals depends on increased ROS production. There the TLR/NF-κB is activated as part of the emergency granulopoiesis, which triggers the production of neutrophils. Noteworthy, the TLR4 is part of the vascular niche and activates this pathway (Manz & Boettcher, 2014).

In addition, increased ROS levels in the PSC lead to the secretion of Spitz into the hemolymph. Spitz activates EGFR signaling in circulating hemocytes and initiates their differentiation (Louradour et al., 2017). The EGFR together with the Toll signaling cascades act in parallel. It might be of further interest to dissect the role of EGFR signaling in differentiating PSC cells into lamellocytes. Similarly, it has been recently demonstrated that EGFR signaling is sufficient to initiate proliferation and conversion from hub cells into stem cells in *Drosophila* testes. Those hub cells are normally quiescent and responsible for secreting signals to adjacent stem cells, comparable to the niche cell function in the lymph gland (Greenspan et al., 2022).

A potential of a niche to trans-differentiate into the cell type, which is normally adjacent to and regulated by the niche, has been identified many studies over the last years. Insights of several types of niche cells, including niches in the *Drosophila* reproductive organs as well as rat limbal niche cells, highlight the growing importance of niche cells in those processes (Greenspan et al., 2022; Rust et al., 2020; Schmitt et al., 2018; Voog et al., 2014; Shiyan Yu et al., 2018; X. Y. Zhao et al., 2018). For instance, this was recently described in *Drosophila* ovary, where a niche for somatic follicle stem cells (FSCs) consists of adjacent escort cells. The escort cells do not give rise to new FSCs under normal

conditions. However, upon environmental stress, these escort cells can convert into new FSCs (Rust et al., 2020). Another similar example of niche cell plasticity was described in *Drosophila* testes, where niche cells send signals to germline stem cells (GSCs) and somatic cyst stem cells (CySCs). Upon genetic ablation of CySCs, the niche cells exit a quiescent state, leave their hub and transdifferentiate into CySCs (Greenspan et al., 2022).

Further investigation of the *Drosophila* niche cells could also help to dissect the role of mammalian niches, because a high similarity to the mammalian bone marrow hematopoiesis is given. It is well known that dividing and non-dividing hematopoietic stem cells reside in perivascular niches. Those are specialized microenvironments in tissues where stem cells and progenitor cells are found in close proximity to blood vessels. These niches provide a supportive environment for stem cells and progenitor cells to maintain their self-renewal capacity and differentiate into specific cell types as needed. Perivascular niches have been identified in various tissues, including bone marrow, brain, skin, and muscle (Komsany & Pezzella, 2020). Similar to *Drosophila*, niche cells and those progenitor stem cells show a noticeable heterogeny composition (Crane et al., 2017).

In summary, the PSC niche has many functions regulating hematopoiesis and differentiation. Results of this work implicate further roles of PSC cells upon immune challenges in signaling relay and direct defense against pathogens. Moreover, those imply that PSC cells act not only as a stem cell niche in larval hematopoiesis but can also contribute as cell reservoir to pupal and adult blood cells.

4.9. Identification and characterization of motile and immune-responsive Posterior Signaling Center cells contributing to hemolymph in *Drosophila*

Until now, most studies on PSC cells focused on their role as a niche. The general mechanisms of how the PSC control hematopoietic maintenance is well studied (Crozatier & Vincent, 2011; Krzemień et al., 2007; Louradour et al., 2017; Luo et al., 2020; Oyallon et al., 2016). Furthermore, it has been shown

that PSC cell number is tightly regulated by various factors (Morin-Poulard et al., 2021). Our study now provides the first evidence that PSC cells can transdifferentiate into lamellocytes, an immune response to wasp infestation, which is normally restricted to larval stages and does not occur in the adult fly (Boulet et al., 2021). Thus, neither the existence nor a definite role for the niche cells in the pupal and adult fly after the disintegration of the lymph gland has been described so far.

In vivo live imaging experiments in this study of both pupal and adult abdomen further revealed the existence of PSC cells (Publication 1, Supplementary Figure S 2 , Supplementary Figure S 3). They are able to switch from random to directed migration towards a wounding site with no significant difference compared to embryonic-derived *hml*-marked plasmatocytes. However, *in vivo* live imaging of the pupal abdomen showed a noteworthy difference between *hml*- and *kn*-positive hemocytes in cell shape and size. The different functions of those different cell types can most likely explain this. On the one hand, embryo-derived reservoir hemocytes mainly function in the phagocytosis of large quantities of histolyzing larval tissue such as muscle and fat cells, the ECM surrounding lymph gland cells, and even other plasmatocytes. This uptake leads to a vacuolization and bloat of the cell shape, and the phagocytic ability declines with age (Horn et al., 2014). In contrast, PSC cells function as a niche and regulate hemocyte differentiation in the lymph gland until its disintegration (Krzemień et al., 2007). They normally do not contribute to the general pool of blood cells but participate in larval response to wasp infestation via signaling (Crozatier et al., 2004). Thus, their role is limited to signaling functions, for which a small cell size with filopodial extensions is sufficient.

It must be in mind that PSC cells primarily play a role in maintaining hemocyte proliferation. During hematopoiesis, those cells require filopodia protrusions for cell-cell communication with progenitor cells next to the niche in the MZ of the lymph gland (Krzemień et al., 2007; Mandal et al., 2007). A similar observation has been made in the ovarian stem cell niche, where filopodia protrusions of cap cells provide Hh signals to escort cells (Csordás et al., 2021). Thus, it can be suggested that these cells partly do not develop means of motility.

However, after the disintegration of the lymph gland, PSC cells are motile and respond to cell damage (Publication 1). The already described explorative function of filopodia can thereby be the main factor for motility. Furthermore, filopods are thought to sense and respond to chemoattractants, facilitating migration promoted by F-Actin polymerization. For instance, in many cancer cells filopodia stability directs cell migration and promotes their invasiveness (Friedl & Wolf, 2010; Jacquemet et al., 2015). Additionally, there is a link between Bone morphogenetic protein (BMP) signaling and filopodia formation. It has been described that BMP induces filopodia protrusions in endothelial cells in zebrafish (Wakayama et al., 2015). Remarkably, BMP signaling also plays an indispensable role in controlling cell size of the PSC at larval stages. However, is not involved in regulating the ability of PSC cells to signal to prohemocytes via filopodia (Pennetier et al., 2012). It might be of further interest to use the available genetic tools investigate if there is a link between BMP signaling and promoting of filopodia extension in pupal or adult stages of *Drosophila*. This has never been addressed so far.

Conclusively, the exact role of filopodia extensions and the underlying mechanism of migration and phagocytosis of PSC cells need to be further evaluated. Further bulk RNA Sequencing of the PSC cell population might reveal the transcriptional profile of actin-related genes. For instance, the upregulation of fascin has been demonstrated in several cancer cells, which utilize filopodia for migration. Additionally, it might be of further interest how PSC cells would act upon knockdown of ROCK. Normally, downregulation of ROCK signaling favors Rac-mediated lamellipodia-based migration. Since filopodia can be formed independently of actin branching by the Arp2/3 complex, which Rac1 induces, the question is whether PSC cells still maintain their signaling functions via filopodia extension and whether they still respond to wound damage.

As mentioned earlier, migration of immune cells mediated by dynamic rearrangement of the actin cytoskeleton is regulated by various proteins. Therefore, dissecting the specific role of regulatory factors in the immune response in these newly described motile PSC cells might be of further interest.

For instance, the regulatory role of a novel interaction partner with the actin branching machinery is described in the following chapters.

4.10. CK1α is a novel interaction partner of WAVE in the regulation of the actin cytoskeleton

A wide screen of putative WAVE interaction partners was performed in *Drosophila* S2 cells (D'Ambrosio & Vale, 2010). Screening 162 kinases using the RNAi system under control of the *Drosophila* hemocyte-specific driver initially revealed CK1α as the most prominent candidate of the kinases regulating the actin machinery. Knockdown of *ck1α* altered the morphology of hemocytes, comparable to the loss of lamellipodia protrusions observed upon *wave* depletion. They proposed that the changes in cell shape could indicate an intermediate state where the barrier to microtubule growth is weakened due to reduced actin retrograde flow. This in turn leads to a stellate phenotype of these knockdown cells similar to a knockdown of *wave* (D'Ambrosio & Vale, 2010).

Retrograde flow has been described to be involved in F-actin assembly. A constant retrograde flow maintains the density of the lamellipodium, and a reduced retrograde flow coincides with a reduced F-actin assembly (Kage et al., 2017). The interplay between different actin regulators is crucial for the overall actin network dynamic and a homeostatic equilibrium within the cytoskeleton. Altering the activity of any of these factors can enhance the formation of different actin structures, including retrograde flow and increased formation of long filopodia protrusion.

Those long filopodia protrusions structures, which are most likely seen in cells upon knockdown of the indispensable WRC components *wave* or *abi*, are formed from parallel bundles of actin filaments by formins or ENA/VASP proteins. Noticeably, parallel actin filaments in filopodia structures are further stabilized by fascin, but they lack microtubules (Etienne-Manneville, 2004). *In vivo* investigation of *ck1α* and *wave* mutant cells demonstrated that filopodial structures are the predominantly actin structures and, thereby essential for the migration with diminished lamellipodia (Publication 2).

Conclusively, the reduction of cell circularity coherently with an impaired migration behavior and immune response in *ck1α* mutant cells is comparable to *wave* mutant cells (Publication 2). This in turn leads to the assumption that disruption of the lamellipodium and enhanced filopodia formation in *ck1α* mutant cells is mainly caused by a diminished activity of the WRC.

Furthermore, co-immunoprecipitation and phosphorylation assay have shown the direct interaction of WAVE and CK1α (Publication 2). However, priming of WAVE by another kinase was not given in this experimental circumstance. It is worth mentioning that both the kinase and the substrate were provided in high concentrations, which may not necessarily display the physiological conditions and just highlights the *in vitro* interaction. CK1α is able to phosphorylate even without priming by another kinase (Flotow & Roach, 1991). Nevertheless, the *in vivo* data strongly underlies the interaction of WAVE and CK1α (Publication 1).

4.11. The role of CK1α and cullin-RING E3 ligases in regulating WAVE stability and degradation and its impact on cell shape

A lot of research demonstrated that phosphorylation regulates the activity of WAVE and thereby the WRC activation and Arp2/3 interaction (Z. Chen et al., 2010; Kramer et al., 2022; Mendoza, 2013; Mendoza et al., 2011; Pocha & Cory, 2009). However, a mechanism behind reduced activity and regulation of the protein level has not been demonstrated *in vivo* so far.

My data imply that basal phosphorylation is crucial in regulating WAVE. Loss of phosphorylation within the VCA domain evoked by knockdown of *ck1α* leads to enhanced degradation of WAVE (Publication 2).

The observations made in this work for the first time point out that phosphorylation by CK1α is indispensable for WAVE stability. As a consequence of observed changes in cell shape and impaired migration behavior, I first thought that the activity of WAVE is diminished upon depletion of CK1α. However, detailed analysis revealed a WAVE degradation (Publication 2). Pharmacological inhibition of CK1α activity leads to reduction of WAVE abundance *in vitro*. Remarkably, this was restored by simultaneously applying the known inhibitor of proteasome activity MG132. Complementary, RNAi

induced CK1α depletion resulted in a substantial reduction of WAVE protein level in larval hemocytes shown by immunoblotting (Publication 2). This was the first evidence of a ubiquitin-proteasomal degradation process, which must be highly regulated to maintain a sufficient protein level and ensure a spatial and temporal control of WAVE activity. An interesting example of this spatiotemporally regulation of WAVE stability was recently described by an interaction between a deubiquitylating module (DUBm) and WAVE in regulating the Arp2/3 complex (Cloud et al., 2019). The DUBm is anchored by Ataxin-7 (Atxn7) to a large complex and is released only temporarily to interact with WAVE and protects it from degradation. Since this interaction with WAVE is not persistent, a constant turnover of WAVE is provided.

Furthermore, it was sought to examine the degradation process. In general, the degradation process is highly regulated and must be protein specific. Once a protein is no longer needed in a cell, for instance due to misfolding or unproper function, it must be removed. As a degradation signal, ubiquitin is covalently attached to the protein. This post-translation modification sets the starting point for a multiple-step process of degradation, which is highly conserved from archaea to eukaryotes. Once ubiquitinylated, the protein to be removed is shuttled to the 26S proteasome, a 2.5 MDa complex (Figure 17). There, selective and ATP-dependent degradation takes place (Finley, 2009; Hershko & Ciechanover, 1998; Lundgren et al., 2005; Saeki, 2017).

In principle, a protein is marked with ubiquitin (Ub), a 76-amino acid protein. The process of ubiquitination involves a sequential action of several enzymes, starting with ubiquitin-activating enzymes (E1), that activate ubiquitin and transfer it to ubiquitin-transferring enzymes (E2). The E2 enzymes then transfer the ubiquitin molecule to the substrate protein, with the help of ubiquitin ligases (E3) (Figure 16, Figure 17) (Komander, 2009; Saeki, 2017).

Protein substrate specificity is mainly determined by E3 ligases, which are highly diverse, with over 600 different E3s in humans (Ketosugbo et al., 2017). They are classified into three main groups based on the properties of the catalytic center responsible for ubiquitin transfer to the substrate: HECT (homologues to the E6AP carboxyl terminus), RING (Really Interesting New Gene), and RBR (RING-between-RING) E3 ligases. RING-type ligases are the

most abundant and are further subdivided into different subtypes, such as cullin-RING ligases. They consist of a Ring-box protein for E2 binding, a cullin as a scaffold, an Adaptor protein, and a substrate receptor. Together, they determine substrate specificity (Figure 16).

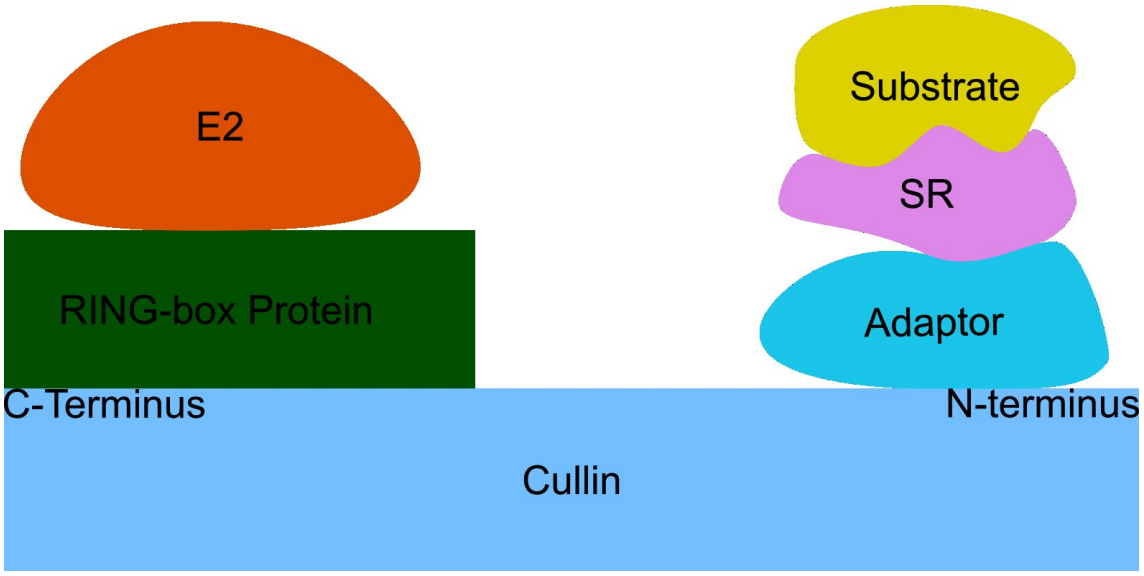

Figure 16 - General composition of the cullin-RING ligase complex, the most abundant type of E3 ligases. *Cullin proteins are scaffold proteins that assemble the cullin-RING ligase complex and thereby brings the substrate in close proximity to the ubiquitin. The C-terminus of a cullin binds the RING-box protein which is linked to the E2 ubiquitin-conjugated enzyme. The N-terminus of a cullin binds to an adaptor protein which in turn is bound to a substrate recognition (SR) protein. Thus, a substrate specificity is given. All together this complex act as an E3 ligase.*

Once a protein is ubiquitinated, it is targeted for degradation by the 26S proteasome, a large multi-subunit complex. The proteasome is composed of two main subunits, a 20S catalytic core and a 19S regulatory complex (Figure 17). The 19S subunit acts as the regulatory unit and is responsible for protein unfolding and activation for degradation, while the 20S subunit is the catalytic core that degrades the protein (Fernández-Cruz et al., 2020). The 20S subunit consists of four heptameric rings composed of seven different alpha subunits and seven different beta subunits arranged in an α7β7β7α7 arrangement. The 19S subunit is composed of six ATPases and four non-ATPases that interact with the alpha subunits of the 20S subunits to transfer the ubiquitinated protein for degradation (Lundgren et al., 2005). The ubiquitin chain is removed from the protein and the substrate protein is then degraded in an ATP-dependent manner. Recent studies have shown that even single ubiquitylation or multiple

short or branched ubiquitin chains can activate protein degradation, and that the size and structural features of the substrate proteins themselves can also affect their recognition and degradation by the proteasome (Matyskiela et al., 2013; Prakash et al., 2004).

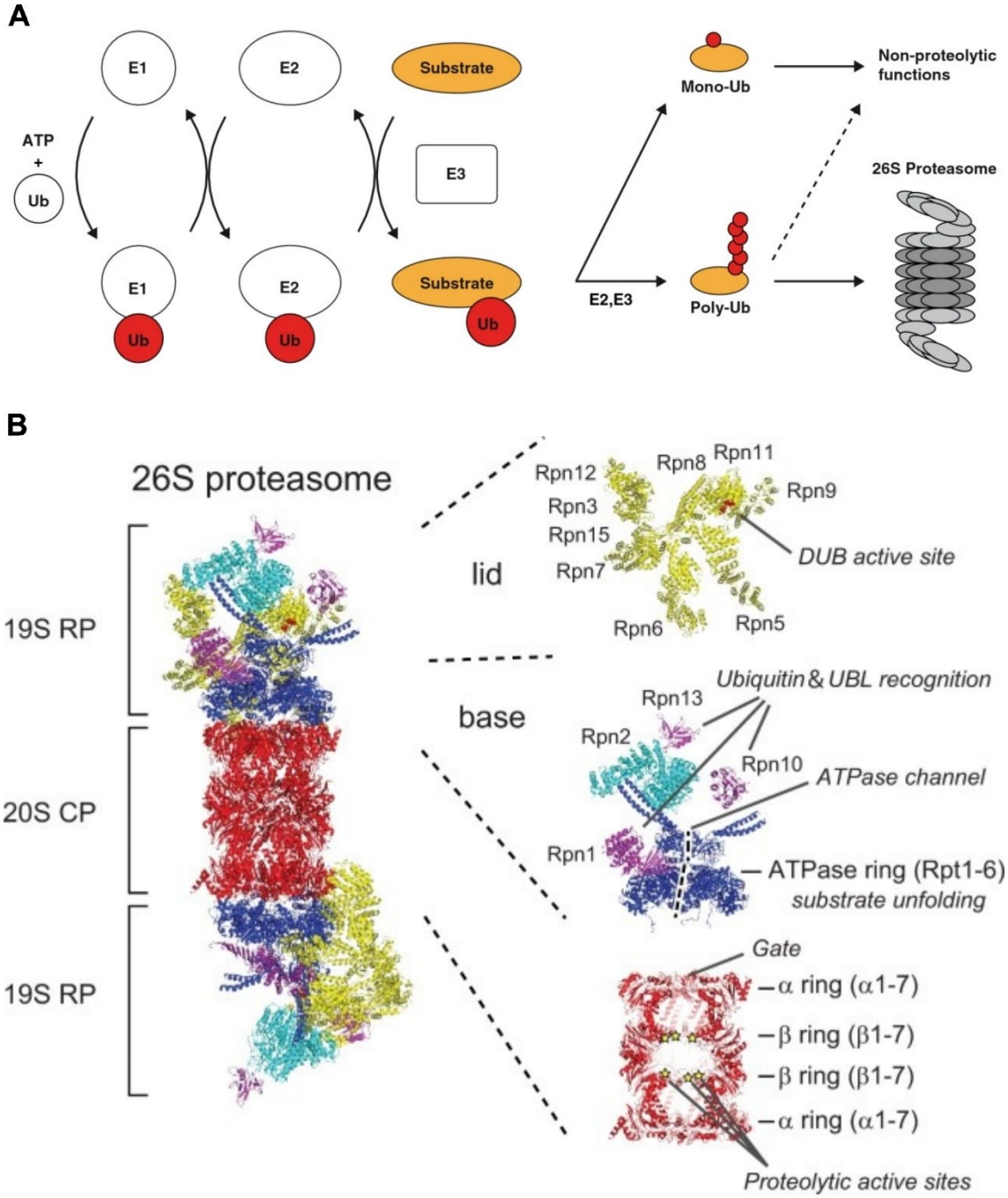

Figure 17 - The ubiquitin proteasome system. *(A) Schematic illustration of the ubiquitin proteasome pathway. The ubiquitin is transferred via E1, E2 and E3 ligases to the substrate, which is supposed to be degraded. Once ubiquitinated, the substrate is shuttled to the 26S Proteasome, where it undergoes proteolytic degradation. Reprinted by permission from Springer Nature Customer Service Centre GmbH* (Sarikas et al., 2011)*. (B) Structure and key subunits of the 26S proteasome. The 26S proteasome is a 2.5 MDa complex and is structurally divided into a 20S catalytic core (CP) and two 19S regulatory complex subunits (RP). The 19 S RP is further divided into a lid and a base, highlighted on the right side. Reprinted from* (Saeki, 2017) *by permission of Oxford University Press.*

As introduced above, protein substrate specificity in the multi-step degradation process is mainly given through the great diversity of different E3 ligases. The most abundant E3 ligases are the cullin-RING E3 ligases. There are six different members of the cullin protein family expressed in the *Drosophila* genome. They serve as a scaffold protein to assemble the multi-subunit cullin-RING E3 ligase (CRL) complex. This complex comprises the main class of the diverse group of known E3 ligases (Sarikas et al., 2011).

The cullin proteins form a substrate-targeting unit and create a distinct substrate specificity by arranging specific proteins (schematic overview see Figure 16). They have also been described as involved in different cellular processes, including actin cytoskeleton remodeling (Ayyub et al., 2015; Yuezhou Chen et al., 2009; Hudson et al., 2015, 2018). Therefore, the cullin proteins were primarily picked to investigate the proteasomal-dependent degradation of WAVE in this work. Indeed, I showed the relevance of Cul2 and Cul3 in the proteasomal degradation process (Publication 2).

Control experiments with RNAi-mediated knockdown of each cullin protein alone support the hypothesis that WAVE stabilization, or in this case abolished degradation, does not lead to enhanced actin polymerization (Publication 2). This suggests that the cell can regulate WAVE turnover independently of a diminished cullin-mediated degradation. Additionally, less WAVE degradation does not result in higher WRC activity. Particularly, an increased availability of WAVE does not necessarily induce the release of the VCA domain, which would initiate enhanced Arp2/3 activity. Depletion by RNAi-knockdown of both CK1α and either Cul2 or Cul3 resembles the evoked phenotype by loss of CK1α phosphorylation (Publication 2). This suggests that CRLs mediate WAVE degradation. However, the exact mechanism of recognition and subsequent ubiquitylation remains unclear. Very little is known so far about the interaction of WAVE with a cullin-adaptor protein-substrate-protein complex.

It is commonly described that ubiquitylation takes place at lysine residues close to the N-terminus. Recently, it has been shown that human WAVE2 undergoes ubiquitylation in a T-cell activation-dependent manner, followed by proteasomal degradation dependent on the VCA domain (Joseph et al., 2017). They proposed that in a resting state, the VCA is sequestered and connects the

components of the WRC with WAVE2, thereby protecting it from degradation. Upon a T-cell-dependent activation, WAVE undergoes a conformational change, releasing the VCA domain and exposing the WAVE WHD domain. Subsequently, WAVE2 undergoes ubiquitylation, which is followed by proteasomal degradation. Specifically, lysine 45 has been described to be the main WAVE2 ubiquitylation site, which is a highly conserved residue within the WHD domain (Joseph et al., 2017).

Rescue experiments with a WAVE^{K48R} mutant performed in this work further point out that the lysine residue in position 48, which is the corresponding lysine residue of *Drosophila* WAVE, is not the main WAVE ubiquitylation site in *Drosophila*. Mutation of a lysine to arginine is a commonly used mutation to investigate the ubiquitylation site. Expression was proven in the wing imaginal disc using the *en*-Gal4 driver determined by F-actin induction (Figure 11, comparable to Publication 2). Immunostaining with an anti-WAVE antibody clearly shows overexpression of WAVE. However, no changes in the cell shape of larval hemocytes were observed in rescue experiments performed in the same way as it has been done with knockdown of each cullin protein (Figure 11, Publication 2). Thus, this suggests that even more ubiquitin target sites are responsible for proteasomal degradation. Supplementary table 1 summarizes putative lysine residues obtained by a computer-based prediction tool.

The exact mechanism underlying the ubiquitylation is still an open question. Even though Joseph and colleagues uncovered that lysine 45 of the human WAVE2 is ubiquitylated, lysine 48 of the fruit fly WAVE has not been successfully determined as the target residue that is essential for ubiquitin-mediated degradation in this work (Figure 11). Interestingly, in a different study, lysine 220 of WASH has been discovered as a target for K63-linked ubiquitination (Hao et al., 2013). This, in turn, leads to exposure of the C-terminal VCA domain, activates the WASH complex, and is subsequently required for endosomal F-actin nucleation and retrograde transport. Jia and colleagues have recognized a high similarity between the WRC and the WASH complex (D. Jia et al., 2010). The WASH lysine 220 exists in a region similar to the meander region of the WRC. As mentioned before, this region is subject to regulation by phosphorylation and controls interaction with the Arp2/3 complex

(Hao et al., 2013). Moreover, using computer-based prediction tools, different lysine residues appear to be more likely ubiquitin targets (Supplementary Table 1). Interestingly lysine 48 of the *Drosophila* WAVE and lysine 45 of the human WAVE do not show confidence with a relatively low prediction score only of 0.79. In contrast, the lysine 200 of *Drosophila* WAVE, which is comparable to the WASH lysine 220, has a score of 3.21 (Supplementary Table 1) (A. Li et al., 2006; Xue et al., 2006). Additionally, Joseph and colleagues pointed out that the mutation of lysine 45 did not completely abolish ubiquitylation, which raises the question if there are further potential lysine residues or ubiquitylation sites in proximity (Joseph et al., 2017). For instance, the same group discovered that activated WASP is ubiquitylated simultaneously on lysine residues 76 and 81 and afterward degraded (Reicher et al., 2012). As mentioned earlier, it must be considered that different ways of ubiquitylation are possible. For this reason, a poly-ubiquitylation on different lysine residues might be indispensable for correct degradation. Further experiments with point mutations of different putative lysine residues will reveal their importance.

Remarkably, there is much evidence that phosphorylation is a key modification for substrate recognition. However, it has been thought for a long time that substrates are only recognized if they are phosphorylated. Recently, it was considered that interaction with CRLs might additionally be influenced by dephosphorylation (Yifan Chen et al., 2021). For example, SPOP is a substrate of the cullin-Ring-ligase 3 that needs to be unphosphorylated for recognition and ubiquitylation (Harper & Schulman, 2021; Q. Zhang et al., 2009). Moreover, they proposed that proteins with S/T rich motifs, called destruction signal (Degron), such as the transcription factor Ci, are recognized by BTB proteins that function as target-recognition components of the cullin-based ligases. Worth to notice is that in this case, phosphorylation might be a negative regulator (which protects the target protein) and this in turn protects Ci from binding to the Cul3-based Ub ligase (Q. Zhang et al., 2009).

To sum up, I pointed out that WAVE is protected from degradation by a basal phosphorylation through CK1α. Proteasomal degradation is mediated by Cul2 and Cul3, and the lysine residue on position 48 is not sufficient as the sole ubiquitylation target. Since the CRLs are part of many cascades for establishing

a sufficient ubiquitylation-dependent protein turnover, the exact mechanism for WAVE degradation needs to be investigated.

4.12. Phosphorylation of the WAVE VCA Domain by CK1α is essential for its function and promotes its stability

In general, phosphorylation plays an important role in activating and stabilizing the WRC. However, until recently, research mostly relied on *in vitro* investigations. Many different kinases, such as Abl, Src, Cdk5, Erk and CK2 are thought to interact with the WRC (Ardern et al., 2006; Danson et al., 2007; Kim et al., 2006; Mendoza, 2013; Nakanishi et al., 2006; Pocha & Cory, 2009; Sossey-Alaoui et al., 2007). Thereby, the main proposed target region is the meander region, which upon phosphorylation, destabilizes the sequestering of the VCA domain to evoke WRC activation (Rottner et al., 2021). Over the last years, phosphorylation of the VCA domain has been subject of different investigations. Somewhat confounding, different publications concluded that phosphorylation of the VCA domain is crucial for the binding affinity and activation of the Arp2/3 complex. However, a clear mechanism *in vivo* remains unclear.

As mentioned in the introduction, the current understanding is that the serine residues of the VCA domain are targets of CK2 phosphorylation which mediates the affinity to the Arp2/3 complex for actin polymerization (Pocha & Cory, 2009; Ura et al., 2012). For instance, Pocha and Cory proposed that CK2 phosphorylates mammalian WAVE2 at positions 482, 484, 488, 489 and 497 within the acidic domain, subsequently regulating the Arp2/3 complex activity *in vitro.* However, those results are limited by various factors. For instance, they did not completely abolish endogenous wild-type protein in rescue experiments with overexpression of phosphorylation-deficient mutants in cultured NIH-3T3 cells. Moreover, their experiments were performed independently of the regulatory multiprotein complex (Pocha & Cory, 2009).

In some way opposing to those results, it has been shown in a more recent study that regulated dephosphorylation is the key step in WAVE activation during pseudopod dynamics (Ura et al., 2012). It was thought that

phosphorylation maintains an inhibited closed state rather than an activated state (Singh & Insall, 2021). With the results of my work, I broadened the spectrum and complexity of phosphorylation-dependent regulation of WAVE, which seems contrary to the previously described results in several points (Publication 2).

The first contradiction is that CK2 was originally described as regulating WAVE. Albeit the fact that both CK1α and CK2 share a similar target sequence, I determined a main regulatory role for CK1α (Publication 2). This is not in contrast to the previous results; it rather expands the knowledge of the regulation. Indeed, CK1α recognition and activity are enhanced by already phosphorylated serine residues N-terminal to the target sequence (Flotow et al., 1990). As shown in other cases, this can be provided by CK2 or other compensating kinases. This may also explain that *in vivo* loss-of CK2 function does not lead to an altered cell morphology. This resembles a hierarchical mechanism of the phosphorylation process as a post-translation step, which has already been described for both kinases in a different background (Flotow et al., 1990)

Secondly, the significance of phosphorylation of the VCA Domain has been demonstrated in this work using the *Drosophila* wing imaginal disc as an *in vivo* model (Publication 2). A mutated version of WAVE, which mimics a phosphorylation state (WAVE-SD^{5x}), induces F-actin in epithelial cells and enhances the actin level similar to the overexpression of WAVE-WT. The observation that the WAVE-SD^{5x} variant additionally increases the WAVE protein level drastically, indicates that phosphorylation of the VCA domain is essential for WAVE stability rather than for its activity. Thus, an increase in stabilization does not subsequently lead to an increase in actin polymerization. Noticeably, the un-phosphorylatable version of WAVE (WAVE-SA^{5x}) does not show the same increase in F-actin polymerization, although the WAVE protein level is similar to WAVE-WT. This also points out that overexpressed WAVE-WT still undergoes a regulation. Particularly, the WAVE protein level is kept in a sufficient amount and a constant turnover is still given. In contrast, the continuous phosphorylated WAVE is not degraded and is thus more stable, but not more active (Publication 2). Furthermore, it was shown that persistent

overaction of the WRC and the Arp2/3 complex subsequently favors its proteasomal degradation (Law et al., 2021).

Taking this into account, it also suggests that phosphorylation prevents it from degradation. Phosphorylation is indispensable for activity but does not enhance it. Correspondingly induced expression of full-length CK1α in *Drosophila* S2 cells did neither induce a mobility shift of endogenous WAVE nor significantly increase the WAVE protein abundance. However, overexpression *in vivo* in the wing imaginal disc showed a slight increase in WAVE protein level (Figure 12). Accordingly, the F-Actin level was also slightly increased compared to the EGFP control, however, it did not resemble the enhanced F-actin polymerization through overexpression of WAVE-WT (Figure 12 D-E). This, again, highlights the diversity and complexity of WAVE regulation. It can be hypothesized that the WAVE amount undergo a constant regulation. Even though the possibility is given that for constant phosphorylation by overexpression of the kinase the activity is limited and maybe the turnover, i.e. the degradation, is accelerated. It can also be suggested that the basal phosphorylation level is already sufficient for maintaining physiological actin dynamics and kinase activity is regulated even in an overexpression situation. To keep in mind, even the WT overexpression seems to be subject to tight regulation.

Rescue experiments performed in this study with a *wave* null mutant furthermore revealed the importance of phosphorylation of the VCA domain (Publication 2). Only the phosphomimetic WAVE-SD^{5x} mutant and not the phosphodeficient SA^{5x} mutant could fully rescue lethality, changes in cell morphology as well as disrupted migration behavior evoked by WAVE loss-of-function. On the other hand, both N-terminal mutants, the phosphodeficient SA^{3x} as well as the phosphomimetic SD^{3x} fully rescued the lethality and defects in lamellipodia formation of *wave* mutants (Publication 2). Thus, the N-terminal SLS motif is indispensable for WAVE function. Remarkably, disruption of the lamellipodia by knockdown of CK1α was not rescued by co-expressing WAVE-WT, but WAVE-SD^{5x} (Publication 2). This clarifies again a substrate specificity of these five serine within the VCA domain to CK1α. Obviously, no other kinase can compensate for the loss of phosphorylation in CK1α RNAi-depleted cells.

Conclusively, this contrasts the previously described CK2-mediated phosphorylation of the VCA domain (Pocha & Cory, 2009).

To further point out the diversity and complexity of WAVE regulation, it is of further interest that even though different kinases have proven to interact with WAVE, a defined role was determined for each kinase. For instance, a knockdown of Protein Kinase A (PKA) also abolishes WAVE expression (Yamashita et al., 2011). However, in case of the PKA-WAVE interaction, it must be noticed that this exclusively happens at the cell membrane. In their model, WAVE recruits the kinase to the membrane. This, in turn, induces the accumulation of PIP_3, leading to a further enrichment of WAVE. This leads to an important aspect of regulation, i.e. both proteins must be located correctly (Knippschild et al., 2005).

For sure, it is of advantage when a kinase and its substrate are equally distributed in time and space. Kinase activity is favored if both proteins are in close contact with each other. Many times, it has been shown that WAVE incorporated in the WRC locates at the leading edge of a cell (revied in Rottner et al., 2021). This for sure is required for a proper function and a rapid regulation of the actin dynamics within the lamellipodium.

However, it is well established that CK1α does normally not localize to the membrane. CK1α is usually active in the cytosol and nucleus (Gross & Anderson, 1998; Santos et al., 1996; J. Zhang et al., 1996). This might underline the fact that WAVE needs to be basally phosphorylated already as a post-translation step before its recruitment to the membrane.

It should also be considered that the assembly of the WRC is a multi-step process with all members tightly regulated and important for an intact and fully assembled complex (Figure 8). Although the exact process remains unclear and is still a remarkably open question, *in vitro* biochemical und structural analysis started to shed light on the underlying mechanism (Kramer et al., 2022; Rottner et al., 2021). For instance, for the WASH complex, which goes through an analogous multi-step assembly procedure as the WRC, it has been shown that the first steps of complex assembling occur at the centrosome (Fokin & Gautreau, 2021). For the WRC, it has only been assumed that the complex

assembly starts similarly. It is known that the association of Abi and WAVE is one of the first steps in the assembly procedure. This is mediated at the centrosome by HSPC300 (also known as BRICK1), which associates with single molecules of Abi and WAVE through a heterotrimeric coiled-coil (Fokin & Gautreau, 2021). Coordinated regulation of these proteins only achieves correct association. This leads to the suggestion that WAVE is already highly regulated by post-translation modifications at the centrosome, where complex assembly starts. That is why it can be hypothesized that phosphorylation by CK1α is already important at the centrosome and not later when the WRC is already recruited to the plasma membrane. Importantly, CK1α has already been described to be associated with the centrosome (Brockman et al., 1992). Though this raises the question whether CK1α phosphorylates WAVE as a first step before the WRC assembly at the centrosome. Regarding the argument that CK1α mediated phosphorylation rather stabilizes the protein than enhances the activity, it can be hypothesized that the interaction takes place before complex assembly. Proteasomal degradation is often initiated at the centrosome (Fokin & Gautreau, 2021; Johnston et al., 1998; Kopito, 2000). Misfolded or incompletely phosphorylated proteins are therefore accumulated around the centrosome. However, it needs to be further addressed if WAVE degradation by CK1α depletion influences the stability of another complex member or subsequently of the whole complex.

Finally, an interesting indication of the essential role of WAVE phosphorylation in actin dynamics not only at the leading edge was shown by Danson and colleagues. They revealed that phosphorylation of WAVE by MAP-Kinase regulates the polarization of the Golgi apparatus (Danson et al., 2007). Disruption of the Golgi apparatus likewise leads to an improper Rac-dependent lamellipodium formation, which is a crucial aspect of cell motility (Danson et al., 2007).

Conclusively, the results of this study imply that WAVE is basally phosphorylated and that a constitutively phosphorylated version of WAVE ($WAVE^{SD5x}$) enhances its stability by protecting it from degradation. Additionally, further phosphorylation of the VCA by CK1α does not appear and is unnecessary for an enhanced Arp2/3 activity (Imaginal Disc, F-actin induction,

Figure 12). Nevertheless, phosphorylation of the five selected serine residues within the VCA domain is indispensable for WAVE activity. However, CK1α is only one of many potential regulators of WAVE activity. The exact mechanism and the interplay between different phosphorylation and dephosphorylation events remain elusive. Moreover, taking all studies of different kinases in the context of WRC activation together led to the conclusion that no kinase can compensate for another.

4.13. CK2 regulates blood cell differentiation rather than cell shape

For a long time, it was suggested that CK2 regulates the activity and stability of the WRC by phosphorylation (Mendoza, 2013; Pocha & Cory, 2009). Results of this study uncovered that CK1α and not CK2 is an important regulator of WAVE function *in vivo*. *Ck2* mutant hemocytes, which lack CK2 kinase activity, form normal lamellipodia but show increased lamellocyte differentiation (Publication 2). This subgroup of blood cells is commonly not seen in healthy flies and is upregulated upon parasitism infestation. They can be recognized by the expression of the surface protein Atilla and ßPS-integrin (Anderl et al., 2016). Furthermore, they can be genetically induced by knockdown of *Ush*, which in turn increases the number of lamellocytes (Fossett et al., 2001; Gajewski et al., 2007). As mentioned before, Ush interacts with the dNuRD complex by binding to the subunit dMi-2. Interestingly, the Ush/dNuRD complex regulates a broad spectrum of genes in both ways, promoting and repressing (Lenz et al., 2021). For instance, a repression of the crystal cell-specific transcription factor complex core factor protein Lz was determined (Muratoglu et al., 2007).

Additionally, a previous study independently revealed dMi-2 as a target of CK2 phosphorylation which in turn regulates nucleosome remodeling activity (Bouazoune & Brehm, 2005). In this case, dephosphorylated dMi-2 shows increased nucleosome binding and activity. This led to the assumption that there might be a genetic correlation between CK2 and the activity of the dNuRD complex.

Results of this work show that an RNAi-mediated knockdown of *dMi-2* in *Drosophila* hemocytes does not induce lamellocyte transdifferentiation (Figure 13). This suggests no impact of dMi-2 downregulation on the interaction of Ush and dNuRD and is in line with previous results of trans-heterozygous dMi-2 mutants, which does not enhance lamellocyte transdifferentiation (Lenz et al., 2021). Since dMi-2 and Ush co-occupy many sites of the chromatin, Ush acts as a suppressor of lamellocyte differentiation and the abolishing phosphorylation of dMi-2 enhances its activity, it can be suggested that this subsequently suppresses Ush interaction leading to forced lamellocyte differentiation.

Taking this into account, phosphorylation is an important post-translation modification to regulate the complex integrity. Accordingly, CK2 might be a crucial regulator of lamellocyte differentiation by phosphorylation of dMi-2, which restrain its enzymatic activity. This in turn affects the NuRD complex binding and enables regular Ush activity (Figure 18).

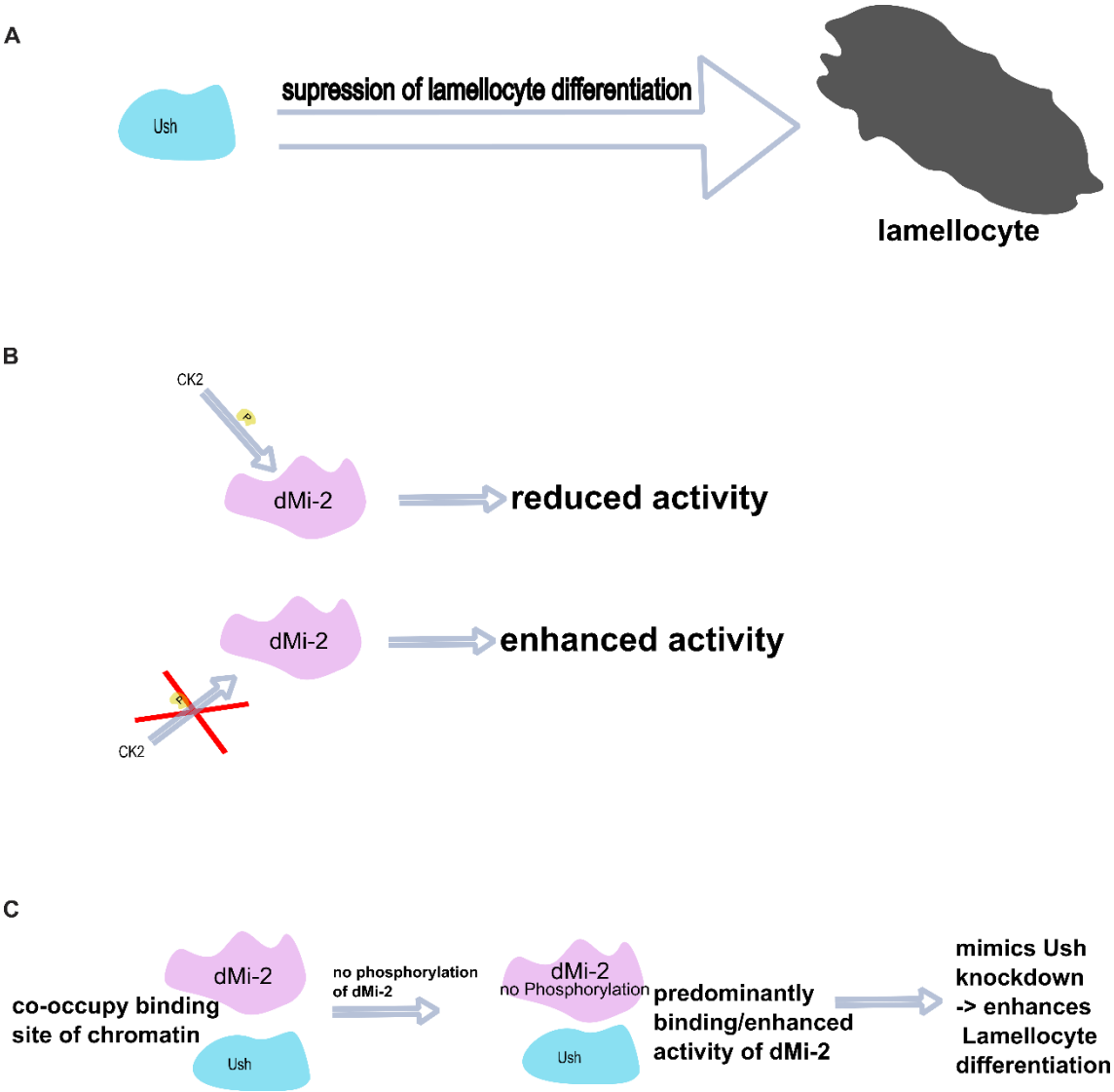

Figure 18 – Schematic overview of Ush and dMi-2 interaction. *(A) Ush suppresses lamellocyte differentiation as a cofactor. (B) Phosphorylation of dMi-2 by CK2 leads to a reduced dMi-2 activity. Without phosphorylation dMi-2 is more active. (C) dMi-2 and Ush co-occupy for binding sites of chromatin. Without phosphorylation, dMi2- binding is favored over Ush binding. This mimics a reduced Ush binding activity which leads to enhanced lamellocyte differentiation.*

5. Conclusion and Outlook

In this work, it was demonstrated that *Drosophila* serves as a powerful *in vivo* model organism to study actin dynamics, cell shape regulation, hematopoiesis, and blood cell differentiation.

With the advances of single cell RNA sequencing, we identified the heterogeneity of *Drosophila* pupal blood cells, which were so far believed to be a homogenous group. Despite the differences in the details of hematopoiesis between flies and vertebrates, many of the cellular mechanisms underlying blood cell development and function are conserved. This makes *Drosophila* an irreplaceable powerful tool for further research as many of the basic pathways and processes of *Drosophila* hematopoietic progenitors and their niche are conserved and therefore similar in vertebrates. Thus, a similar heterogeneity among vertebrate blood cells modulated by developmental stage and immune challenges can be further investigated in *Drosophila*. The dataset of this work reveals the presence of already described embryonic derived mixed with lymph gland derived blood cells, as well as previously undescribed effector cell types. Those subgroups mainly reflect the physiological changes with the onset of metamorphosis and persist into adulthood. Remarkably, the dataset clearly discriminates between undifferentiated *srp*-high expressing plasmatocytes and immune-active plasmatocyte populations. This outlines the diversity in functions of either the innate immune system like antimicrobial peptide production, formation of adhesion structures, cellular junctions and fatty acid β-oxidation or endocytic and phagocytic processes that come along with the onset of pupal development.

Results of this work enable the future application of Gal4-enhancer traps and GFP-exon traps for distinct marker genes to determine how hematopoiesis and immune response are regulated in a different environment like an induced immune challenge or starvation. This could be, for instance, the relationship between immune response and metabolic shift as well as mechanisms behind the mammalian emergency hematopoiesis, as they are so far poorly understood. Likewise, it could reveal if any of the subpopulation still have the potential to further differentiate or switch their characteristics to effector cells.

In addition to the plasmatocyte subpopulations with their specific roles in the common immune functions combined with an adaptive metabolism, the dataset uncovers a small group of immune cells which resembles cells from the PSC niche. After lymph gland disintegration, those cells show high motility and immune response. Furthermore, lineage tracing revealed their ability to differentiate into lamellocytes upon wasp infestation. This leads to the question about the role of niche like cells beyond the maintenance of progenitors. It is of further interest if those cells might have different functions in the pupal and adult immune response compared to mature plasmatocytes.

What intrinsic signaling pathways lead to the differentiation of PSC cells to lamellocytes? Since lamellocytes derived from PSC cells are barely present in the larval state, do they have a distinct feature in the pupal state? The use of the versatile tools of *Drosophila* genetic manipulation would reveal, for instance whether the EGFR pathway act in parallel to the Toll/NFκB pathway to initiate PSC cell differentiation besides the lymph gland progenitors.

Furthermore, bulk RNAseq of this subgroup, best sorted by a distinct marker like *tau*, will gain more insight into the molecular signature. Since they show a small spiky cell morphology, a detailed expression profile would uncover the regulation of actin cytoskeleton genes. For instance, fascin has been shown to be upregulated in cancer cells that use filopodia for migration. We uncovered that PSC cells perform a comparable filopodia based migration. So far, there is less known why PSC cells do not use lamellipodia based motility, as this is normally the predominantly way. Studying the effects of tissue specific gene knockdown of various actin regulators might determine changes in PSC cell shape. Additionally, this could be a powerful tool to investigate more details about how the signaling mechanisms are regulated. Remarkably, niche function has been connected to cancer studies as they show conserved functions.

In addition to their role in encapsulating parasitic wasp eggs, recent studies have suggested that lamellocytes may also have other functions in the immune system of *Drosophila*. For example, they have been shown to be capable of phagocytosing both microbial and self-tissue debris, suggesting that they may play a broader role in the clearance of cellular waste. Overall, lamellocytes are a fascinating and important cell type in the immune system of *Drosophila*

melanogaster, and their study is shedding new light on the mechanisms underlying host-parasite interactions and cellular immune responses.

Another point is that so far, TEP4 has not been explored as a marker for lamellocytes. Though Dstálová and colleagues proposed a role of TEP4 in response to wasp infestation, they did neither clarify the importance nor show *ex vivo* images of TEP4 marked cells. The pluripotent role of TEP4 outlines its indispensable role in both the innate immune response and hematopoiesis. Now, with the results of this work, the role of TEP4 can be additionally described as a marker for lamellocytes. *In vivo* investigations of TEP mutant flies will outline the role of TEP-positive cells depending on external immune challenges.

TEP4 is also a marker gene of the Secretory-PL cluster together with several other serine proteases. Since a distinct function could not be clearly distinguished, it will be of further interest to dissect the role of the serine proteases upregulated in this cluster in the innate immune response. Although serine proteases involved in regulating melanization and Toll signaling pathways processes have been already elucidated (Dudzic et al., 2019; Shichao Yu et al., 2022), it is still unclear whether the activation is further regulated by distinct serine protease cascades. This opens the question if the Secretory-PL serine proteases are involved in either activation of crystal cells, through induction of PPO activity, or in another activation cascade. Since this cluster is not present in early developmental stages, their specific role in the onset of metamorphosis should be addressed. Does this cluster represent an activator subpopulation?

The ability to migrate and phagocytose is indispensable for immune cells. This is provided through the dynamic ability to reorganize the actin cytoskeleton. Here, I outlined that CK1α phosphorylation protects the NPF WAVE from degradation and thus enables the promoting of actin branching by Arp2/3. However, the exact mechanism of WAVE degradation is still unclear. Because the lysine residue at position 45 of WAVE is not the only target of ubiquitylation, as a first step online prediction tools could forecast more putative lysine residues. Afterwards, site direct mutagenesis combined with rescue experiments could characterize the lysine residue dependency for ubiquitin

recognition. Clarifying the degradation process would provide an efficient tool in mammals to prevent the cell from undesirable actin nucleation. This in turn has been described to favor chronic inflammatory responses induced by unfavorable activation of T cells (Joseph et al., 2017). Furthermore, it still remains unclear at which time point CK1α phosphorylation occurs. One hypothesis is that WAVE is phosphorylated already during the assembly process. However, it was proposed recently, that phosphorylation only occurs following activation (Singh & Insall, 2021). Thus, it might be used as a readout of complex activation.

Besides this novel role of CK1α, I identified an unknown role for CK2, another member of the casein kinase family, in blood cell differentiation. Accordingly, previous data showed that constitutive phosphorylation of the chromatin remodeling enzyme dMi2 by CK2 affects its nucleosome binding activity, however the importance is still unclear (Bouazoune & Brehm, 2005). Generally, dMi2 and Ush compete for many binding sites. Moreover, phosphorylation of dMi2 leads to downregulation of its activity and thus a preferred binding of Ush to regulation sites. This in turn abolishes lamellocyte differentiation. It would be of further interest to dissect the interaction of CK2 and dMi2 in controlling transdifferentiation. Using the versatile advances of *Drosophila* gene manipulation, experiments with dMi2 and CK2 double mutant flies could outline dependency of CK2 phosphorylation.

6. References

Akhshi, T. K., Wernike, D., & Piekny, A. (2014). Microtubules and actin crosstalk in cell migration and division. *Cytoskeleton*, *71*(1), 1–23. https://doi.org/10.1002/cm.21150

Alekhina, O., Burstein, E., & Billadeau, D. D. (2017). Cellular functions of WASP family proteins at a glance. *Journal of Cell Science*. https://doi.org/10.1242/jcs.199570

Alfonso, T. B., & Jones, B. W. (2002). gcm2 Promotes Glial Cell Differentiation and Is Required with glial cells missing for Macrophage Development in Drosophila. *Developmental Biology*, *248*(2), 369–383. https://doi.org/10.1006/dbio.2002.0740

Anderl, I., Vesala, L., Ihalainen, T. O., Vanha-aho, L.-M., Andó, I., Rämet, M., & Hultmark, D. (2016). Transdifferentiation and Proliferation in Two Distinct Hemocyte Lineages in Drosophila melanogaster Larvae after Wasp Infection. *PLOS Pathogens*, *12*(7), e1005746. https://doi.org/10.1371/journal.ppat.1005746

Antón, I. M., Jones, G. E., Wandosell, F., Geha, R., & Ramesh, N. (2007). WASP-interacting protein (WIP): working in polymerisation and much more. *Trends in Cell Biology*, *17*(11), 555–562. https://doi.org/10.1016/j.tcb.2007.08.005

Ardern, H., Sandilands, E., Machesky, L. M., Timpson, P., Frame, M. C., & Brunton, V. G. (2006). Src-dependent phosphorylation of Scar1 promotes its association with the Arp2/3 complex. *Cell Motility and the Cytoskeleton*, *63*(1), 6–13. https://doi.org/10.1002/cm.20101

Ayyaz, A., Giammarinaro, P., Liégeois, S., Lestradet, M., & Ferrandon, D. (2013). A negative role for MyD88 in the resistance to starvation as revealed in an intestinal infection of Drosophila melanogaster with the Gram-positive bacterium Staphylococcus xylosus. *Immunobiology*, *218*(4), 635–644. https://doi.org/10.1016/j.imbio.2012.07.027

Ayyub, C., Banerjee, K. K., & Joti, P. (2015). Reduction of Cullin-2 in somatic cells disrupts differentiation of germline stem cells in the Drosophila ovary.

Developmental Biology, *405*(2), 269–279. https://doi.org/10.1016/j.ydbio.2015.07.019

Baer, M. M., Bilstein, A., Caussinus, E., Csiszar, A., Affolter, M., & Leptin, M. (2010). The role of apoptosis in shaping the tracheal system in the Drosophila embryo. *Mechanisms of Development*, *127*(1–2), 28–35. https://doi.org/10.1016/j.mod.2009.11.003

Bandyopadhyay, M., Arbet, S., Bishop, C., & Bidwai, A. (2016). Drosophila Protein Kinase CK2: Genetics, Regulatory Complexity and Emerging Roles during Development. *Pharmaceuticals*, *10*(4), 4. https://doi.org/10.3390/ph10010004

Banerjee, U., Girard, J. R., Goins, L. M., & Spratford, C. M. (2019). Drosophila as a Genetic Model for Hematopoiesis. *Genetics*, *211*(2), 367–417. https://doi.org/10.1534/genetics.118.300223

Basset, A., Khush, R. S., Braun, A., Gardan, L., Boccard, F., Hoffmann, J. A., & Lemaitre, B. (2000). The phytopathogenic bacteria Erwinia carotovora infects Drosophila and activates an immune response. *Proceedings of the National Academy of Sciences*, *97*(7), 3376–3381. https://doi.org/10.1073/pnas.97.7.3376

Bear, J. E., Rawls, J. F., & Saxe, C. L. (1998). SCAR, a WASP-related protein, isolated as a suppressor of receptor defects in late Dictyostelium development. *Journal of Cell Biology*, *142*(5), 1325–1335. https://doi.org/10.1083/jcb.142.5.1325

Benmimoun, B., Polesello, C., Haenlin, M., & Waltzer, L. (2015). The EBF transcription factor Collier directly promotes Drosophila blood cell progenitor maintenance independently of the niche. *Proceedings of the National Academy of Sciences*, *112*(29), 9052–9057. https://doi.org/10.1073/pnas.1423967112

Bergman, P., Seyedoleslami Esfahani, S., & Engström, Y. (2017). Drosophila as a Model for Human Diseases—Focus on Innate Immunity in Barrier Epithelia. *Current Topics in Developmental Biology*, *121*, 29–81. https://doi.org/10.1016/bs.ctdb.2016.07.002

Bidla, G., Dushay, M. S., & Theopold, U. (2007). Crystal cell rupture after injury in Drosophila requires the JNK pathway, small GTPases and the TNF homolog Eiger. *Journal of Cell Science*, *120*(7), 1209–1215. https://doi.org/10.1242/jcs.03420

Binggeli, O., Neyen, C., Poidevin, M., & Lemaitre, B. (2014). Prophenoloxidase Activation Is Required for Survival to Microbial Infections in Drosophila. *PLoS Pathogens*, *10*(5), e1004067. https://doi.org/10.1371/journal.ppat.1004067

Bischof, J., Maeda, R. K., Hediger, M., Karch, F., & Basler, K. (2007). An optimized transgenesis system for Drosophila using germ-line-specific C31 integrases. *Proceedings of the National Academy of Sciences*, *104*(9), 3312–3317. https://doi.org/10.1073/pnas.0611511104

Bischoff, M. C., Lieb, S., Renkawitz-Pohl, R., & Bogdan, S. (2021). Filopodia-based contact stimulation of cell migration drives tissue morphogenesis. *Nature Communications*, *12*(1), 1–18. https://doi.org/10.1038/s41467-020-20362-2

Bisi, S., Disanza, A., Malinverno, C., Frittoli, E., Palamidessi, A., & Scita, G. (2013). Membrane and actin dynamics interplay at lamellipodia leading edge. *Current Opinion in Cell Biology*, *25*(5), 565–573. https://doi.org/10.1016/j.ceb.2013.04.001

Blanchoin, L., Boujemaa-Paterski, R., Sykes, C., & Plastino, J. (2014). Actin dynamics, architecture, and mechanics in cell motility. *Physiological Reviews*, *94*(1), 235–263. https://doi.org/10.1152/physrev.00018.2013

Bogdan, S., & Klämbt, C. (2003). Kette regulates actin dynamics and genetically interacts with Wave and Wasp. *Development*, *130*(18), 4427–4437. https://doi.org/10.1242/dev.00663

Bou Aoun, R., Hetru, C., Troxler, L., Doucet, D., Ferrandon, D., & Matt, N. (2011). Analysis of thioester-containing proteins during the innate immune response of Drosophila melanogaster. *Journal of Innate Immunity*, *3*(1), 52–64. https://doi.org/10.1159/000321554

Bouazoune, K., & Brehm, A. (2005). dMi-2 chromatin binding and remodeling

activities are regulated by dCK2 phosphorylation. *Journal of Biological Chemistry*, *280*(51), 41912–41920. https://doi.org/10.1074/jbc.M507084200

Boulet, M., Renaud, Y., Lapraz, F., Benmimoun, B., Vandel, L., & Waltzer, L. (2021). Characterization of the Drosophila Adult Hematopoietic System Reveals a Rare Cell Population With Differentiation and Proliferation Potential. *Frontiers in Cell and Developmental Biology*, *9*. https://doi.org/10.3389/fcell.2021.739357

Bretscher, A. J., Honti, V., Binggeli, O., Burri, O., Poidevin, M., Kurucz, E., Zsamboki, J., Ando, I., & Lemaitre, B. (2015). The Nimrod transmembrane receptor Eater is required for hemocyte attachment to the sessile compartment in Drosophila melanogaster. *Biology Open*, *4*(3), 355–363. https://doi.org/10.1242/bio.201410595

Brinkmann, K., Winterhoff, M., Önel, S.-F., Schultz, J., Faix, J., & Bogdan, S. (2015). WHAMY is a novel actin polymerase promoting myoblast fusion, macrophage cell motility and sensory organ development. *Journal of Cell Science*. https://doi.org/10.1242/jcs.179325

Brockman, J. L., Gross, S. D., Sussman, M. R., & Anderson, R. A. (1992). Cell cycle-dependent localization of casein kinase I to mitotic spindles. *Proceedings of the National Academy of Sciences*, *89*(20), 9454–9458. https://doi.org/10.1073/pnas.89.20.9454

Brooks, S P. (2004). Identification of the gene for Nance-Horan syndrome (NHS). *Journal of Medical Genetics*, *41*(10), 768–771. https://doi.org/10.1136/jmg.2004.022517

Brooks, Simon P., Coccia, M., Tang, H. R., Kanuga, N., Machesky, L. M., Bailly, M., Cheetham, M. E., & Hardcastle, A. J. (2010). The Nance-Horan syndrome protein encodes a functional WAVE homology domain (WHD) and is important for co-ordinating actin remodelling and maintaining cell morphology. *Human Molecular Genetics*, *19*(12), 2421–2432. https://doi.org/10.1093/hmg/ddq125

Buchon, N., Silverman, N., & Cherry, S. (2014). Immunity in Drosophila melanogaster-from microbial recognition to whole-organism physiology.

Nature Reviews Immunology, *14*(12), 796–810. https://doi.org/10.1038/nri3763

Buracco, S., Singh, S., Claydon, S., Paschke, P., Tweedy, L., Whitelaw, J., McGarry, L., Thomason, P. A., & Insall, R. H. (2022). The Scar/WAVE complex drives normal actin protrusions without the Arp2/3 complex, but proline-rich domains are required. *BioRxiv*, 2022.05.14.491902. https://www.biorxiv.org/content/10.1101/2022.05.14.491902v1%0Ahttps://www.biorxiv.org/content/10.1101/2022.05.14.491902v1.abstract

Campellone, K. G., Cheng, H. C., Robbins, D., Siripala, A. D., McGhie, E. J., Hayward, R. D., Welch, M. D., Rosen, M. K., Koronakis, V., & Leong, J. M. (2008). Repetitive N-WASP-binding elements of the enterohemorrhagic Escherichia coli effector EspFU synergistically activate actin assembly. *PLoS Pathogens*, *4*(10). https://doi.org/10.1371/journal.ppat.1000191

Campellone, K. G., & Welch, M. D. (2010). A nucleator arms race: cellular control of actin assembly. *Nature Reviews Molecular Cell Biology*, *11*(4), 237–251. https://doi.org/10.1038/nrm2867

Caria, S., Magtoto, C. M., Samiei, T., Portela, M., Lim, K. Y. B., How, J. Y., Stewart, B. Z., Humbert, P. O., Richardson, H. E., & Kvansakul, M. (2018). Drosophila melanogaster Guk-holder interacts with the Scribbled PDZ1 domain and regulates epithelial development with Scribbled and Discs Large. *Journal of Biological Chemistry*, *293*(12), 4519–4531. https://doi.org/10.1074/jbc.M117.817528

Cattenoz, P. B., Monticelli, S., Pavlidaki, A., & Giangrande, A. (2021). Toward a Consensus in the Repertoire of Hemocytes Identified in Drosophila. *Frontiers in Cell and Developmental Biology*, *9*(March), 1–14. https://doi.org/10.3389/fcell.2021.643712

Cattenoz, P. B., Sakr, R., Pavlidaki, A., Delaporte, C., Riba, A., Molina, N., Hariharan, N., Mukherjee, T., & Giangrande, A. (2020). Temporal specificity and heterogeneity of Drosophila immune cells. *The EMBO Journal*, *39*(12), 1–25. https://doi.org/10.15252/embj.2020104486

Cegielska, A., Gietzen, K. F., Rivers, A., & Virshup, D. M. (1998). Autoinhibition

of Casein Kinase I ε (CKIε) Is Relieved by Protein Phosphatases and Limited Proteolysis. *Journal of Biological Chemistry*, *273*(3), 1357–1364. https://doi.org/10.1074/jbc.273.3.1357

Chan, C., Beltzner, C. C., & Pollard, T. D. (2009). Cofilin Dissociates Arp2/3 Complex and Branches from Actin Filaments. *Current Biology*, *19*(7), 537–545. https://doi.org/10.1016/j.cub.2009.02.060

Charroux, B., & Royet, J. (2009). Elimination of plasmatocytes by targeted apoptosis reveals their role in multiple aspects of the Drosophila immune response. *Proceedings of the National Academy of Sciences*, *106*(24), 9797–9802. https://doi.org/10.1073/pnas.0903971106

Chen, B., Chou, H.-T., Brautigam, C. A., Xing, W., Yang, S., Henry, L., Doolittle, L. K., Walz, T., & Rosen, M. K. (2017). Rac1 GTPase activates the WAVE regulatory complex through two distinct binding sites. *ELife*, *6*. https://doi.org/10.7554/eLife.29795

Chen, X. J., Squarr, A. J., Stephan, R., Chen, B., Higgins, T. E., Barry, D. J., Martin, M. C., Rosen, M. K., Bogdan, S., & Way, M. (2014). Ena/VASP Proteins Cooperate with the WAVE Complex to Regulate the Actin Cytoskeleton. *Developmental Cell*, *30*(5), 569–584. https://doi.org/10.1016/J.DEVCEL.2014.08.001

Chen, Yifan, Shao, X., Cao, J., Zhu, H., Yang, B., He, Q., & Ying, M. (2021). Phosphorylation regulates cullin-based ubiquitination in tumorigenesis. *Acta Pharmaceutica Sinica B*, *11*(2), 309–321. https://doi.org/10.1016/j.apsb.2020.09.007

Chen, Yongbin, Sasai, N., Ma, G., Yue, T., Jia, J., Briscoe, J., & Jiang, J. (2011). Sonic Hedgehog dependent Phosphorylation by CK1α and GRK2 is required for Ciliary Accumulation and Activation of Smoothened. *PLoS Biology*, *9*(6). https://doi.org/10.1371/journal.pbio.1001083

Chen, Yuezhou, Yang, Z., Meng, M., Zhao, Y., Dong, N., Yan, H., Liu, L., Ding, M., Peng, H. B., & Shao, F. (2009). Cullin Mediates Degradation of RhoA through Evolutionarily Conserved BTB Adaptors to Control Actin Cytoskeleton Structure and Cell Movement. *Molecular Cell*, *35*(6), 841–

855. https://doi.org/10.1016/j.molcel.2009.09.004

Chen, Z., Borek, D., Padrick, S. B., Gomez, T. S., Metlagel, Z., Ismail, A. M., Umetani, J., Billadeau, D. D., Otwinowski, Z., & Rosen, M. K. (2010). Structure and control of the actin regulatory WAVE complex. *Nature*, *468*(7323), 533–538. https://doi.org/10.1038/nature09623

Chereau, D., Kerff, F., Graceffa, P., Grabarek, Z., Langsetmo, K., & Dominguez, R. (2005). Actin-bound structures of Wiskott-Aldrich syndrome protein (WASP)-homology domain 2 and the implications for filament assembly. *Proceedings of the National Academy of Sciences of the United States of America*, *102*(46), 16644–16649. https://doi.org/10.1073/pnas.0507021102

Chesarone, M. A., Dupage, A. G., & Goode, B. L. (2010). Unleashing formins to remodel the actin and microtubule cytoskeletons. *Nature Reviews Molecular Cell Biology*, *11*(1), 62–74. https://doi.org/10.1038/nrm2816

Chesarone, M. A., & Goode, B. L. (2009). Actin nucleation and elongation factors: mechanisms and interplay. *Current Opinion in Cell Biology*, *21*(1), 28–37. https://doi.org/10.1016/j.ceb.2008.12.001

Chia, R., Haddock, S., Beilina, A., Rudenko, I. N., Mamais, A., Kaganovich, A., Li, Y., Kumaran, R., Nalls, M. A., & Cookson, M. R. (2014). Phosphorylation of LRRK2 by casein kinase 1α regulates trans-Golgi clustering via differential interaction with ARHGEF7. *Nature Communications*, *5*(1), 5827. https://doi.org/10.1038/ncomms6827

Cho, B., Yoon, S.-H., Lee, D., Koranteng, F., Tattikota, S. G., Cha, N., Shin, M., Do, H., Hu, Y., Oh, S. Y., Lee, D., Vipin Menon, A., Moon, S. J., Perrimon, N., Nam, J.-W., & Shim, J. (2020). Single-cell transcriptome maps of myeloid blood cell lineages in Drosophila. *Nature Communications*, *11*(1), 4483. https://doi.org/10.1038/s41467-020-18135-y

Clemmons, A. W., Lindsay, S. A., & Wasserman, S. A. (2015). An Effector Peptide Family Required for Drosophila Toll-Mediated Immunity. *PLoS Pathogens*, *11*(4), 1–17. https://doi.org/10.1371/journal.ppat.1004876

Cloud, V., Thapa, A., Morales-Sosa, P., Miller, T. M., Miller, S. A., Holsapple, D., Gerhart, P. M., Momtahan, E., Jack, J. L., Leiva, E., Rapp, S. R.,

Shelton, L. G., Pierce, R. A., Martin-Brown, S., Florens, L., Washburn, M. P., & Mohan, R. D. (2019). Ataxin-7 and Non-stop coordinate SCAR protein levels, subcellular localization, and actin cytoskeleton organization. *ELife*, *8*. https://doi.org/10.7554/eLife.49677

Cooper, J. A., & Sept, D. (2008). *New Insights into Mechanism and Regulation of Actin Capping Protein* (pp. 183–206). https://doi.org/10.1016/S1937-6448(08)00604-7

Cory, G. O. C., Cramer, R., Blanchoin, L., & Ridley, A. J. (2003). Phosphorylation of the WASP-VCA Domain Increases Its Affinity for the Arp2/3 Complex and Enhances Actin Polymerization by WASP. *Molecular Cell*, *11*(5), 1229–1239. https://doi.org/10.1016/S1097-2765(03)00172-2

Crane, G. M., Jeffery, E., & Morrison, S. J. (2017). Adult haematopoietic stem cell niches. *Nature Reviews Immunology*, *17*(9), 573–590. https://doi.org/10.1038/nri.2017.53

Crozatier, M., & Meister, M. (2007). Drosophila haematopoiesis. *Cellular Microbiology*, *9*(5), 1117–1126. https://doi.org/10.1111/j.1462-5822.2007.00930.x

Crozatier, M., Ubeda, J.-M., Vincent, A., & Meister, M. (2004). Cellular Immune Response to Parasitization in Drosophila Requires the EBF Orthologue Collier. *PLoS Biology*, *2*(8), e196. https://doi.org/10.1371/journal.pbio.0020196

Crozatier, M., & Vincent, A. (2011). Drosophila: A model for studying genetic and molecular aspects of haematopoiesis and associated leukaemias. *DMM Disease Models and Mechanisms*, *4*(4), 439–445. https://doi.org/10.1242/dmm.007351

Csordás, G., Gábor, E., & Honti, V. (2021). There and back again: The mechanisms of differentiation and transdifferentiation in Drosophila blood cells. *Developmental Biology*, *469*, 135–143. https://doi.org/10.1016/j.ydbio.2020.10.006

D'Ambrosio, M. V., & Vale, R. D. (2010). A whole genome RNAi screen of Drosophila S2 cell spreading performed using automated computational

image analysis. *Journal of Cell Biology*, *191*(3), 471–478. https://doi.org/10.1083/jcb.201003135

Danson, C. M., Pocha, S. M., Bloomberg, G. B., & Cory, G. O. (2007). Phosphorylation of WAVE2 by MAP kinases regulates persistent cell migration and polarity. *Journal of Cell Science*, *120*(23), 4144–4154. https://doi.org/10.1242/jcs.013714

Defaye, A., Evans, I., Crozatier, M., Wood, W., Lemaitre, B., & Leulier, F. (2009). Genetic Ablation of Drosophila Phagocytes Reveals Their Contribution to Both Development and Resistance to Bacterial Infection. *Journal of Innate Immunity*, *1*(4), 322–334. https://doi.org/10.1159/000210264

Derry, J. M., Ochs, H. D., & Francke, U. (1994). Isolation of a novel gene mutated in Wiskott-Aldrich syndrome. *Cell*, *79*(5), 635–644. https://doi.org/10.1542/peds.96.2.411a

Dostálová, A., Rommelaere, S., Poidevin, M., & Lemaitre, B. (2017). Thioester-containing proteins regulate the Toll pathway and play a role in Drosophila defence against microbial pathogens and parasitoid wasps. *BMC Biology*, *15*(1), 79. https://doi.org/10.1186/s12915-017-0408-0

Dudzic, J. P., Hanson, M. A., Iatsenko, I., Kondo, S., & Lemaitre, B. (2019). More Than Black or White: Melanization and Toll Share Regulatory Serine Proteases in Drosophila. *Cell Reports*, *27*(4), 1050-1061.e3. https://doi.org/10.1016/j.celrep.2019.03.101

Edwards, M., Zwolak, A., Schafer, D. A., Sept, D., Dominguez, R., & Cooper, J. A. (2014). Capping protein regulators fine-tune actin assembly dynamics. *Nature Reviews Molecular Cell Biology*, *15*(10), 677–689. https://doi.org/10.1038/nrm3869

Eleftherianos, I., Heryanto, C., Bassal, T., Zhang, W., Tettamanti, G., & Mohamed, A. (2021). Haemocyte-mediated immunity in insects: Cells, processes and associated components in the fight against pathogens and parasites. *Immunology*, *164*(3), 401–432. https://doi.org/10.1111/imm.13390

Emtenani, S., Martin, E. T., Gyoergy, A., Bicher, J., Genger, J., Köcher, T., Akhmanova, M., Guarda, M., Roblek, M., Bergthaler, A., Hurd, T. R., Rangan, P., & Siekhaus, D. E. (2022). Macrophage mitochondrial bioenergetics and tissue invasion are boosted by an Atossa-Porthos axis in Drosophila. *The EMBO Journal*, *41*(12). https://doi.org/10.15252/embj.2021109049

Etienne-Manneville, S. (2004). Actin and Microtubules in Cell Motility: Which One is in Control? *Traffic*, *5*(7), 470–477. https://doi.org/10.1111/j.1600-0854.2004.00196.x

Evans, C. J., Hartenstein, V., & Banerjee, U. (2003). Thicker Than Blood. *Developmental Cell*, *5*(5), 673–690. https://doi.org/10.1016/S1534-5807(03)00335-6

Evans, C. J., Liu, T., & Banerjee, U. (2014). Drosophila hematopoiesis: Markers and methods for molecular genetic analysis. *Methods*, *68*(1), 242–251. https://doi.org/10.1016/j.ymeth.2014.02.038

Evans, C. J., Olson, J. M., Ngo, K. T., Kim, E., Lee, N. E., Kuoy, E., Patananan, A. N., Sitz, D., Tran, P., Do, M.-T., Yackle, K., Cespedes, A., Hartenstein, V., Call, G. B., & Banerjee, U. (2009). G-TRACE: rapid Gal4-based cell lineage analysis in Drosophila. *Nature Methods*, *6*(8), 603–605. https://doi.org/10.1038/nmeth.1356

Faas, M. M., & de Vos, P. (2020). Mitochondrial function in immune cells in health and disease. *Biochimica et Biophysica Acta (BBA) - Molecular Basis of Disease*, *1866*(10), 165845. https://doi.org/10.1016/j.bbadis.2020.165845

Facchetti, F., Blanzuoli, L., Vermi, W., Notarangelo, L. D., Giliani, S., Fiorini, M., Fasth, A., Stewart, D. M., & Nelson, D. L. (1998). Defective actin polymerization in EBV-transformed B-cell lines from patients with the Wiscott-Aldrich syndrome. *Journal of Pathology*, *185*(1), 99–107. https://doi.org/10.1002/(SICI)1096-9896(199805)185:1<99::AID-PATH48>3.0.CO;2-L

Fernández-Cruz, I., Sánchez-Díaz, I., Narváez-Padilla, V., & Reynaud, E.

(2020). Rpt2 proteasome subunit reduction causes Parkinson's disease like symptoms in Drosophila. *IBRO Reports*, *9*(July), 65–77. https://doi.org/10.1016/j.ibror.2020.07.001

Ferrandon, D. (1998). A drosomycin-GFP reporter transgene reveals a local immune response in Drosophila that is not dependent on the Toll pathway. *The EMBO Journal*, *17*(5), 1217–1227. https://doi.org/10.1093/emboj/17.5.1217

Ferrandon, Dominique, Imler, J.-L., & Hoffmann, J. A. (2004). Sensing infection in Drosophila: Toll and beyond. *Seminars in Immunology*, *16*(1), 43–53. https://doi.org/10.1016/j.smim.2003.10.008

Fessler, J. H., & Fessler, L. I. (1989). Drosophila Extracellular Matrix. *Annual Review of Cell Biology*, *5*(1), 309–339. https://doi.org/10.1146/annurev.cb.05.110189.001521

Finley, D. (2009). Recognition and Processing of Ubiquitin-Protein Conjugates by the Proteasome. *Annual Review of Biochemistry*, *78*(1), 477–513. https://doi.org/10.1146/annurev.biochem.78.081507.101607

Flotow, H., Graves, P. R., Wang, A., Fiol, C. J., Roeske, R. W., & Roach, P. J. (1990). Phosphate groups as substrate determinants for casein kinase I action. *Journal of Biological Chemistry*, *265*(24), 14264–14269. http://www.jbc.org/content/265/24/14264.long

Flotow, H., & Roach, P. J. (1991). Role of acidic residues as substrate determinants for casein kinase I. *Journal of Biological Chemistry*, *266*(6), 3724–3727. http://www.jbc.org/content/266/6/3724.long

Fokin, A. I., & Gautreau, A. M. (2021). Assembly and Activity of the WASH Molecular Machine: Distinctive Features at the Crossroads of the Actin and Microtubule Cytoskeletons. *Frontiers in Cell and Developmental Biology*, *9*(April), 1–9. https://doi.org/10.3389/fcell.2021.658865

Fossett, N., Hyman, K., Gajewski, K., Orkin, S. H., & Schulz, R. A. (2003). Combinatorial interactions of Serpent, Lozenge, and U-shaped regulate crystal cell lineage commitment during Drosophila hematopoiesis. *Proceedings of the National Academy of Sciences*, *100*(20), 11451–11456.

https://doi.org/10.1073/pnas.1635050100

Fossett, N., & Schulz, R. A. (2001). Functional conservation of hematopoietic factors in Drosophila and vertebrates. *Differentiation*, *69*(2–3), 83–90. https://doi.org/10.1046/j.1432-0436.2001.690202.x

Fossett, N., Tevosian, S. G., Gajewski, K., Zhang, Q., Orkin, S. H., & Schulz, R. A. (2001). The Friend of GATA proteins U-shaped, FOG-1, and FOG-2 function as negative regulators of blood, heart, and eye development in Drosophila. *Proceedings of the National Academy of Sciences*, *98*(13), 7342–7347. https://doi.org/10.1073/pnas.131215798

Franc, N. C., Dimarcq, J.-L., Lagueux, M., Hoffmann, J., & Ezekowitz, R. A. B. (1996). Croquemort, A Novel Drosophila Hemocyte/Macrophage Receptor that Recognizes Apoptotic Cells. *Immunity*, *4*(5), 431–443. https://doi.org/10.1016/S1074-7613(00)80410-0

Fregoso, F. E., van Eeuwen, T., Simanov, G., Rebowski, G., Boczkowska, M., Zimmet, A., Gautreau, A. M., & Dominguez, R. (2022). Molecular mechanism of Arp2/3 complex inhibition by Arpin. *Nature Communications*, *13*(1), 1–12. https://doi.org/10.1038/s41467-022-28112-2

Fricke, R., Gohl, C., Dharmalingam, E., Grevelhörster, A., Zahedi, B., Harden, N., Kessels, M., Qualmann, B., & Bogdan, S. (2009). Drosophila Cip4/Toca-1 Integrates Membrane Trafficking and Actin Dynamics through WASP and SCAR/WAVE. *Current Biology*, *19*(17), 1429–1437. https://doi.org/10.1016/j.cub.2009.07.058

Friedl, P., & Wolf, K. (2010). Plasticity of cell migration: A multiscale tuning model. *Journal of Cell Biology*, *188*(1), 11–19. https://doi.org/10.1083/jcb.200909003

Fu, Y., Huang, X., Zhang, P., van de Leemput, J., & Han, Z. (2020). Single-cell RNA sequencing identifies novel cell types in Drosophila blood. *Journal of Genetics and Genomics*, *47*(4), 175–186. https://doi.org/10.1016/j.jgg.2020.02.004

Gajewski, K. M., Sorrentino, R. P., Lee, J. H., Zhang, Q., Russell, M., & Schulz, R. A. (2007). Identification of a crystal cell-specific enhancer of the black

cells prophenoloxidase gene in drosophila. *Genesis*, *45*(4), 200–207. https://doi.org/10.1002/dvg.20285

Galindo, L. A., Lagune, M., Glatigny, S., Herrmann, J., Girard-, F., Waterhouse, M., & Gue, I. (2023). *Mycobacterium abscessus resists the innate cellular response by surviving cell lysis of infected phagocytes*. 1–26. https://doi.org/10.1371/journal.ppat.1011257

Gallego, M. D., Santamaría, M., Peña, J., & Molina, I. J. (1997). Defective actin reorganization and polymerization of Wiskott-Aldrich T cells in response to CD3-mediated stimulation. *Blood*, *90*(8), 3089–3097. https://doi.org/10.1182/blood.v90.8.3089

Gautreau, A., Ho, H. Y. H., Li, J., Steen, H., Gygi, S. P., & Kirschner, M. W. (2004). Purification and architecture of the ubiquitous Wave complex. *Proceedings of the National Academy of Sciences of the United States of America*, *101*(13), 4379–4383. https://doi.org/10.1073/pnas.0400628101

Ghosh, S., Singh, A., Mandal, S., & Mandal, L. (2015). Active Hematopoietic Hubs in Drosophila Adults Generate Hemocytes and Contribute to Immune Response. *Developmental Cell*, *33*(4), 478–488. https://doi.org/10.1016/j.devcel.2015.03.014

Gietzen, K. F., & Virshup, D. M. (1999). Identification of Inhibitory Autophosphorylation Sites in Casein Kinase I ε. *Journal of Biological Chemistry*, *274*(45), 32063–32070. https://doi.org/10.1074/jbc.274.45.32063

Gold, K. S., & Brückner, K. (2014). Drosophila as a model for the two myeloid blood cell systems in vertebrates. *Experimental Hematology*, *42*(8), 717–727. https://doi.org/10.1016/j.exphem.2014.06.002

Gold, K. S., & Brückner, K. (2015). Macrophages and cellular immunity in Drosophila melanogaster. *Seminars in Immunology*, *27*(6), 357–368. https://doi.org/10.1016/j.smim.2016.03.010

Gold, K. S., & Brückner, K. (2016). Seminars in Immunology Macrophages and cellular immunity in Drosophila melanogaster. *Seminars in Immunology*, *27*(6), 357–368. https://doi.org/10.1016/j.smim.2016.03.010

Goley, E. D., & Welch, M. D. (2006). The ARP2/3 complex: An actin nucleator comes of age. *Nature Reviews Molecular Cell Biology*, *7*(10), 713–726. https://doi.org/10.1038/nrm2026

Gomez, T. S., & Billadeau, D. D. (2009). A FAM21-Containing WASH Complex Regulates Retromer-Dependent Sorting. *Developmental Cell*, *17*(5), 699–711. https://doi.org/10.1016/j.devcel.2009.09.009

Goodsell, D. S. (2022). Actin Branching by Arp2/3 Complex. *RCSB Protein Data Bank*. https://doi.org/10.2210/rcsb_pdb/mom_2022_11

Graves, P. R., & Roach, P. J. (1995). Role of COOH-terminal Phosphorylation in the Regulation of Casein Kinase Iδ. *Journal of Biological Chemistry*, *270*(37), 21689–21694. https://doi.org/10.1074/jbc.270.37.21689

Greenspan, L. J., de Cuevas, M., Le, K. H., Viveiros, J. M., & Matunis, E. L. (2022). Activation of the EGFR/MAPK pathway drives transdifferentiation of quiescent niche cells to stem cells in the Drosophila testis niche. *ELife*, *11*, 1–28. https://doi.org/10.7554/eLife.70810

Grigorian, M., Mandal, L., & Hartenstein, V. (2011). Hematopoiesis at the onset of metamorphosis: terminal differentiation and dissociation of the Drosophila lymph gland. *Development Genes and Evolution*, *221*(3), 121–131. https://doi.org/10.1007/s00427-011-0364-6

Gross, S. D., & Anderson, R. A. (1998). Casein kinase I: Spatial organization and positioning of a multifunctional protein kinase family. *Cellular Signalling*, *10*(10), 699–711. https://doi.org/10.1016/S0898-6568(98)00042-4

Guillou, A., Troha, K., Wang, H., Franc, N. C., & Buchon, N. (2016). The Drosophila CD36 Homologue croquemort Is Required to Maintain Immune and Gut Homeostasis during Development and Aging. *PLOS Pathogens*, *12*(10), e1005961. https://doi.org/10.1371/journal.ppat.1005961

Gyoergy, A., Roblek, M., Ratheesh, A., Valoskova, K., Belyaeva, V., Wachner, S., Matsubayashi, Y., Sánchez-Sánchez, B. J., Stramer, B., & Siekhaus, D. E. (2018). Tools Allowing Independent Visualization and Genetic Manipulation of Drosophila melanogaster Macrophages and Surrounding

Tissues. *G3 Genes|Genomes|Genetics*, *8*(3), 845–857. https://doi.org/10.1534/g3.117.300452

Han, Y., Wang, B., Cho, Y. S., Zhu, J., Wu, J., Chen, Y., & Jiang, J. (2019). Phosphorylation of Ci/Gli by Fused Family Kinases Promotes Hedgehog Signaling. *Developmental Cell*, *50*(5), 610-626.e4. https://doi.org/10.1016/j.devcel.2019.06.008

Handke, B., Poernbacher, I., Goetze, S., Ahrens, C. H., Omasits, U., Marty, F., Simigdala, N., Meyer, I., Wollscheid, B., Brunner, E., Hafen, E., & Lehner, C. F. (2013). The Hemolymph Proteome of Fed and Starved Drosophila Larvae. *PLoS ONE*, *8*(6), 1–10. https://doi.org/10.1371/journal.pone.0067208

Hanson, M. A., Dostálová, A., Ceroni, C., Poidevin, M., Kondo, S., & Lemaître, B. (2019). Erratum: Correction: Synergy and remarkable specificity of antimicrobial peptides in vivo using a systematic knockout approach (eLife (2019) 8 PII: e48778). *ELife*, *8*, 1–24. https://doi.org/10.7554/eLife.48778

Hanson, M. A., & Lemaitre, B. (2020). New insights on Drosophila antimicrobial peptide function in host defense and beyond. *Current Opinion in Immunology*, *62*, 22–30. https://doi.org/10.1016/j.coi.2019.11.008

Hao, Y. H., Doyle, J. M., Ramanathan, S., Gomez, T. S., Jia, D., Xu, M., Chen, Z. J., Billadeau, D. D., Rosen, M. K., & Potts, P. R. (2013). Regulation of WASH-dependent actin polymerization and protein trafficking by ubiquitination. *Cell*, *152*(5), 1051–1064. https://doi.org/10.1016/j.cell.2013.01.051

Harper, J. W., & Schulman, B. A. (2021). Cullin-RING Ubiquitin Ligase Regulatory Circuits: A Quarter Century Beyond the F-Box Hypothesis. *Annual Review of Biochemistry*, *90*(1), 403–429. https://doi.org/10.1146/annurev-biochem-090120-013613

Hartenstein, V. (2006). Blood Cells and Blood Cell Development in the Animal Kingdom. *Annual Review of Cell and Developmental Biology*, *22*(1), 677–712. https://doi.org/10.1146/annurev.cellbio.22.010605.093317

Hershko, A., & Ciechanover, A. (1998). THE UBIQUITIN SYSTEM. *Annual*

Review of Biochemistry, *67*(1), 425–479. https://doi.org/10.1146/annurev.biochem.67.1.425

Higgs, H. N., Blanchoin, L., & Pollard, T. D. (1999). Influence of the C terminus of Wiskott-Aldrich syndrome protein (WASp) and the Arp2/3 complex on actin polymerization. *Biochemistry*, *38*(46), 15212–15222. https://doi.org/10.1021/bi991843+

Hirota, T., Lee, J. W., Lewis, W. G., Zhang, E. E., Breton, G., Liu, X., Garcia, M., Peters, E. C., Etchegaray, J.-P., Traver, D., Schultz, P. G., & Kay, S. A. (2010). High-Throughput Chemical Screen Identifies a Novel Potent Modulator of Cellular Circadian Rhythms and Reveals CKIα as a Clock Regulatory Kinase. *PLoS Biology*, *8*(12), e1000559. https://doi.org/10.1371/journal.pbio.1000559

Holmes, K. C., Popp, D., Gebhard, W., & Kabsch, W. (1990). Atomic model of the actin filament. *Nature*, *347*(6288), 44–49. https://doi.org/10.1038/347044a0

Holz, A., Bossinger, B., Strasser, T., Janning, W., & Klapper, R. (2003). The two origins of hemocytes in Drosophila. *Development*, *130*(20), 4955–4962. https://doi.org/10.1242/dev.00702

Honti, V., Kurucz, É., Csordás, G., Laurinyecz, B., Márkus, R., & Andó, I. (2009). In vivo detection of lamellocytes in Drosophila melanogaster. *Immunology Letters*, *126*(1–2), 83–84. https://doi.org/10.1016/j.imlet.2009.08.004

Horn, L., Leips, J., & Starz-Gaiano, M. (2014). Phagocytic ability declines with age in adult Drosophila hemocytes. *Aging Cell*, *13*(4), 719–728. https://doi.org/10.1111/acel.12227

Howell, L., Sampson, C. J., Xavier, M. J., Bolukbasi, E., Heck, M. M. S., & Williams, M. J. (2012). A directed miniscreen for genes involved in the Drosophila anti-parasitoid immune response. *Immunogenetics*, *64*(2), 155–161. https://doi.org/10.1007/s00251-011-0571-3

Hudson, A. M., Mannix, K. M., & Cooley, L. (2015). Actin Cytoskeletal Organization in Drosophila Germline Ring Canals Depends on Kelch

Function in a Cullin-RING E3 Ligase. *Genetics*, *201*(3), 1117–1131. https://doi.org/10.1534/genetics.115.181289

Hudson, A. M., Mannix, K. M., Gerdes, J. A., Kottemann, M. C., & Cooley, L. (2018). Targeted substrate degradation by Kelch controls the actin cytoskeleton during ring canal expansion. *Development*. https://doi.org/10.1242/dev.169219

Hultmark, D., & Andó, I. (2022). Hematopoietic plasticity mapped in Drosophila and other insects. *ELife*, *11*, 1–36. https://doi.org/10.7554/eLife.78906

Innocenti, M., Zucconi, A., Disanza, A., Frittoli, E., Areces, L. B., Steffen, A., Stradal, T. E. B., Paolo, P., Fiore, D., Carlier, M., & Scita, G. (2004). *Abi1 is essential for the formation and activation of a WAVE2 signalling complex*. *6*(4), 319–327. https://doi.org/10.1038/ncb1105

Irving, P., Ubeda, J.-M., Doucet, D., Troxler, L., Lagueux, M., Zachary, D., Hoffmann, J. A., Hetru, C., & Meister, M. (2005). New insights into Drosophila larval haemocyte functions through genome-wide analysis. *Cellular Microbiology*, *7*(3), 335–350. https://doi.org/10.1111/j.1462-5822.2004.00462.x

Iwasaki, A., & Medzhitov, R. (2015). Control of adaptive immunity by the innate immune system. *Nature Immunology*, *16*(4), 343–353. https://doi.org/10.1038/ni.3123

Jacquemet, G., Hamidi, H., & Ivaska, J. (2015). Filopodia in cell adhesion, 3D migration and cancer cell invasion. *Current Opinion in Cell Biology*, *36*, 23–31. https://doi.org/10.1016/j.ceb.2015.06.007

Janeway, C. A., & Medzhitov, R. (2002). Innate Immune Recognition. *Annual Review of Immunology*, *20*(1), 197–216. https://doi.org/10.1146/annurev.immunol.20.083001.084359

Jia, D., Gomez, T. S., Metlagel, Z., Umetani, J., Otwinowski, Z., Rosen, M. K., & Billadeau, D. D. (2010). WASH and WAVE actin regulators of the Wiskott-Aldrich syndrome protein (WASP) family are controlled by analogous structurally related complexes. *Proceedings of the National Academy of Sciences of the United States of America*, *107*(23), 10442–10447.

https://doi.org/10.1073/pnas.0913293107

Jia, H., Liu, Y., Yan, W., & Jia, J. (2009). PP4 and PP2A regulate Hedgehog signaling by controlling Smo and Ci phosphorylation. *Development*, *136*(2), 307–316. https://doi.org/10.1242/dev.030015

Jia, J., Zhang, L., Zhang, Q., Tong, C., Wang, B., Hou, F., Amanai, K., & Jiang, J. (2005). Phosphorylation by double-time/CKIε and CKIα targets Cubitus Interruptus for Slimb/β-TRCP-mediated proteolytic processing. *Developmental Cell*, *9*(6), 819–830. https://doi.org/10.1016/j.devcel.2005.10.006

Jiang, J. (2017). *CK1 in Developmental Signaling* (pp. 303–329). https://doi.org/10.1016/bs.ctdb.2016.09.002

Johnson, D. M., Wells, M. B., Fox, R., Lee, J. S., Loganathan, R., Levings, D., Bastien, A., Slattery, M., & Andrew, D. J. (2020). CrebA increases secretory capacity through direct transcriptional regulation of the secretory machinery, a subset of secretory cargo, and other key regulators. *Traffic*, *21*(9), 560–577. https://doi.org/10.1111/tra.12753

Johnston, J. A., Ward, C. L., & Kopito, R. R. (1998). Aggresomes: A Cellular Response to Misfolded Proteins. *Journal of Cell Biology*, *143*(7), 1883–1898. https://doi.org/10.1083/jcb.143.7.1883

Joo, H.-S., Fu, C.-I., & Otto, M. (2016). Bacterial strategies of resistance to antimicrobial peptides. *Philosophical Transactions of the Royal Society B: Biological Sciences*, *371*(1695), 20150292. https://doi.org/10.1098/rstb.2015.0292

Joseph, N., Biber, G., Fried, S., Reicher, B., Levy, O., Sabag, B., Noy, E., & Barda-Saad, M. (2017). A conformational change within the WAVE2 complex regulates its degradation following cellular activation. *Scientific Reports*, *7*(1), 44863. https://doi.org/10.1038/srep44863

Jung, S. H., Evans, C. J., Uemura, C., & Banerjee, U. (2005). The Drosophila lymph gland as a developmental model of hematopoiesis. *Development*, *132*(11), 2521–2533. https://doi.org/10.1242/dev.01837

Kage, F., Döring, H., Mietkowska, M., Schaks, M., Grüner, F., Stahnke, S.,

Steffen, A., Müsken, M., Stradal, T. E. B., & Rottner, K. (2022). Lamellipodia-like actin networks in cells lacking WAVE regulatory complex. *Journal of Cell Science*, *135*(15). https://doi.org/10.1242/jcs.260364

Kage, F., Winterhoff, M., Dimchev, V., Mueller, J., Thalheim, T., Freise, A., Brühmann, S., Kollasser, J., Block, J., Dimchev, G., Geyer, M., Schnittler, H.-J., Brakebusch, C., Stradal, T. E. B., Carlier, M.-F., Sixt, M., Käs, J., Faix, J., & Rottner, K. (2017). FMNL formins boost lamellipodial force generation. *Nature Communications*, *8*(1), 14832. https://doi.org/10.1038/ncomms14832

Kanwal, A., Joshi, P. V., Mandal, S., & Mandal, L. (2021). Ubx-Collier signaling cascade maintains blood progenitors in the posterior lobes of the Drosophila larval lymph gland. *PLoS Genetics*, *17*(8), 1–29. https://doi.org/10.1371/journal.pgen.1009709

Karp, G. C., & Solursh, M. (1985). Dynamic activity of the filopodia of sea urchin embryonic cells and their role in directed migration of the primary mesenchyme in vitro. *Developmental Biology*, *112*(2), 276–283. https://doi.org/10.1016/0012-1606(85)90398-7

Kenney, D., Cairns, L., Remold-O'Donnell, E., Peterson, J., Rosen, F., & Parkman, R. (1986). Morphological abnormalities in the lymphocytes of patients with the Wiskott-Aldrich syndrome. *Blood*, *68*(6), 1329–1332. https://doi.org/10.1182/blood.V68.6.1329.1329

Ketosugbo, K. F., Bushnell, H. L., & Johnson, R. I. (2017). A screen for E3 ubiquitination ligases that genetically interact with the adaptor protein Cindr during Drosophila eye patterning. *PLOS ONE*, *12*(11), e0187571. https://doi.org/10.1371/journal.pone.0187571

Kim, Y., Sung, J. Y., Ceglia, I., Lee, K.-W., Ahn, J.-H., Halford, J. M., Kim, A. M., Kwak, S. P., Park, J. B., Ho Ryu, S., Schenck, A., Bardoni, B., Scott, J. D., Nairn, A. C., & Greengard, P. (2006). Phosphorylation of WAVE1 regulates actin polymerization and dendritic spine morphology. *Nature*, *442*(7104), 814–817. https://doi.org/10.1038/nature04976

Knippschild, U., Gocht, A., Wolff, S., Huber, N., Löhler, J., & Stöter, M. (2005).

The casein kinase 1 family: participation in multiple cellular processes in eukaryotes. *Cellular Signalling*, *17*(6), 675–689. https://doi.org/10.1016/j.cellsig.2004.12.011

Kocks, C., Cho, J. H., Nehme, N., Ulvila, J., Pearson, A. M., Meister, M., Strom, C., Conto, S. L., Hetru, C., Stuart, L. M., Stehle, T., Hoffmann, J. A., Reichhart, J.-M., Ferrandon, D., Rämet, M., & Ezekowitz, R. A. B. (2005). Eater, a Transmembrane Protein Mediating Phagocytosis of Bacterial Pathogens in Drosophila. *Cell*, *123*(2), 335–346. https://doi.org/10.1016/j.cell.2005.08.034

Komander, D. (2009). The emerging complexity of protein ubiquitination. *Biochemical Society Transactions*, *37*(5), 937–953. https://doi.org/10.1042/BST0370937

Komsany, A., & Pezzella, F. (2020). The perivascular niche. *Tumor Vascularization*, 113–127. https://doi.org/10.1016/B978-0-12-819494-2.00007-9

Kopito, R. R. (2000). Aggresomes, inclusion bodies and protein aggregation. *Trends in Cell Biology*, *10*(12), 524–530. https://doi.org/10.1016/S0962-8924(00)01852-3

Koranteng, F., Cho, B., & Shim, J. (2022). Intrinsic and Extrinsic Regulation of Hematopoiesis in Drosophila. *Molecules and Cells*, *45*(3), 101–108. https://doi.org/10.14348/molcells.2022.2039

Kramer, D. A., Piper, H. K., & Chen, B. (2022). WASP family proteins: Molecular mechanisms and implications in human disease. *European Journal of Cell Biology*, *101*(3), 151244. https://doi.org/10.1016/j.ejcb.2022.151244

Krause, M., & Gautreau, A. (2014). Steering cell migration: lamellipodium dynamics and the regulation of directional persistence. *Nature Reviews Molecular Cell Biology*, *15*(9), 577–590. https://doi.org/10.1038/nrm3861

Krejčová, G., Danielová, A., Nedbalová, P., Kazek, M., Strych, L., Chawla, G., Tennessen, J. M., Lieskovská, J., Jindra, M., Doležal, T., & Bajgar, A. (2019). Drosophila macrophages switch to aerobic glycolysis to mount effective antibacterial defense. *ELife*, *8*, 1–22.

https://doi.org/10.7554/eLife.50414

Krzemień, J., Dubois, L., Makki, R., Meister, M., Vincent, A., & Crozatier, M. (2007). Control of blood cell homeostasis in Drosophila larvae by the posterior signalling centre. *Nature*, *446*(7133), 325–328. https://doi.org/10.1038/nature05650

Kurucz, É., Márkus, R., Zsámboki, J., Folkl-Medzihradszky, K., Darula, Z., Vilmos, P., Udvardy, A., Krausz, I., Lukacsovich, T., Gateff, E., Zettervall, C.-J., Hultmark, D., & Andó, I. (2007). Nimrod, a Putative Phagocytosis Receptor with EGF Repeats in Drosophila Plasmatocytes. *Current Biology*, *17*(7), 649–654. https://doi.org/10.1016/j.cub.2007.02.041

Kurucz, É., Váczi, B., Márkus, R., Laurinyecz, B., Vilmos, P., Zsámboki, J., Csorba, K., Gateff, E., Hultmark, D., & Andó, I. (2007). Definition of Drosophila hemocyte subsets by cell-type specific antigens. *Acta Biologica Hungarica*, *58*(Supplement 1), 95–111. https://doi.org/10.1556/ABiol.58.2007.Suppl.8

Labrosse, C., Eslin, P., Doury, G., Drezen, J. M., & Poirié, M. (2005). Haemocyte changes in D. Melanogaster in response to long gland components of the parasitoid wasp Leptopilina boulardi: a Rho-GAP protein as an important factor. *Journal of Insect Physiology*, *51*(2), 161–170. https://doi.org/10.1016/j.jinsphys.2004.10.004

Lam, V. H., Li, Y. H., Liu, X., Murphy, K. A., Diehl, J. S., Kwok, R. S., & Chiu, J. C. (2018). CK1α Collaborates with DOUBLETIME to Regulate PERIOD Function in the Drosophila Circadian Clock. *The Journal of Neuroscience*, *38*(50), 10631–10643. https://doi.org/10.1523/JNEUROSCI.0871-18.2018

Lämmermann, T., & Sixt, M. (2009). Mechanical modes of “amoeboid” cell migration. *Current Opinion in Cell Biology*, *21*(5), 636–644. https://doi.org/10.1016/j.ceb.2009.05.003

Lanot, R., Zachary, D., Holder, F., & Meister, M. (2001). Postembryonic Hematopoiesis in Drosophila. *Developmental Biology*, *230*(2), 243–257. https://doi.org/10.1006/dbio.2000.0123

Law, A. L., Jalal, S., Pallett, T., Mosis, F., Guni, A., Brayford, S., Yolland, L.,

Marcotti, S., Levitt, J. A., Poland, S. P., Rowe-Sampson, M., Jandke, A., Köchl, R., Pula, G., Ameer-Beg, S. M., Stramer, B. M., & Krause, M. (2021). Nance-Horan Syndrome-like 1 protein negatively regulates Scar/WAVE-Arp2/3 activity and inhibits lamellipodia stability and cell migration. *Nature Communications*, *12*(1). https://doi.org/10.1038/s41467-021-25916-6

Lebensohn, A. M., & Kirschner, M. W. (2009). Activation of the WAVE Complex by Coincident Signals Controls Actin Assembly. *Molecular Cell*, *36*(3), 512–524. https://doi.org/10.1016/j.molcel.2009.10.024

Lebestky, T., Chang, T., Hartenstein, V., & Banerjee, U. (2000). Specification of Drosophila Hematopoietic Lineage by Conserved Transcription Factors. *Science*, *288*(5463), 146–149. https://doi.org/10.1126/science.288.5463.146

Legent, K., Steinhauer, J., Richard, M., & Treisman, J. E. (2012). A Screen for X-Linked Mutations Affecting Drosophila Photoreceptor Differentiation Identifies Casein Kinase 1α as an Essential Negative Regulator of Wingless Signaling. *Genetics*, *190*(2), 601–616. https://doi.org/10.1534/genetics.111.133827

Lehmann, M. (1996). Drosophila Sgs genes: Stage and tissue specificity of hormone responsiveness. *BioEssays*, *18*(1), 47–54. https://doi.org/10.1002/bies.950180110

Lehne, F., Pokrant, T., Parbin, S., Salinas, G., Großhans, J., Rust, K., Faix, J., & Bogdan, S. (2022). Calcium bursts allow rapid reorganization of EFhD2/Swip-1 cross-linked actin networks in epithelial wound closure. *Nature Communications*, *13*(1), 2492. https://doi.org/10.1038/s41467-022-30167-0

Leitão, A. B., Arunkumar, R., Day, J. P., Geldman, E. M., Morin-Poulard, I., Crozatier, M., & Jiggins, F. M. (2020). Constitutive activation of cellular immunity underlies the evolution of resistance to infection in Drosophila. *ELife*, *9*, 1–24. https://doi.org/10.7554/eLife.59095

Lemaitre, B., & Hoffmann, J. (2007). The Host Defense of Drosophila

melanogaster. *Annual Review of Immunology*, *25*(1), 697–743. https://doi.org/10.1146/annurev.immunol.25.022106.141615

Leng, Y., Zhang, J., Badour, K., Arpaia, E., Freeman, S., Cheung, P., Siu, M., & Siminovitch, K. (2005). Abelson-interactor-1 promotes WAVE2 membrane translocation and Abelson-mediated tyrosine phosphorylation required for WAVE2 activation. *Proceedings of the National Academy of Sciences*, *102*(4), 1098–1103. https://doi.org/10.1073/pnas.0409120102

Lenz, J., Liefke, R., Funk, J., Shoup, S., Nist, A., Stiewe, T., Schulz, R., Tokusumi, Y., Albert, L., Raifer, H., Förstemann, K., Vázquez, O., Tokusumi, T., Fossett, N., & Brehm, A. (2021). Ush regulates hemocyte-specific gene expression, fatty acid metabolism and cell cycle progression and cooperates with dNuRD to orchestrate hematopoiesis. *PLOS Genetics*, *17*(2), e1009318. https://doi.org/10.1371/journal.pgen.1009318

Letourneau, M., Lapraz, F., Sharma, A., Vanzo, N., Waltzer, L., & Crozatier, M. (2016). Drosophila hematopoiesis under normal conditions and in response to immune stress. *FEBS Letters*, *590*(22), 4034–4051. https://doi.org/10.1002/1873-3468.12327

Li, A., Gao, X., Ren, J., Jin, C., & Xue, Y. (2006). *BDM-PUB: Computational Prediction of Protein Ubiquitination Sites with a Bayesian Discriminant Method*. http://bdmpub.biocuckoo.org/

Li, H., Janssens, J., De Waegeneer, M., Kolluru, S. S., Davie, K., Gardeux, V., Saelens, W., David, F. P. A., Brbić, M., Spanier, K., Leskovec, J., McLaughlin, C. N., Xie, Q., Jones, R. C., Brueckner, K., Shim, J., Tattikota, S. G., Schnorrer, F., Rust, K., … Zinzen, R. P. (2022). Fly Cell Atlas: A single-nucleus transcriptomic atlas of the adult fruit fly. *Science*, *375*(6584). https://doi.org/10.1126/science.abk2432

Ligoxygakis, P., Pelte, N., Hoffmann, J. A., & Reichhart, J. M. (2002). Activation of Drosophila toll during fungal infection by a blood serine protease. *Science*, *297*(5578), 114–116. https://doi.org/10.1126/science.1072391

Ligoxygakis, P., Pelte, N., Ji, C., Leclerc, V., Duvic, B., Belvin, M., Jiang, H., Hoffmann, J. A., & Reichhart, J. M. (2002). A serpin mutant links Toll

activation to melanization in the host defence of Drosophila. *EMBO Journal*, *21*(23), 6330–6337. https://doi.org/10.1093/emboj/cdf661

Liu, Y., Liu, H., Liu, S., Wang, S., Jiang, R. J., & Li, S. (2009). Hormonal and nutritional regulation of insect fat body development and function. *Archives of Insect Biochemistry and Physiology*, *71*(1), 16–30. https://doi.org/10.1002/arch.20290

Louradour, I., Sharma, A., Morin-Poulard, I., Letourneau, M., Vincent, A., Crozatier, M., & Vanzo, N. (2017). Reactive oxygen species-dependent Toll/NF-κB activation in the Drosophila hematopoietic niche confers resistance to wasp parasitism. *ELife*, *6*, 1–22. https://doi.org/10.7554/eLife.25496

Lundgren, J., Masson, P., Mirzaei, Z., & Young, P. (2005). Identification and Characterization of a Drosophila Proteasome Regulatory Network. *Molecular and Cellular Biology*, *25*(11), 4662–4675. https://doi.org/10.1128/MCB.25.11.4662-4675.2005

Luo, F., Yu, S., & Jin, L. H. (2020). The Posterior Signaling Center Is an Important Microenvironment for Homeostasis of the Drosophila Lymph Gland. *Frontiers in Cell and Developmental Biology*, *8*(May), 1–15. https://doi.org/10.3389/fcell.2020.00382

Machesky, L. M., & Insall, R. H. (1998). Scar1 and the related Wiskott-Aldrich syndrome protein, WASP, regulate the actin cytoskeleton through the Arp2/3 complex. *Current Biology*, *8*(25), 1347–1356. https://doi.org/10.1016/S0960-9822(98)00015-3

Machesky, L. M., Mullins, R. D., Higgs, H. N., Kaiser, D. A., Blanchoin, L., May, R. C., Hall, M. E., & Pollard, T. D. (1999). Scar, a WASp-related protein, activates nucleation of actin filaments by the Arp2/3 complex. *Proceedings of the National Academy of Sciences of the United States of America*, *96*(7), 3739–3744. https://doi.org/10.1073/pnas.96.7.3739

Makhijani, K., Alexander, B., Tanaka, T., Rulifson, E., & Brückner, K. (2011). The peripheral nervous system supports blood cell homing and survival in the Drosophila larva. *Development*, *138*(24), 5379–5391.

https://doi.org/10.1242/dev.067322

Makki, R., Meister, M., Pennetier, D., Ubeda, J.-M., Braun, A., Daburon, V., Krzemień, J., Bourbon, H.-M., Zhou, R., Vincent, A., & Crozatier, M. (2010). A Short Receptor Downregulates JAK/STAT Signalling to Control the Drosophila Cellular Immune Response. *PLoS Biology*, *8*(8), e1000441. https://doi.org/10.1371/journal.pbio.1000441

Malinda, K. M., Fisher, G. W., & Ettensohn, C. A. (1995). Four-Dimensional Microscopic Analysis of the Filopodial Behavior of Primary Mesenchyme Cells during Gastrulation in the Sea Urchin Embryo. *Developmental Biology*, *172*(2), 552–566. https://doi.org/10.1006/dbio.1995.8044

Mandal, L., Banerjee, U., & Hartenstein, V. (2004). Evidence for a fruit fly hemangioblast and similarities between lymph-gland hematopoiesis in fruit fly and mammal aorta-gonadal-mesonephros mesoderm. *Nature Genetics*, *36*(9), 1019–1023. https://doi.org/10.1038/ng1404

Mandal, L., Martinez-Agosto, J. A., Evans, C. J., Hartenstein, V., & Banerjee, U. (2007). A Hedgehog- and Antennapedia-dependent niche maintains Drosophila haematopoietic precursors. *Nature*, *446*(7133), 320–324. https://doi.org/10.1038/nature05585

Manz, M. G., & Boettcher, S. (2014). Emergency granulopoiesis. *Nature Reviews Immunology*, *14*(5), 302–314. https://doi.org/10.1038/nri3660

Marchand, J. B., Kaiser, D. A., Pollard, T. D., & Higgs, H. N. (2001). Interaction of WASP/Scar proteins with actin and vertebrate Arp2/3 complex. *Nature Cell Biology*, *3*(1), 76–82. https://doi.org/10.1038/35050590

Marin, O., Bustos, V. H., Cesaro, L., Meggio, F., Pagano, M. A., Antonelli, M., Allende, C. C., Pinna, L. A., & Allende, J. E. (2003). A noncanonical sequence phosphorylated by casein kinase 1 in β-catenin may play a role in casein kinase 1 targeting of important signaling proteins. *Proceedings of the National Academy of Sciences*, *100*(18), 10193–10200. https://doi.org/10.1073/pnas.1733909100

Marin, O., MEGGIO, F., SARNO, S., ANDRETTA, M., & PINNA, L. A. (1994). Phosphorylation of synthetic fragments of inhibitor-2 of protein

phosphatase-1 by casein kinase-1 and -2. Evidence that phosphorylated residues are not strictly required for efficient targeting by casein kinase-1. *European Journal of Biochemistry*, *223*(2), 647–653. https://doi.org/10.1111/j.1432-1033.1994.tb19037.x

Martínez, B. A., Hoyle, R. G., Yeudall, S., Granade, M. E., Harris, T. E., David Castle, J., Leitinger, N., & Bland, M. L. (2020). Innate immune signaling in Drosophila shifts anabolic lipid metabolism from triglyceride storage to phospholipid synthesis to support immune function. In *PLoS Genetics* (Vol. 16, Issue 11). https://doi.org/10.1371/journal.pgen.1009192

Massaad, M. J., Ramesh, N., & Geha, R. S. (2013). Wiskott-Aldrich syndrome: a comprehensive review. *Annals of the New York Academy of Sciences*, *1285*(1), 26–43. https://doi.org/10.1111/nyas.12049

Matsubayashi, Y., Louani, A., Dragu, A., Sánchez-Sánchez, B. J., Serna-Morales, E., Yolland, L., Gyoergy, A., Vizcay, G., Fleck, R. A., Heddleston, J. M., Chew, T.-L., Siekhaus, D. E., & Stramer, B. M. (2017). A Moving Source of Matrix Components Is Essential for De Novo Basement Membrane Formation. *Current Biology*, *27*(22), 3526-3534.e4. https://doi.org/10.1016/j.cub.2017.10.001

Mattila, P. K., & Lappalainen, P. (2008). Filopodia: Molecular architecture and cellular functions. *Nature Reviews Molecular Cell Biology*, *9*(6), 446–454. https://doi.org/10.1038/nrm2406

Matyskiela, M. E., Lander, G. C., & Martin, A. (2013). Conformational switching of the 26S proteasome enables substrate degradation. *Nature Structural & Molecular Biology*, *20*(7), 781–788. https://doi.org/10.1038/nsmb.2616

McNally, A. K., & Anderson, J. M. (2011). *Macrophage Fusion and Multinucleated Giant Cells of Inflammation* (pp. 97–111). https://doi.org/10.1007/978-94-007-0763-4_7

Medzhitov, R. (2007). Recognition of microorganisms and activation of the immune response. *Nature*, *449*(7164), 819–826. https://doi.org/10.1038/nature06246

Medzhitov, R., & Janeway, C. (2000). Innate Immunity. *New England Journal of*

Medicine, *343*(5), 338–344. https://doi.org/10.1056/NEJM200008033430506

Mendoza, M. C. (2013). Phosphoregulation of the WAVE regulatory complex and signal integration. *Seminars in Cell and Developmental Biology*, *24*(4), 272–279. https://doi.org/10.1016/j.semcdb.2013.01.007

Mendoza, M. C., Er, E. E., Zhang, W., Ballif, B. A., Elliott, H. L., Danuser, G., & Blenis, J. (2011). ERK-MAPK Drives Lamellipodia Protrusion by Activating the WAVE2 Regulatory Complex. *Molecular Cell*, *41*(6), 661–671. https://doi.org/10.1016/j.molcel.2011.02.031

Miki, H., Miura, K., & Takenawa, T. (1996). N-WASP, a novel actin-depolymerizing protein, regulates the cortical cytoskeletal rearrangement in a PIP2-dependent manner downstream of tyrosine kinases. *EMBO Journal*, *15*(19), 5326–5335. https://doi.org/10.1002/j.1460-2075.1996.tb00917.x

Miki, H., Suetsugu, S., & Takenawa, T. (1998). WAVE, a novel WASP-family protein involved in actin reorganization induced by Rac. *EMBO Journal*, *17*(23), 6932–6941. https://doi.org/10.1093/emboj/17.23.6932

Mogilner, A., & Oster, G. (1996). Cell motility driven by actin polymerization. *Biophysical Journal*, *71*(6), 3030–3045. https://doi.org/10.1016/S0006-3495(96)79496-1

Molina, I. J., Kenney, D. M., Rosen, F. S., & Remold-O'donnell, E. (1992). T cell lines characterize events in the pathogenesis of the wiskott-aldrich syndrome. *Journal of Experimental Medicine*, *176*(3), 867–874. https://doi.org/10.1084/jem.176.3.867

Morin-Poulard, I., Tian, Y., Vanzo, N., & Crozatier, M. (2021). Drosophila as a Model to Study Cellular Communication Between the Hematopoietic Niche and Blood Progenitors Under Homeostatic Conditions and in Response to an Immune Stress. *Frontiers in Immunology*, *12*. https://doi.org/10.3389/fimmu.2021.719349

Mullins, R. D., Heuser, J. A., & Pollard, T. D. (1998). The interaction of Arp2/3 complex with actin: Nucleation, high affinity pointed end capping, and formation of branching networks of filaments. *Proceedings of the National*

Academy of Sciences, *95*(11), 6181–6186. https://doi.org/10.1073/pnas.95.11.6181

Muratoglu, S., Hough, B., Mon, S. T., & Fossett, N. (2007). The GATA factor Serpent cross-regulates lozenge and u-shaped expression during Drosophila blood cell development. *Developmental Biology*, *311*(2), 636–649. https://doi.org/10.1016/j.ydbio.2007.08.015

Nadkarni, A. V., & Brieher, W. M. (2014). Aip1 destabilizes cofilin-saturated actin filaments by severing and accelerating monomer dissociation from ends. *Current Biology*, *24*(23), 2749–2757. https://doi.org/10.1016/j.cub.2014.09.048

Nagel, B. (2018). *The role of Drosophila WASH and its interaction partner CCDC22 in endosomal trafficking*.

Nagel, B. M., Bechtold, M., Rodriguez, L. G., & Bogdan, S. (2017). Drosophila WASH is required for integrin-mediated cell adhesion, cell motility and lysosomal neutralization. *Journal of Cell Science*, *130*(2), 344–359. https://doi.org/10.1242/jcs.193086

Nakamura-Ishizu, A., Ito, K., & Suda, T. (2020). Hematopoietic Stem Cell Metabolism during Development and Aging. *Developmental Cell*, *54*(2), 239–255. https://doi.org/10.1016/j.devcel.2020.06.029

Nakanishi, O., Suetsugu, S., Yamazaki, D., & Takenawa, T. (2006). Effect of WAVE2 Phosphorylation on Activation of the Arp2/3 Complex. *Journal of Biochemistry*, *141*(3), 319–325. https://doi.org/10.1093/jb/mvm034

Nappi, A. J., & Carton, Y. (2001). Immunogenetic aspects of the cellular immune response of Drosophila against parasitoids. *Immunogenetics*, *52*(3–4), 157–164. https://doi.org/10.1007/s002510000272

Nelson, R. E., Fessler, L. I., Takagi, Y., Blumberg, B., Keene, D. R., Olson, P. F., Parker, C. G., & Fessler, J. H. (1994). Peroxidasin: a novel enzyme-matrix protein of Drosophila development. *The EMBO Journal*, *13*(15), 3438–3447. https://doi.org/10.1002/j.1460-2075.1994.tb06649.x

O'Neill, L. A. J., & Pearce, E. J. (2016). Immunometabolism governs dendritic cell and macrophage function. *Journal of Experimental Medicine*, *213*(1),

15–23. https://doi.org/10.1084/jem.20151570

Oikawa, T., Yamaguchi, H., Itoh, T., Kato, M., Ijuin, T., Yamazaki, D., Suetsugu, S., & Takenawa, T. (2004). PtdIns(3,4,5)P3 binding is necessary for WAVE2-induced formation of lamellipodia. *Nature Cell Biology*, *6*(5), 420–426. https://doi.org/10.1038/ncb1125

Orange, J. S., Ramesh, N., Remold-O'Donnell, E., Sasahara, Y., Koopman, L., Byrne, M., Bonilla, F. A., Rosen, F. S., Geha, R. S., & Strominger, J. L. (2002). Wiskott-Aldrich syndrome protein is required for NK cell cytotoxicity and colocalizes with actin to NK cell-activating immunologic synapses. *Proceedings of the National Academy of Sciences of the United States of America*, *99*(17), 11351–11356. https://doi.org/10.1073/pnas.162376099

Oyallon, J., Vanzo, N., Krzemień, J., Morin-Poulard, I., Vincent, A., & Crozatier, M. (2016). Two Independent Functions of Collier/Early B Cell Factor in the Control of Drosophila Blood Cell Homeostasis. *PLOS ONE*, *11*(2), e0148978. https://doi.org/10.1371/journal.pone.0148978

Padrick, S. B., Cheng, H.-C., Ismail, A. M., Panchal, S. C., Doolittle, L. K., Kim, S., Skehan, B. M., Umetani, J., Brautigam, C. A., Leong, J. M., & Rosen, M. K. (2008). Hierarchical Regulation of WASP/WAVE Proteins. *Molecular Cell*, *32*(3), 426–438. https://doi.org/10.1016/j.molcel.2008.10.012

Padrick, S. B., Doolittle, L. K., Brautigam, C. A., King, D. S., & Rosen, M. K. (2011). Arp2/3 complex is bound and activated by two WASP proteins. *Proceedings of the National Academy of Sciences of the United States of America*, *108*(33), 472–479. https://doi.org/10.1073/pnas.1100236108

Padrick, S. B., & Rosen, M. K. (2010). Physical Mechanisms of Signal Integration by WASP Family Proteins. *Annual Review of Biochemistry*, *79*(1), 707–735. https://doi.org/10.1146/annurev.biochem.77.060407.135452

Pennetier, D., Oyallon, J., Morin-Poulard, I., Dejean, S., Vincent, A., & Crozatier, M. (2012). Size control of the Drosophila hematopoietic niche by bone morphogenetic protein signaling reveals parallels with mammals. *Proceedings of the National Academy of Sciences*, *109*(9), 3389–3394.

https://doi.org/10.1073/pnas.1109407109

Petraki, S., Alexander, B., & Brückner, K. (2015). Assaying Blood Cell Populations of the Drosophila melanogaster Larva. *Journal of Visualized Experiments*, *105*. https://doi.org/10.3791/52733

Pettersen, E. F., Goddard, T. D., Huang, C. C., Meng, E. C., Couch, G. S., Croll, T. I., Morris, J. H., & Ferrin, T. E. (2021). <scp>UCSF ChimeraX</scp> : Structure visualization for researchers, educators, and developers. *Protein Science*, *30*(1), 70–82. https://doi.org/10.1002/pro.3943

Pfisterer, K., Levitt, J., Lawson, C. D., Marsh, R. J., Heddleston, J. M., Wait, E., Ameer-Beg, S. M., Cox, S., & Parsons, M. (2020). FMNL2 regulates dynamics of fascin in filopodia. *Journal of Cell Biology*, *219*(5). https://doi.org/10.1083/jcb.201906111

Pinna, L. A. (1994). A historical view of protein kinase CK2. *Cellular & Molecular Biology Research*, *40*(5–6), 383–390. http://www.ncbi.nlm.nih.gov/pubmed/7735312

Pinto-Costa, R., & Sousa, M. M. (2020). Profilin as a dual regulator of actin and microtubule dynamics. *Cytoskeleton*, *77*(3–4), 76–83. https://doi.org/10.1002/cm.21586

Pocha, S. M., & Cory, G. O. (2009). WAVE2 is regulated by multiple phosphorylation events within its VCA domain. *Cell Motility and the Cytoskeleton*, *66*(1), 36–47. https://doi.org/10.1002/cm.20323

Pollard, T. D. (2016). Actin and Actin-Binding Proteins. *Cold Spring Harbor Perspectives in Biology*, *8*(8), a018226. https://doi.org/10.1101/cshperspect.a018226

Pollard, T. D., & Borisy, G. G. (2003). Cellular Motility Driven by Assembly and Disassembly of Actin Filaments. *Cell*, *112*(4), 453–465. https://doi.org/10.1016/S0092-8674(03)00120-X

Prakash, S., Tian, L., Ratliff, K. S., Lehotzky, R. E., & Matouschek, A. (2004). An unstructured initiation site is required for efficient proteasome-mediated degradation. *Nature Structural and Molecular Biology*, *11*(9), 830–837. https://doi.org/10.1038/nsmb814

Price, M. A. (2006). CKI, there's more than one: casein kinase I family members in Wnt and Hedgehog signaling. *Genes & Development*, *20*(4), 399–410. https://doi.org/10.1101/gad.1394306

Pulgar, V., Marin, O., Meggio, F., Allende, C. C., Allende, J. E., & Pinna, L. A. (1999). Optimal sequences for non-phosphate-directed phoshorylation by protein kinase CK1 (casein kinase-1) - a re-evaluation. *European Journal of Biochemistry*, *260*(2), 520–526. https://doi.org/10.1046/j.1432-1327.1999.00195.x

Rashkovan, M., & Ferrando, A. (2019). Metabolic dependencies and vulnerabilities in leukemia. *Genes & Development*, *33*(21–22), 1460–1474. https://doi.org/10.1101/gad.326470.119

Regan, J. C., Brandão, A. S., Leitão, A. B., Mantas Dias, Â. R., Sucena, É., Jacinto, A., & Zaidman-Rémy, A. (2013). Steroid Hormone Signaling Is Essential to Regulate Innate Immune Cells and Fight Bacterial Infection in Drosophila. *PLoS Pathogens*, *9*(10), e1003720. https://doi.org/10.1371/journal.ppat.1003720

Rehorn, K. P., Thelen, H., Michelson, A. M., & Reuter, R. (1996). A molecular aspect of hematopoiesis and endoderm development common to vertebrates and Drosophila. *Development*, *122*(12), 4023–4031. https://doi.org/10.1242/dev.122.12.4023

Reicher, B., Joseph, N., David, A., Pauker, M. H., Perl, O., & Barda-Saad, M. (2012). Ubiquitylation-Dependent Negative Regulation of WASp Is Essential for Actin Cytoskeleton Dynamics. *Molecular and Cellular Biology*, *32*(15), 3153–3163. https://doi.org/10.1128/MCB.00161-12

Rivers, A., Gietzen, K. F., Vielhaber, E., & Virshup, D. M. (1998). Regulation of Casein Kinase I ε and Casein Kinase I δ by anin Vivo Futile Phosphorylation Cycle. *Journal of Biological Chemistry*, *273*(26), 15980–15984. https://doi.org/10.1074/jbc.273.26.15980

Rizki, T. M. (1962). Experimental Analysis of Hemocyte Morphology in Insects. *American Zoologist*, *2*(2), 247–256. http://www.jstor.org/stable/3881212

Rodrigues, D., Renaud, Y., VijayRaghavan, K., Waltzer, L., & Inamdar, M. S.

(2021). Differential activation of JAK-STAT signaling reveals functional compartmentalization in Drosophila blood progenitors. *ELife*, *10*. https://doi.org/10.7554/eLife.61409

Rogers, S. L., Wiedemann, U., Stuurman, N., & Vale, R. D. (2003). Molecular requirements for actin-based lamella formation in Drosophila S2 cells. *Journal of Cell Biology*, *162*(6), 1079–1088. https://doi.org/10.1083/jcb.200303023

Rottner, K., Hänisch, J., & Campellone, K. G. (2010). WASH, WHAMM and JMY: regulation of Arp2/3 complex and beyond. *Trends in Cell Biology*, *20*(11), 650–661. https://doi.org/10.1016/j.tcb.2010.08.014

Rottner, K., & Schaks, M. (2019). Assembling actin filaments for protrusion. *Current Opinion in Cell Biology*, *56*, 53–63. https://doi.org/10.1016/J.CEB.2018.09.004

Rottner, K., Stradal, T. E. B., & Chen, B. (2021). WAVE regulatory complex. *Current Biology*, *31*(10), R512–R517. https://doi.org/10.1016/j.cub.2021.01.086

Rotty, J. D. (2020). Actin Cytoskeleton: Profilin Gives Cells an Edge. *Current Biology*, *30*(14), R807–R809. https://doi.org/10.1016/j.cub.2020.05.041

Rotty, J. D., Wu, C., & Bear, J. E. (2013). New insights into the regulation and cellular functions of the ARP2/3 complex. *Nature Reviews Molecular Cell Biology*, *14*(1), 7–12. https://doi.org/10.1038/nrm3492

Russo, J., Brehélin, M., & Carton, Y. (2001). Haemocyte changes in resistant and susceptible strains of D. melanogaster caused by virulent and avirulent strains of the parasitic wasp Leptopilina boulardi. *Journal of Insect Physiology*, *47*(2), 167–172. https://doi.org/10.1016/S0022-1910(00)00102-5

Russo, J., Dupas, S., Frey, F., Carton, Y., & Brehelin, M. (1996). Insect immunity: early events in the encapsulation process of parasitoid (Leptopilina boulardi) eggs in resistant and susceptible strains of Drosophila. *Parasitology*, *112*(1), 135–142. https://doi.org/10.1017/S0031182000065173

Rust, K., Byrnes, L. E., Yu, K. S., Park, J. S., Sneddon, J. B., Tward, A. D., & Nystul, T. G. (2020). A single-cell atlas and lineage analysis of the adult Drosophila ovary. *Nature Communications*, *11*(1), 1–17. https://doi.org/10.1038/s41467-020-19361-0

Saeki, Y. (2017). Ubiquitin recognition by the proteasome. *Journal of Biochemistry*, mvw091. https://doi.org/10.1093/jb/mvw091

Sanchez Bosch, P., Makhijani, K., Herboso, L., Gold, K. S., Baginsky, R., Woodcock, K. J., Alexander, B., Kukar, K., Corcoran, S., Jacobs, T., Ouyang, D., Wong, C., Ramond, E. J. V., Rhiner, C., Moreno, E., Lemaitre, B., Geissmann, F., & Brückner, K. (2019). Adult Drosophila Lack Hematopoiesis but Rely on a Blood Cell Reservoir at the Respiratory Epithelia to Relay Infection Signals to Surrounding Tissues. *Developmental Cell*, *51*(6), 787-803.e5. https://doi.org/10.1016/j.devcel.2019.10.017

Santos, J. a, Logarinho, E., Tapia, C., Allende, C. C., Allende, J. E., & Sunkel, C. E. (1996). The casein kinase 1 alpha gene of Drosophila melanogaster is developmentally regulated and the kinase activity of the protein induced by DNA damage. *Journal of Cell Science*, *109 (Pt 7*, 1847–1856. http://www.ncbi.nlm.nih.gov/pubmed/8832407

Sarikas, A., Hartmann, T., & Pan, Z.-Q. (2011). The cullin protein family. *Genome Biology*, *12*(4), 220. https://doi.org/10.1186/gb-2011-12-4-220

Schaks, M., Giannone, G., & Rottner, K. (2019). Actin dynamics in cell migration. *Essays in Biochemistry*, *63*(5), 483–495. https://doi.org/10.1042/EBC20190015

Schmitt, M., Schewe, M., Sacchetti, A., Feijtel, D., van de Geer, W. S., Teeuwssen, M., Sleddens, H. F., Joosten, R., van Royen, M. E., van de Werken, H. J. G., van Es, J., Clevers, H., & Fodde, R. (2018). Paneth Cells Respond to Inflammation and Contribute to Tissue Regeneration by Acquiring Stem-like Features through SCF/c-Kit Signaling. *Cell Reports*, *24*(9), 2312-2328.e7. https://doi.org/10.1016/j.celrep.2018.07.085

Sears, H. C., Kennedy, C. J., & Garrity, P. A. (2003). Macrophage-mediated corpse engulfment is required for normal Drosophila CNS morphogenesis.

Development, *130*(15), 3557–3565. https://doi.org/10.1242/dev.00586

Shokal, U., & Eleftherianos, I. (2017a). Thioester-Containing Protein-4 Regulates the Drosophila Immune Signaling and Function against the Pathogen Photorhabdus. *Journal of Innate Immunity*, *9*(1), 83–93. https://doi.org/10.1159/000450610

Shokal, U., & Eleftherianos, I. (2017b). Evolution and Function of Thioester-Containing Proteins and the Complement System in the Innate Immune Response. *Frontiers in Immunology*, *8*. https://doi.org/10.3389/fimmu.2017.00759

Shresthaa, R., & Gateff, E. (1982). Ultrastructure and Cytochemistry of the Cell Types in the Larval Hematopoietic Organs and Hemolymph of Drosophila Melanogaster. (drosophila/hematopoiesis/blool cells/ultrastructure/cytochemistry). *Development, Growth and Differentiation*, *24*(1), 65–82. https://doi.org/10.1111/j.1440-169X.1982.00065.x

Sinenko, S. A., & Mathey-Prevot, B. (2004). Increased expression of Drosophila tetraspanin, Tsp68C, suppresses the abnormal proliferation of ytr-deficient and Ras/Raf-activated hemocytes. *Oncogene*, *23*(56), 9120–9128. https://doi.org/10.1038/sj.onc.1208156

Sinenko, S. A., Shim, J., & Banerjee, U. (2012). Oxidative stress in the haematopoietic niche regulates the cellular immune response in Drosophila. *EMBO Reports*, *13*(1), 83–89. https://doi.org/10.1038/embor.2011.223

Singh, S. P., & Insall, R. H. (2021). Adhesion stimulates Scar/WAVE phosphorylation in mammalian cells. *Communicative and Integrative Biology*, *14*(1), 1–4. https://doi.org/10.1080/19420889.2020.1855854

Singh, S. P., Thomason, P. A., & Insall, R. H. (2021). Extracellular signalling modulates scar/wave complex activity through abi phosphorylation. *Cells*, *10*(12). https://doi.org/10.3390/cells10123485

Skruber, K., Warp, P. V., Shklyarov, R., Thomas, J. D., Swanson, M. S., Henty-Ridilla, J. L., Read, T. A., & Vitriol, E. A. (2020). Arp2/3 and Mena/VASP

Require Profilin 1 for Actin Network Assembly at the Leading Edge. *Current Biology*, *30*(14), 2651-2664.e5. https://doi.org/10.1016/j.cub.2020.04.085

Sossey-Alaoui, K., Safina, A., Li, X., Vaughan, M. M., Hicks, D. G., Bakin, A. V., & Cowell, J. K. (2007). Down-Regulation of WAVE3, a Metastasis Promoter Gene, Inhibits Invasion and Metastasis of Breast Cancer Cells. *The American Journal of Pathology*, *170*(6), 2112–2121. https://doi.org/10.2353/ajpath.2007.060975

Steffen, A., Rottner, K., Ehinger, J., Innocenti, M., Scita, G., Wehland, J., & Stradal, T. E. B. (2004). Sra-1 and Nap1 link Rac to actin assembly driving lamellipodia formation. *The EMBO Journal*, *23*(4), 749–759. https://doi.org/10.1038/sj.emboj.7600084

Stradal, T. E. B., Rottner, K., Disanza, A., Confalonieri, S., Innocenti, M., & Scita, G. (2004). Regulation of actin dynamics by WASP and WAVE family proteins. *Trends in Cell Biology*, *14*(6), 303–311. https://doi.org/10.1016/j.tcb.2004.04.007

Suetsugu, S., Miki, H., & Takenawa, T. (1999). Identification of two human WAVE/SCAR homologues as general actin regulatory molecules which associate with the Arp2/3 complex. *Biochemical and Biophysical Research Communications*, *260*(1), 296–302. https://doi.org/10.1006/bbrc.1999.0894

Svitkina, T. (2018). The actin cytoskeleton and actin-based motility. *Cold Spring Harbor Perspectives in Biology*, *10*(1). https://doi.org/10.1101/cshperspect.a018267

Svitkina, T. M., Bulanova, E. A., Chaga, O. Y., Vignjevic, D. M., Kojima, S., Vasiliev, J. M., & Borisy, G. G. (2003). Mechanism of filopodia initiation by reorganization of a dendritic network. *The Journal of Cell Biology*, *160*(3), 409–421. https://doi.org/10.1083/jcb.200210174

T., B. (2002). Origin and evolution of arthropod hemocyanins and related proteins. *Journal of Comparative Physiology B: Biochemical, Systemic, and Environmental Physiology*, *172*(2), 95–107. https://doi.org/10.1007/s00360-001-0247-7

Takenawa, T., & Suetsugu, S. (2007). The WASP-WAVE protein network:

Connecting the membrane to the cytoskeleton. *Nature Reviews Molecular Cell Biology*, *8*(1), 37–48. https://doi.org/10.1038/nrm2069

Tattikota, S. G., Cho, B., Liu, Y., Hu, Y., Barrera, V., Steinbaugh, M. J., Yoon, S.-H., Comjean, A., Li, F., Dervis, F., Hung, R.-J., Nam, J.-W., Ho Sui, S., Shim, J., & Perrimon, N. (2020). A single-cell survey of Drosophila blood. *ELife*, *9*. https://doi.org/10.7554/eLife.54818

Tepass, U., Fessler, L. I., Aziz, A., & Hartenstein, V. (1994). Embryonic origin of hemocytes and their relationship to cell death in Drosophila. *Development*, *120*(7), 1829–1837. https://doi.org/10.1242/dev.120.7.1829

Tevosian, S. G., Deconinck, A. E., Cantor, A. B., Rieff, H. I., Fujiwara, Y., Corfas, G., & Orkin, S. H. (1999). FOG-2: A novel GATA-family cofactor related to multitype zinc-finger proteins Friend of GATA-1 and U-shaped. *Proceedings of the National Academy of Sciences*, *96*(3), 950–955. https://doi.org/10.1073/pnas.96.3.950

Tiwari, S. K., Toshniwal, A. G., Mandal, S., & Mandal, L. (2020). Fatty acid β-oxidation is required for the differentiation of larval hematopoietic progenitors in Drosophila. *ELife*, *9*. https://doi.org/10.7554/eLife.53247

Tokusumi, T., Sorrentino, R. P., Russell, M., Ferrarese, R., Govind, S., & Schulz, R. A. (2009). Characterization of a Lamellocyte Transcriptional Enhancer Located within the misshapen Gene of Drosophila melanogaster. *PLoS ONE*, *4*(7), e6429. https://doi.org/10.1371/journal.pone.0006429

Trapnell, C., Cacchiarelli, D., Grimsby, J., Pokharel, P., Li, S., Morse, M., Lennon, N. J., Livak, K. J., Mikkelsen, T. S., & Rinn, J. L. (2014). The dynamics and regulators of cell fate decisions are revealed by pseudotemporal ordering of single cells. *Nature Biotechnology*, *32*(4), 381–386. https://doi.org/10.1038/nbt.2859

Tuazon, P. T., & Traugh, J. A. (1991). Casein kinase I and II--multipotential serine protein kinases: structure, function, and regulation. *Advances in Second Messenger and Phosphoprotein Research*, *23*, 123–164. http://www.ncbi.nlm.nih.gov/pubmed/1997039

Tzou, P., Ohresser, S., Ferrandon, D., Capovilla, M., Reichhart, J.-M., Lemaitre,

B., Hoffmann, J. A., & Imler, J.-L. (2000). Tissue-Specific Inducible Expression of Antimicrobial Peptide Genes in Drosophila Surface Epithelia. *Immunity*, *13*(5), 737–748. https://doi.org/10.1016/S1074-7613(00)00072-8

Uhlén, M., Fagerberg, L., Hallström, B. M., Lindskog, C., Oksvold, P., Mardinoglu, A., Sivertsson, Å., Kampf, C., Sjöstedt, E., Asplund, A., Olsson, I., Edlund, K., Lundberg, E., Navani, S., Szigyarto, C. A.-K., Odeberg, J., Djureinovic, D., Takanen, J. O., Hober, S., … Pontén, F. (2015). Tissue-based map of the human proteome. *Science*, *347*(6220). https://doi.org/10.1126/science.1260419

Ura, S., Pollitt, A. Y., Veltman, D. M., Morrice, N. A., Machesky, L. M., & Insall, R. H. (2012). Pseudopod Growth and Evolution during Cell Movement Is Controlled through SCAR/WAVE Dephosphorylation. *Current Biology*, *22*(7), 553–561. https://doi.org/10.1016/j.cub.2012.02.020

Valanne, S., Wang, J.-H., & Rämet, M. (2011). The Drosophila Toll Signaling Pathway . *The Journal of Immunology*, *186*(2), 649–656. https://doi.org/10.4049/jimmunol.1002302

Vanha-Aho, L.-M., Anderl, I., Vesala, L., Hultmark, D., Valanne, S., & Rämet, M. (2015). Edin Expression in the Fat Body Is Required in the Defense Against Parasitic Wasps in Drosophila melanogaster. *PLOS Pathogens*, *11*(5), e1004895. https://doi.org/10.1371/journal.ppat.1004895

Vignjevic, D., Kojima, S. I., Aratyn, Y., Danciu, O., Svitkina, T., & Borisy, G. G. (2006). Role of fascin in filopodial protrusion. *Journal of Cell Biology*, *174*(6), 863–875. https://doi.org/10.1083/jcb.200603013

Vivancos, Roberto Bernardoni, V., & Giangrande, A. (1997). glide/gcmls Expressed and Required in the Scavenger Cell Lineage. *Developmental Biology*, *191*(1), 118–130. https://doi.org/10.1006/dbio.1997.8702

Vlisidou, I., & Wood, W. (2015). Drosophila blood cells and their role in immune responses. *FEBS Journal*, *282*(8), 1368–1382. https://doi.org/10.1111/febs.13235

Voog, J., Sandall, S. L., Hime, G. R., Resende, L. P. F., Loza-Coll, M., Aslanian, A., Yates, J. R., Hunter, T., Fuller, M. T., & Jones, D. L. (2014). Escargot

Restricts Niche Cell to Stem Cell Conversion in the Drosophila Testis. *Cell Reports*, *7*(3), 722–734. https://doi.org/10.1016/j.celrep.2014.04.025

Wakayama, Y., Fukuhara, S., Ando, K., Matsuda, M., & Mochizuki, N. (2015). Cdc42 mediates Bmp - Induced sprouting angiogenesis through Fmnl3-driven assembly of endothelial filopodia in zebrafish. *Developmental Cell*, *32*(1), 109–122. https://doi.org/10.1016/j.devcel.2014.11.024

Wan, B., Poirié, M., & Gatti, J. L. (2020). Parasitoid wasp venom vesicles (venosomes) enter Drosophila melanogaster lamellocytes through a flotillin/lipid raft-dependent endocytic pathway. *Virulence*, *11*(1), 1512–1521. https://doi.org/10.1080/21505594.2020.1838116

Wang, L., Lu, A., Zhou, H. X., Sun, R., Zhao, J., Zhou, C. J., Shen, J. P., Wu, S. N., & Liang, C. G. (2013). Casein Kinase 1 Alpha Regulates Chromosome Congression and Separation during Mouse Oocyte Meiotic Maturation and Early Embryo Development. *PLoS ONE*, *8*(5). https://doi.org/10.1371/journal.pone.0063173

Wang, P. C., Vancura, A., Mitcheson, T. G. M., & Kuret, J. (1992). Two genes in Saccharomyces cerevisiae encode a membrane-bound form of casein kinase-1. *Molecular Biology of the Cell*, *3*(3), 275–286. https://doi.org/10.1091/mbc.3.3.275

Watanabe, N., & Mitchison, T. J. (2002). Single-Molecule Speckle Analysis of Actin Filament Turnover in Lamellipodia. *Science*, *295*(5557), 1083–1086. https://doi.org/10.1126/science.1067470

Whitelaw, J. A., Lilla, S., Paul, N. R., Fort, L., Zanivan, S., & Machesky, L. M. (2019). CYRI/ Fam49 Proteins Represent a New Class of Rac1 Interactors. *Communicative and Integrative Biology*, *12*(1), 112–118. https://doi.org/10.1080/19420889.2019.1643665

Williams, M. J., Ando, I., & Hultmark, D. (2005). Drosophila melanogaster Rac2 is necessary for a proper cellular immune response. *Genes to Cells*, *10*(8), 813–823. https://doi.org/10.1111/j.1365-2443.2005.00883.x

Wood, W., Faria, C., & Jacinto, A. (2006). Distinct mechanisms regulate hemocyte chemotaxis during development and wound healing in

Drosophila melanogaster. *Journal of Cell Biology*, *173*(3), 405–416. https://doi.org/10.1083/jcb.200508161

Wood, W., & Jacinto, A. (2007). Drosophila melanogaster embryonic haemocytes: Masters of multitasking. *Nature Reviews Molecular Cell Biology*, *8*(7), 542–551. https://doi.org/10.1038/nrm2202

Xavier, M. J., & Williams, M. J. (2011). The Rho-Family GTPase Rac1 Regulates Integrin Localization in Drosophila Immunosurveillance Cells. *PLoS ONE*, *6*(5), e19504. https://doi.org/10.1371/journal.pone.0019504

Xue, Y., Li, A., Wang, L., Feng, H., & Yao, X. (2006). PPSP: prediction of PK-specific phosphorylation site with Bayesian decision theory. *BMC Bioinformatics*, *7*(1), 163. https://doi.org/10.1186/1471-2105-7-163

Yamashita, H., Ueda, K., & Kioka, N. (2011). WAVE2 forms a complex with PKA and is involved in PKA enhancement of membrane protrusions. *Journal of Biological Chemistry*, *286*(5), 3907–3914. https://doi.org/10.1074/jbc.M110.145409

Yang, L., Qiu, L., Fang, Q., Stanley, D. W., & Ye, G. (2021). Cellular and humoral immune interactions between Drosophila and its parasitoids. *Insect Science*, *28*(5), 1208–1227. https://doi.org/10.1111/1744-7917.12863

Yang, S., Tang, Y., Liu, Y., Brown, A. J., Schaks, M., Ding, B., Kramer, D. A., Mietkowska, M., Ding, L., Alekhina, O., Billadeau, D. D., Chowdhury, S., Wang, J., Rottner, K., & Chen, B. (2022). Arf GTPase activates the WAVE regulatory complex through a distinct binding site. *Science Advances*, *8*(50), 1–17. https://doi.org/10.1126/sciadv.add1412

Yasothornsrikul, S., Davis, W. J., Cramer, G., Kimbrell, D. A., & Dearolf, C. R. (1997). viking: identification and characterization of a second type IV collagen in Drosophila. *Gene*, *198*(1–2), 17–25. https://doi.org/10.1016/S0378-1119(97)00274-6

Younes, S., Al-Sulaiti, A., Nasser, E. A. A., Najjar, H., & Kamareddine, L. (2020). Drosophila as a Model Organism in Host–Pathogen Interaction Studies. *Frontiers in Cellular and Infection Microbiology*, *10*.

https://doi.org/10.3389/fcimb.2020.00214

Yu, Shichao, Luo, F., Xu, Y., Zhang, Y., & Jin, L. H. (2022). Drosophila Innate Immunity Involves Multiple Signaling Pathways and Coordinated Communication Between Different Tissues. *Frontiers in Immunology*, *13*(July), 1–23. https://doi.org/10.3389/fimmu.2022.905370

Yu, Shiyan, Tong, K., Zhao, Y., Balasubramanian, I., Yap, G. S., Ferraris, R. P., Bonder, E. M., Verzi, M. P., & Gao, N. (2018). Paneth Cell Multipotency Induced by Notch Activation following Injury. *Cell Stem Cell*, *23*(1), 46-59.e5. https://doi.org/10.1016/j.stem.2018.05.002

Zelenak, C., Eberhard, M., Jilani, K., Qadri, S. M., Macek, B., & Lang, F. (2012). Protein Kinase CK1α Regulates Erythrocyte Survival. *Cellular Physiology and Biochemistry*, *29*(1–2), 171–180. https://doi.org/10.1159/000337598

Zettervall, C.-J., Anderl, I., Williams, M. J., Palmer, R., Kurucz, E., Ando, I., & Hultmark, D. (2004). A directed screen for genes involved in Drosophila blood cell activation. *Proceedings of the National Academy of Sciences*, *101*(39), 14192–14197. https://doi.org/10.1073/pnas.0403789101

Zhang, J., Gross, S. D., Schroeder, M. D., & Anderson, R. A. (1996). Casein kinase I α and αL: Alternative splicing-generated kinases exhibit different catalytic properties. *Biochemistry*, *35*(50), 16319–16327. https://doi.org/10.1021/bi9614444

Zhang, L., Jia, J., Wang, B., Amanai, K., Wharton, K. A., & Jiang, J. (2006). Regulation of wingless signaling by the CKI family in Drosophila limb development. *Developmental Biology*, *299*(1), 221–237. https://doi.org/10.1016/j.ydbio.2006.07.025

Zhang, Q., Shi, Q., Chen, Y., Yue, T., Li, S., Wang, B., & Jiang, J. (2009). Multiple Ser/Thr-rich degrons mediate the degradation of Ci/Gli by the Cul3-HIB/SPOP E3 ubiquitin ligase. *Proceedings of the National Academy of Sciences of the United States of America*, *106*(50), 21191–21196. https://doi.org/10.1073/pnas.0912008106

Zhao, J. L., & Baltimore, D. (2015). Regulation of stress-induced hematopoiesis. *Current Opinion in Hematology*, *22*(4), 286–292.

https://doi.org/10.1097/MOH.0000000000000149

Zhao, X. Y., Xie, H. T., Duan, C. Y., Li, J., & Zhang, M. C. (2018). Rat limbal niche cells can induce transdifferentiation of oral mucosal epithelial cells into corneal epithelial-like cells in vitro. *Stem Cell Research and Therapy*, *9*(1), 1–16. https://doi.org/10.1186/s13287-018-0996-9

Zuchero, J. B., Belin, B., & Mullins, R. D. (2012). Actin binding to WH2 domains regulates nuclear import of the multifunctional actin regulator JMY. *Molecular Biology of the Cell*, *23*(5), 853–863. https://doi.org/10.1091/mbc.E11-12-0992

Zuchero, J. B., Coutts, A. S., Quinlan, M. E., La Thangue, N. B., & Mullins, R. D. (2009). p53-cofactor JMY is a multifunctional actin nucleation factor. *Nature Cell Biology*, *11*(4), 451–459. https://doi.org/10.1038/ncb1852

7. Appendix

7.1. Supplementary Figures

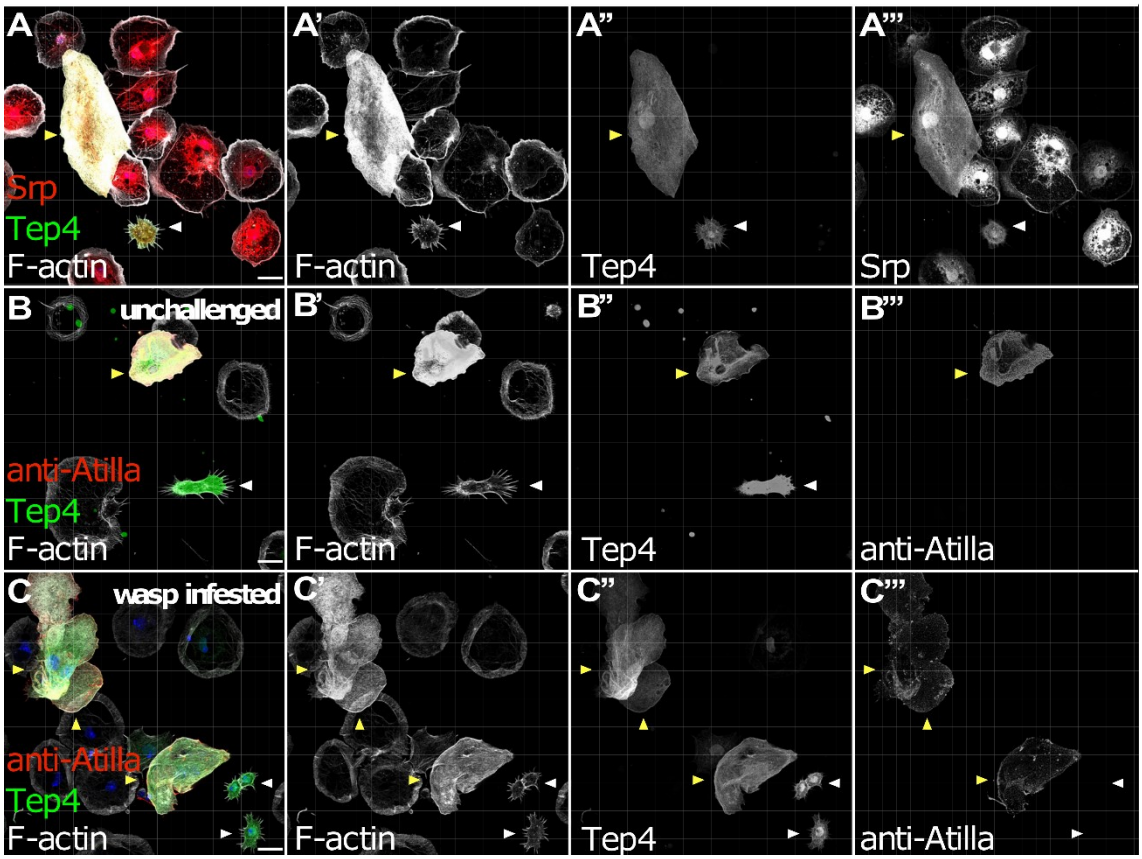

Supplementary Figure S 1 – Tep4 marks rare giant cells with lamellocyte morphology. *Maximum intensity projection of confocal images of pupal hemocytes; Alexa568-labeled phalloidin was used to stain the actin cytoskeleton. (A) Coexpression of srpHemo::3xmCherry and Tep4-Gal4 > UAS-GFP. Spiky small cells express the transcription factor srp. Tep4 and Srp double positive cells are marked by arrowheads. (B,C) Tep4-Gal4 > UAS-GFP cells were stained for the lamellocyte marker gene atilla (red) either in unchallenged condition (B) or upon wasp infestation (C). Large Tep4-expressing cells show characteristic lamellocyte morphology, marked by a yellow asterisk.*

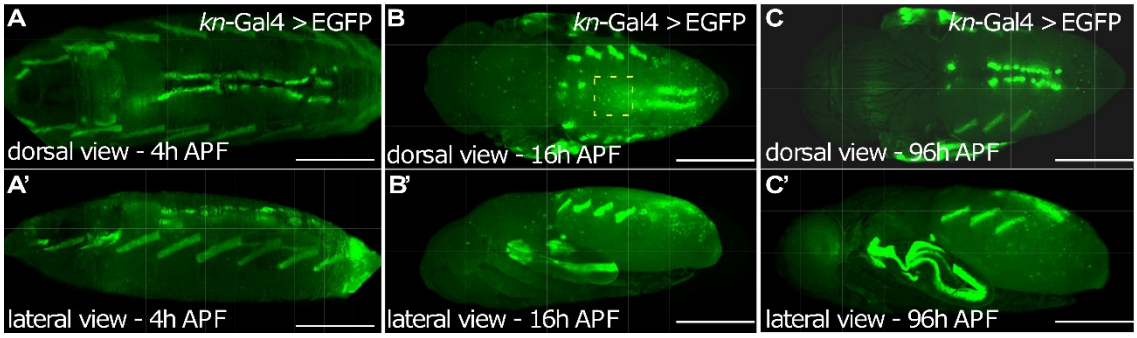

Supplementary Figure S 2 – Representative in vivo images of GFP expression under the control of the collier promoter kn-Gal4. *Scale bar represents 50 µm. (A) Dorsal and (A') lateral view of a pupae 4h APF. (B) Dorsal and (B') lateral view of a pupae 16h APF. The rectangle marks the region of accumulation of PSCs visualized by spinning disc microscopy (Publication 2). The expression on the pupal wing represents the A/P boundary. (C) Dorsal and (C') lateral view of a pupae 96h APF.*

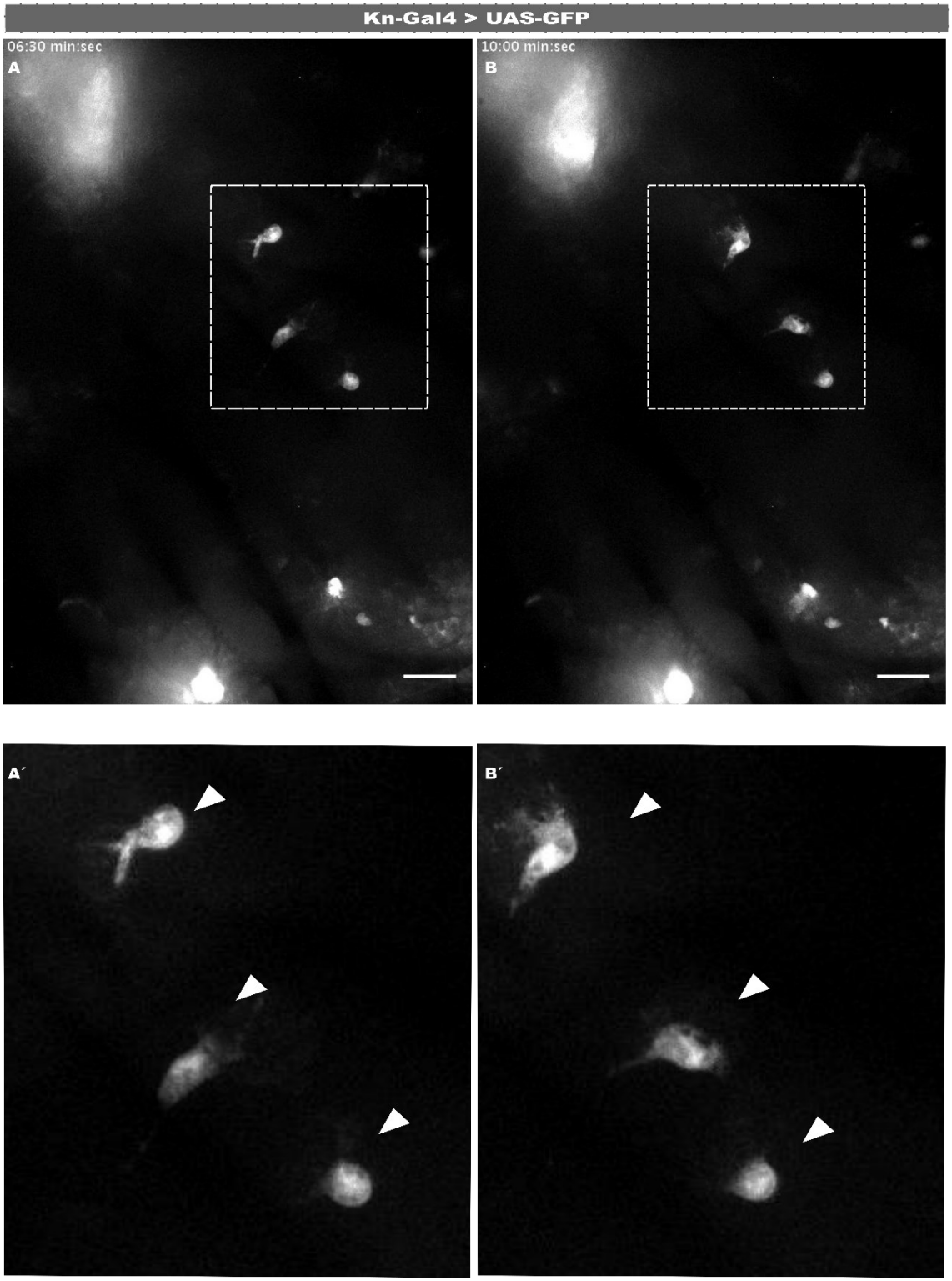

Supplementary Figure S 3 – Kn-Gal4 positive cells persist until adulthood. *Frames of a spinning disc time-lapse movie of randomly migrating 96h APF hemocytes marked by GFP expression under the control of kn-Gal4. A-B) Images after 6:30 min and 10 min, respectively. A´-B´) Enlarged box region from A) and B) show kn-positive cells marked by white arrows.*

7.2. Supplementary table

Supplementary Table 1 – Putative protein ubiquitylation sites at lysine residues were predicted by BDM-PUB (http://bdmpub.biocuckoo.org/prediction.php). *Selected lysine residues highlighted in red are discussed in chapter 4.11* (Xue et al., 2006).

Protein	*Peptide*	*Position*	*Score*
Drosophila WAVE			
	RQLSSLSKHAEDVFG	48	0.79
	RIDRLAIKVTQLDST	81	1.91
	PLTDITRKKAFKSAK	100	2.62
	ITRKKAFKSAKVFDQ	104	2.50
	KKAFKSAKVFDQQIF	107	1.90
	DKPPPLDKLNVYRDD	138	1.47
	TERVMHDKGKKLNRP	178	0.60
	RVMHDKGKKLNRPRQ	180	1.07
	VMHDKGKKLNRPRQD	181	1.22
	GAAGRGNKKQKTKIR	200	3.21
	AAGRGNKKQKTKIRV	201	1.24
	GRGNKKQKTKIRVPH	203	1.01
	GNKKQKTKIRVPHNT	205	0.54
	PGTPSRNKPRPSQPP	407	0.74
	NSGHMAAKLLGRANS	475	1.66
	VPDQHSPKMSPPNAA	536	1.49
	RPHQILPKSLANGEM	573	1.72
	VPHIVAPKKMLPPFH	596	0.78
	PHIVAPKKMLPPFHD	597	0.56
	RDGITLRKVEKSEQK	621	0.76
	KVEKSEQKEIERNAA	628	0.41
Drosophila WASH			
	RLARNGSKVEDINNR	57	1.42
	EDINNRVKRAQAKID	66	0.38
	RVKRAQAKIDALVGS	71	1.58
	IDALVGSKRAIQIFA	79	1.30
	SHSAADQKPDDADIF	133	0.92
	SPLVAERKITNRTAG	158	2.03
	GEDLNAWKRSLPPQN	198	2.08
	STQLTGEKQLAPAPH	220	1.45
	SLAHGTTKLATPAGD	235	2.30
	IPGPVRRKSVGQCPS	322	1.88
	SPPPFPTKGAVKPLS	365	2.65
	FPTKGAVKPLSPSLA	369	3.33
	VVDNSRSKAGGAVTG	427	0.45
	PPPVQPRKGSKSSDE	482	2.95
	VQPRKGSKSSDEHSE	485	2.14

Human WAVE2

RQLGSLSKYAEDIFG	45	0.32
RVDRLQVKVTQLDPK	78	1.02
KVTQLDPKEEEVSLQ	85	0.34
DDGKEALKFYTDPSY	148	1.43
EKMLQDTKDIMKEKR	169	0.31
TKDIMKEKRKHRKEK	175	0.70
DIMKEKRKHRKEKKD	177	2.12
KEKRKHRKEKKDNPN	180	1.90
KRKHRKEKKDNPNRG	182	2.36
RKHRKEKKDNPNRGN	183	1.08
RGNVNPRKIKTRKEE	195	1.64
NVNPRKIKTRKEEWE	197	1.24
GQEFVESKEKLGTSG	216	0.88
GSGLAGPKRSSVVSP	290	3.97
LGSPPGPKPGFAPPP	313	1.89
PPLSDTTKPKSSLPA	425	1.00
LSDTTKPKSSLPAVS	427	1.36

7.3. Author contribution

Publication 1

Hirschhäuser, A., Molitor, D., Salinas, G., Großhans, J., Rust, K., & Bogdan, S. Single-cell transcriptomics identifies new blood cell populations in *Drosophila* released at the onset of metamorphosis. Submitted to Development; under review.

Figure 1: (A) I performed the hemocyte isolation step from *Drosophila* pupae before the transfer to scRNA-Seq approach.

Figure 2: (C-D) I performed the experiments.

Figure 4: (H-L) I performed the experiments.

Figure 5: (G-K) I performed the experiments and quantifications.

Figure 6: I performed all experiments and quantifications.

Figure 8: (A, D-F) I performed the experiments and quantifications.

Movies M1, M3: I performed all experiments.

Supplementary Figure S7: I performed all experiments.

Sven Bogdan and Katja Rust wrote the manuscript and I commented on it.

Publication 2:

Hirschhäuser, A., van Cann, M., & Bogdan, S. (2021). CK1α protects WAVE from degradation to regulate cell shape and motility in the immune response. Journal of Cell Science, 134(23). https://doi.org/10.1242/jcs.258891

Figure 1: I performed all experiments and quantifications.

Figure 2: I performed all experiments and quantifications.

Figure 3: I performed all experiments and quantifications.

Figure 4: (C-F) I designed and performed the experiments and quantifications.

Figure 5: I performed all experiments and quantifications.

Figure 6: (B-G) I performed all experiments and quantifications.

Figure 7: I designed and performed the experiments and quantifications.

Figure S1: I performed all experiments and quantifications.

Movie 1: I created the movie animation based on the available amino acid sequence of CK1α using the UCSF Chimera software.

Movie 2 & 3: I performed all experiments.

I performed the methodology and data curation.

Sven Bogdan wrote the manuscript and I commented on it.

7.4. *Drosophila* transgenic lines used in this work

Genotype	Description	Reference/Stock Number
; CK1α[RNAi] VDRC 16645 ; ;	CK1α RNAi #1	VDRC 16645
; ; CK1α[RNAi] BL 25786 ;	CK1α RNAi #2	BL# 25786
y[1] w[*] CK1α [A] P{ry[+t7.2]=neoFRT}19A/FM7c, P{w[+mC]=GAL4-Kr.C}DC1, P{w[+mC]=UAS-GFP.S65T}DC5, sn[+]	CK1α mutation L141M	BL# 57084
y[1] w[*] CK1α [8B12] P{ry[+t7.2]=neoFRT}19A/FM6; CyO/Sco	CK1α mutation G43D	BL# 63802
y[1] w[*] CK1α [B] P{ry[+t7.2]=neoFRT}19A/FM7c, P{w[+mC]=GAL4-Kr.C}DC1, P{w[+mC]=UAS-GFP.S65T}DC5, sn[+]	CK1α mutation G148S	BL# 64459
hsFLP, tubP-Gal80, w[*], neoFRT19A ; hmlΔGal4, UASeGFP	hsFLP with marker for hemocytes for MARCM Analyses	Publication 2
P{ry[+t7.2]=neoFRT}19A; ry[506]	MARCM control stock	BL# 1709
mys[1] P{ry[+t7.2]=neoFRT}19A/FM7c	myospheroid loss of function allel for MARCM	BL# 23862
ck1α-F000940FlyOrf/TM6B	CK1α-3xHA overexpression	Rumpf Lab
hmlΔGal4, UAS-eGFP; ck1α-F000940FlyOrf/TM6B	CK1α-3xHA overexpression in hemocytes	this work
enGal4/Cyo; ck1α-F000940FlyOrf/TM6B	CK1α-3xHA overexpression in wing imaginal disc	this work
;hmlΔGal4, UASeGFP; CK1α RNAi BL 25786/TM6B;	knockdown and rescue experiments in hemocytes	Publication 2
y[*] w[*]; ; CK2α$^{[TikR]}$/Tm6b	CK2α kinase dead mutant; homozygous lethal	BL# 24511
y[*] w[*]; ; CK2α$^{[Tik]}$/Tm6b	CK2α kinase dead mutant; homozygous lethal	BL# 24512
y[*] w[*]; ; CK2α$^{[P1]}$/Tm6b	CK2α loss-of-function; homozygous lethal;	Kyoto 141869

	transheterozygous with kinase dead mutant viable until pupal stage	
;Bl/Cyo; pUAST-WAVE^{SA5X} / TM6B ;	wing imaginal disc	injectetion in 68E
;Bl/Cyo; pUASP-WAVE^{SA5X} / TM6B ;	hemocyte rescue	injectetion in 68E
;Bl/Cyo; pUAST-WAVE^{SD5X} / TM6B ;	wing imaginal disc	injectetion in 68E
;Bl/Cyo; pUASP-WAVE^{SD5X} / TM6B ;	hemocyte rescue	injectetion in 68E
;Bl/Cyo; pUAST-WAVE-WT / TM6B ;	wing imaginal disc	injectetion in 68E
;Bl/Cyo; pUASP-WAVE-WT / TM6B ;	hemocyte rescue	injectetion in 68E
;hmlΔ-dsRed, FRT40A scarΔ37/ CyO$^{Wee\text{-}P\text{-}GFP}$; daGal4 / TM6B ;	*in vivo* rescue experiment	Bogdan lab
; scar[Δ37], FRT40A / CyO^{Dfd}; UAS-WAVE^{SA5X} / TM6;	*in vivo* rescue experiment	injectetion in 68E
; scar[Δ37], FRT40A / CyO^{Dfd}; UAS-WAVE WT / TM6B;	*in vivo* rescue experiment	injectetion in 68E
; scar[Δ37], FRT40A / CyO^{Dfd};UAS-WAVE^{SD5x} / TM6;	*in vivo* rescue experiment	injectetion in 68E
;Bl/Cyo; pUAST-WAVE^{K48R} / TM6B	point mutation putative ubi site	injectetion in 68E
y[1] sc[*] v[1] sev[21]; P{y[+t7.7] v[+t1.8]=TRiP.HMS00119}attP2	Prosβ5 RNAi	BL# 34810
y[1] sc[*] v[1] sev[21]; P{y[+t7.7] v[+t1.8]=TRiP.HMS00068}attP2	Prosα7 RNAi	BL# 33660
y[1] sc[*] v[1] sev[21]; P{y[+t7.7] v[+t1.8]=TRiP.HMS00071}attP2	Rpn11 RNAi	BL# 33662
y[1] v[1]; P{y[+t7.7] v[+t1.8]=TRiP.JF03317}attP2	Rpn6 RNAi	BL# 29385
Cul1 RNAi	Cullin 1 RNAi	BL# 36601
Cul 2 RNAi	Cullin 2 RNAi	VDRC 19297
Cul 3 RNAi	Cullin 3 RNAi	VDRC 25875
Cul4 RNAi	Cullin 4 RNAi	BL# 50614
Cul 5 RNAi	Cullin 5 RNAi	VDRC 52176
Cul 6 RNAi	Cullin 6 RNAi	VDRC 31479
w[*] / ; P{w[+mC]=UAS-RedStinger}4, P{w[+mC]=UAS-FLP.D}JD1, P{w[+mC]=Ubi-p63E(FRT.STOP)Stinger}9F6 / CyO ; ;	G-TRACE	BL# 28280
w[*] / ; ; P{w[+mC]=UAS-RedStinger}6, P{w[+mC]=UAS-FLP.Exel}3, P{w[+mC]=Ubi-p63E(FRT.STOP)Stinger}15F2 / ;	G-TRACE	BL# 28281
w ; sp / Cyo ; SRP-H2A-3XmCherry / TM3Ser #3 ;	nuclear localized 3x mCherry	(Gyoergy et al., 2018)

	fusion with srpHemo promoter	
w ; sp / CyO ; SRP-3XmCherry / TM6B ;	3x mCherry fusion with srpHemo promoter	(Gyoergy et al., 2018)
P{w[+mC]=GAL4-Antp.P1.A}1, y[1] w[*]; wg[Sp-1]/CyO	*Antp* Gal4-enhaner trap	BL# 26817
y[1] w[*]; Mi{Trojan-GAL4.2}kn[MI15480-TG4.2]/SM6a	*kn* Gal4-enhancer trap	BL# 67516
w[1118]; PBac{w[+mC]=IT.GAL4}tau[4021-G4]	*tau* Gal4 enhancer-trap	BL# 77641
w[1118]; Mi{GFP[E.3xP3]=ET1}CG31174[MB02966]	CG31174 GFP trap	BL# 24040
w[1118]; P{y[+t7.7] w[+mC]=GMR80G10-GAL4}attP2	*Ham* Gal4-enhancer trap	BL# 40090
y[1] w[*]; Mi{Trojan-GAL4.2}Tep4[MI13472-TG4.2]/SM6a	*Tep4* Gal4-enhacner trap	BL# 76750
y[1] w[67c23]; Mi{PT-GFSTF.1}Ance[MI05748-GFSTF.1]/SM6a	Ance GFP trap	BL# 59828
UAS-mCherry-NLS/CyO; CG31174-GFP/TM6B	for cross-validation	this work
msnF9-moesin-mCherry, eater-GFP-NLS; ; ;	dual reporter for lamellocytes and plasmatocytes, used for wasp infestiation	(Anderl et al., 2016)
; BI / CyO; WAVE[RNAi] NIG / TM6B ;	WAVE RNAi	NIG Fly 4636R-1
; HmlΔ-Gal4; ;	hemocyte specific driver, used for knockdown and rescue experiments	(Sinenko & Mathey-Prevot, 2004)
; ; da-Gal4, UAS-eGFP;	ubiquitous expression driver	(Lehne et al., 2022)
; HmlΔ-Gal4, UAS-eGFP; ;	hemocyte specific, used for knockdown, rescue, and *in vivo* experiments	(Sinenko & Mathey-Prevot, 2004)
; knGal4, UAS-eGFP; ;	recombination, *in vivo* experiments	Publication 1
; Tep4Gal4, UAS-Lifeact-GFP; ;	recombination, wasp infestiation	Publication 1

7.5. List of Gal4-enhancer trap and GFP-exon trap fly lines used for ex vivo validation from Publication 1

Genotyp	Source	Gen	Cluster	Expression in isolated Hemocytes
P{w[+mGT]=GT1}CG13377[BG01596] asRNA:CR43906[BG01596] w[1118]/Binsinscy	BL 12547	CG13377	Adhesive-PL	no
y[1] w[*] Mi{y[+mDint2]=MIC}ovo[MI01236]	BL 34411	Ovo	Adhesive-PL	no
w[1118]; PBac{y[+mDint2] w[+mC]=EcR-EGFP.S}VK00033	BL 59040	EcR	Adhesive-PL	no
y[1] w[67c23]; Mi{PT-GFSTF.1}EcR[MI05320-GFSTF.1]/SM6a	BL 59823	EcR	Adhesive-PL	no
y[1] w[*]; Mi{y[+mDint2]=MIC}EcR[MI05320]	BL 38619	EcR	Adhesive-PL	no
w[1118]; P{w[+mC]=EcR.GET-BD-GAL4}1	BL 5910	EcR	Adhesive-PL	no
w[*]; P{w[+mC]=rst.F6-GAL4}2/CyO, P{ry[+t7.2]=elav-lacZ.H}Y H2	BL 23302	rst	Adhesive-PL & Muscle-PL	no
dipt- GFP - term drs	Jean-Luc Imler	diptericin	AMP-PL	no
drc- GFP - term drc	Jean-Luc Imler	drosocin	AMP-PL	no
metch- GFP - term drs	Jean-Luc Imler	metchnikowin	AMP-PL	no
Def- GFP - term drs	Jean-Luc Imler	defensin	AMP-PL	no
CecA1- GFP - term drs (M3or)	Jean-Luc Imler	cecropin A1	AMP-PL	no
y[1] w[*]; TI{GFP[3xP3.cLa]=CRIMIC.TG4.1}Myd88[CR02479-TG4.1]	BL 92678	Myd88	Chitinase-PL	no
w[1118]; PBac{w[+mC]=IT.GAL4}Tep2[0635-G4]	BL 63457	Tep2	Chitinase-PL	no

y[1] w[*]; Mi{Trojan-GAL4.0}btl[MI03286-TG4.0]/TM3, Sb[1] Ser[1]	BL 66790	btl	Chitinase-PL	no
w[*]; P{w[+m*]=vvl-FLP1.M}2/CyO; P{w[+mC]=btl-moe.mRFP1}3	BL 64233	btl	Chitinase-PL	no
w[1118]; Mi{GFP[E.3xP3]=ET1}pyr[MB02808]/CyO	BL 23827	Pyr	Chitinase-PL	no
P{w[+mC]=UAS-btl.lambda}1, w[*]	BL 29046	btl	Chitinase-PL	no
w[1118]; Mi{GFP[E.3xP3]=ET1}TotA[MB06977]	BL 25343	TotA	LSP-Bomanin-PL	no
y[1] w[*]; Mi{y[+mDint2]=MIC}Lsp1beta[MI11032]	BL 55576	Lsp1Beta	LSP-Bomanin-PL	no
y[1] w[*]; Mi{y[+mDint2]=MIC}Lsp1beta[MI05460]	BL 40782	Lsp1Beta	LSP-Bomanin-PL	no
P{w[+mC]=GAL4-twi.G}108.4, w[1]	BL 914	Twi	Muscle	no
y[1] w[*]; PBac{y[+mDint2] w[+mC]=twi-GFP.FPTB}VK00033	BL 79615	Twi	Muscle	no
y[1] w[*]; Mi{y[+mDint2]=MIC}Kah[MI01396]	BL 34187	Kah	Muscle	no
w[1118]; P{y[+t7.7] w[+mC]=Kah-GFP.FPTB}attP40	BL 64829	Kah	Muscle	no
y[1] w[*]; Mi{y[+mDint2]=MIC}Dp1[MI11574] imd[MI11574]/SM6a	BL 56344	Imd	Muscle	no
y[1] w[*]; Mi{y[+mDint2]=MIC}imd[MI03451]/CyO	BL 37054	Imd	Muscle	no

w[*]; P{w[+mC]=mdelta0.5-GAL4}2	BL 41795	HLH	Muscle	no
y[1] w[*]; P{y[+t7.7] w[+mC]=E(spl)m3-HLH-GFP.FPTB}attP40	BL 66402	HLH	Muscle	no
y[1] w[*]; PBac{y[+mDint2] w[+mC]=scro-GFP.FPTB}VK00037	BL 92387	Scro	Neuron	no
w[1118]; Mi{GFP[E.3xP3]=ET1}scro[MB09728]	BL 27801	Scro	Neuron	no
y[1] w[*]; Mi{y[+mDint2]=MIC}smog[MI04401]	BL 37662	Smog	Neuron	no
y[1] w[*]; TI{GFP[3xP3.cLa]=CRIMIC.TG4.0}smog[CR00977-TG4.0]	BL 83229	Smog	Neuron	no
y[1] w[*]; Mi{y[+mDint2]=MIC}RhoGAP100F[MI12278]	BL 57912	RhoGAP100F	Neuron	no
w[1118]; PBac{w[+mC]=IT.GAL4}RhoGAP100F[0379-G4]	BL 62816	RhoGAP100F	Neuron	no
PBac{w[+mC]=IT.GAL4}Appl[0293-G4] w[1118]	BL 77544	Appl	Neuron	no
y[1] Mi{Trojan-GAL4.0}Appl[MI11551-TG4.0] w[*]/FM7c	BL 66900	Appl	Neuron	no
y[1] w[*] Mi{Trojan-GAL4.2}fne[MI09399-TG4.2]	BL 77796	Fne	Neuron	no
y[1] w[*] Mi{y[+mDint2]=MIC}fne[MI06476]	BL 41101	Fne	Neuron	no

y[1] w[*]; P{y[+t7.7] w[+mC]=nerfin-1-GFP.FPTB}attP40	BL 67385	nerfin-1	Neuron	no
P{w[+m*]=Appl-GAL4.G1a}1, y[1] w[*]	BL 32040	Appl	Neuron	no
w[1118]; Mi{GFP[E.3xP3]=ET1}nerfin-1[MB09839]	BL 27810	nerfin-1	Neuron	no
w[1118] P{w[+mGT]=GT1}NetA[BG02298]	BL 12856	NetA	Osiris-PL	no
y[1] w[*] Mi{PT-GFSTF.1}NetA[MI04563-GFSTF.1]/FM7j, B[1]	BL 59409	NetA	Osiris-PL	no
y[1] w[*]; PBac{y[+mDint2] w[+mC]=esg-GFP.FPTB}VK00031	BL 83386	Esg	Osiris-PL	no
y[1] w[*]; TI{GFP[3xP3.cLa]=CRIMIC.TG4.2}CG4914[CR01749-TG4.2] ome[CR01749-TG4.2-X]/TM3 Sb[1] Ser[1]	BL 86504	CG4914	Osiris-PL	no
y[1] w[67c23]; P{w[+mC]=lacW}esg[k00606]/CyO	BL 10359	esg	Osiris-PL	no
P{ry[+t7.2]=PZ}esg[05729]/CyO	BL 83153	esg	Osiris-PL	no
y[1] w[*]; Mi{y[+mDint2]=MIC}NimC1[MI13732]	BL 59190	NimC1	Pan-Hemocytes	yes
y[1] w[*]; Mi{y[+mDint2]=MIC}eater[MI15531]	BL 61081	Eater	Pan-Hemocytes	yes
Mi{ET1}CREGMB00443	BL 22800	CREG	Precurso-PL-3	no
Mi{MIC}CREGMI06250	BL 42140	CREG	Precurso-PL-4	no
Mi{ET1}CG31102MB10157	BL 29096	CG31102	Precursor-PL-1	no

Mi{ET1}CG5002MB08327	BL 26108	CG5002	Precursor-PL-1&2	no
TI{2A-GAL4}Pdfr[2A-GAL4] w[*]/FM7a	BL 84684	Pdfr	Precursor-PL-3	no
y[1] w[67c23]; Mi{GFP[E.3xP3]=ET1}CG33791[MB00772] CG12105[MB00772] CG18170[MB00772]	BL 23173	CG12105	Precursor-PL-3	no
w[1118]; P{y[+t7.7] w[+mC]=GMR18H11-GAL4}attP2	BL 48832	Pdfr	Precursor-PL-3	no
w[*]; P{w[+mC]=Pdfr-GAL4.B}2/CyO	BL 68215	Pdfr	Precursor-PL-3	no
y[1] w[*]; TI{GFP[3xP3.cLa]=CRIMIC.TG4.1}Pdfr[CR01422-TG4.1]	BL 86375	Pdfr	Precursor-PL-3	no
Mi{ET1}CG7720MB01330	BL 23059	CG7720	Precursor-PL-3 & AMP-PL	no
y[1] w[*] Mi{y[+mDint2]=MIC}CG13012[MI12082]	BL 56720	CG13012	Precursor-PL-6	no
y[1] w[*]; TI{GFP[3xP3.cLa]=CRIMIC.TG4.1}Toll-4[CR00920-TG4.1]	BL 79358	Toll-4	PSC	no
P{w[+mC]=GAL4-Antp.P1.A}1, y[1] w[*]; wg[Sp-1]/CyO	BL 26817	Antp	PSC	yes
y[1] w[*]; Mi{PT-GFSTF.0}Antp[MI02272-GFSTF.0]/TM6C, Sb[1] Tb[1]	BL 59790	Antp	PSC	no
y[1] w[*]; Mi{y[+mDint2]=MIC}kn[MI15480]/SM6a	BL 61064	Kn	PSC	no
y[1] w[*]; Mi{Trojan-GAL4.2}kn[MI15480-TG4.2]/SM6a	BL 67516	Kn	PSC	yes

w[1118]; PBac{w[+mC]=IT.GAL4}tau[4021-G4]	BL 77641	Tau	PSC	yes
y[1] w[*]; Mi{PT-GFSTF.0}tau[MI03440-GFSTF.0]/TM6C, Sb[1] Tb[1]	BL 60199	Tau	PSC	no
y[1] w[*]; Mi{y[+mDint2]=MIC}MstProx[MI02994]	BL 35889	MstProx	PSC	no
Mi{MIC}glob1MI02798	BL 36147	glob	PSC	no
Mi{MIC}glob1MI14203	BL 59679	glob	PSC	no
y[1] w[67c23]; Mi{PT-GFSTF.1}Ance[MI05748-GFSTF.1]/SM6a	BL 59828	Ance	Secretory-PL	yes
y[1] w[*]; Mi{Trojan-GAL4.1}Ance[MI05748-TG4.1]/CyO; D[1]/TM3, Sb[1] Ser[1]	BL 76676	Ance	Secretory-PL	yes
y[1] w[*]; Mi{y[+mDint2]=MIC}CG30083[MI04386]	BL 37445	CG30083	Secretory-PL	no
y[1] w[*]; Mi{y[+mDint2]=MIC}mthl11[MI11235]	BL 55597	Mthl11	Secretory-PL	no
TI{2A-GAL4}mthl11[2A-GAL4]	BL 84658	Mthl11	Secretory-PL	no
y[1] w[*]; TI{GFP[3xP3.cLa]=CRIMIC.TG4.2}Tep1[CR02497-TG4.2]	BL 92681	Tep1	Secretory-PL	no
w[1118]; Mi{GFP[E.3xP3]=ET1}CG31174[MB02966]	BL 24040	CG31174	Secretory-PL	yes

y[1] w[*]; PBac{y[+mDint2] w[+mC]=ham-GFP.FPTB}VK00033/TM6C, Sb[1]	BL 83660	Ham	Secretory-PL	no
w[1118]; P{y[+t7.7] w[+mC]=GMR80G10-GAL4}attP2	BL 40090	Ham	Secretory-PL	yes
FlyFos016332(pRedFlp-Hgr)(CG588526810::2XTY1-T2A-SGFP-NLS-3XFLAG)dFRT	VDRC 318411	CG5885	Secretory-PL	no
FlyFos016332(pRedFlp-Hgr)(CG588526810::2xTY1-SGFP-3xFLAG)dFRT	VDRC 318480	CG5885	Secretory-PL	no
y[1] w[*]; Mi{Trojan-GAL4.2}Tep4[MI13472-TG4.2]/SM6a	BL 76750	Tep4	Secretory-PL & PSC	no
y[1] w[*]; Mi{y[+mDint2]=MIC}Tep4[MI06806]	BL 51209	Tep4	Secretory-PL & PSC	yes
y[1] w[*]; Mi{Trojan-GAL4.0}Trim9[MI00398-TG4.0] w-cup[MI00398-TG4.0-X]	BL 76133	w-cup	Spermatid-Marker-PL	no
y[1] w[*]; Mi{y[+mDint2]=MIC}Trim9[MI00398] w-cup[MI00398]/CyO	BL 30984	w-cup	Spermatid-Marker-PL	no
w[1118]; Mi{GFP[E.3xP3]=ET1}wa-cup[MB07475]	BL 26503	Wa-cup	Spermatid-Marker-PL	no
w[1118]; Mi{GFP[E.3xP3]=ET1}soti[MB07998]/TM6C, Sb[1]	BL 26092	Soti	Spermatid-Marker-PL	no

7.6. Plasmids generated in this work

pUASTattb - WAVE^{SA5x}

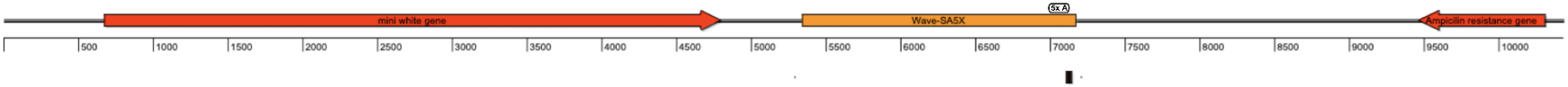

pUASTattb - WAVE^{SD5x}

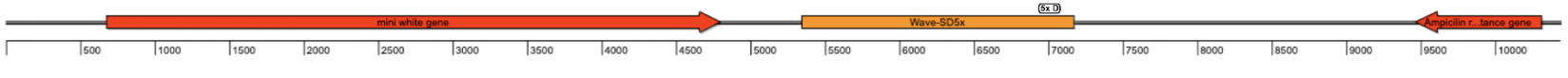

pUASTattb - WAVE WT

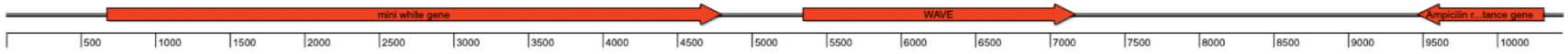

pUASTattb - WAVE^{K48R}

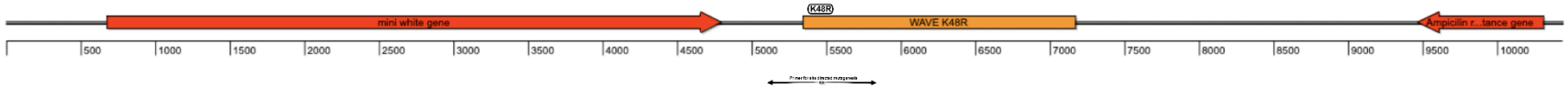

pMT-CK1-6xMyc

CK1α-eGFP

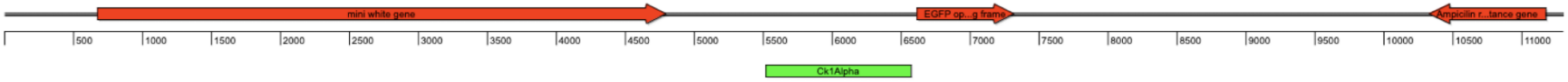

7.7. List of PCR primers

WAVE K48R_for	CTCGCTGTCCaggCACGCAGAGG
WAVE K48R_rev	GACAGCTGGCGAATGATGTTCG
CK1α seq_for	CCCTCGCTGGAGGATCTG
CK1α seq_rev	CAGTCGCGGCGTGACGAC
WAVE SA5x_for	GGCTATCGAATTAGCCGAGGCCGAGGATGCGGATGCCGAAGACGACGCCGAGGGA
WAVE SA5x_rev	GCCCTCGGAGTCGTCTTCGGCATCCGCATCCTCGGCCTCGGCTAATTCGATAGCC
WAVE SD5x_for	TGGGCCAGACGTGTGGCTATCGAATTAGACGAGGACGAGGATGACGATGACGAAGACGACGACGAGGGCTGGATGGA
WAVE SD5x_rev	TCCATCCAGCCCTCGTCGTCGTCTTCGTCATCGTCATCCTCGTCCTCGTCTAATTCGATAGCCACACGTCTGGCCAA

7.8. Verzeichnis der akademischen Lehrerinnen und Lehrer

Meine akademischen Lehrenden in Frankfurt waren die Damen und Herren:

PD Dr. Abele, Prof. Auner, Dr. Bauer, Prof. Bruls, Prof. Delecluse, Prof. Dötsch, Jun. Prof. Ernst, Dr. Jan-Peter Ferner, Prof. Frangakis, Prof. Glaubitz, Prof. Gottschallk, Prof. Göbel, Prof. Grininger, Prof. Güntert, Prof. Heckel, Prof. Klein, Dr. Koch, Prof. Ludwig, Prof. Osiewacz, Prof. Pos, Prof. Schmidt, Prof. Schwalbe, Prof. Tampé, Dr. Trowitzsch

7.9. Danksagung

„Ausdauer wird früher oder später belohnt, meistens aber später.“ Das waren die Worte zu meinem letzten Geburtstag in der Arbeitsgruppe. Eine Doktorarbeit benötigt viel Ausdauer und ist geprägt von häufigen unvorhergesehen Umständen. Daher möchte ich dir, Prof. Dr. Sven Bogdan, meinen großen Dank aussprechen. Weil ich die Möglichkeit bekommen habe die Doktorarbeit zu beginnen, aber auch weil trotz aller Stolpersteine ein Vertrauen in meine Arbeit existierte. Die Zeit in deiner Arbeitsgruppe hat mich nachhaltig geprägt und mich viel gelernt. An dem Punkt auch ein großes Dankeschön an alle aus der Arbeitsgruppe, die mich auf diesem Weg begleitet und sehr unterstütz haben. Vielen Dank!

Danke an Claudia. Allein um dich zu finden hat es sich gelohnt das Kapitel Doktorarbeit in Marburg zu verfassen. Worte können nicht beschreiben, was du für eine Bedeutung in dieser Geschichte hast. Alles, was ich sagen kann, ist, dass ich dich liebe für alles, was war und das, was kommen wird. Danke für deine Unterstützung.

Eigentlich das Wichtigste ist der Dank an meine Eltern. Ihr habt mich auf dem ganzen Weg begleitet und mir immer die Möglichkeit gegeben, nach etwas neuem zu streben. Ich danke euch für alles, was ihr mir auf diesem Weg mitgegeben habt und hoffe, dass ich es irgendwann wieder zurückgeben kann.

„Manche sind gestorben, andere gingen weg. Doch wir haben einfach immer alles überlegt. Wir sind anders als die anderen, auch wenn´s keine anderen gibt. Wir schwören uns immer wieder, dass das Beste vor uns liegt!“ – Danke Marcel. Danke für alle Worte und Taten im Studium und der Promotion. Ich hoffe in Zukunft wird es weiterhin heißen: „Und wieder ist ein Jahr vorüber, und wieder ist ein Bierglas leer!“

„Der Zahn der Zeit schlägt sich ins Fleisch. Vom Bummern der Jugend zu den Enten am Teich. Wir bleiben die, die wir waren, dass man daran überhaupt zweifeln kann. Wir bleiben die, die wir waren, nicht alles endet irgendwann“

Danke Tobi für deine Begleitung und immer offene und ehrliche Meinung!